# HOLOGRAPHIC INTERFEROMETRY OF THE FLOW FIELD BETWEEN A FIN AND FLAT PLATE

Robert Ward Heyer

NAVAL POSTGRADUATE SCHOOL
Monterey, California

THESIS

Holographic Interferometry of The Flow

Field Between a Fin And Flat Plate

by

Robert Ward Heyer

Thesis Advisor: D. G. Collins

March 1972

Holographic Interferometry of The Flow

Field Between a Fin And Flat Plate

by

Robert Ward Heyer
Lieutenant, United States Navy
B.S.E.E., Duke University, 1964

Submitted in partial fulfillment of the
requirements for the degree of

MASTER OF SCIENCE IN AERONAUTICAL ENGINEERING

from the

NAVAL POSTGRADUATE SCHOOL
March 1972

ABSTRACT

This study was an attempt to map the density field in a fin-flat plate junction three-dimensionally using holographic interferometry. This investigation has extended the density studies by Matulka [12, 13] and Jagota [3, 4] to include, for the first time, interferometric fringe information obtained through a transparent model in supersonic flow. The fringe information was then inverted by a FORTRAN computer program to produce a plot of the density field around the model. The feasibility of the method was demonstrated.

The factors which are thought to have limited the success of the experiment include vibration of the model, fluctuations of the tunnel flow and the fact that the model was somewhat too large in relation to the size of the wind tunnel test section. Schlieren photography was used to look through and around the model and to verify that the same flow was established as was reported by Thomas [23, 24] and Winkelman [26, 27].

The data reduction of holographic interferograms was, for the first time, accomplished using photographic enlargements. This technique is considered to be much easier and more accurate than the one used in the previous investigations. However, the data reduction step, because of the time and labor involved, is considered to be the rate controlling process of the whole analysis.

TABLE OF CONTENTS

4

ACKNOWLEDGEMENTS

I. INTRODUCTION

The determination of the flow field in the wing-body junction of an aircraft in supersonic flight presents many problems. The typical approach has been to measure the static pressure on the surface using many small pressure taps [23, 24] and to determine the velocity field in the junction using translatable pressure probes [18, 19, 25]. Thomas [23, 24] and Winkelmann [26, 27] used azobenzene and oil-smear tests to view the flow field around a flat plate-fin junction. From the streak patterns on the plate and fin, they were able to illustrate the three-dimensional flow field, although in a partially speculative fashion. This study has attempted to map the density field in a fin-flat plate junction three-dimensionally using holographic interferometry. Although this objective was not fully achieved, the feasibility of the method has been demonstrated.

By using a Q-switched laser with exposure times of about twenty nanoseconds, it was possible to obtain three-dimensional holographic interferograms of the density field in the fin-flat plate junction. From holograms taken at a number of viewing angles the fringe shifts in different planes could be obtained. By integrating this information using a FORTRAN computer program, the density field can be determined. This technique has been previously demonstrated for the flow field of a free jet by Matulka [12, 13] and for the supersonic flow field around a cone at angle of attack by Jagota [3, 4] .

The tests were performed at the Naval Postgraduate School, using the four-inch supersonic wind tunnel.

II. EXPERIMENTAL APPARATUS

A. THE WIND TUNNEL

The investigation was conducted in the Naval Postgraduate School
blowdown-to-atmosphere supersonic wind tunnel. The test section is
four inches by four inches in cross section and six inches long with
two different sets of side walls. The two-inch thick plexiglas side
walls, which have a refraction index of 1.49, present a complete field
of view of the flow from the nozzle throat to aft of the test section
mounting bracket (Figure 1 (a)). The second set of sidewalls used are
aluminum with high quality optical glass portholes located in the test
section area (Figure 1 (b)). The interchangeable nozzle for a test
section Mach number of 2.8 was used for all tests. The nominal run
time is five minutes at Mach 2.8 with the maximum stagnation pressure
of about 105 pounds per square inch.

B. THE HOLOGRAPHIC ARRANGEMENT

The holographic arrangement is illustrated in Figure 2 and shown in
photographs included as Figures 3, 4, and 5. The equipment stand was
rested on a portion of the building floor that was vibrationally isolated.
A Konrad K-1 pulsed ruby laser with a Pockels cell Q-switching unit was
used to produce monochromatic light at a wave length of 6943 Angstroms
and exposure time of twenty nano-seconds. The laser cavity length was
seventy-three cm. giving a coherence length of about ten cm. To main-
tain the laser head and output etalon at a constant temperature of 27.5
degrees centigrade, a Lauda constant temperature circulator Model N was
used. This was controlled by an electronic relay type R-10 coupled with
a Culligan de-ionizer.

Holograms were obtained by routing the reference beam under the wind tunnel and the scene beam through the test section, and intersecting the two beams on the hologram plate at an intersecting angle of approximately 50 degrees. The beam sizes were controlled by translating the concave lenses located between the beam splitter and hologram plate in each beam (Figure 2). The Q-switched laser and optics were aligned using a continuous wave helium-neon laser. For reference purposes, grids were mounted on the outside tunnel walls and aligned using a surveyor's transit. The holographic stand and test section were completely enclosed in a wooden box to enable holograms to be taken in the daylight (Figure 6).

C. THE WIND TUNNEL MODELS

The fin-flat plate models used are shown in Figures 7 (a), (b), (c), and (d). The metal portions of both models were stainless steel. The center section, part of one strake, and all of the other strake of the first model in Figure 7 (a) were made of epoxy while the center section of the second model, Figures 7 (b) and 7 (c), was fabricated from plexiglas. The flat plate grids in both models were etched into the plastic surface and coated with a clear plastic to achieve a smooth surface.

The models were rotated about their sting mounts as shown in Figure 7 (d). Alignment for the desired rotation angle was accomplished by aligning prescribed lines on the sting mount collar with a scribed mark on the sting stand using a surveyor's transit.

8

III. ANALYTICAL EVALUATION OF THE DENSITY FIELD

A. THE BASIC INTERFEROMETRIC EQUATION

Interferograms are created when two coherent light beams are super-
imposed on each other and projected on a viewing screen. The light and
dark regions observed correspond to the relative phase difference be-
tween the two beams which are caused by a difference in the two optical
path lengths. Consider a coherent beam which is split and then recom-
bined on a viewing screen. A difference in optical path lengths of the
two beams may be achieved in two ways in order to create an interfero-
gram. The first is to make the physical distance traveled by the two
beams different. In a vacuum this path length difference is expressed
as $L = c_0 \Delta t$ where c_0 is the speed of light in a vacuum. The second
way is to maintain equal physical path lengths but to have the beams
traverse through different media prior to recombining. In this case
each light beam will travel at a speed $\frac{c_0}{n}$ where n is the index of re-
fraction for the medium traversed. The optical path length difference
then becomes:

$$\Delta L = L (n_2 - n_1) = c_0 \Delta t \tag{1}$$

The interference pattern or fringes observed may be expressed as a
function of the optical path length difference or

$$g = \frac{\Delta L}{\lambda} \tag{2}$$

where: g = fringe shift

λ = wave length of the light source

ΔL = change in optical path

Combining equations (1) and (2), the fringe shift is then

$$g = \frac{L}{\lambda}(n_2 - n_1) \tag{3}$$

The index of refraction is known to be a function of density. Since the speed of light is only slightly less in gases than in a vacuum, the index of refraction could be closely approximated by the series expansion [8]

$$n = 1 + \beta \frac{\rho}{\rho_s} \tag{4}$$

where

β = dimensionless constant related to the Gladstone-Dale

constant by $K = \frac{\beta}{\rho_s}$

ρ_s = reference density of 0° C, 760 mm. Hg.

The variation of with wavelength is small and has a value of 0.000292 for λ = 5893 angstroms.

Considering a fixed difference in the index of refraction between the two beams in Equation (3), then

$$g = \beta \frac{L}{\lambda}\left(\frac{\rho_2 - \rho_\infty}{\rho_s}\right) \tag{5}$$

If the density varies in a beam path, the net change in the optical path length will be the integrated effect along the beam path or

$$g = \frac{\beta}{\lambda \rho_s} \int_0^L (\rho - \rho_\infty)ds = Q \int_0^L f(x,y,z_c)ds \tag{6}$$

where

$$Q = \frac{\beta \rho_\infty}{\lambda \rho_s} \tag{6a}$$

10

$$f(x, y, z_c) = \frac{\rho(x, y z_c)}{\rho_\infty} - 1 \tag{6b}$$

z_c = a plane of constant Z

ds = incremental distance along the ray

In order to determine the density along the beam path where the fringe shift is known from an interferogram, Equation (6) must be inverted.

B. THE INTEGRAL INVERSION

The integral inversion technique was first reported by C. D. Maldonado et al in 1965 [9, 10, 11]. R.D. Matulka [12, 13] and R. C. Jagota [3, 4] used this method to determine the density variation in an asymmetric free jet and about a cone at angle of attack, respectively. The technique involves representing the function, $f(x,y,z_c)$ in Equation (6) by a complete set of orthogonal functions where the unknown coefficients are evaluated using the orthogonality relationship between the set of functions. The functions are orthogonal over the entire plane and also have the propery of being invariant in form to any rotation of the coordinate system. Figure 8 illustrates the coordinate system for the inversion where x and y are the fixed laboratory coordinates and x' and y' are the coordinates in which the fringe number function is defined. As the view through the test section is varied the primed coordinates are rotated with respect to the fixed coordinates x and y.

The fringe shift expressed in Equation (6) may be written as the transform

$$g(\xi, y, z_c) = f(x, y, z_c) \tag{7}$$

11

or, inverting the equation, the density function, f, is equal to:

$$f(x, y, z_c) = T^{-1} g(\xi, y, z_c) \tag{8}$$

The density function can be expanded in the following manner using a set of polynomial functions, $U_{m+2k}^{\pm m}(\alpha x, \alpha y)$, and unknown comples coefficients, $C_{m+2k}^{\pm m}(\alpha)$

$$f(x,y,z_c) = \sum_{m=0}^{\infty} \sum_{k=0}^{\infty} \epsilon_m \left[C_{m+2k}^{m}(\alpha) U_{m+2k}^{m}(\alpha x, \alpha y) + C_{m+2k}^{-m}(\alpha) U_{m+2k}^{-m}(\alpha x, \alpha y) \right] \cdot e^{-(\alpha^2 x^2 + \alpha^2 y^2)} \tag{9}$$

where

$$\epsilon_m = \begin{cases} \frac{1}{2} & m=0 \\ 1 & m=1,2,3,\cdots \end{cases}$$

$$\alpha = \text{arbitrary scale factor}$$

The polynomial functions, $U_{m+2k}^{\pm m}(\alpha x, \alpha y)$, are invariant in form to a rotation of the coordinate system $[10, 12, 13]$. They also have a Gauss transform which makes them adaptable to the physical situation and to manipulating into the form of Equation (7). The functions are defined as:

$$U_{m+2k}^{\pm m}(\alpha x, \alpha y) = (-1)^k \alpha \left[\frac{k! (\alpha^2 x^2 + \alpha^2 y^2)^m}{\pi (m+k)!} \right]^{\frac{1}{2}} e^{\pm im\phi} L_k^m (\alpha^2 x^2 + \alpha^2 y^2) \tag{10}$$

where

$$\phi = \tan^{-1}\left(\frac{y}{x}\right) - \frac{\pi}{2} \tag{10a}$$

$$L_k^m = \text{Laguerre polynomial}$$

$$= \sum_{s=0}^{k} \left[\frac{(m+k)!}{(k-s)!(m-s)!s!} \right] \left[(-1)(\alpha^2 x^2 + \alpha^2 y^2) \right]^s \tag{10b}$$

And the Gauss Transform of $U_{m+2k}^{\pm m}$ is:

$$I_{m+2k}^{\pm m}(\alpha y; \xi) = \int_{-\infty}^{\infty} U_{m+2k}^{\pm m}(\alpha x, \alpha y) e^{-\alpha^2 x'^2} dx' = \frac{e^{\pm im\xi} H_{m+2k}(\alpha y')}{\left[k! (m+k)! \right]^{\frac{1}{2}} 2^{m+2k}} \tag{11}$$

where $H_{m+2k}(\alpha y') = $ Hermite polynomials

By applying the transform above to Equation (9), the fringe function in

Equation (7) can be written as:

$$g(\xi, y, z_c) = \sum_{m=0}^{\infty} \sum_{k=0}^{\infty} \frac{\epsilon_m [C_{m+2k}^m(\alpha) e^{im\xi} + C_{m+2k}^{-m}(\alpha) e^{-im\xi}] H_{m+2k}(\alpha) e^{-\alpha^2 y'^2}}{[k!(m+k)! \, 2^{2(m+k)}]^{1/2}} \quad (12)$$

using the following orthogonality relationship on Equation (12)

$$\int_{-\pi}^{\pi} e^{\pm im\xi} e^{\mp in\xi} d\xi \int_{-\infty}^{\infty} H_{m+2k}(\alpha y') H_{n+2\ell}(\alpha y') e^{-\alpha^2 y^2} dy' =$$

$$\frac{2\pi^{3/2}}{\alpha} \left[(m+2k)!(n+2\ell)! \, 2^{m+2k} 2^{n+2\ell} \, \delta_{mn} \delta_{(m+2k)(n+2\ell)} \right] \quad (13)$$

where δ is the kroneker delta, the expansion coefficients $C_{m+2k}^{\pm m}$, can be determined by:

$$C_{m+2k}^{\pm m}(\alpha) = \frac{\alpha}{2\pi^{3/2}} \left[\frac{(k!(m+k)!)^{1/2}}{(m+2k)!} \right] \int_{-\pi}^{\pi} g(y', \xi, z_c) H_{m+2k}(\alpha y') e^{\mp im\xi} dy' d\xi \quad (14)$$

Substitution of the coefficients in Equation (14) bact into Equation (9) results in the density variation being expressed as:

$$f(x, y, z_c) = \left(\frac{\alpha}{\pi}\right)^2 \sum_{m=0}^{\infty} \sum_{k=0}^{\infty} \epsilon_m [k!(m+k)!]^{1/2} e^{-(\alpha^2 x^2 + \alpha^2 y^2)} \cdot$$

$$\text{REAL} \left[\int_{-\pi}^{\pi} \int_{-\infty}^{\infty} g(y', \xi, z_c) e^{-im\xi} H_{m+2k}(\alpha y') dy' d\xi \right] U_{m+2k}^m(\alpha x, \alpha y) \quad (15)$$

or by inserting Equation (10):

$$f(x, y, z_c) = \left(\frac{\alpha}{\pi}\right)^2 \sum_{m=0}^{\infty} \sum_{k=0}^{\infty} \epsilon_m \frac{(-1)^k k!}{(m+2k)!} (\alpha^2 x^2 + \alpha^2 y^2)^{m/2} L_k^m (\alpha^2 x^2 + \alpha^2 y^2) \cdot$$

$$\left[B_{m+2k}^m(\alpha) \cos(m\phi) + D_{m+2k}^m(\alpha) \sin(m\phi) \right] e^{-(\alpha^2 x^2 + \alpha^2 y^2)} \quad (16)$$

where:

$$B_{m+2k}^m(\alpha) = \int_{-\pi}^{\pi} \int_{-\infty}^{\infty} g(y', \xi, z_c) \cos(m\xi) H_{m+2k}(\alpha y') dy' d\xi \quad (17)$$

$$D_{m+2k}^m(\alpha) = \int_{-\pi}^{\pi} \int_{-\infty}^{\infty} g(y', \xi, z_c) \sin(m\xi) H_{m+2k}(\alpha y') dy' d\xi \quad (18)$$

13

Equations (16), (17), and (18) are the basic equations used to calculate the density distribution from the experimentally determined fringe variations.

C. THE NUMERICAL PROCEDURE

The form of the density distribution in Equations (16), (17), and (18) must be modified in order to input the experimentally determined fringe distribution. First from Figure 8 and Equation (6b) it can be seen that it is only necessary to integrate Equations (17) and (18) over an area where the density is changing from a known density, ρ_∞. Outside of this region where there is no change in density, the function $f(x, y, z_0) = 0$, i.e. outside the test section. Also since the fringe distribution is taken in small increments over the test area the coefficients, B and D, can be approximated as

$$B^m_{m+2k}(\alpha) = \sum_{i=1}^{I-1} \sum_{j=0}^{J-1} g(\xi_j + \Delta\xi_j, x_i + \Delta x_i) \int_{\xi_j}^{\xi_{j+1}} \cos(m\xi)\,d\xi \int_{x_i}^{x_{i+1}} H_{m+2k}(\alpha x)\,dx \quad (19)$$

$$D^m_{m+2k}(\alpha) = \sum_{i=1}^{I-1} \sum_{j=0}^{J-1} g(\xi_j + \Delta\xi_j, x_i + \Delta x_i) \int_{\xi_j}^{\xi_{j+1}} \sin(m\xi)\,d\xi \int_{x_i}^{x_{i+1}} H_{m+2k}(\alpha x)\,dx \quad (20)$$

The integral of ξ is easily determined and by using the derivative formula for Hermite polynomials the integral of x may be manipulated to yield

$$B^m_{m+2k}(\alpha) = \left[\frac{1}{2\alpha m}\, \frac{1}{(m+2k+1)} \right] \sum_{i=0}^{I-1} \sum_{j=0}^{J-1} g(\xi_j + \Delta\xi_j, x_i + \Delta x_i) \cdot$$

$$\left[\sin(m\xi_{j+1}) - \sin(m\xi_j) \right] \left[H_{m+2k+1}(\alpha x_{i+1}) - H_{m+2k+1}(\alpha x_i) \right] \quad (21)$$

$$D^m_{m+2k}(\alpha) = -\left[\frac{1}{2\alpha m(m+2k+1)} \right] \sum_{i=0}^{I-1} \sum_{j=0}^{J-1} g(\xi_j + \Delta\xi_j, x_i + \Delta x_i) \cdot \quad (22)$$

$$\left[\cos(m\xi_{j+1}) - \cos(m\xi_j) \right] \left[H_{m+2k+1}(\alpha x_{i+1}) - H_{m+2k+1}(\alpha x_i) \right]$$

In the computation of the density function from Equation (16), obtaining the infinite summations experimentally is not plausible or

possible. It has been demonstrated that by using a finite number of
terms and by adjusting the values of $\Delta \xi$, Δx and α, it is possible
to obtain the density distribution with very good accuracy [3, 4, 12,
13]. Equation (16) then becomes:

$$
\rho(x,y,z_c) = \left(\frac{\alpha}{\pi}\right)^2 \sum_{k=0}^{K} \sum_{m=0}^{M} \epsilon_m (-1)^K \left[\frac{k!}{(m+2k)!}\right] (\alpha^2 x^2 + \alpha^2 y^2) \cdot
$$

$$
L_k^m (\alpha^2 x^2 + \alpha^2 y^2) \left[B_{m+2k}^m(\alpha) \cos(m\phi) + D_{m+2k}^m(\alpha) \sin(m\phi) \right] \cdot
$$

$$
e^{-(\alpha^2 x^2 + \alpha^2 y^2)}
$$

(23)

IV. EXPERIMENTAL PROCEDURE

A. LABORATORY TECHNIQUES

The analysis of a free jet by Matulka [12, 13] illustrated how
holographic interferometry can be used to obtain a complete three dimen-
sional plot of the density within a moving transparent flow field.
Jagota [3, 4] in his study of a cone at angle of attack in supersonic
flow went one step further by introducing an opaque object into an
assumed steady state flow field and describing the density field three-
dimensionally.

This investigation has attempted to determine the three-dimensional
density field around a transparent object in a supersonic flow field by
passing a light beam through the object. Specifically the interest was
to describe the flow field existing in the junction of a fin-root inter-
section.

1. Model Considerations

In order to obtain uniform flow around the fin-root area, a model
of the form shown in Figure 9 was selected. The flat plate has a knife

edge and is intended to remain at zero degrees angle of attack so as

to establish the flow conditions illustrated. The fin edges were made

circular in order to approach flow conditions similar to those estab-

lished in Winkelmann's [26, 27] investigation. Plastic and metal strakes

were added on the model sides so as to maintain two-dimensional flow as

well as to add strength to the flat plate. In the first model constructed

(Figure 7(a)), maximum visibility of the plastic fin-flat plate center

section was achieved by bolting the leading edge and aft plate together

through the plastic center section. Due to model flexure, this design

was found to be unsuitable and the second model in Figures 7(b) and 7(c)

was constructed. The model was made from a single piece of stainless

steel. The model rigidity was satisfactory but unfortunately the strength-

ening borders around the plastic center section reduced the holographic

visibility somewhat.

Since the wind tunnel blocks were fixed, it was possible to make

multiple test runs with the same flow conditions over the model provided

supersonic flow had been established over the model.

2. Holographic Techniques

In order to obtain holographic interferograms it was necessary to

ensure that the optical path lengths of the scene and reference beams

remained approximately equal. Since the ruby laser is believed to have

a coherency length of approximately ten centimeters, the equality of

lengths is far less critical than in the classical Mach-Zehner inter-

ferometric approach. Consequently a string was used in the experiment

to trace the reference beam and then adjust the scene beam. This method

kept the two beam lengths within one centimeter of each other. Since the

scene beam traversed approximately 4.5 inches of plastic tunnel walls and

grids which the reference beam did not, it was necessary to compensate by making the scene beam physically 2.25 inches shorter than the reference beam. The reference beam varied in length from 61 inches to 68 inches during the experimentation.

To determine the fringe/density field, finite fringe interferograms were made by three different techniques. In the direct fin-root flow approach the diffuser plate was part of the model. Either the mirror, M_5, in Figure 2 or the hologram plate holder was translated between the no-flow exposure and the flow-established exposure. In the total model flow method the diffuser plate was located between scene beam lens, L_3, and the test section (See Figure 2) and it was translated horizontally or vertically. Translations were varied from .001 inches to .006 inches with the translation distance of .003 inches yielding the best fringe separation.

Most of the holograms taken using basically the holographic arrangement shown in Figure 2 gave well-defined fringe patterns. In order to improve upon the fringe definition, a variety of techniques was attempted. The transverse mode selector was varied from 1.0 mm. to 2.5 mm. in increments of 0.5 mm. to determine the best lighting of the model. The hologram plate holder was rotated horizontally to various positions. These positions varied between being perpendicular to the scene beam to being perpendicular to the bisection of the angle between the scene and reference beams. Polarization plates were added in both the scene and reference beams between the test section and hologram plate in the scene beam and between the last mirror, M_4, and the hologram plate in the reference beam. A one-quarter wave plate was also placed between the first lens, L_1, and the beam splitter as recommended by Okayama and Emori [14].

17

The holograms were taken using 4" x 5" Agfa-Gavaert 8E-75 holo-
gram plates. The developing process involved:

1. Five minutes in Kodak D-19 developer

2. Thirty seconds in an acetic acid stop bath

3. Five minutes in standard fixer

4. Five minutes in a flowing water bath

5. One minute emersion in Kodak Photo Flo wetting agent

6. Drying using blowing cool air

a. Direct Fin-Root Flow Method

Since the flow field in the fin-root junction is assumed to
be identical on either side of the fin, then it is only necessary to
determine the density on one side of the fin. To accomplish this it is
necessary to obtain holograms for 180° of view as shown in Figure 10.
The holograms for the views from 0° to 90° can be obtained by using a
frosted fin and flat plate as shown in Figure 11. The advantage of
having the frosted plate as part of the model is that the fringe/density
information obtained by the interferogram is believed to be only for the
area between the fin-root intersection to the tunnel wall vice the whole
test section, but this was not verified. In order to obtain the fringe
information for angles greater than 90° but less than 180° the fin
would be exchanged for one containing a stainless steel reflective sur-
face. The scene beam would then enter the test area from the viewing
port below the tunnel and be reflected to the hologram plate as shown
in Figure 12.

b. Total Model Flow Method

In this method the diffuser plate was located in the scene
beam outside the test section as shown in Figure 14 and the flat plate

18

center section and fin were made of optically clear plexiglas. By
translating the diffuser plate between exposures of the hologram, an
interferogram of the whole density field in the test section about the
model was obtained. From Figure 13 it can be seen that due to symmetry
only 90° of view was required to obtain the density field. This makes
it much easier experimentally to take the holograms than the previous
method described.

3. Schlieren Analysis

A standard Schlieren knife-edge system was used to verify the
establishment of the supersonic flow network around the model as shown
in Figure 9. Photographs were also taken of the flow with the model at
0° and 90° rotation in order to compare the fin shock conditions with
those obtained by Winkelmann [26, 27].

B. PHOTOGRAPHIC TECHNIQUES

By illuminating the holograms with a helium-neon laser beam which
has a wave length of 6328 Angstroms, the original scene was reconstructed.
Since the original scene beam and the reconstructed beam were of different
wave lengths, there is actually a small distortion in the reconstructed
scene but of neglectable effect because the hologram plate emulsion in
the development process also shrinks.

The typical method for reconstructing the scene is to illuminate the
hologram as illustrated in Figure 15. The diffuse glass used in the con-
struction of the hologram appears to act as an infinite light source of
non-parallel rays which illuminates the scene. If a small aperture is
positioned at the focal plane of the imaging lense, an almost parallel
set of rays may then be selected as shown in Figure 16. A third method

19

illustrated in Figure 17 uses a small diameter conjugate beam to illu-
minate the hologram. A large depth of field is achieved because the
narrow beam acts as an aperture. This effect was of considerable ad-
vantage since it enabled both the front and rear grids, the model, and
the fringe patterns to be simultaneously projected on the screen. The
best photographs were obtained by focusing on the plane of the fringes.

C. DATA REDUCTION

Photographic interferograms were obtained by illuminating the holo-
gram scene with a thin laser beam and using a camera with a viewing screen
located in the film plane as shown in Figure 15. The line of sight in
the plane desired was achieved by translating the hologram until common
points on the front and rear grids were aligned. The camera, with the
aperture set wide open at 7.7, was then adjusted to give the best focus
on the fringe plane. The best photographic results were achieved by
using an exposure time of 1/10 second with Polaroid Type 55 P/N film.

It was felt that the density field could be well defined three-di-
mensionally along the fin if the density fields were determined in four
planes perpendicular to the Z-axis and equally spaced along the fin as
shown in Figure 18. In obtaining the fringe data across a constant Z-
plane it would be necessary to take six photographs per rotation angle,
aligned at appropriate intervals down the y' axis, and then graphically
mate the fringe data to form one complete set. The six photos across the
field were felt necessary because the optical path length from the model
to the hologram plate varied for those points not on the aligned plane.

The fringe shift reduction was accomplished using two different tech-
niques. The first was to project the negative, using a photo enlarger,

onto a sheet of paper and trace out the fringe pattern, model surfaces and grid lines. The light fringes were traced out since it was much easier to judge their center line. From the fringe lines forward of the fin in the region of uniform flow one fringe line which appeared the straightest and compatible with most others was selected as the bench mark. A straight line was then drawn over that fringe and extended past the aligned Z plane (i.e. y' axis). Lines parallel to the bench mark line were then drawn likewise over the remaining fringe lines. The fringe displacements were then read relative to the lines drawn at the points of intersection of the fringes with the y' axis. The radius of the inversion circle was selected so that the fin-root intersection was the origin and the fin tip was the 100 percent point.

In the second technique an enlarged positive photograph was made from the negative. Again one fringe line in the uniform flow region just forward of the fin which appeared to be parallel with the majority of the fringes was selected as the bench mark. The remaining fringes were likewise traced over with lines parallel to the first. The fringe displacements were then measured relative to the lines drawn. For further details see Appendix A.

The locations at which reference lines crossed the y' axis in both techniques above were further adjusted to account for the tunnel wall refraction displacement as shown in Figure 19 and computed by a computer program in Appendix B. Once these corrections were made, the radial variation of the fringe number could then be plotted for the various y' alignment planes and a smooth curve drawn through the data points. The fringe number at 201 equidistant points across the field can then be obtained for input into the computer program, HOLOFER, in MODE 3. For

21

further details on how to use the computer program, HOLOFER, see Appendix C. Once the data from all the rotation angles of the model have been put into the computer program, the program will then calculate the density field across the inversion circle for that Z-plane. After the density has been calculated for all four Z-planes in Figure 18, a three-dimensional plot of the density field can be made by connecting points of equal density across the fin.

V. EXPERIMENTAL RESULTS AND DISCUSSION

The initial attempts to establish uniform flow over the flat plate shown in Figure 7(a) were unsuccessful due to model vibration and flexure. Movement of the model sting within its holder and flexure of the model plastic center section allowed the model leading edge to establish a little over 1° angle of attack upward when flow was established. Due to various modifications made in attempts to eliminate the vibration, the sting finally fractured.

In an attempt to eliminate these problems, the second model shown in Figures 7(b) and 7(c) was made of a single piece of stainless steel and the sting was mated to its holder to within .001 inches. The model center section was made of poured epoxy and the strakes were both made of stainless steel with plexiglas inserts. The model rotation about the sting was reduced to approximately 0.3° angle of attack upward. Due to the vibration in passing through the transonic range and a weak glue seal between the metal strakes and plexiglas inserts, the inserts were found to break loose. They were subsequently removed and not replaced.

In order to determine the flow field using the direct fin-root approach, the epoxy fin and model center section were frosted on one side using fine

emery paper (see Figure 20). Holograms were taken of the model at rotation angles of 0°, 12°, 45° and 90° using the holographic arrangement in Figure 2 excluding the diffuser plate between lens, L_3, and the test section. The mirror, M_5, was translated in various directions from towards to parallel to the test section between the exposures without flow and with flow established. Fringe patterns were obtained around the model, but only at 0° and 12° rotation could any fringe patterns be observed across the fin. It was found that the fin fringe pattern appeared to remain almost unchanged no matter how or how much the mirror, M_5, was translated while the fringe around the model changed appropriately. For instance, in Figure 21 the mirror was not translated and in Figure 22 the mirror was translated .006 inches horizontally parallel to the tunnel.

Since fringes could not be observed across the flat plate at 45° and 90°, it was felt that the epoxy center section might be too imperfect optically. Consequently double-exposed holograms were taken with no flow through the test section and various translation distances from 0 to .005 inches. The fringe patterns were excellent across the whole model and their spacing decreased according to the increase in the translation of M_5. Next the diffuser plate in the scene beam in Figure 2 was inserted with the model at 0° rotation angle and translated between no flow and flow exposures of the hologram. The fringes about the model were of excellent quality but the double diffusion of the scene beam through the model caused all fringe patterns on the model (fin) to disappear.

It was felt at this point that the fringe pattern obtained across the fin was caused by the movement of the model to an angle of attack and possibly by model vibration, although none was observed visually. The

lack of any fringes across the flat plate center section is not well understood but is believed to be caused by vibration of the model.

Since it was not possible to obtain acceptable interferograms with the diffuser plate as part of the model due to model motion, it was felt that the effect of minor model movements could be eliminated by using an optically clear model and an external translating diffuser plate. Therefore the fin and model center sections were replaced with optically clear plexiglas. With these changes it was found that the flat-plate leading-edge angle of attack had been reduced to approximately 0.1^o.

Initially double-exposure holograms were taken using the arrangement in Figure 2 and translating the diffuser horizontally. At 0° model rotation the holographic interferograms were excellent. But as observed in Figure 23 it would be extremely difficult to determine the fringe change across the fin since no free stream reference fringes were available, due to the flat plate leading edge Prandtl-Meyer expansion and fin shock intersecting the tunnel top just above the fin. With a larger tunnel or smaller model this would be an excellent technique.

The diffuser plate was then translated vertically between exposures and excellent horizontal fringe patterns were obtained as shown in Figure 24. The model was then rotated to $22\frac{1}{2}^o$ and the same holographic technique was used. Excellent fringe patterns were obtained above and below the flat plate center section. Fringe patterns across the flat plate center section and fin in this area were very light and usable interferograms could not be photographed with the polaroid camera. In an attempt to improve on the fringe quality, polarizer plates were inserted in the reference beam between the mirror, M_4, and the hologram plate and in the scene beam between the lens, L_3, and the diffuser plate in order to ensure

polarization of both beams. No significant improvement could be noticed and they were subsequently removed. A one-quarter wave polarizer plate was then placed between the lens, L_1 and the beam splitter in order to utilize circularly polarized light for the reference and scene beams. Okayama and Emori [14] found that their image resolution improved considerably; however, with this particular arrangement little to no improvement in the fringe resolution was observed and the approach was abandoned.

The transverse mode selector was then varied from 2.0 mm. to 1.5 mm. and later to 1.0 mm. in an effort to improve the coherency length of the laser light and consequently the image resolution. Due to the decrease in output light intensity, up to six exposures were taken during a run with flow established. Image and fringe definition were not found to increase possibly due to model vibration which was not visible to the eye.

The model was rotated to 45° and $67\frac{1}{2}^\circ$ and double exposure holograms were taken with a 2.5 mm. transverse mode selector. There were no observable fringe patterns in any portion of the test section. Consequently it was believed that supersonic flow was not established due to tunnel blockage caused by the shock wave from the model and by slight model vibrations in passing through the transonic range. In the transition to supersonic flow, the model leading edge would sometimes flex as much as 0.2° depending upon the transition time.

The test section walls were changed from the total plexiglas side walls shown in Figure 1(a) to the aluminum walls with the optical quality glass port holes (Figure 1(b)). The better quality glass would hopefully improve the viewing and the port holes made the model much more accessible. The metal strakes were also removed from the model since they appeared to have a minimal effect on the flow, were an interference optically,

25

and appeared to add very little structurally. Flow tests were run and the model was found to attain an angle of attack of about 0.14° upward when flow was established at Mach 2.84. The angle of attack was tolerable, however the model also maintained a visible high frequency vibration of about ± 0.05°. Double exposure holograms were taken with the model at 0° rotation and fringes could only be observed forward of the Prandtl-Meyer expansion on the top of the model and forward of the flat plate leading edge shock on the bottom. The tunnel seals were found to leak and were replaced and resealed. The same angle of attack and high frequency model vibration still persisted. Double exposure holograms were again taken and a very faint fringe pattern was observed across the model. In reproducing the scene when aligned along a constant Z-plane passing through the fin, it was impossible to photograph the fringe pattern across the fin because of a bad speckle effect. Double exposure holograms were made at model rotation angles of 45° and 90° without and with flow. The holograms taken without flow gave excellent fringe patterns across the model however no fringes could be observed with flow.

At this point a knife edge Schlieren system was set up to determine just what the flow conditions were in the tunnel and around the model. The first runs were made at a model rotation angle of 90° and presented the shock knee in front of the fin (Figures 25(a) and 25 (b)) which was pointed out by Thomas [23, 24] and Winkelman [26, 27]. Due to the model vibration, the shock extending out from the shock knee was observed to flutter about $\pm\frac{1}{2}$ cm.

The model was then rotated back to 0° and Schlieren photographs were taken as shown in Figure 26. During all but one of the runs at this rotation angle, the model would pitch up approximately 0.14° angle of attack and continue to vibrate about ± 0.05° at a high frequency when

26

flow was established. The plate leading edge shock and fin shock appeared quite fuzzy and light. Due to oil from the tunnel supply reservoir mixing in the flow, a light oil smear pattern can be observed across the fin in Figure 26. During one run, which could not be duplicated, the model pitched up as flow was established but did not vibrate. The plate shock and Prandtl-Meyer waves, fin shock system, and tunnel Mach lines became very distinct and well defined as seen in Figure 27. The schematic of the Schlieren photographs in Figure 28 points out the cause for the various flow lines observed. The non-uniformity of the free stream caused by tunnel leakage can be easily seen. Consequently the experimental work was discontinued due to tunnel conditions and time considerations.

It was felt at this point that if the holographic interferogram taken of the clear plexiglas fin at 0° rotation angle could be reduced to useful data for the computer program then the holographic method would be to a certain extent verified even though the actual density field could not yet be determined.

In obtaining interferograms from the hologram, the reconstruction technique shown in Figure 15 was used. The plane of constant Z across the model to be reduced was chosen to be the forward most vertical grid line crossing the fin. It should be pointed out that in order to simplify the hologram alignment process, all four reduction planes across the model should have been scribed on the exterior grids. The three photographic points across the Z plane on the y' axis were, for convenience, chosen to be where horizontal exterior grid lines crossed the y' axis on the fin. Five interferogram photographs were taken at points A, B, and C as shown in Figure 29. Photographs 2 and 5 were taken using a Kodak Wratten Gelatin Filter N.D. 2.0 placed in the reconstruction beam in order to reduce the

beam intensity and increase the fringe definition. These two photographs were also used to provide a check on the consistency of the reduction process.

All five negatives were blown up on the photo enlarger in the dark room and the plate, fin, grid lines and fringes were traced out on a sheet of white paper as shown in Figures 30-34. It was very difficult to trace the fringes in the region of the fin tip and fin root due to the photographic resolution and the fin tip shadow. Also fringes were not visible in the region of the fin leading edge shock. Consequently, connecting the fringe in front of the fin to the correct fringe on the fin was a best guess effort. Typical of the problem was that fringe lines in two of the drawings were initially improperly connected across the fin leading edge shock. After being checked against the photograph negatives, the fringes were reconnected and the data taken correlated well with the data from other drawings. The fringes in the fin root area were extremely light in some photographs which made it quite difficult to determine their centerline crossing the y' axis. Another point of difficulty was determing the location of the top and bottom of the fin. An error in drawing here will have an effect later when the fringe locations are normalized with respect to the fin height.

Enlarged positives were then made from the negatives as shown in Figures 35-39 to see if the data accuracy could be improved by eliminating the difficulties of tracing the fringes in the dark room. This method also made it possible usually to reassess the assumed path of the fringe lines at a later time if the data did no appear to correlate properly. The same problems of locating the fringe lines in the region of the fin tip and of connecting the fringe lines across the fin shock are readily apparent in the figures.

To obtain the fringe change across the fin one of the straightest fringes in the free stream region which paralleled the majority of other free stream fringes was selected. A straight line was drawn through its centerline and extended to cross the y' axis. The other free stream reference lines were then drawn parallel to the first and adjusted so as to best follow the centerline of the selected fringe. This method actually averages the free stream conditions and is only valid if the free stream is essentially uniform. Since it was not possible to obtain in the photographs the free stream fringe pattern forward of the leading edge Prandtl-Meyer expansion for the lower fin region, the fringe reference lines in photo enlargements were drawn over the fringes just prior to the fin shock. In order to adjust them to free stream conditions their location was moved downward a distance equal to 1.1 times the average fringe interval for that photograph. The figure 1.1 was observed in all the enlarged photographs to be the approximate fringe change across the Prandtl-Meyer expansion. In the drawings (Figures 30-34), fringe reference lines for the lower fringes (generally $y' \leqslant .8$) were initially aligned along the straightest portion of the fringe prior to intercepting the fin shock. By comparing the reference line location on the drawing with the fringe pattern in the photographic enlargements the reference line location and fringe change were adjusted by an appropriate portion or all of the 1.1 fringe change caused by the Prandtl-Meyer expansion. All of the reference lines were then corrected for the tunnel wall and grid plastic parrallax shown in Figure 19 and computed in Appendix B. The reference fringe locations were then normalized with respect to the wing height and the fringe numbers calculated by dividing the fringe change by the average fringe interval. For further details and calculations see Appendix A.

The data obtained for alignment points A and C by the two different reduction processes are plotted in Figures 40-43. The data obtained from the photo enlargements aligned at point C and shown in Figure 43 gave the best data agreement between two photographs. The worst data agreement was obtained from the reduction of the drawings aligned at the same point. The inconsistency in the data was probably caused by connecting the wrong fringe lines across the fin leading edge shock. The data fluctuations and discrepencies between the curves in the figures could have been caused by a number of things. It could have been caused, for instance, by not drawing the fringe reference line parallel to or exactly on the free stream fringe center line or slightly missing the fringe center as it crosses the y' axis or by misconnecting fringe lines across the fin shock as was illustrated in Figure 42. Fringe location errors could be caused by misdrawing the fin tip and root lines as was mentioned earlier. Another contributer would be measurement errors.

To analyze these sources for error, first consider that the typical fin size in the drawings and photo enlargements averaged about 2.5 inches high and 2.75 inches wide and that the fringe spacing averaged about 0.10 inches. All measurements were taken using a ruler graduated in 0.01 inches and readings were made to the nearest .005 inches. Since the average difference between the data points and curves ran around $\frac{1}{4}$ fringe, some figures were calculated to determine what measurement errors could produce this fringe error. It was found that an error of .025 inches in alignment of the fringe reference line with the free stream fringe center line and/or fringe center line crossing the y' axis could produce $\frac{1}{4}$ fringe error. This fringe error will also occur if the fringe reference line differs from the free stream center line by more than 1.4° when drawn 1 inch from the y' axis or by more than 0.36° when drawn 4 inches from the

y' axis. A difference of .01 inches in the average fringe interval

could also produce a $\frac{1}{4}$-fringe error; however, this is not too likely

since it is an average of fifteen to twenty-five intervals. By com-

paring the actual height-to-width ratio with those found in all the

drawings and photo enlargements it was found that average error was

around 2% or a distance of .02 on the y'-axis.

In order to compare the interferogram negative quality and the two

different reduction techniques, a plot of the data for each negative was

made as shown in Figures 44-48. Photographs 1 and 3 in Figures 44 and

46 gave the smoothest curves indicating the highest interferogram re-

solution. Photograph 5 (Figure 48) gave the worst dispersion indicating

poor interferogram resolution; yet looking at the enlargement in Figure

39, the fringe line contrast is very good. In comparing Figures 40-48

it appears that the reduction technique using the photographic enlarge-

ments gave the most consistent data. This technique also provides a

much easier and faster recheck on the proper tracing of fringe lines

because it is extremely difficult and tedious to duplicate the fringe

pattern to the same scale over the drawings using the photo-enlarger in

the dark room.

All the data obtained by either method for one alignment point were

then plotted in Figures 49 and 50 in order to observe the dispersion.

A fringe number dispersion of about 0.6 fringes was observed in the data

taken from the negatives aligned at point A and a dispersion of about

0.8 fringes for the data about point C. The dispersion is attributable

to the inaccuracies in the drawings, to the photographic quality of the

interferograms, and to the inaccuracies in correcting the lower fringe

reference lines to free stream conditions. The last point is based upon

the increased dispersion between the fin tip and fin root data.

Figures 51 and 52 show an integrated curve of the fringe change across the wing as determined by each reduction method. In constructing the curve, the data from the three aligned points was plotted so as to just overlap each other. These two curves were then compared in Figure 53. The maximum variation in the fringe number is about ½ a fringe but the variations in the location of the fringe maximums and minimums average about 0.1 inches on the fin. The location difference is probably due to improper drawing of the fringe reference lines compounded with not being able to measure the wing height accurately. Due to the inaccuracies introduced in tracing the negative and then reducing the data it is felt that the photo enlargement method is the more accurate reduction method.

With fringe data from only one field of view, the density field, obviously, could not be obtained. It was felt useful to consider the flow field axisymmetric in order to exercise the computer program and to provide a check on the program's ability to handle these particular curve shapes. Fringe data at 101 equidistant points across the fin from $0 \leqslant Y' \leqslant 1.0$ was obtained from Figure 53 for both curves and fed in HOLOFER in Mode 3 for the axisymmetric case. For further details on HOLOFER see Appendix C. The scale factor, α, in Equation 9 was then varied from 0.2 to 2.5 and a value to 1.0 was determined to yield the most accurate density solutions. This value was verified by feeding the function data, $(\rho/\rho_\infty -1)$, calculated by Mode 3 back into the program in Mode 1 and comparing the fringe data calculated with the original fringe data obtained from Figure 53.

The density distribution for both the drawing and photographic reduction cases is plotted in Figure 54. The density as Y' approaches zero actually goes as the drawn lines even though the points indicate a dip.

32

Matulka [12, 13] pointed out that the computer program accuracy does not converge at the origin. The large variations of the density curves at values of $Y' > 0.8$ are caused by the program trying to adapt to a step or shock wave type function at $Y' = 1.0$. If the remainder of the fringe data in Figure 53 for values of $Y' > 1.0$ had been included as input data the density curves would have smoothed out. This shock wave step function effect was demonstrated and analyzed by Matulka [12, 13].

The low values of density for the photographic data curve around $Y' = 0.38$ were unexpected but not surprising. First, the photographic fringe data curve is more extreme than the drawing fringe data curve and second, the density curves are not true values anyway since the field was considered axisymmetric and this is not the case in reality.

In general the density curves are felt to be reasonable under the assumed conditions. Consequently it is believed that the computer program could very easily and accurately handle a complete analysis of the flow field around the fin-flat plate.

In completing the analysis there are some data reduction problems which would have been encountered in reducing the interferograms at other model rotation angles which merit discussion. With no model rotation, adjusting the fringe reference lines close to the fin root to account for the leading edge Prandtl-Meyer expansion was relatively easy. However, when the model is rotated, the fringe shift across the Prandtl-Meyer expansion can no longer be considered a constant and it will be very difficult to adjust the fringe lines at lower values of Y' to free stream conditions. The best solution would be to increase the scene beam diameter and/or reduce the model size in order to photograph the free stream fringe lines forward of the plate leading edge. The free

stream lines could be connected to the appropriate fringe lines forward of the fin and this would eliminate the numerical correction and increase the fringe data accuracy.

Also at the rotated angles, fringe information will not be available for portions of the reduction plane due to shadows cast by the model sides as shown in Figure 55. In the lower portion of the hologram the fringe curve can be connected with a smooth line because the density field in that portion should be essentially constant. Care must be taken in completing the curve, though, since this information will be used in the integration of other rotation angles. The fringe curve in the upper portion must also be completed carefully but should be easier since the shadow will be smaller. For this particular model it was calculated that for angles greater than 46.6° the upper shadow would not penetrate the fin.

There are two more problems to be coped with which do not have apparent solutions at this time. The first has to do with the superimposing of fringe information from different locations onto one scene beam line as illustrated in Figure 56. In case I the superimposing of the fringe change in Region A onto that in Region C and locating the fringe reference line at point C' is tolerable because the density field in Region A should be fairly constant and uniform. However in case II where the fringe change in all three regions are superimposed and located at point C", the answer is not readily apparent. If the plate and fin were of equal thicknesses then points A" and C" would be the same and the error would be somewhat reduced. If, in addition, the thicknesses were made as thin as structurally possible, the error would be reduced to a minimum. Also it might be possible to integrate the model geometry into the computer program but this has not been attempted.

With the model at rotation angles between 0° and 90° scene beam defraction at the fin root and tip areas would also present problems as seen in Figure 57. A minimization of the problem could again be achieved by minimizing the fin and plate thicknesses.

VI. CONCLUSIONS AND RECOMMENDATIONS

The investigation, although not totally successful, has demonstrated the feasibility of using holographic interferometry to determine the flow field around a transparent model by looking through the model. The problems of model vibration and movement, of superimposing different fringe information on one beam, and of scene beam divergence through the fin root and tip regions must still be solved. The model vibrations and rotation to an angle of attack are attributable to the tunnel pressure fluctuations caused by tunnel leaks and to possible movement of the sting holder. It is felt that all three problems could be decreased to neglectable effects by reducing the overall model size and by incorporating the model geometry into the computer program.

The basic holographic arrangement was found to work quite well for this type of experiment. The holograms were generally high quality except when unfavorable tunnel flow conditions existed. The use of circularly polarized light recommended by Okayama and Emori [14] did not increase the hologram resolution appreciably but the method merits further considerations because of their excellent results.

The data reduction process was found to be the rate-controlling step in the investigation due to the time and labor involved. Reducing the data from enlarged photographs of the interferogram saved some time and appeared to increase the data accuracy. The data scatter of ± 1/8 fringe

was considered acceptable considering the fringe resolution in the holo-
grams. It was felt that this could be reduced by using either a larger
tunnel or a smaller model. With either of the changes it would be pos-
sible either to use the free stream fringe pattern forward of the model
as the reference conditions across the whole model or to use a vertical
fringe pattern, since the leading edge Prandtl-Meyer expansion and fin
shock would not block out the free stream fringes above the fin. It
appears that the use of vertical fringes would also considerably reduce
the data reduction time.

With the use of Schlieren the flow network described by both Thomas
[23, 24] and Winkelmann [26, 27] was verified to exist. From the top
view (90° model rotation) the fin shock and its fluctuations were ob-
served and photographed through the flat plate plastic center section.

The computer program, HOLOFER, was found to be quite capable of
handling the type of flow field fringe data which would be generated in
a complete analysis of this type. As pointed out before it is believed
that the program should be modified to incorporate the model geometry.
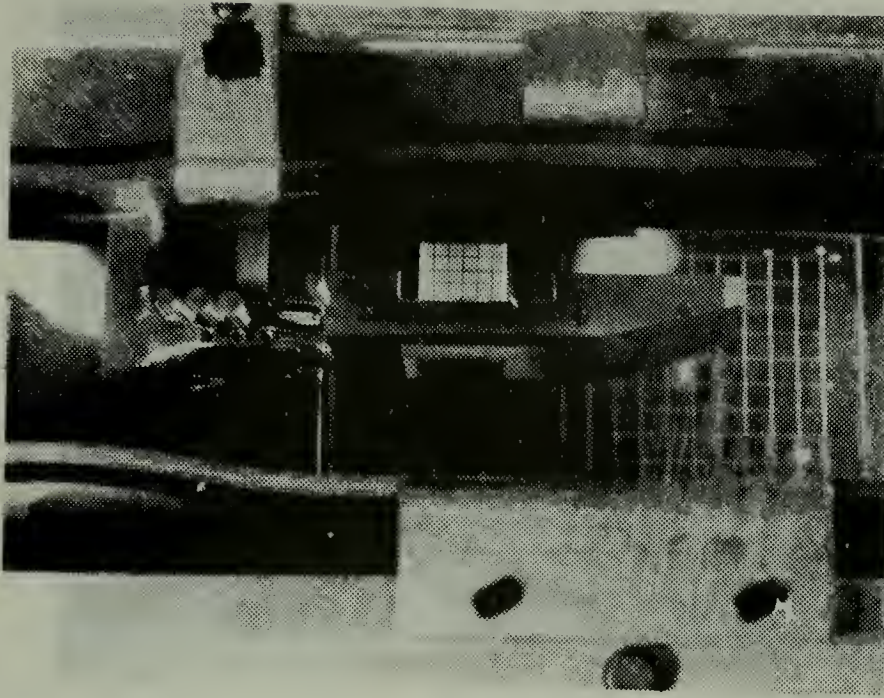
Figure 1(a). Wind Tunnel Test Section with Clear Plastic Side Walls
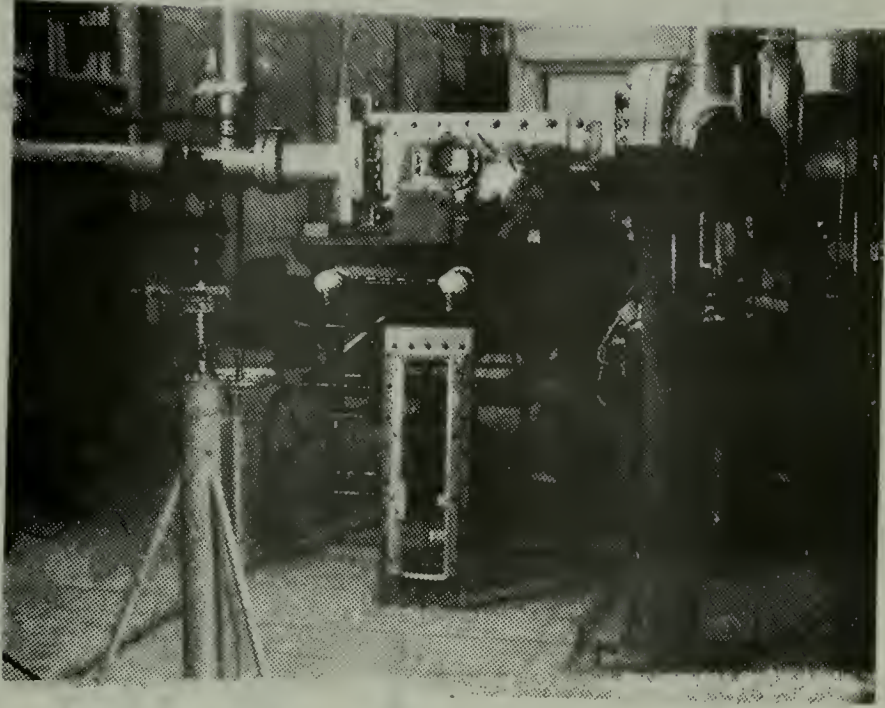
Figure 1(b). Wind Tunnel Test Section with Aluminum Side Walls
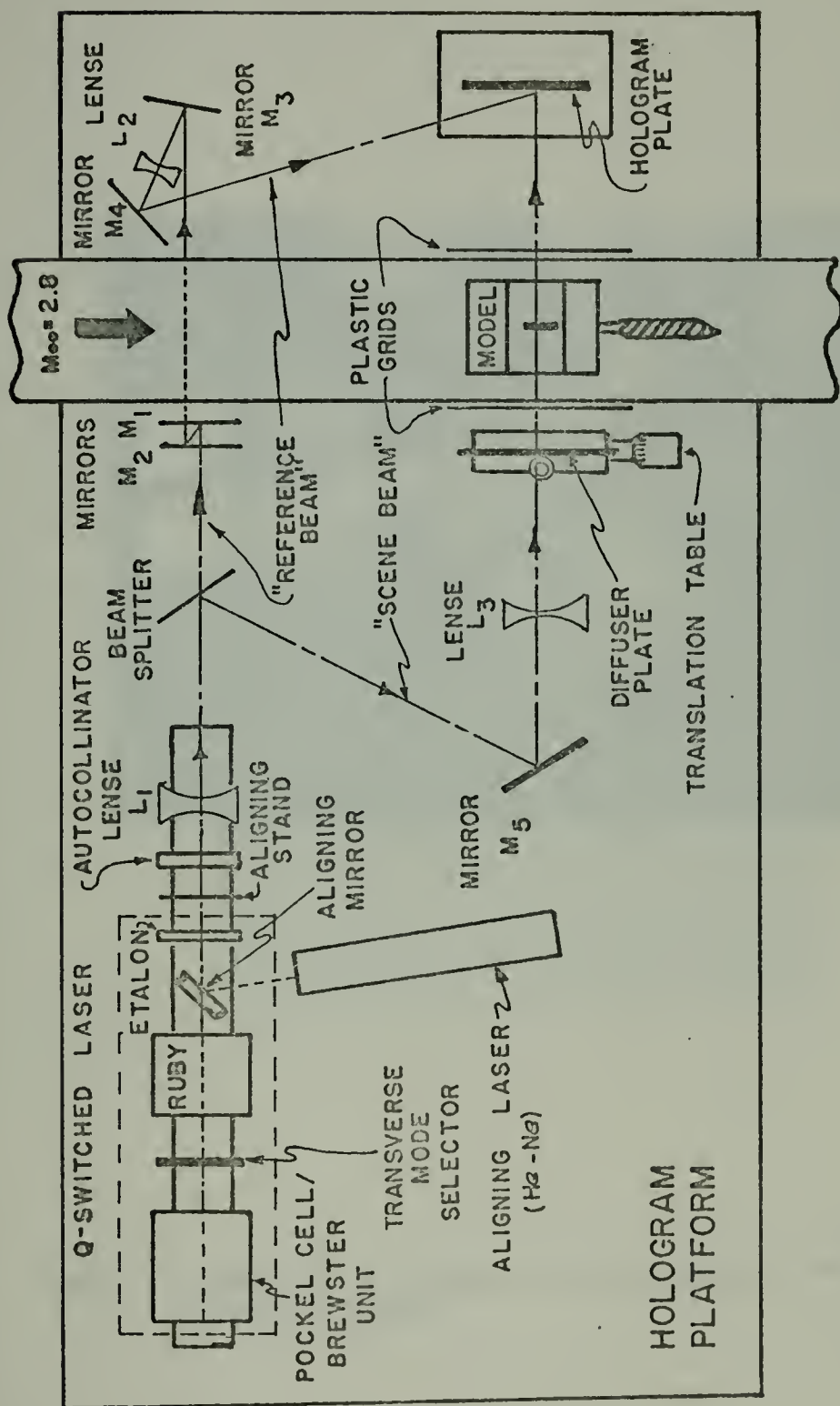
Figure 2. Schematic Representation of the Holographic Arrangement
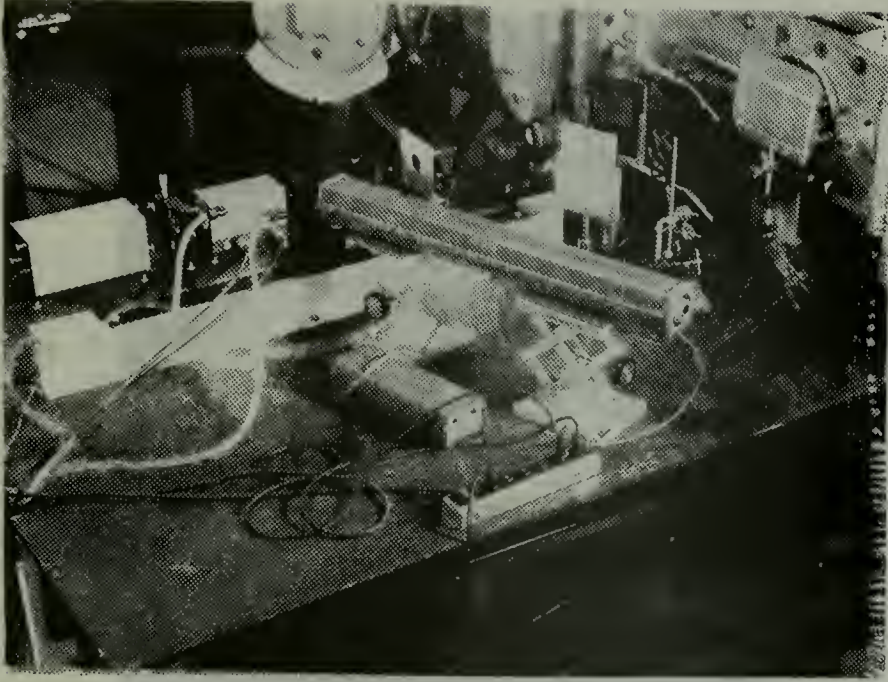
Figure 3. Holographic Arrangement Including the Laser Cooling and Aligning Equipment
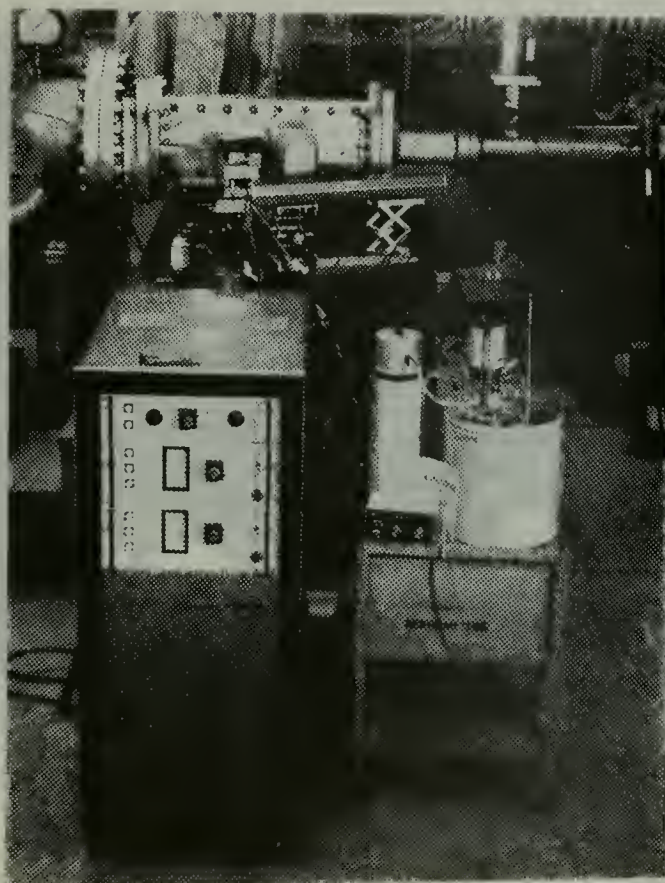
Figure 4. Ruby Laser Power Supply and Cooling Unit

Figure 5. Hologram Plate Holder and Mirrors on the Reverse Side
of the Wind Tunnel
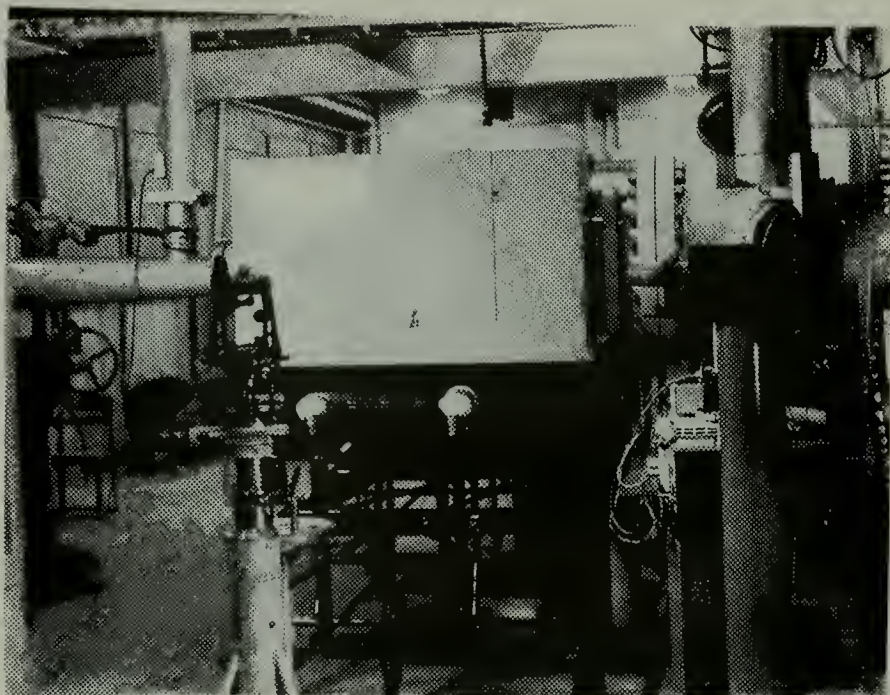
Figure 6.   Hologram Platform Box Cover for Daylight Photography

43
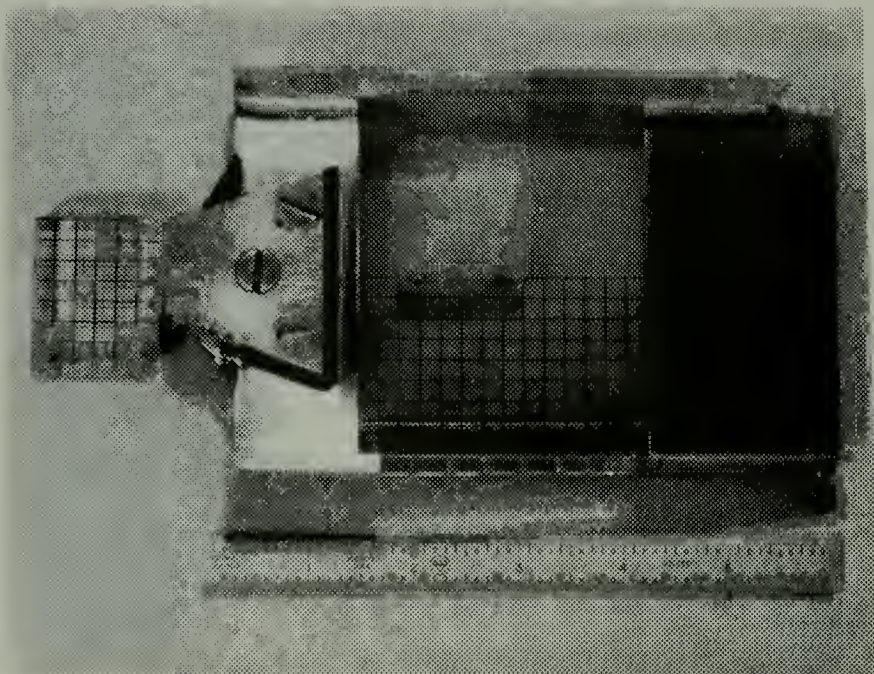
Figure 7(a). Initial Fin-Flat Plate Model Used in the Experiment
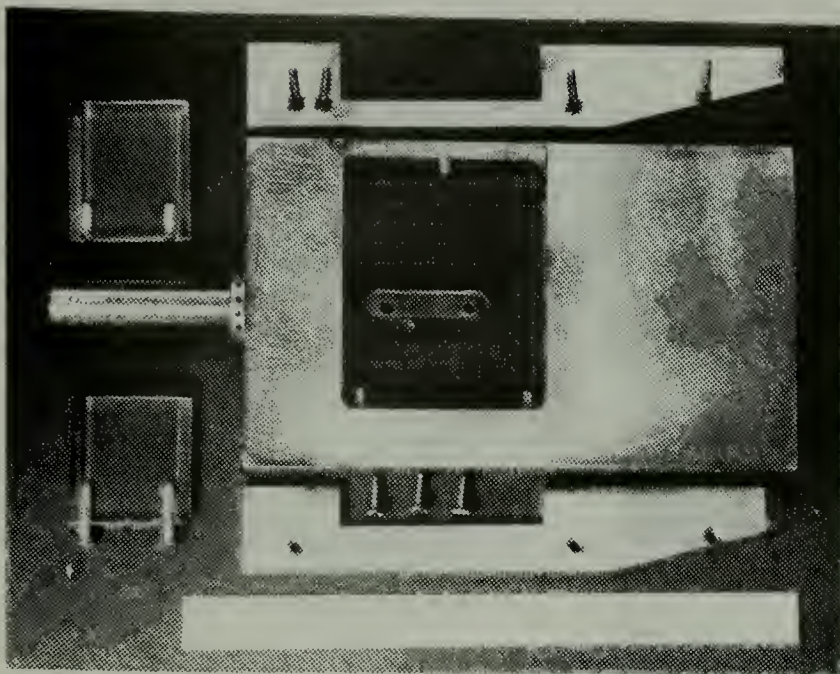
Figure 7(b). Second Fin-Flat Plate Model Used in the Experiment

COMMODE DI D. GIOVANNI DELL'ARCHITETTURA (XIII SECOLO)
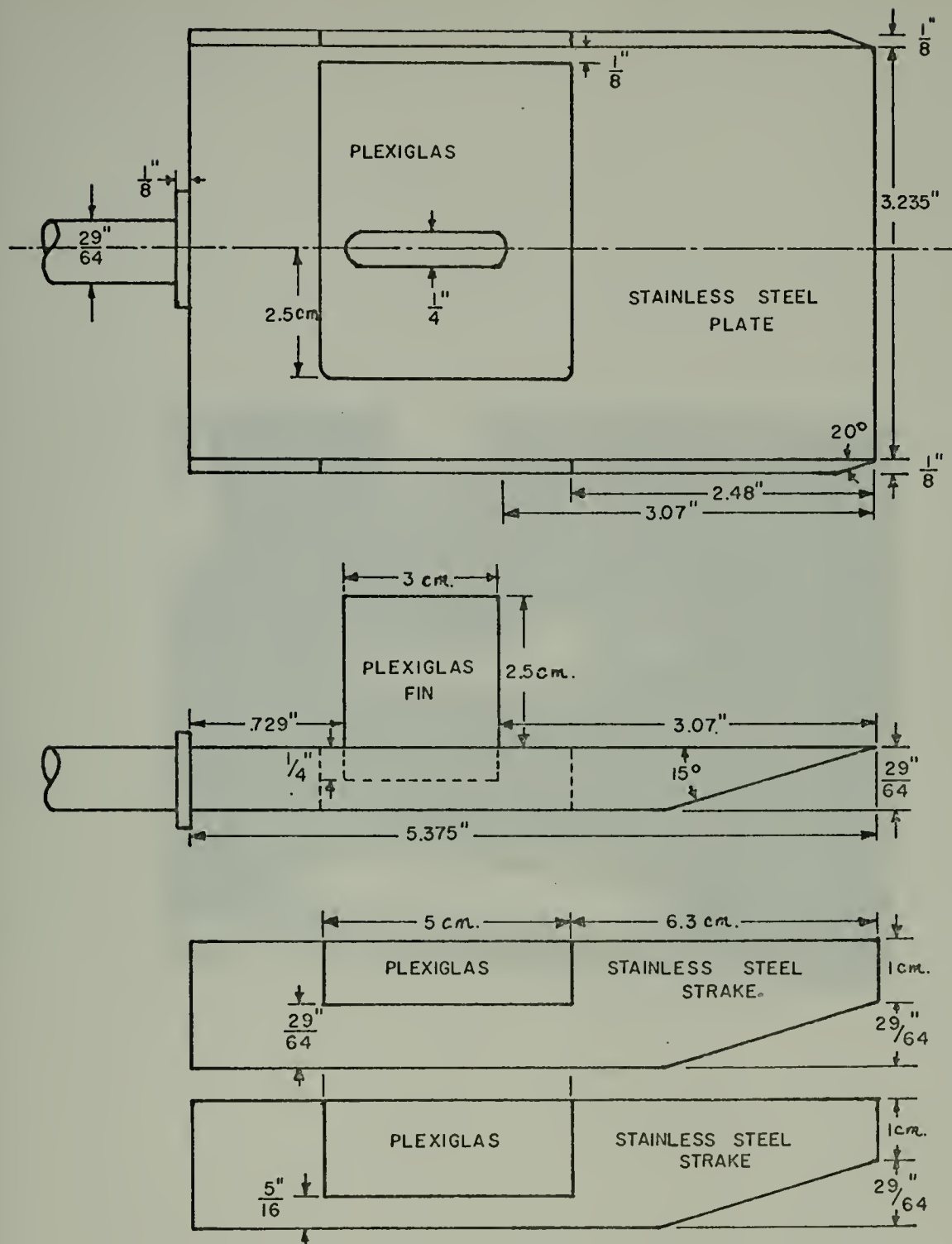
Figure 7(c). Details of the Second Fin-Flat Plate Model

46
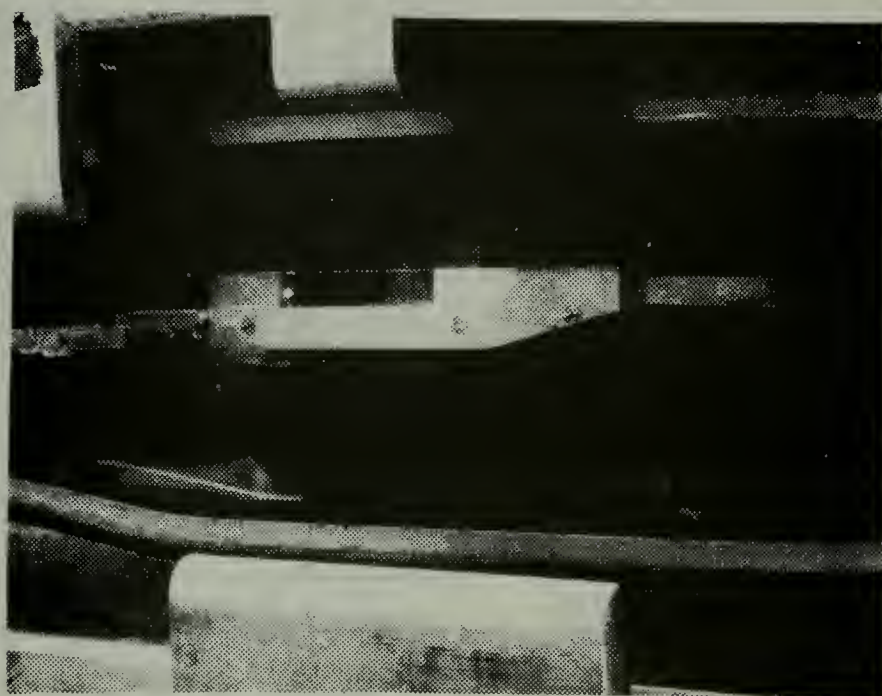
Figure 7(d). Model Mounting in the Wind Tunnel Test Section
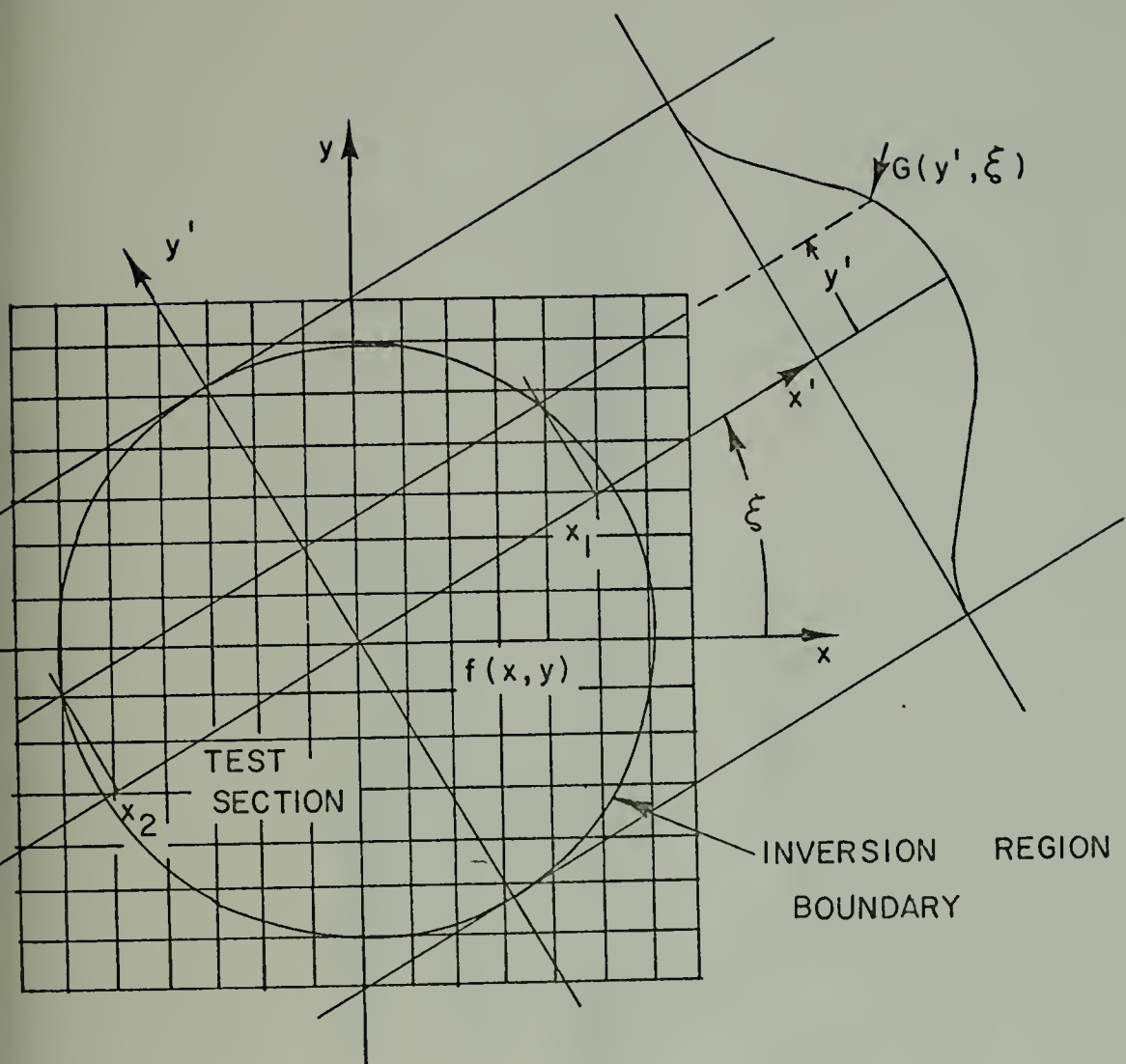
FIGURE 8. CO-ORDINATE SYSTEM USED FOR THE INVERSION OF FRINGE NUMBER TO DENSITY
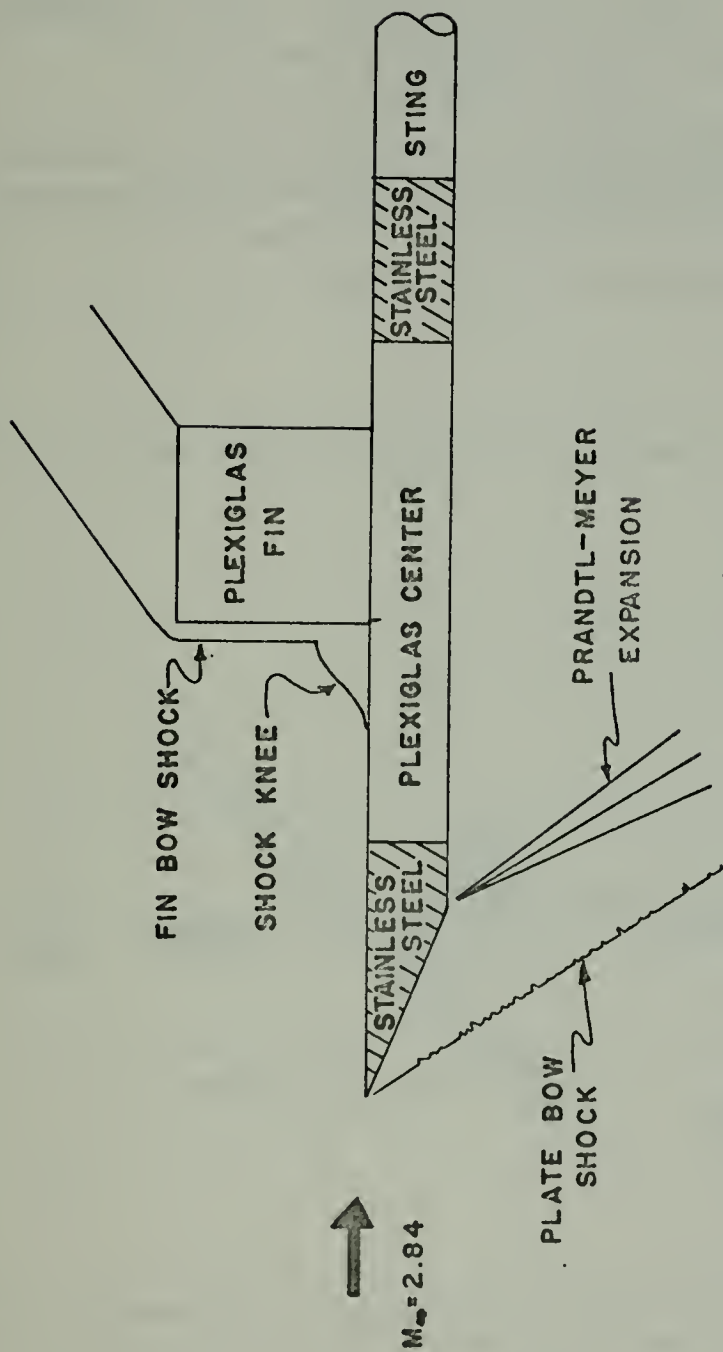
Figure 9. Schematic of the Desired Model Flow Network

49
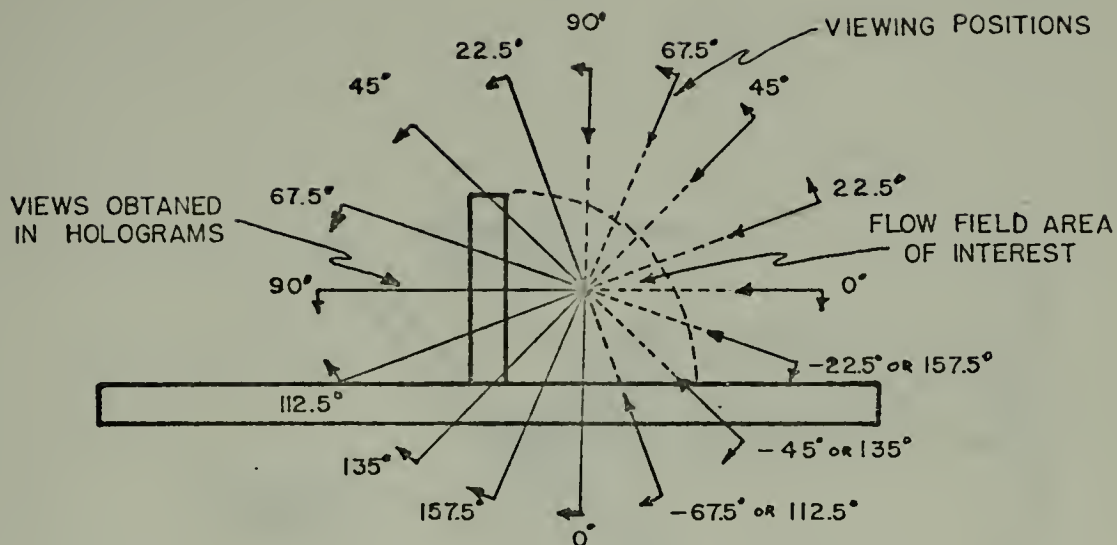
Figure 10. Desired Holographic Views in the Direct Fin-Root Method
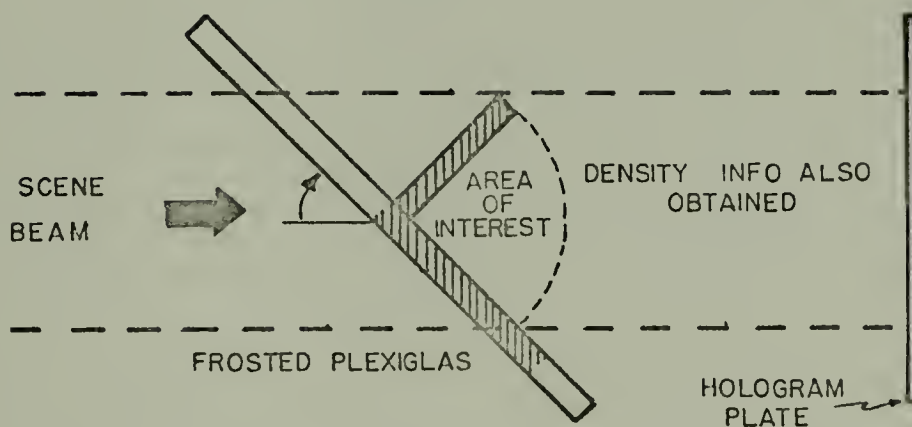
Figure 11. Schematic of the Model Used to Obtain Holographic Views Between 0° and 90° in the Direct Fin-Root Method
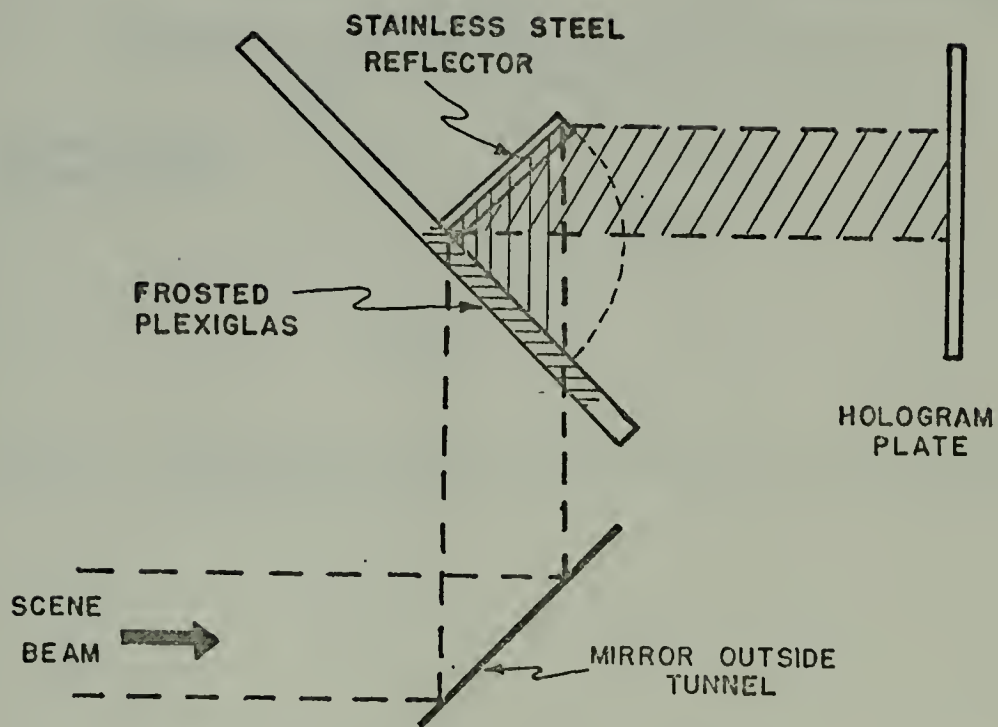
Figure 12. Schematic of the Model Used to Obtain Holographic Views Between 90° and 180° in the Direct Fin-Root Method

51
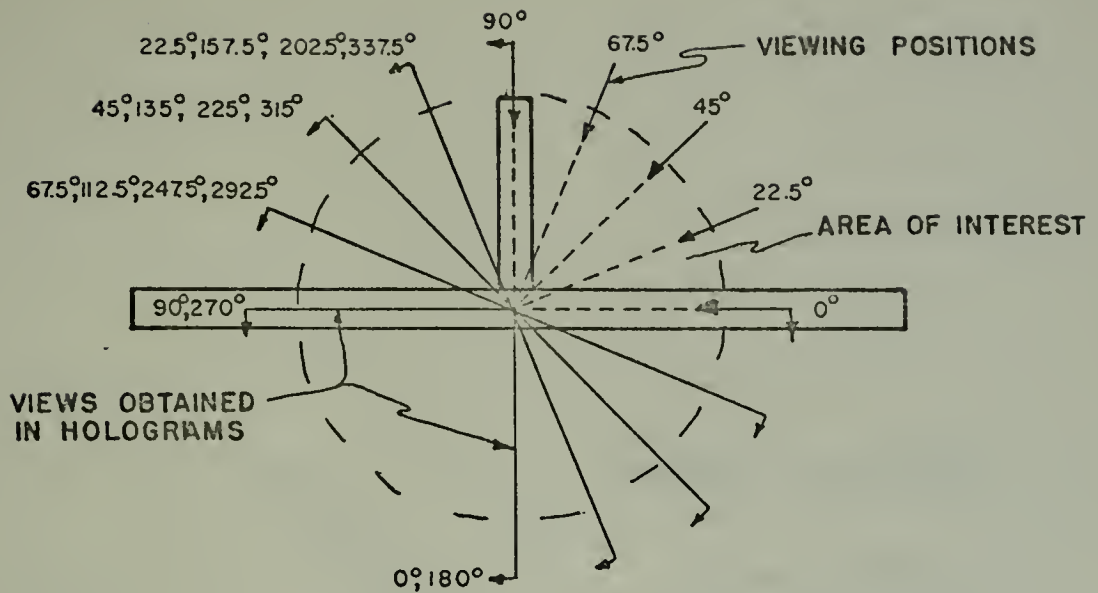
Figure 13.   Holographic Viewing Angles Required in the Total Model
Flow Method
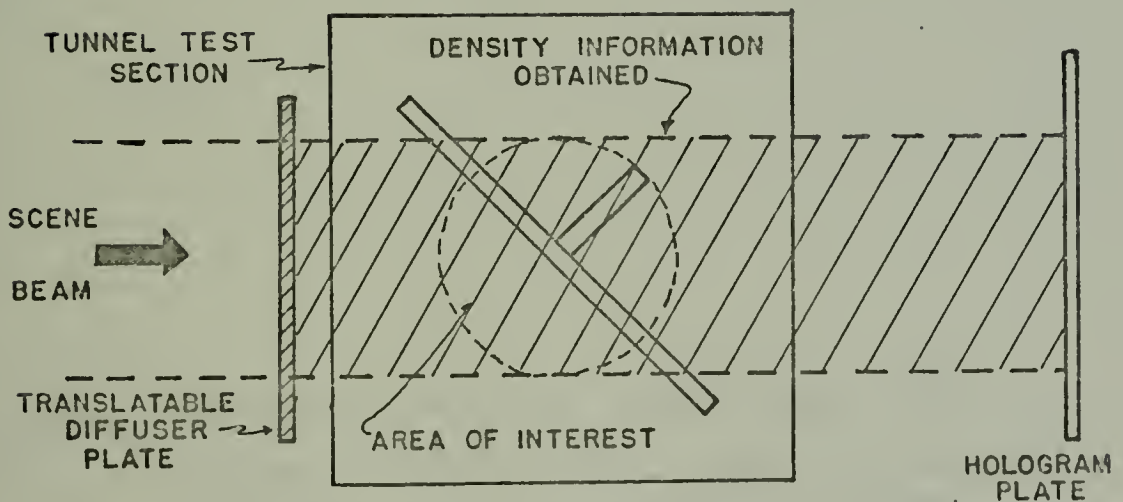
Figure 14.   Schematic of the Technique Used to Obtain Holograms in
the Total Model Flow Method
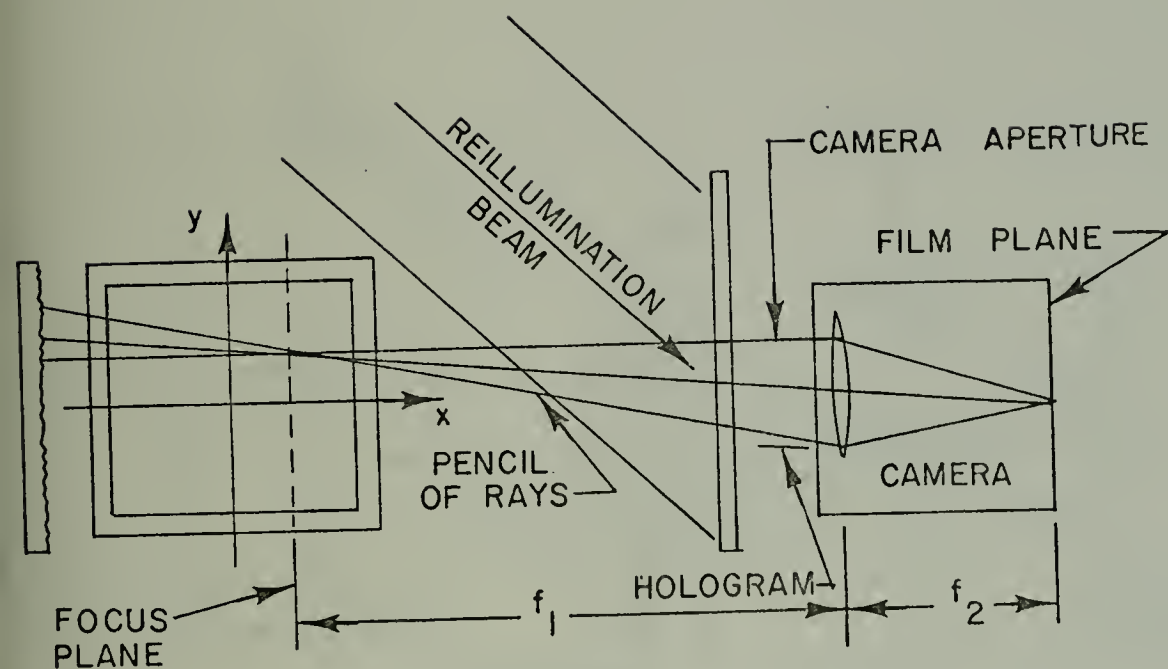
FIGURE I5. EFFECT OF APERTURE SIZE FOCUS PLANE
POSITION ON THE PENCIL SIZE OF RAYS ABOUT
A LINE OF SIGHT RECORDED BY CAMERA
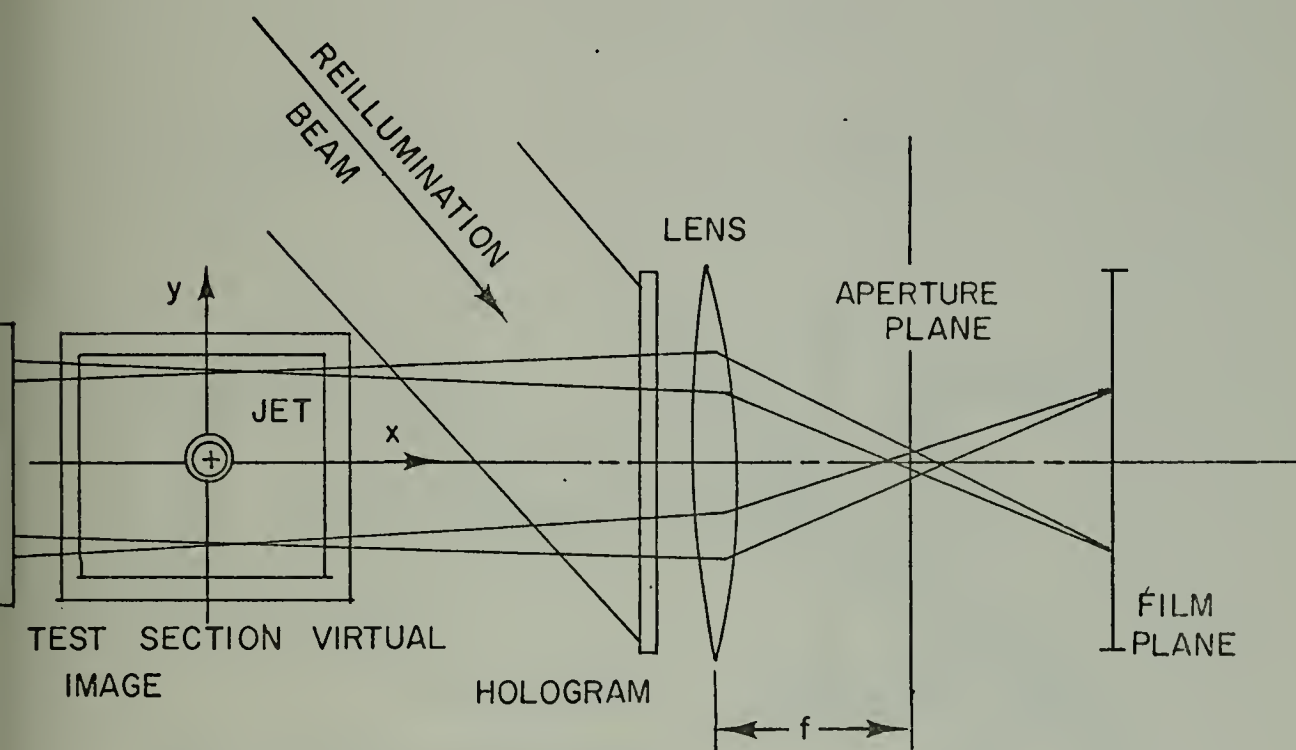
FIGURE 16. SPATIAL FILTERING TECHNIQUE FOR SELECTING PHOTOGRAPH OF CONSTANT ANGLE LINES OF LIGHT
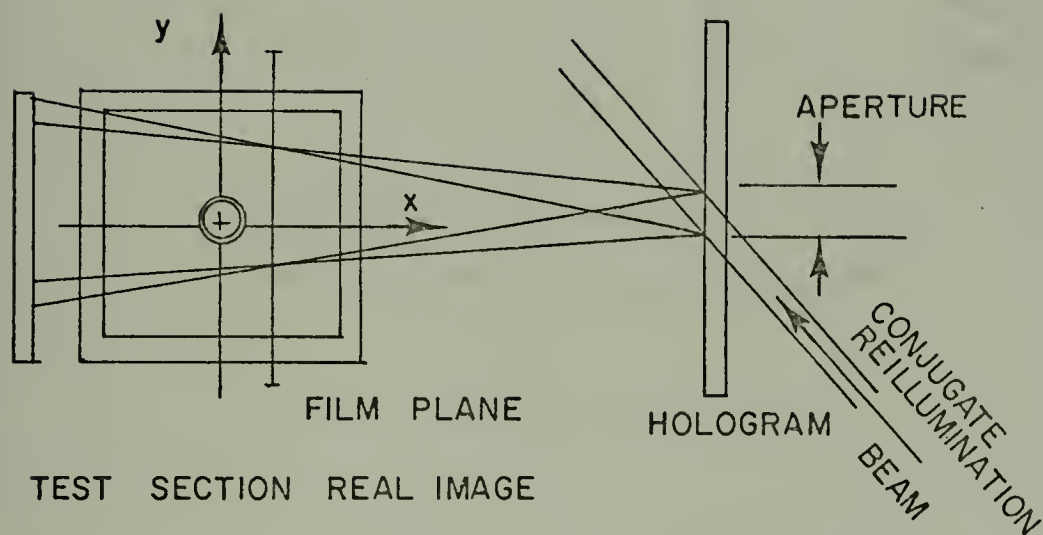
FIGURE 17. LENSLESS PHOTOGRAPHIC TECHNIQUE USING A
CONJUGATE REFERENCE BEAM OF SMALL DIAMETER
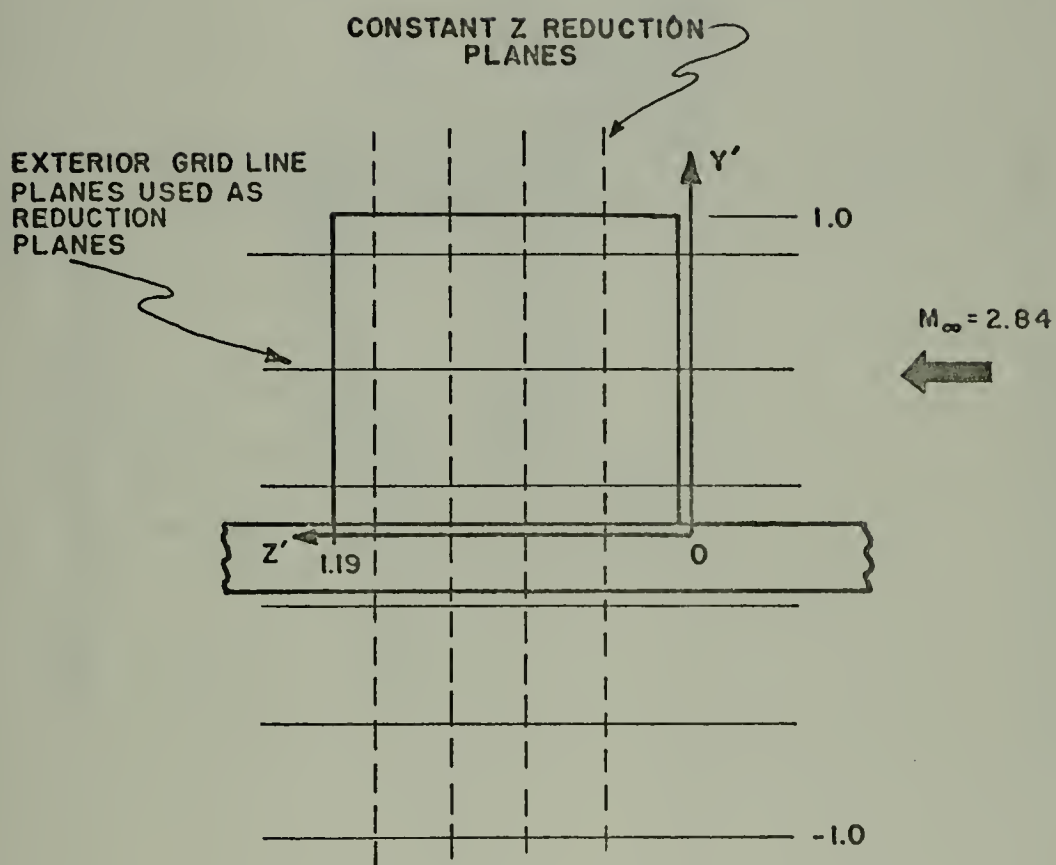
Figure 18. Data Reduction Planes Desired to Describe the Density Field Down the Fin

Figure 19. Schematic of the Refraction Displacement in the Photographs of Points Not Located on the Aligned Axis Caused by the Plastic Grid and Tunnel Wall

57

FROSTED AREAS

CLEAR
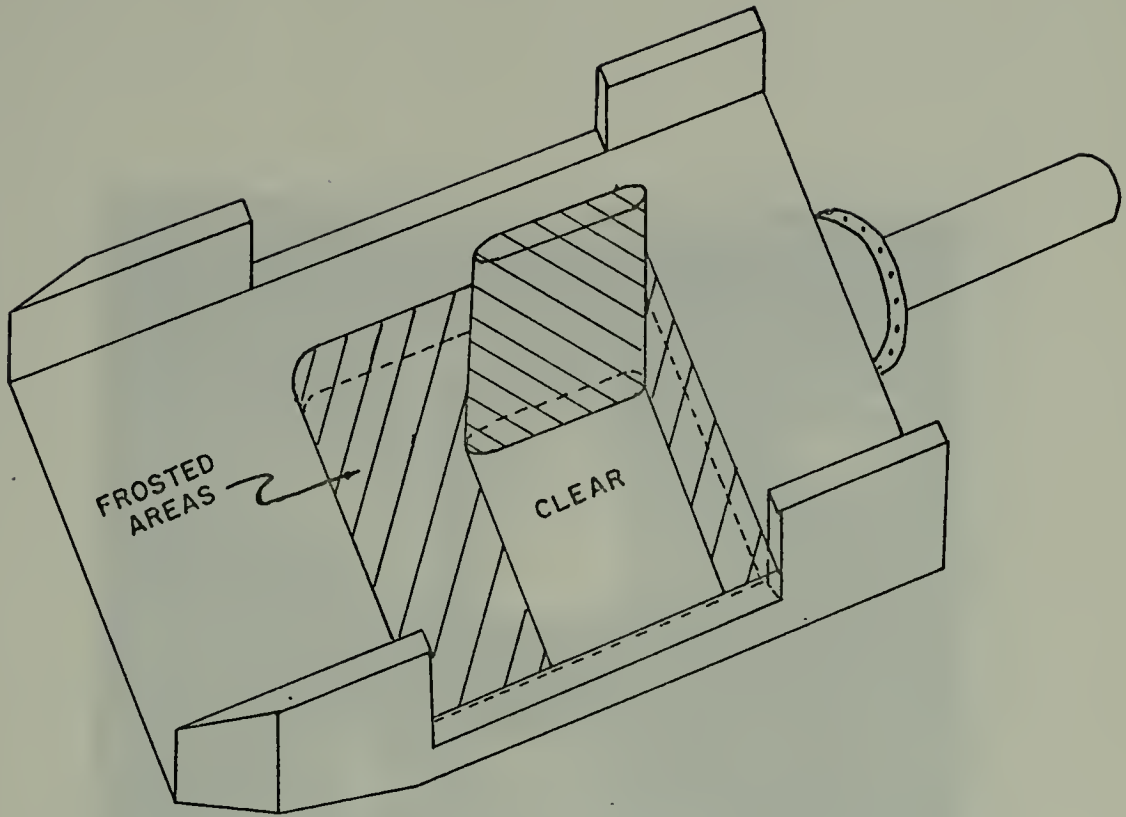
Figure 20. Schematic of the Diffused Plastic Portion of the Model
Required in the Direct Fin Flow Method

58
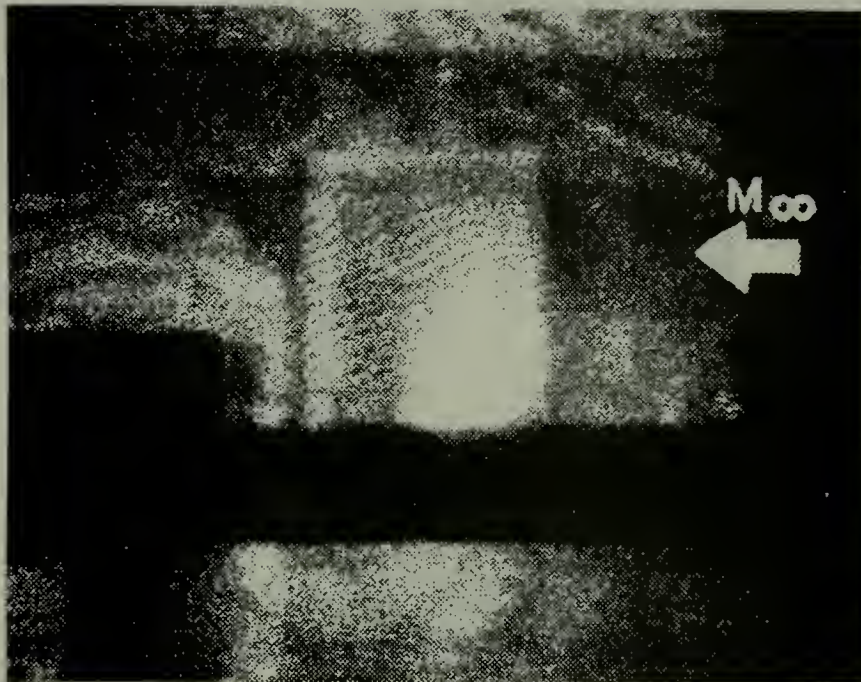
Figure 21. Interferogram Obtained in the Direct Fin Flow Method with
the Model at 0° Rotation, Mach 2.84 and no Translation
of Mirror, M_5
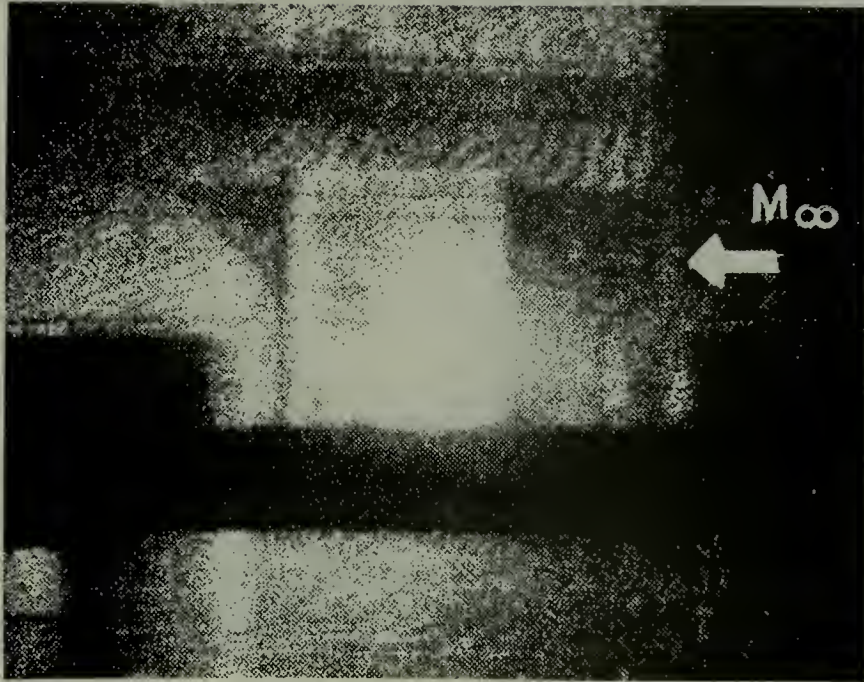
Figure 22. Interferogram Obtained in the Direct Fin Flow Method with
the Model at 0° Rotation, Mach 2.84 and a .006 inches
Translation of Mirror, M_5, Parallel to the Test Section
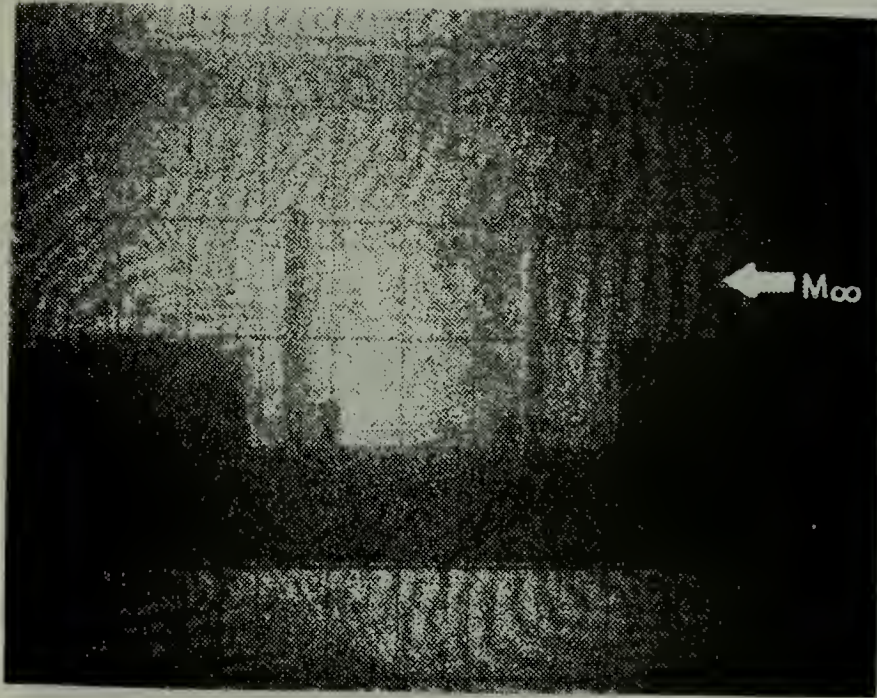
Figure 23. Interferogram Obtained in the Total Flow Method with the
Clear Plexiglas Fin Model at 0° Rotation, Mach 2.84 and
a .0015 inches Horizontal Translation of the Diffuser
Plate Parallel to the Test Section

Figure 24. Interferogram Obtained in the Total Flow Method with the
Clear Plexiglas Fin Model at 0° Rotation, Mach 2.84 and
a .0045 Vertical Translation of the Diffuser Plate
Parallel to the Test Section
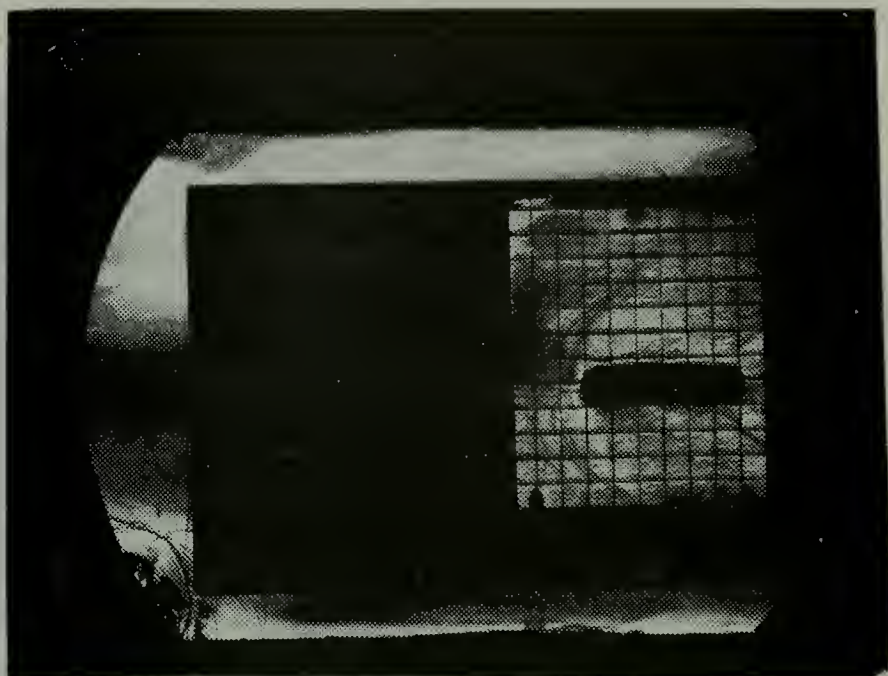
Figure 25(a). Illustration of the Shock Network Around the Fin at
Mach 2.84 with a 90° Model Rotation Angle Using a
Horizontal Knife Edge Schlieren System
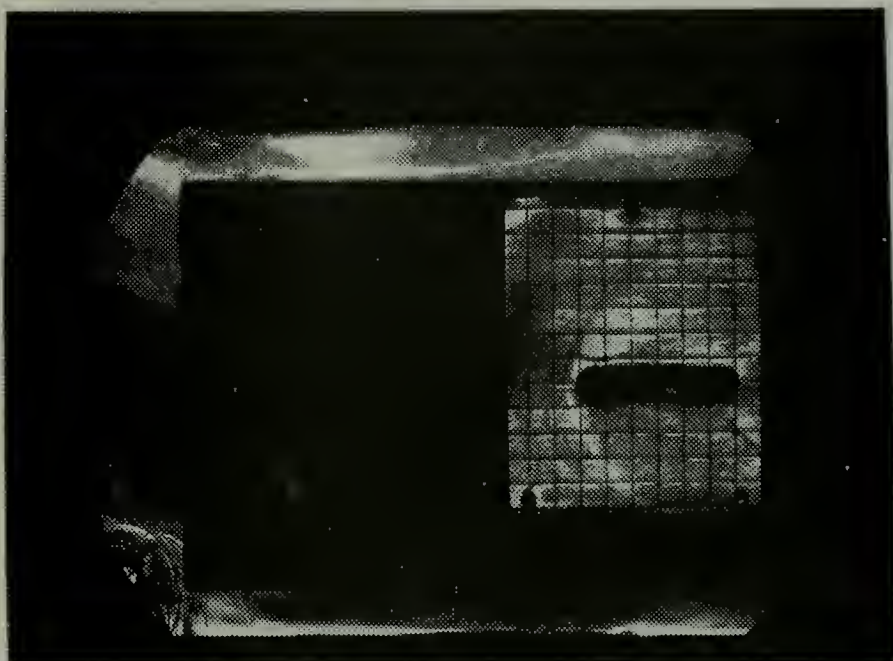
Figure 25(b). Illustration of the Shock Network Around the Fin at Mach 2.84 with a 90° Model Rotation Angle Using a Vertical Knife Edge Schlieren System
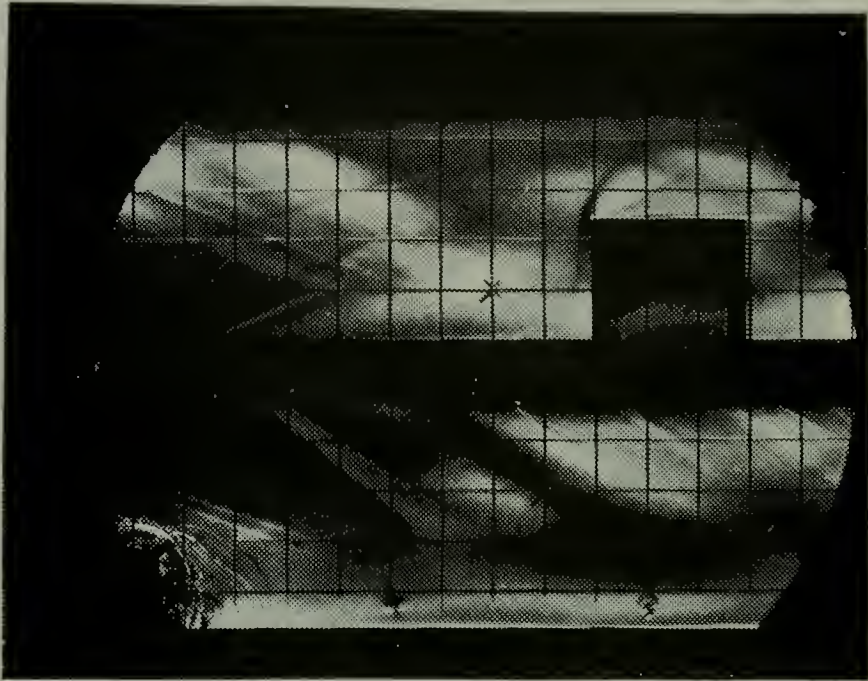
Figure 26. Illustration of the Model Flow Network at Mach 2.84, 0°
Model Rotation and a Plate Vibration of $\pm.05$ Angle of
Attack Using a Schlieren System
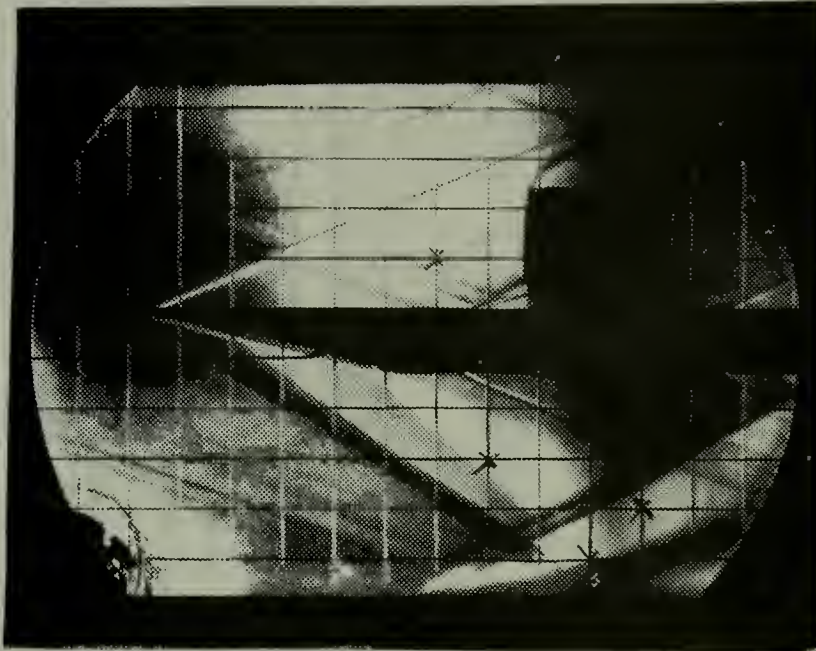
Figure 27. Illustration of the Model Flow Network at Mach 2.84, 0°
Model Rotation and No Plate Vibration Using a Schlieren
System
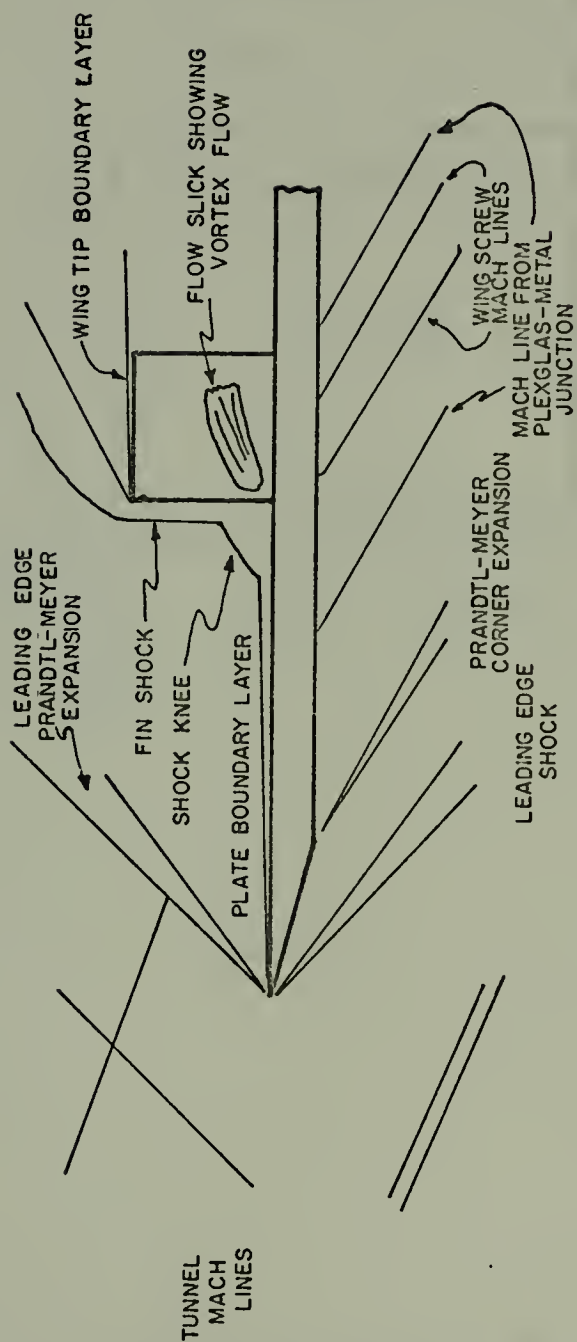
Figure 28. Schematic of the Flow Observed in the Schlieren Photographs
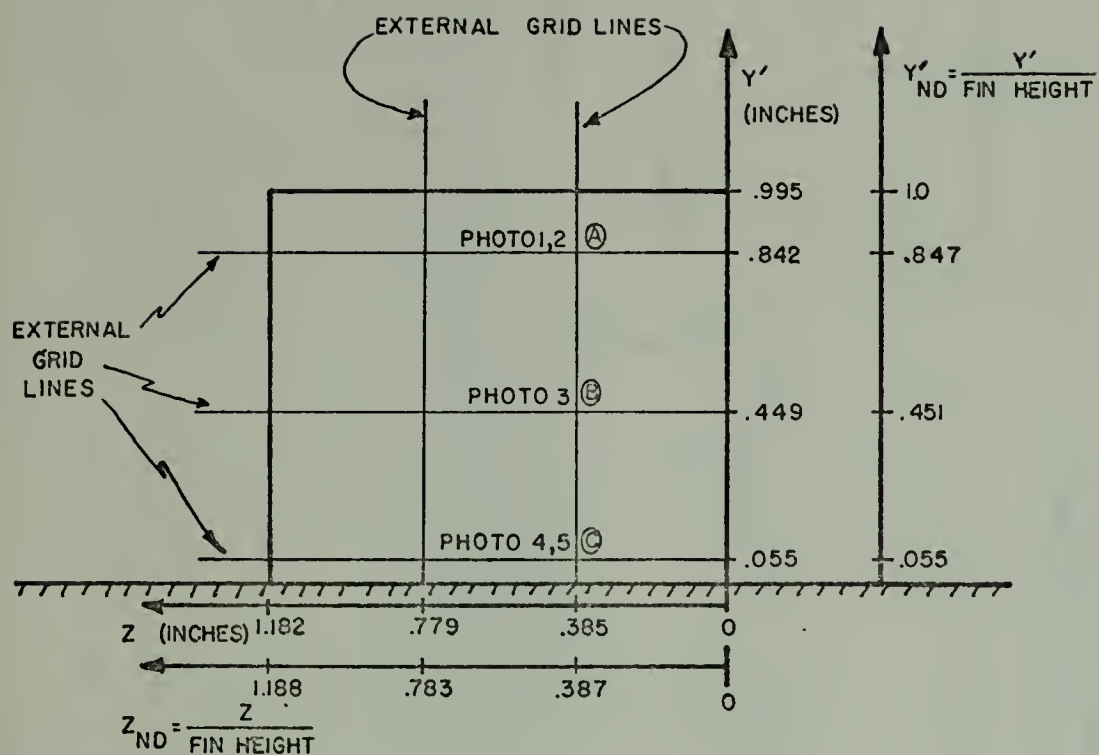
Figure 29. Schematic of the Fin at 0° Rotation Showing the Locations of the External Grid Lines and of the Interferogram Photographic Points
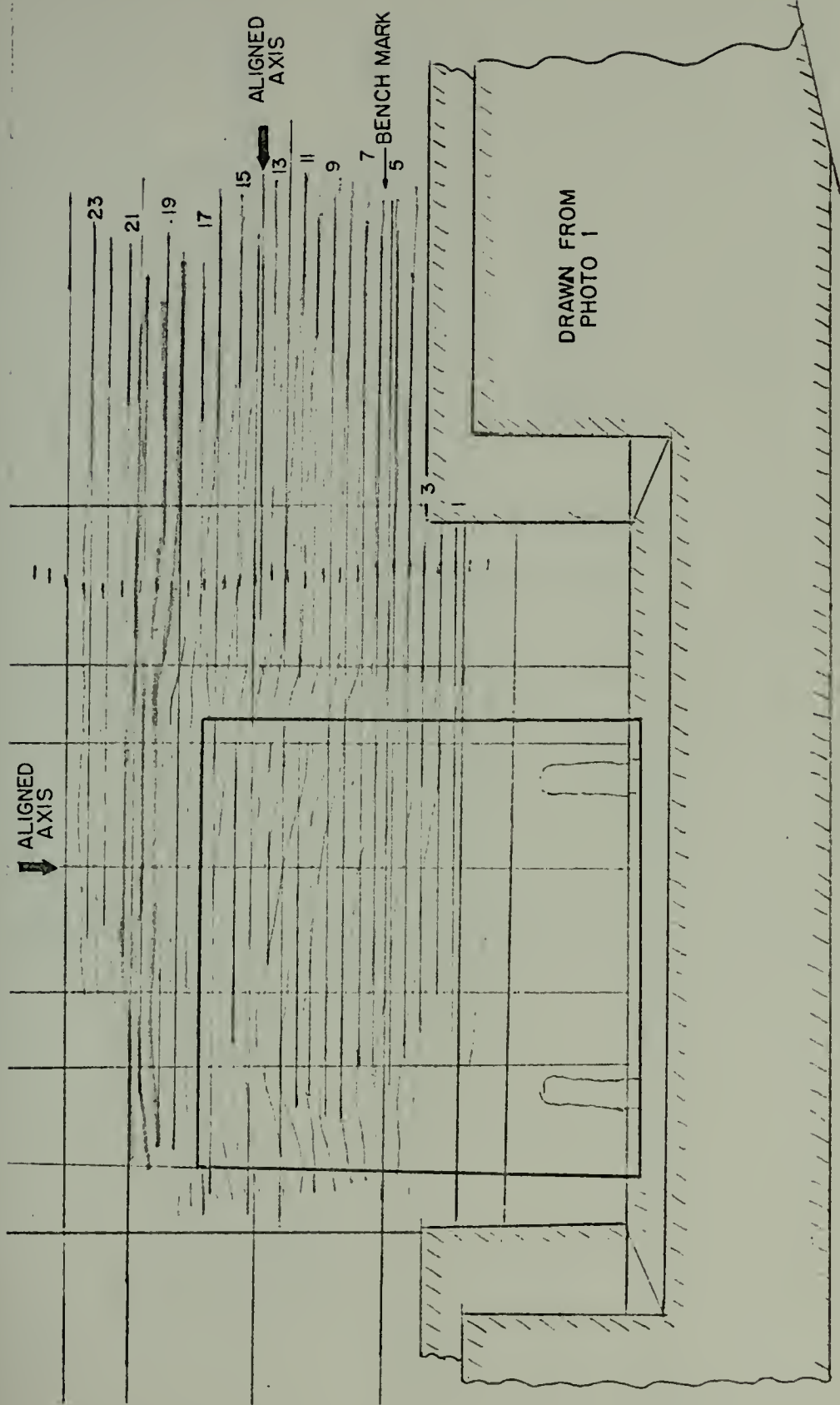
Figure 30. Actual Drawing and Data Reduction of Interferogram Photograph 1 Aligned at Z = 0.387, Y' = 0.847 for Mach 2.84 and 0° Model Rotation Angle
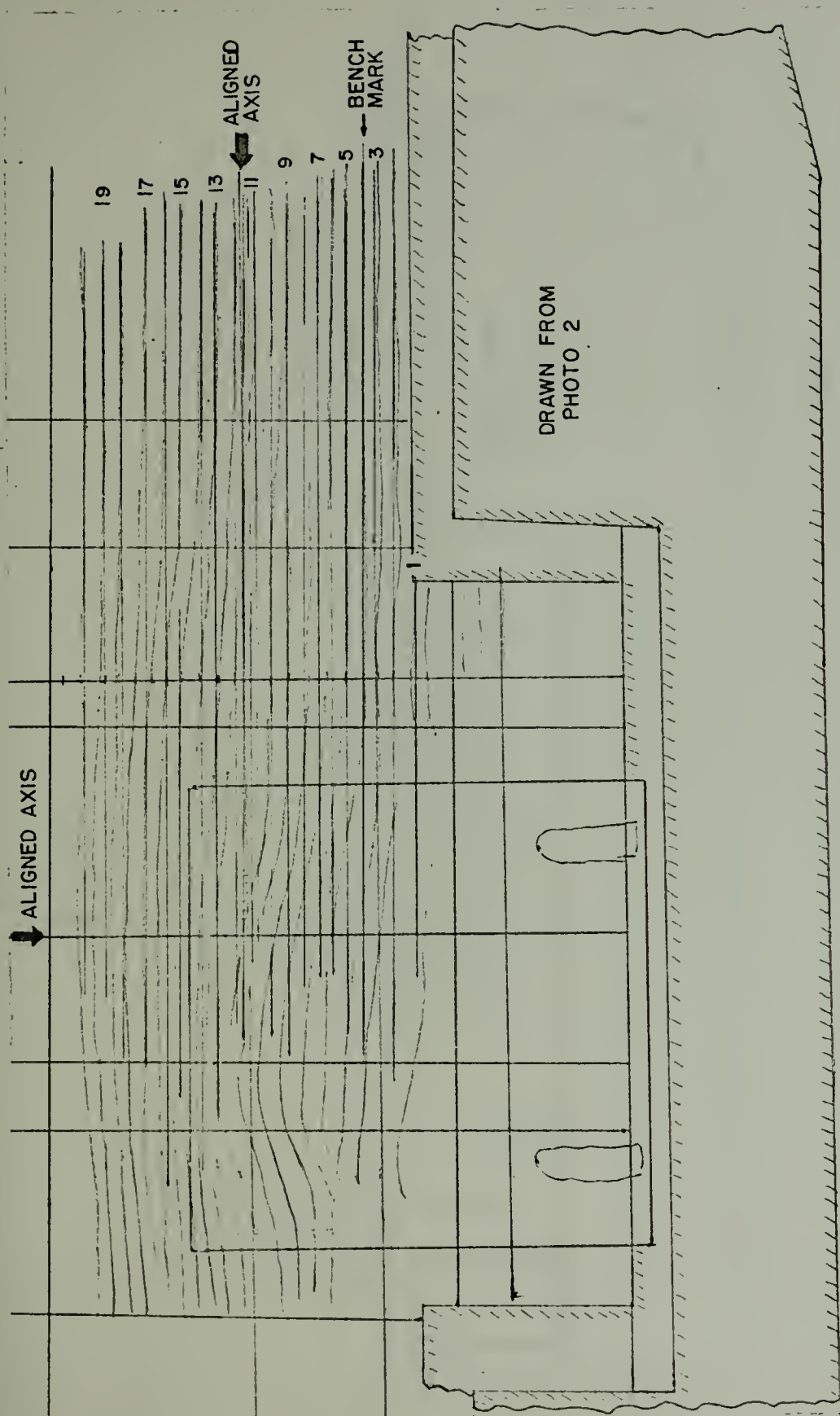
Figure 31. Actual Drawing and Data Reduction of Interferogram Photograph 2 Aligned at Z = 0.387, Y' = 0.847 for Mach 2.84 and 0° Model Rotation Angle
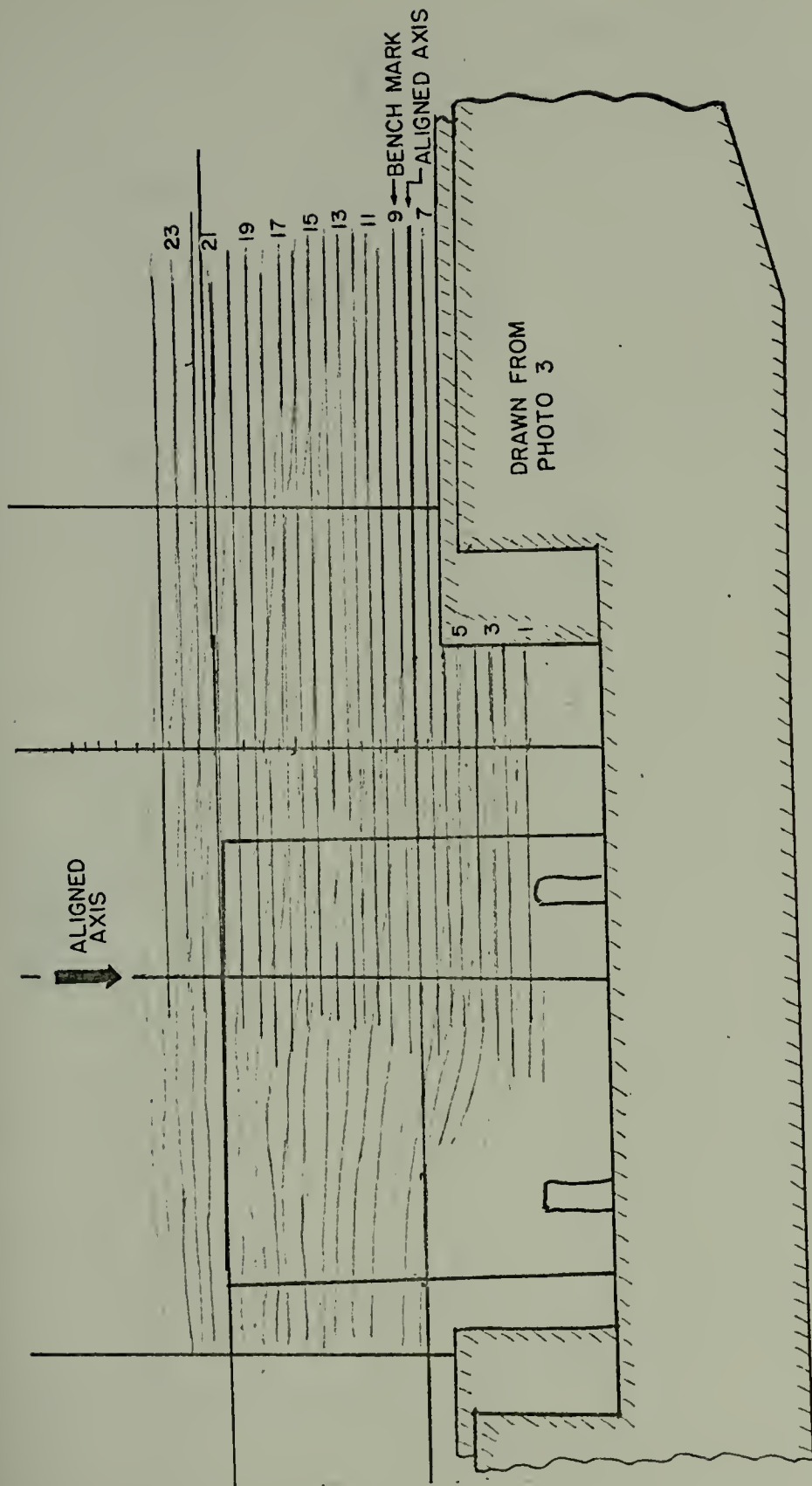
Figure 32. Actual Drawing and Data Reduction of Interferogram Photograph 3 Aligned at Z = 0.381, Y' = 0.451 for Mach 2.84 and 0° Model Rotation Angle

71
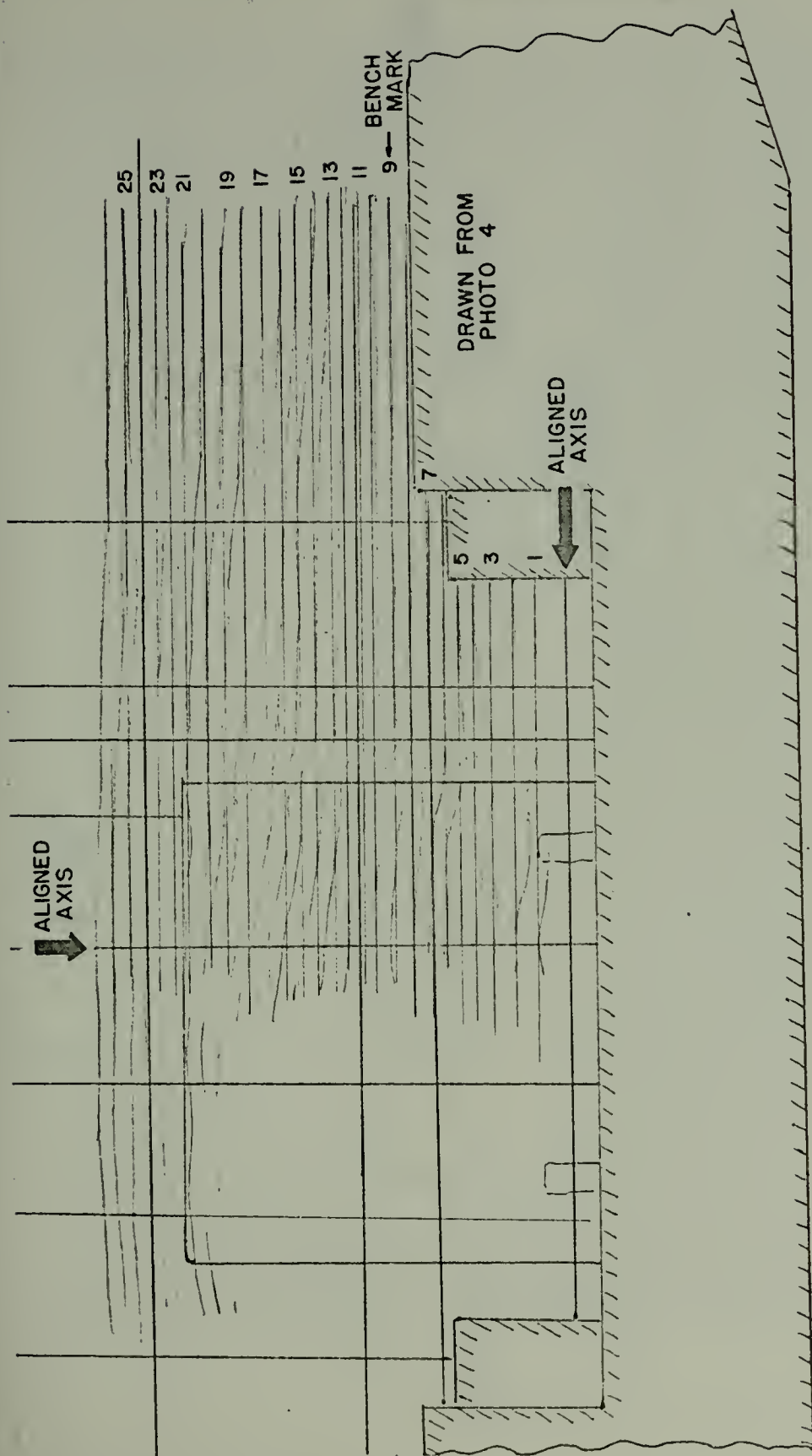
Figure 33. Actual Drawing and Data Reduction of Interferogram Photograph 4 Aligned at $Z = 0.387$, $Y' = 0.055$ for Mach 2.84 and 0° Model Rotation Angle
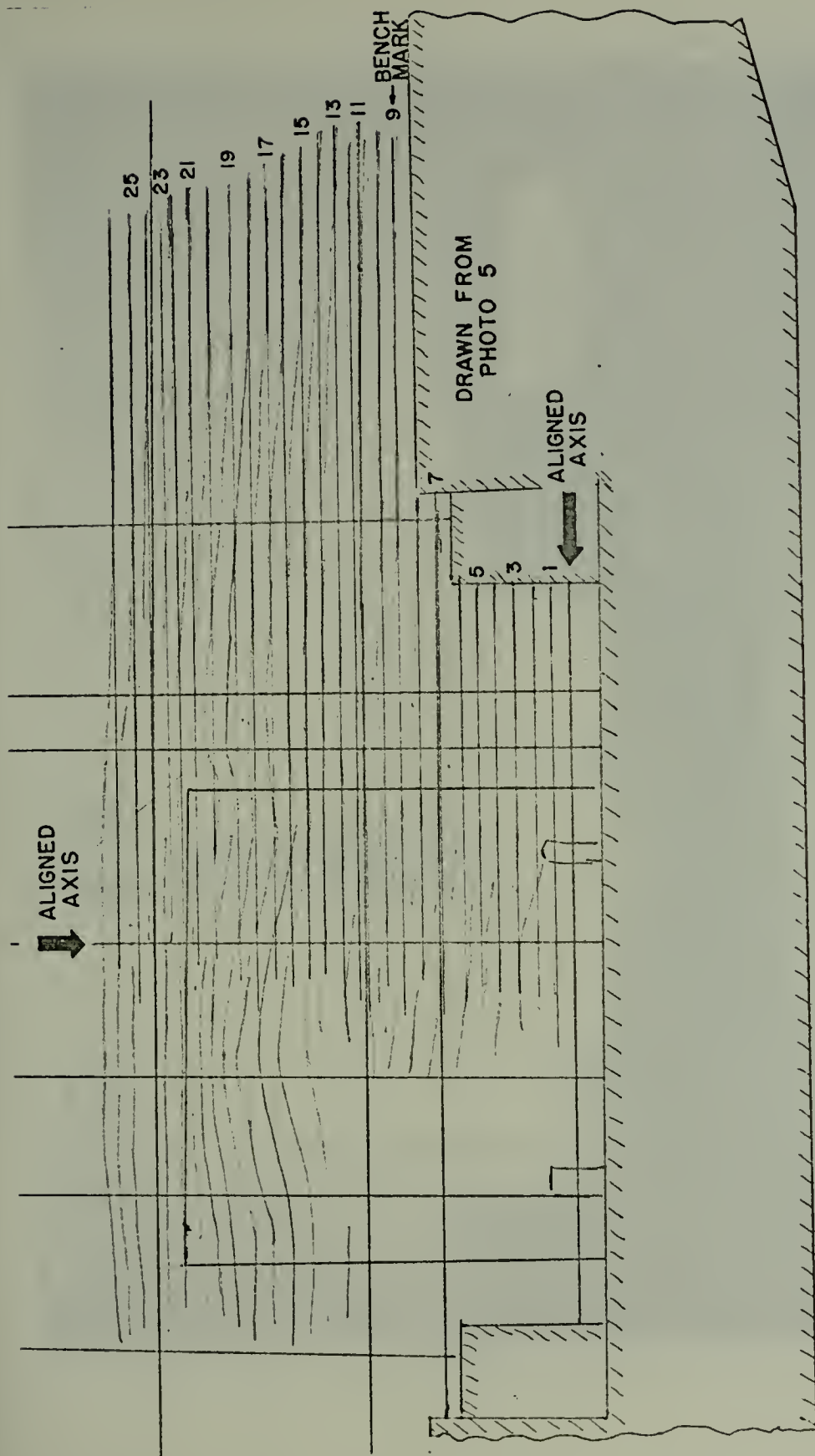
Figure 34. Actual Drawing and Data Reduction of Interferogram Photograph 5 Aligned at Z = 0.387, Y' = 0.055 for Mach 2.84 and 0° Model Rotation Angle

73
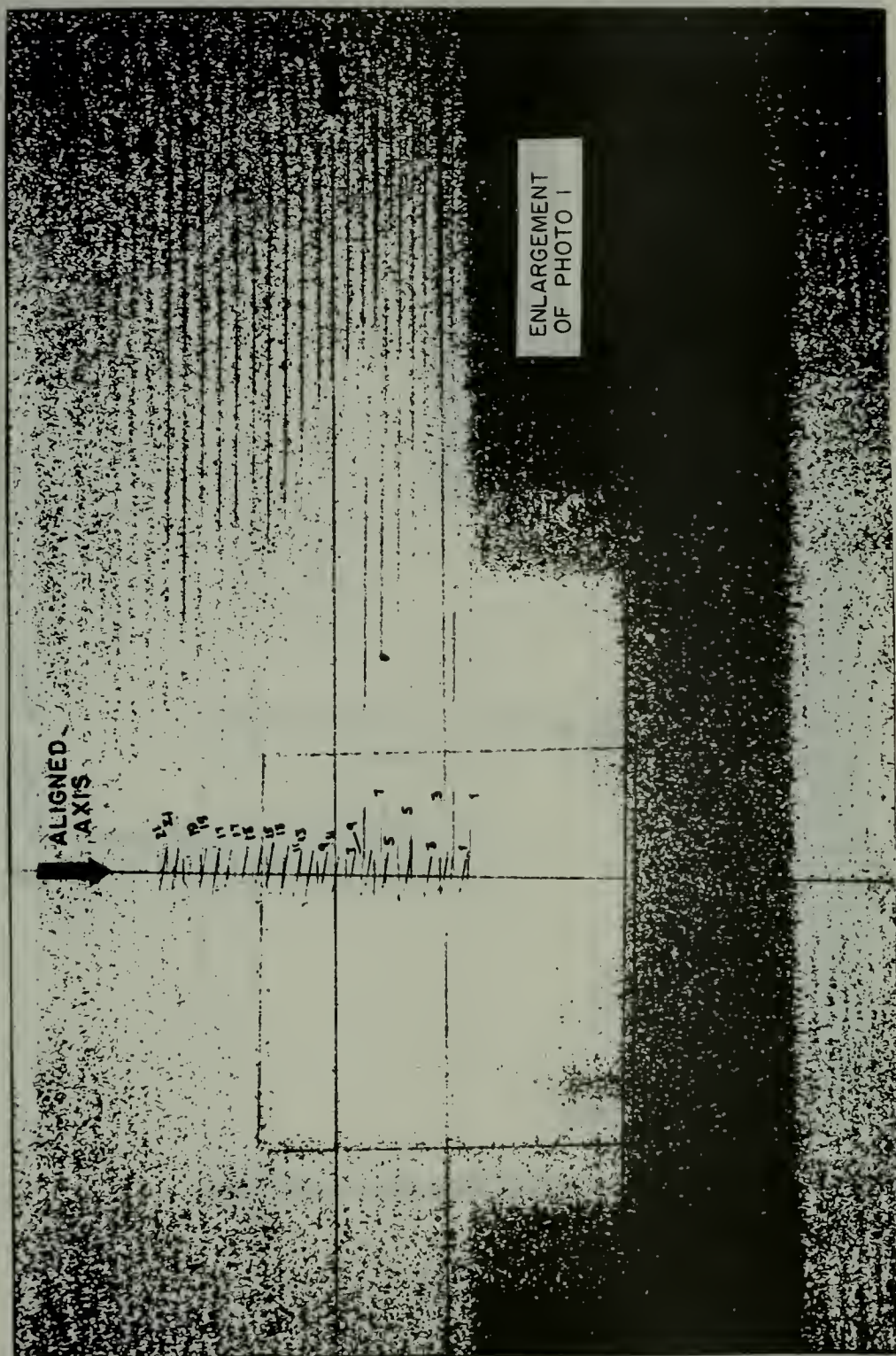
Figure 35. Actual Enlarged Photograph Used for the Data Reduction of Interferogram Photograph 1
Aligned at Z = 0.387, Y' = 0.847 for Mach 2.84 and 0° Model Rotation Angle
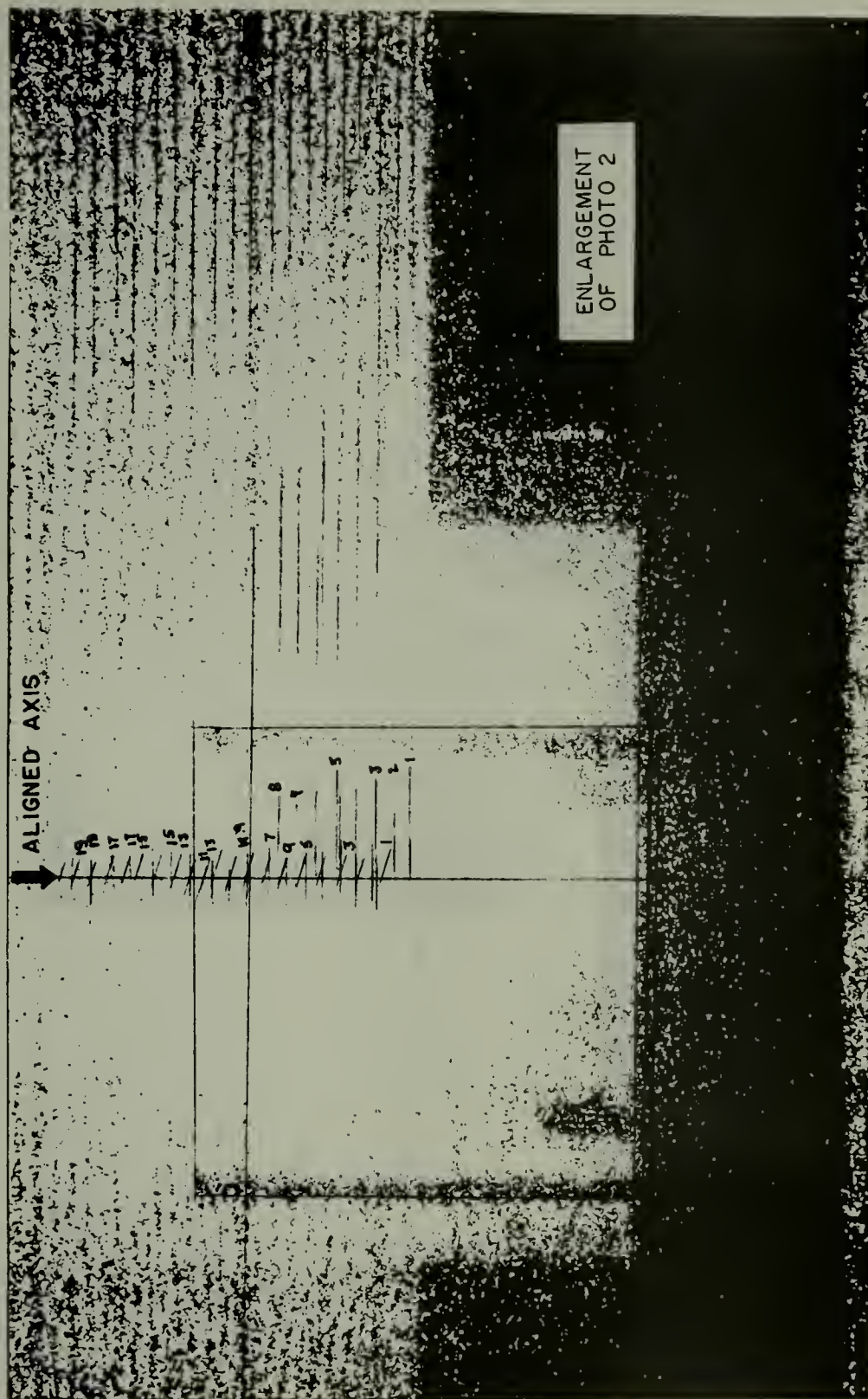
Figure 36. Actual Enlarged Photograph Used for the Data Reduction of Interferogram Photograph 2 Aligned at Z = 0.387, Y' = 0.847 for Mach 2.84 and 0° Model Rotation Angle
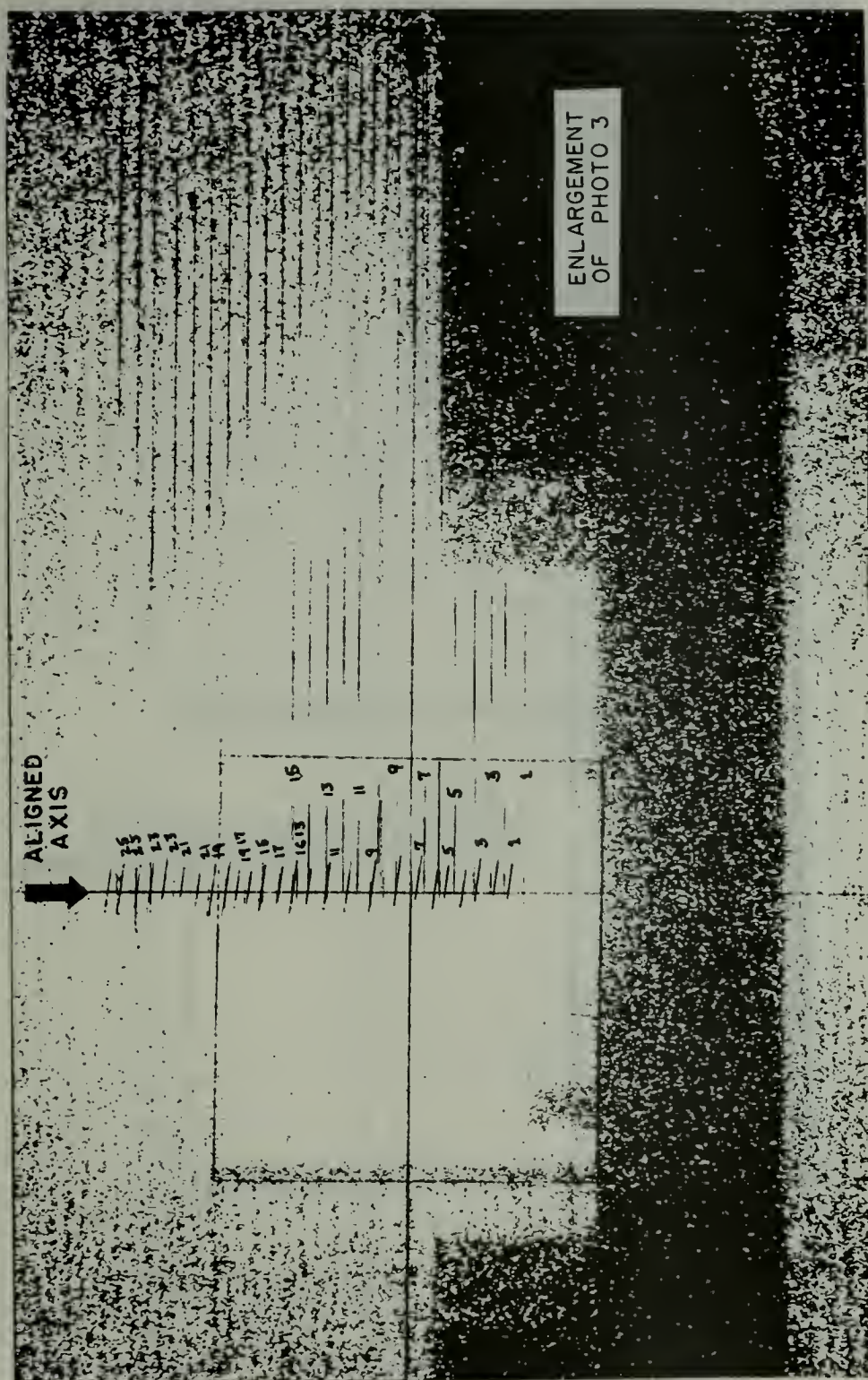
Figure 37. Actual Enlarged Photograph Used for the Data Reduction of Interferogram Photograph 3 Aligned at Z = 0.387, Y' = 0.451 for Mach 2.84 and 0 Model Rotation Angle
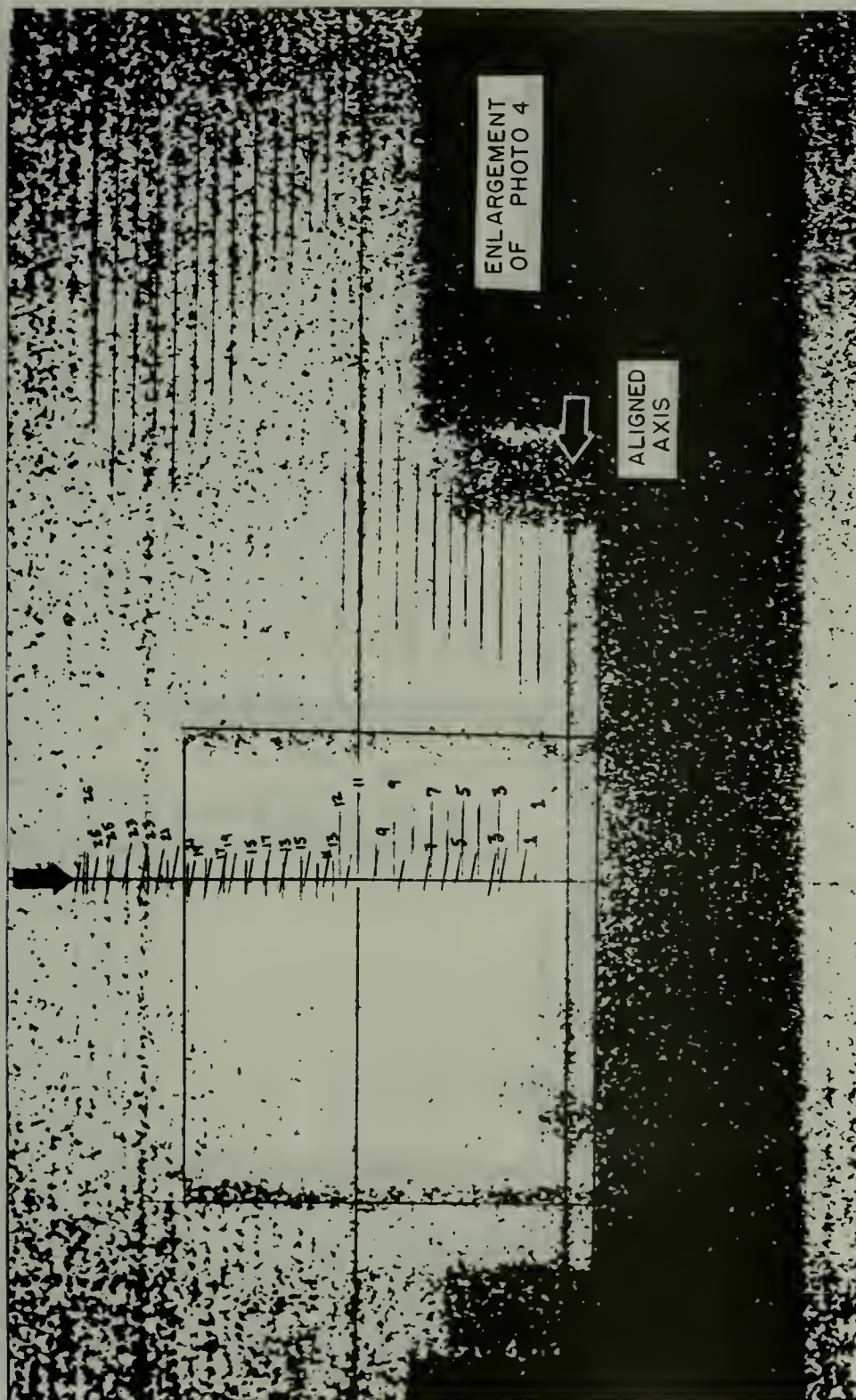
Figure 38. Actual Enlarged Photograph Used for the Data Reduction of Interferogram Photograph 4 Aligned at Z = 0.387, Y' = 0.055 for Mach 2.84 and 0° Model Rotation Angle

77
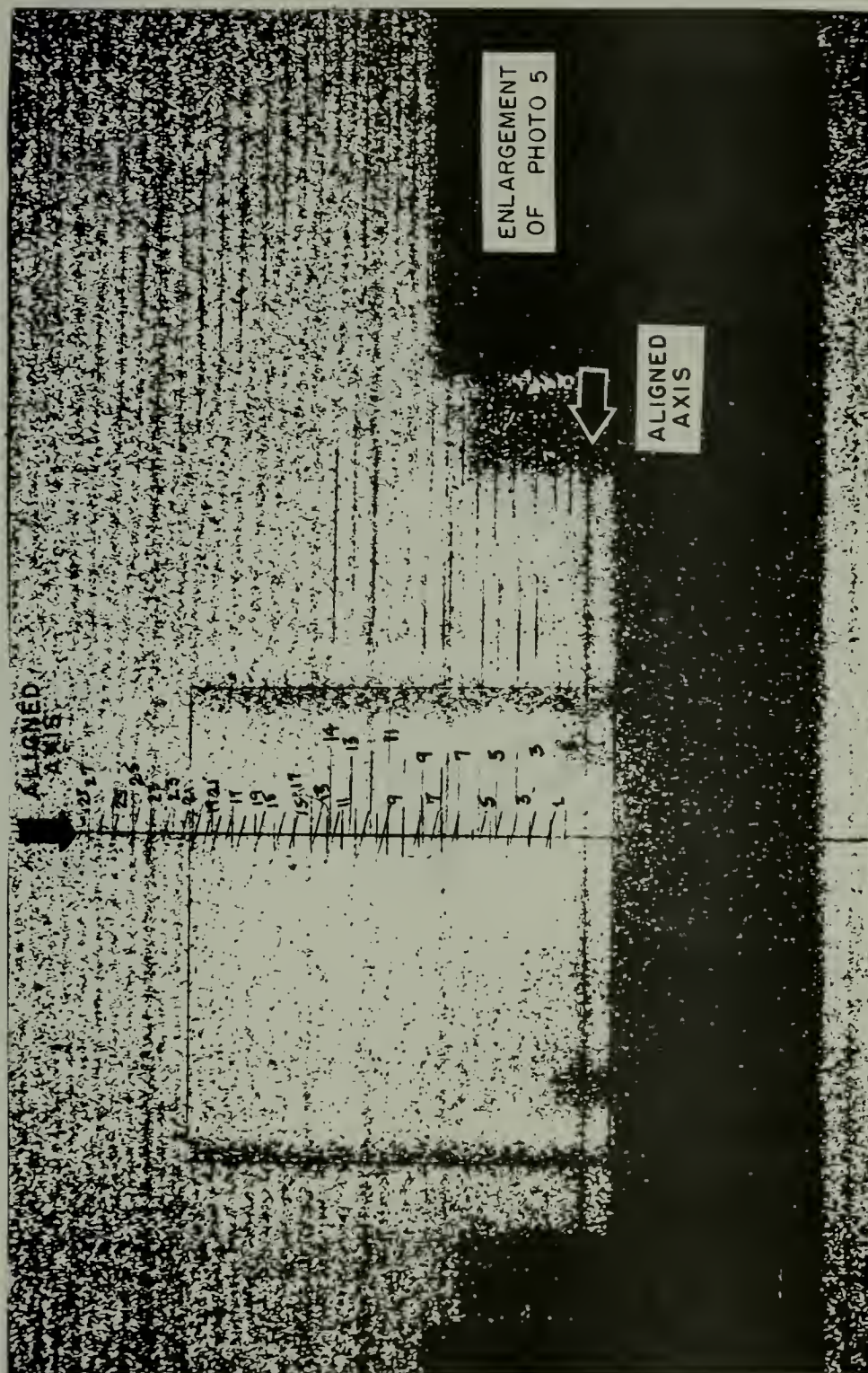
Figure 39. Actual Enlarged Photograph Used for the Data Reduction of Interferogram Photograph 5
Aligned at Z = 0.387, Y' = 0.055 for Mach 2.84 and 0° Model Rotation Angle

Figure 40. Comparison of Fringe Data Obtained from Drawings of
Interferogram Photographs 1 and 2 Aligned at $Y' = 0.847$

79

Figure 41. Comparison of Fringe Data Obtained from Photographic
Enlargements of Interferogram Photographs 1 and 2 Aligned
at Y' = 0.847
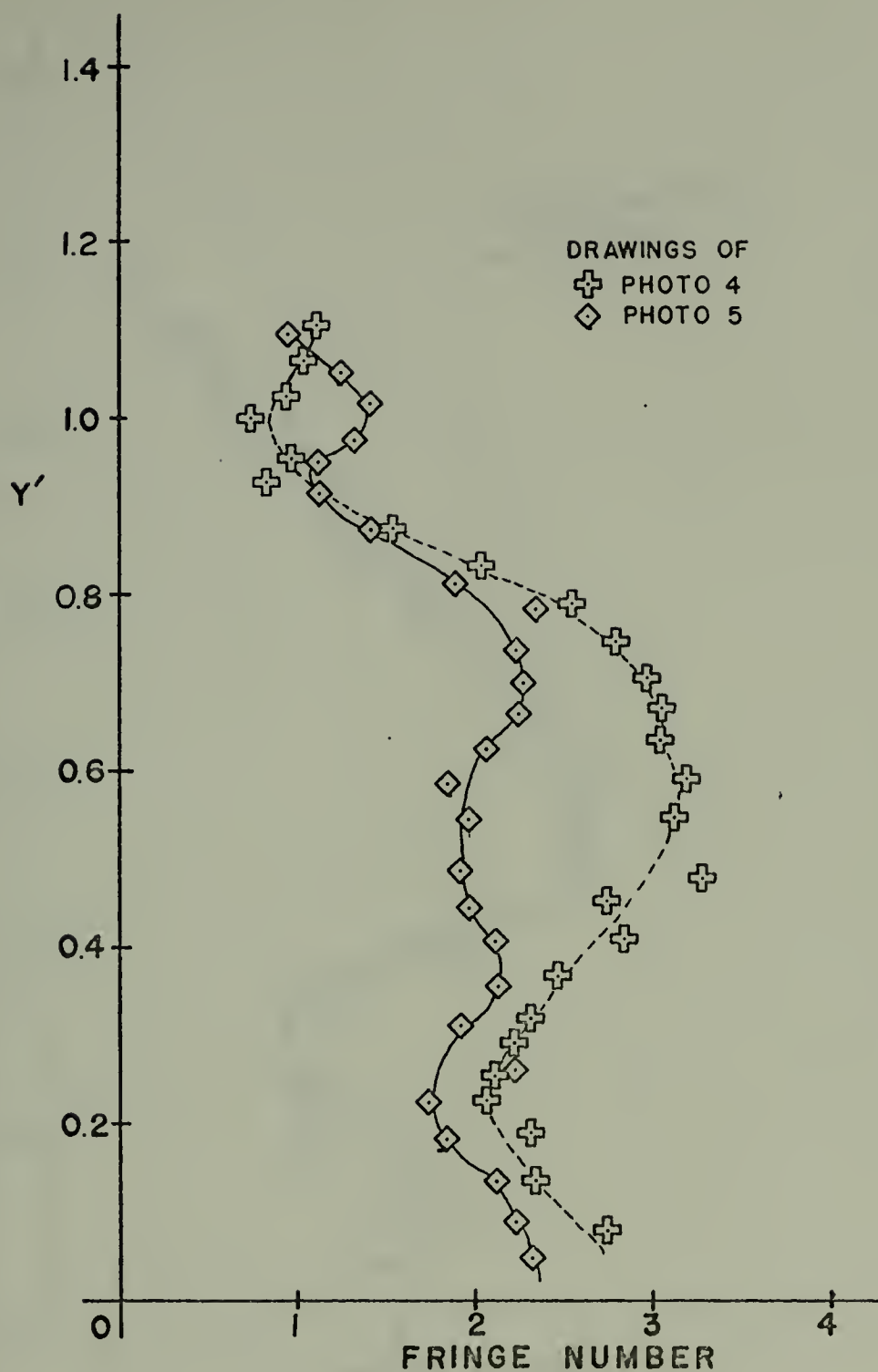
Figure 42. Comparison of Fringe Data Obtained from Drawings of
Interferogram Photographs 4 and 5 Aligned at Y' = 0.055
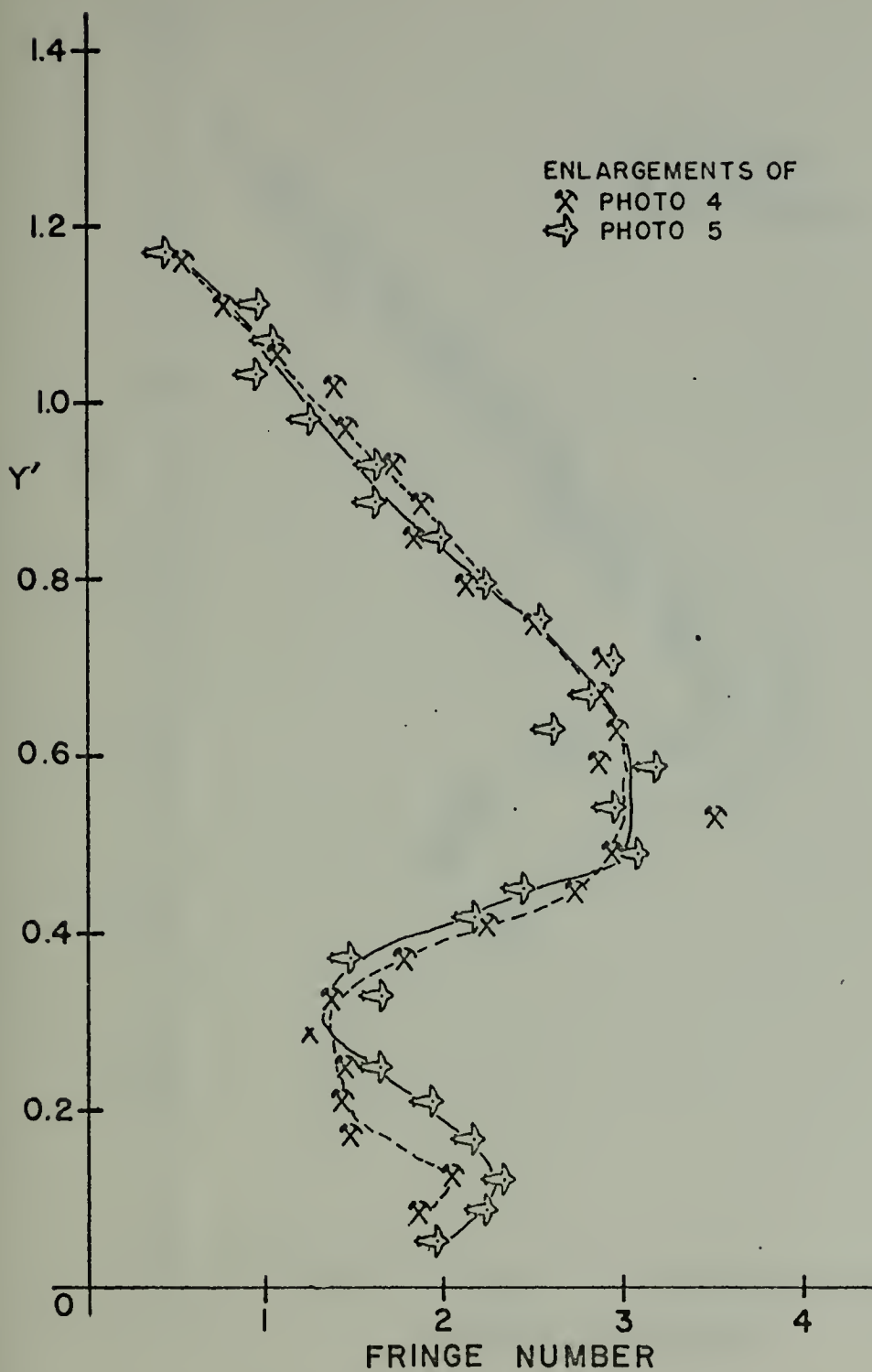
Figure 43. Comparison of Fringe Data Obtained from Photographic
Enlargements of Interferogram Photographs 4 and 5 Aligned
at Y' = 0.055
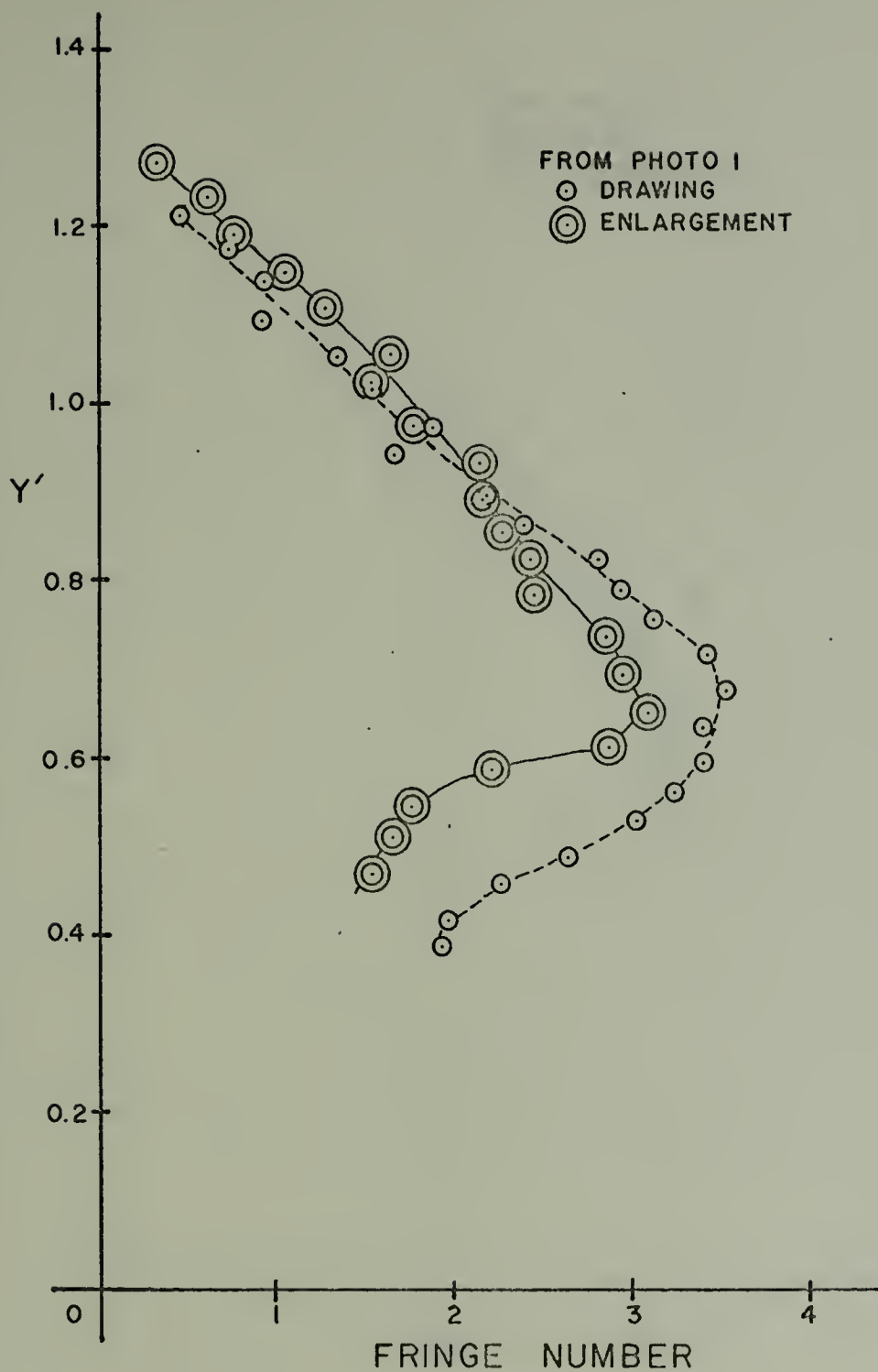
Figure 44. Comparison of Fringe Data Obtained from the Drawing and Photographic Enlargement of Interferogram Photograph 1 Aligned at Y' = 0.847
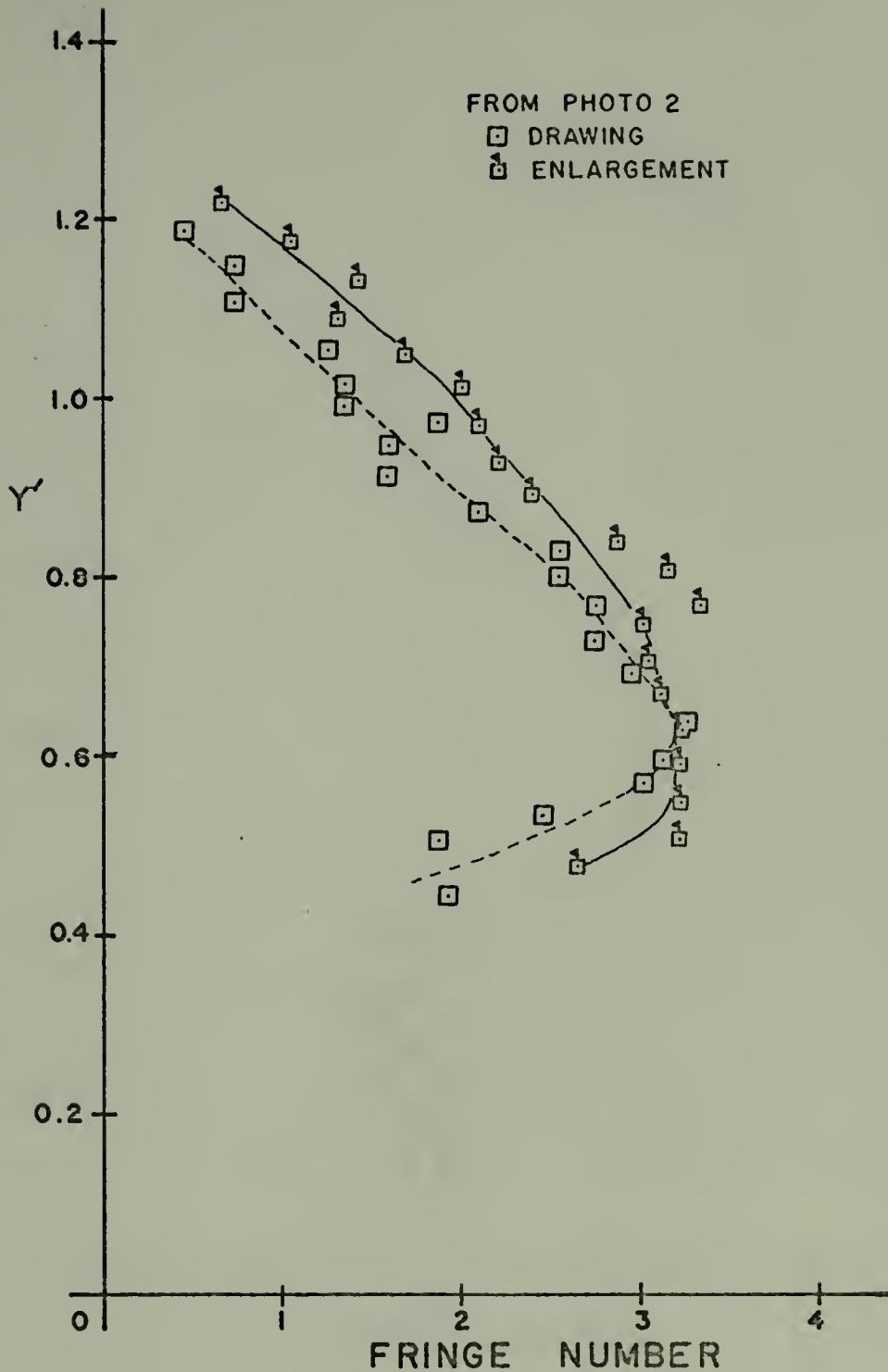
Figure 45. Comparison of Fringe Data Obtained from the Drawing and Photographic Enlargement of Interferogram Photograph 2 Aligned at Y' = 0.847
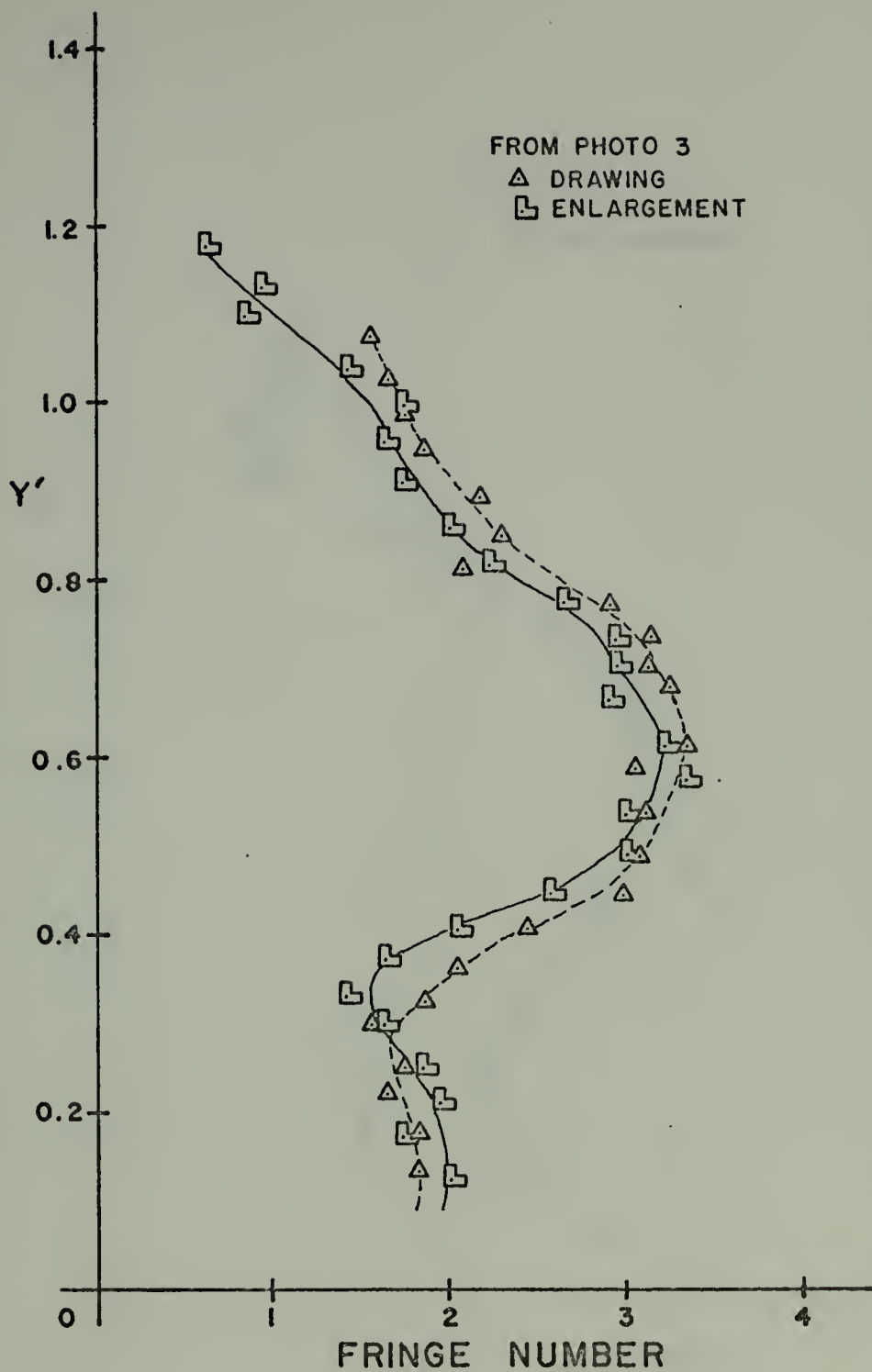
Figure 46. Comparison of Fringe Data Obtained from the Drawing and Photographic Enlargement of Interferogram Photograph 3 Aligned at Y' = 0.451
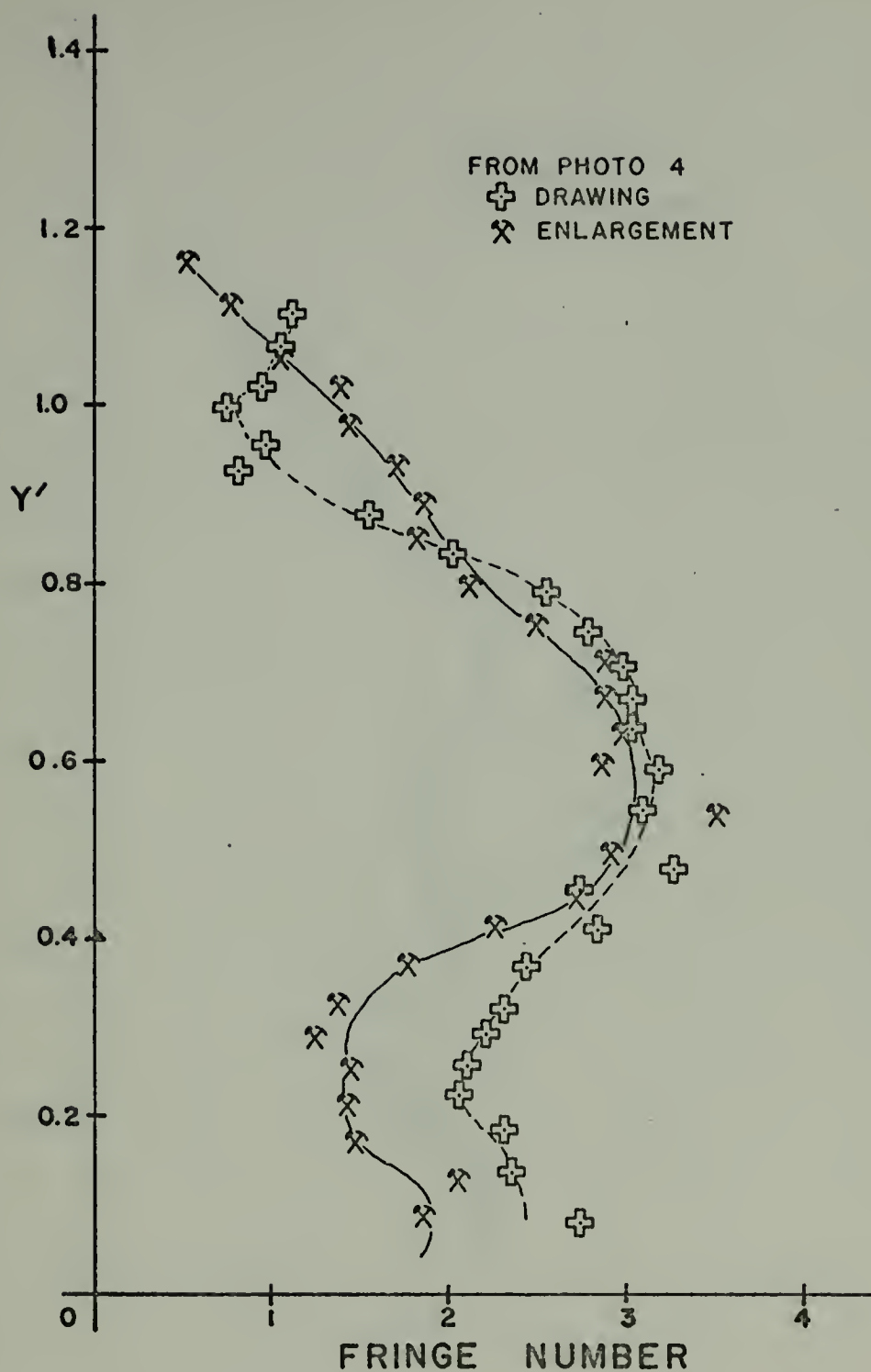
Figure 47. Comparison of Fringe Data Obtained from the Drawing and
Photographic Enlargement of Interferogram Photograph 4
Aligned at Y' = 0.055

86
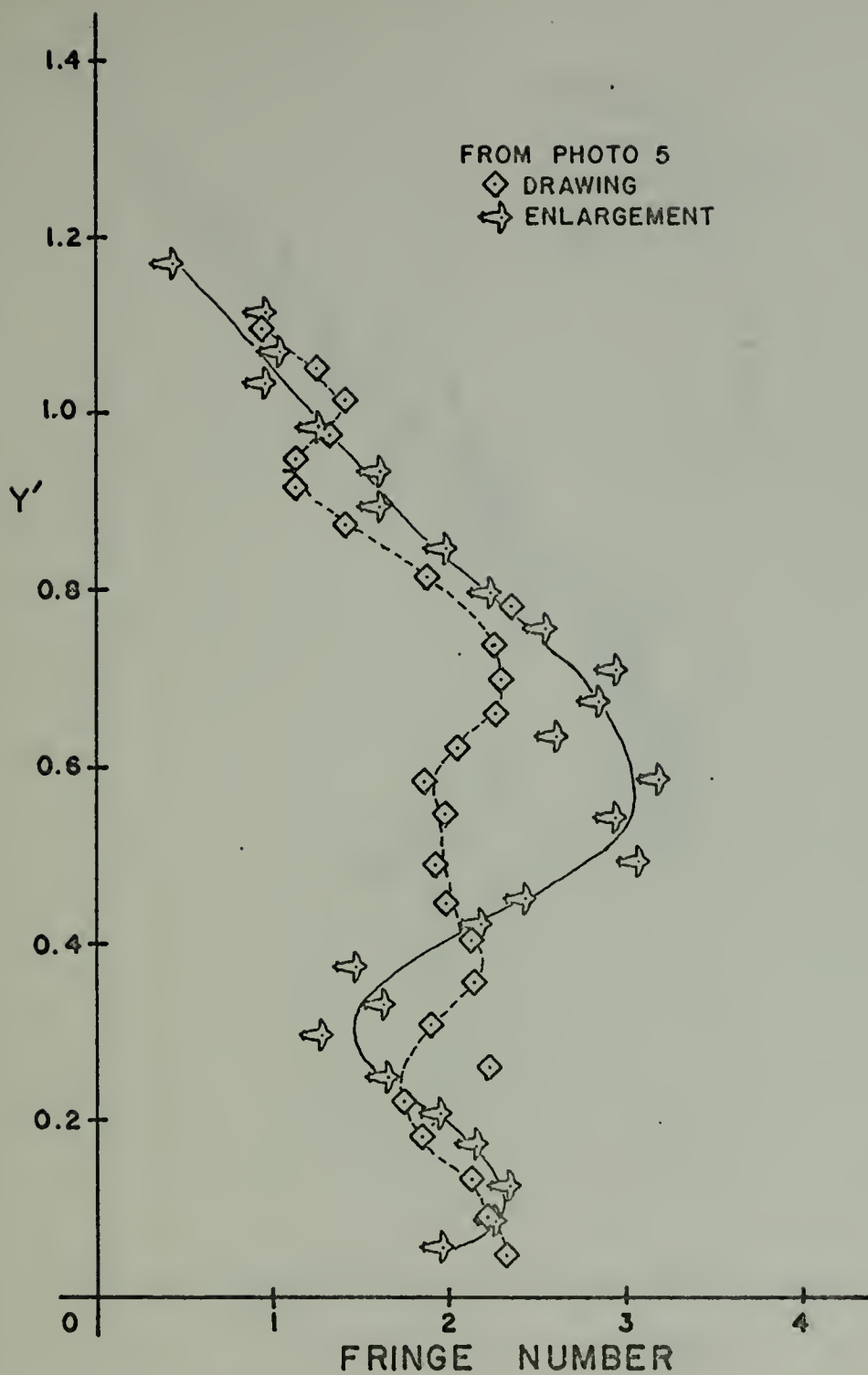
Figure 48. Comparison of Fringe Data Obtained from the Drawing and
Photographic Enlargement of Interferogram Photograph 5
Aligned at Y' = 0.055
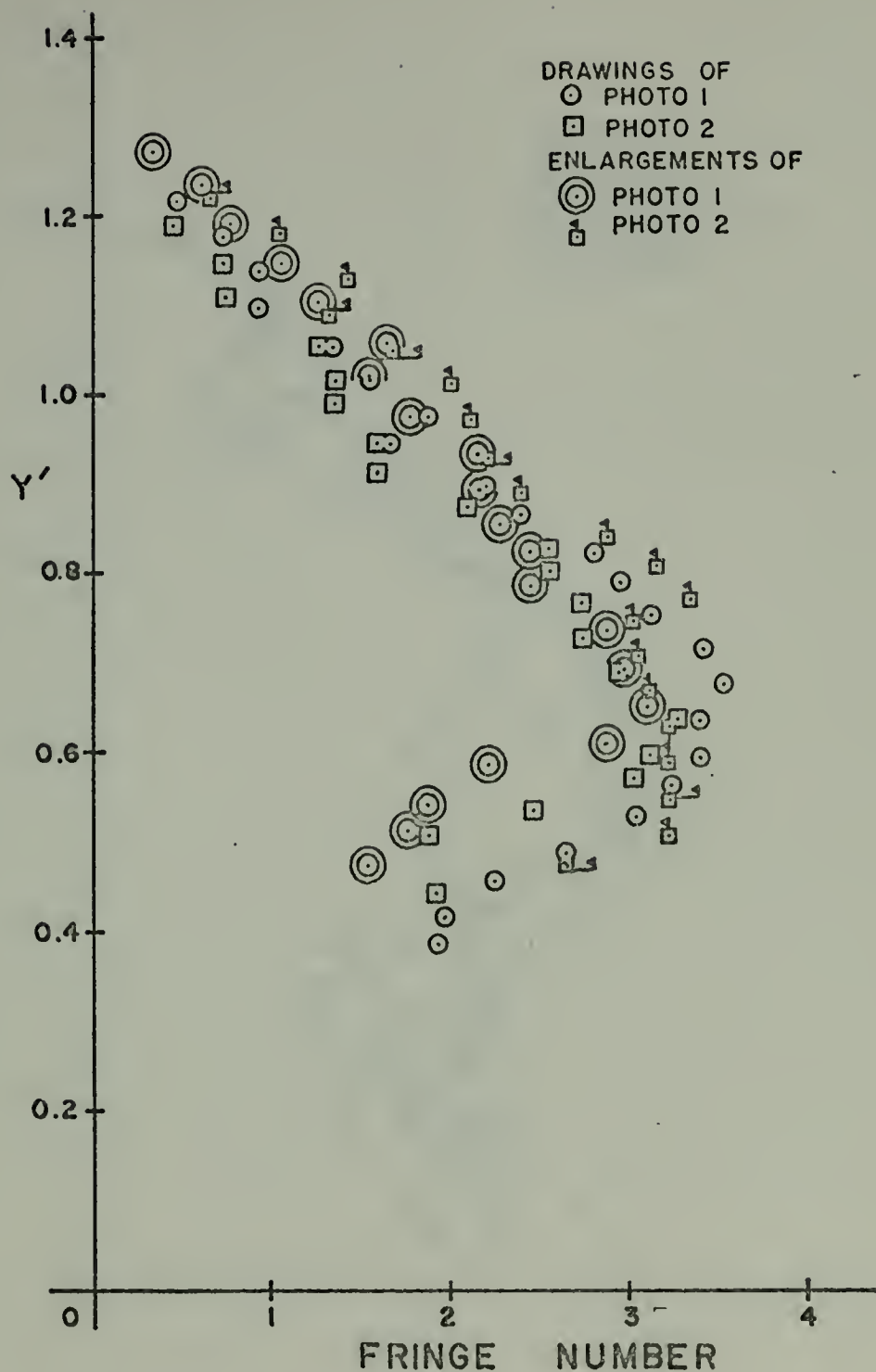
Figure 49. Comparison of Fringe Data Obtained from the Drawings and
Photographic Enlargements of Interferogram Photographs 1
and 2 Aligned at Y' = 0.847
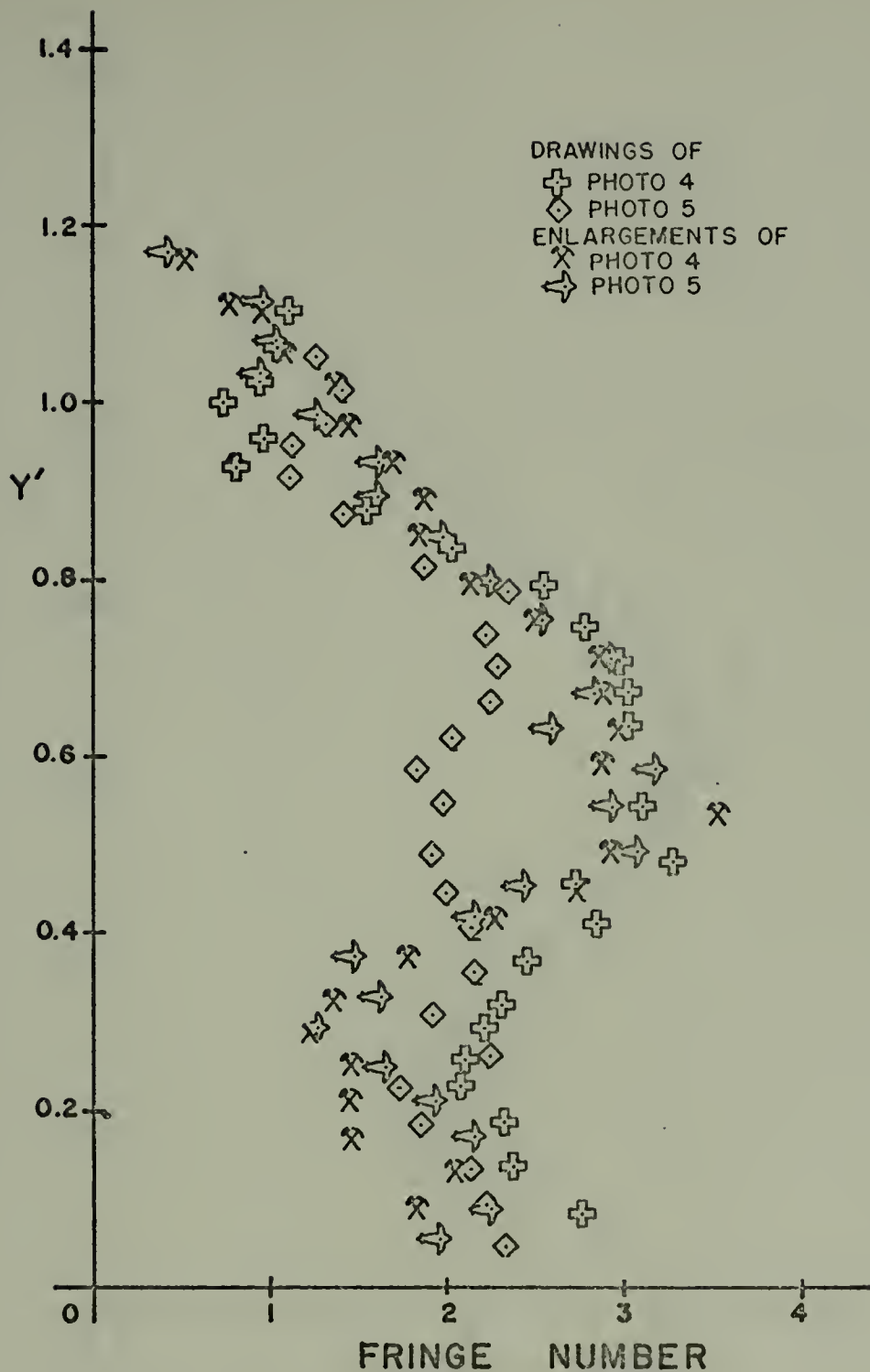
Figure 50. Comparison of Fringe Data Obtained from the Drawings and Photographic Enlargements of Interferogram Photographs 4 and 5 Aligned at Y' = 0.055
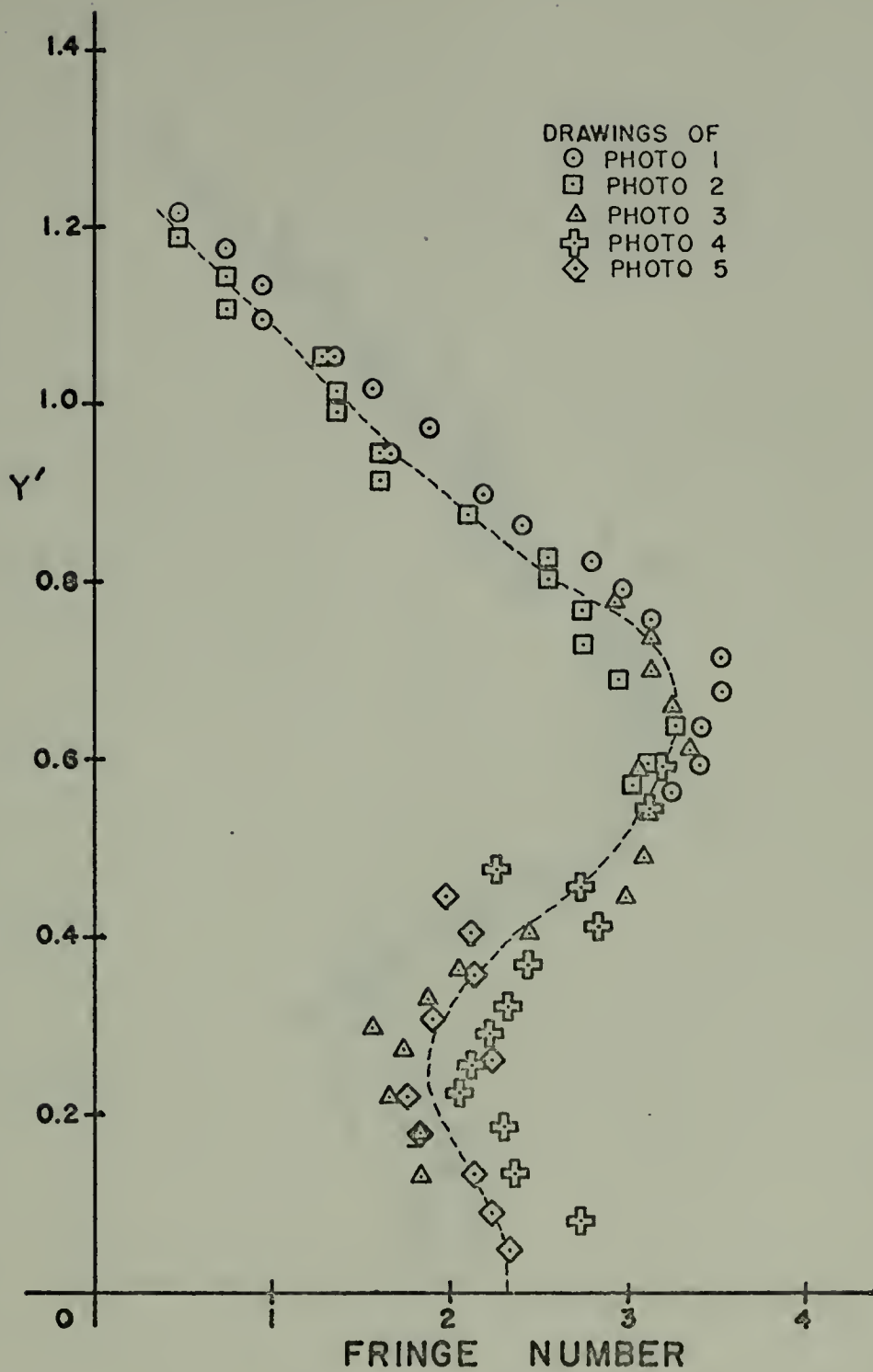
Figure 51.   Fringe Number Across the Fin in the Z = 0.387 Plane for $\beta = 0^\circ$, Mach 2.84 as Determined from the Drawings of the Interferogram Photographs
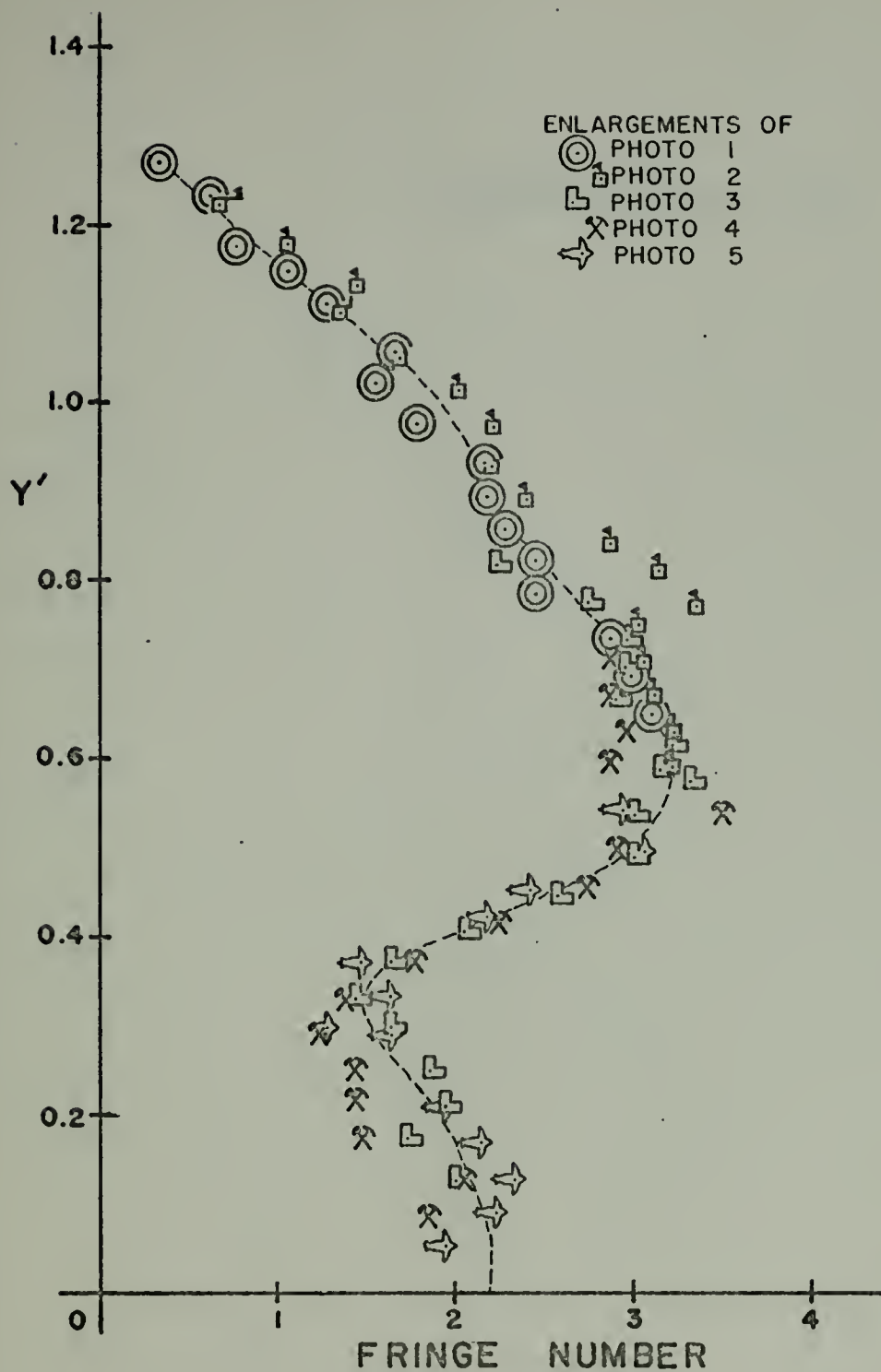
Figure 52. Fringe Number Across the Fin in the Z = 0.387 Plane for
ξ = 0°, Mach 2.84 as Determined from the Photographic
Enlargements of the Interferogram Photographs
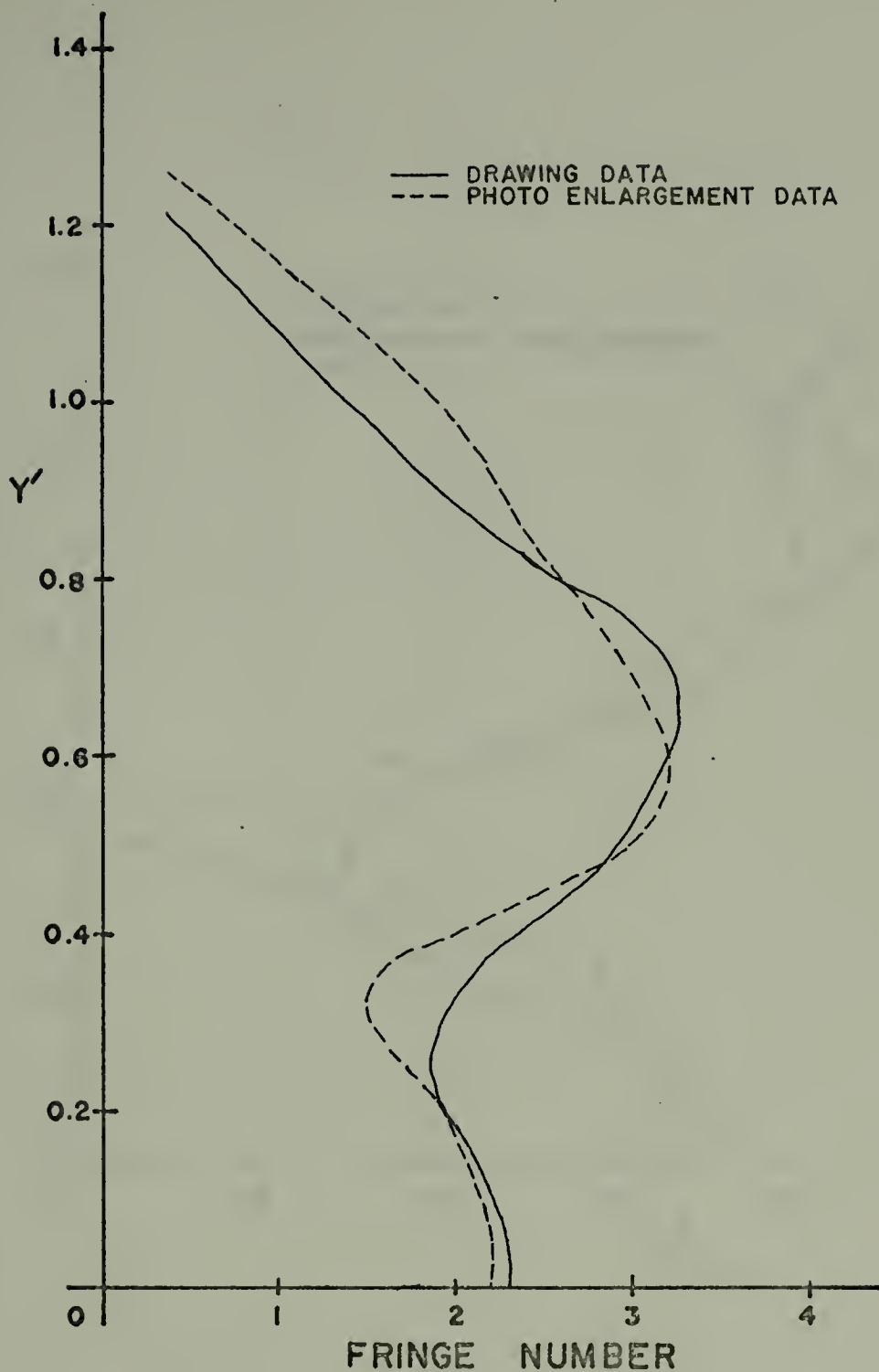
Figure 53. Comparison of the Fringe Numbers Across the Fin in the Z = 0.387 Plane for ξ = 0°, Mach 2.84 as Determined from the Drawings and Photographic Enlargements of the Interferogram Photographs
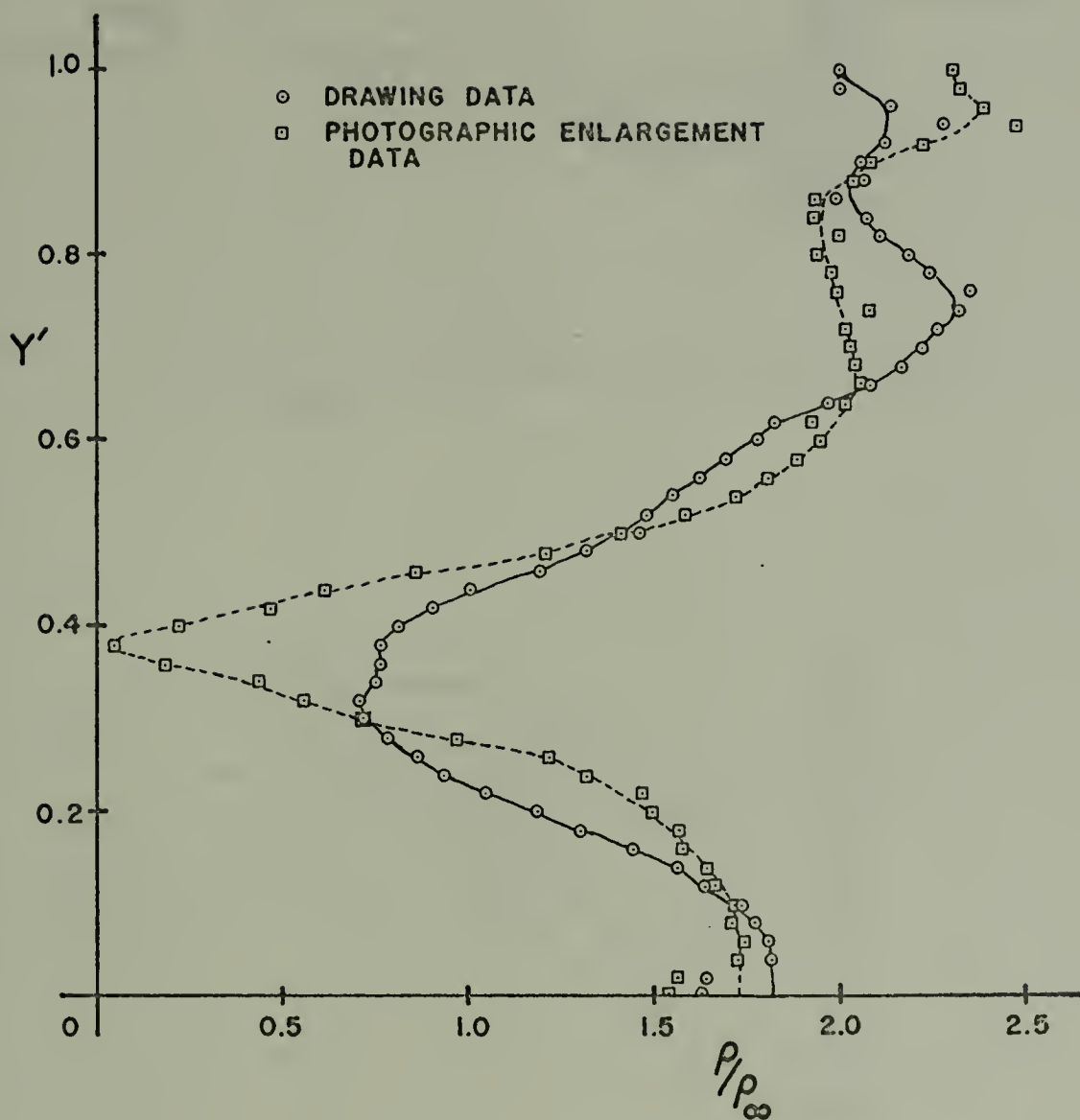
Figure 54. Comparison of the Density Distributions Calculated by
HOLOVLR for an Axisymmetric Case

94
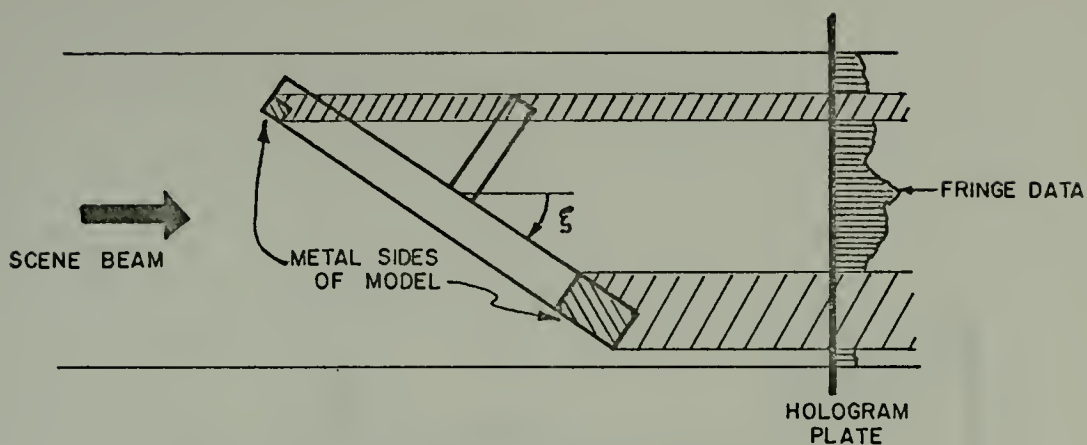
Figure 55. Schematic of the Model Center Section Rotated to Illustrate
the Loss of Fringe Information Due to Model Shadows on
the Hologram
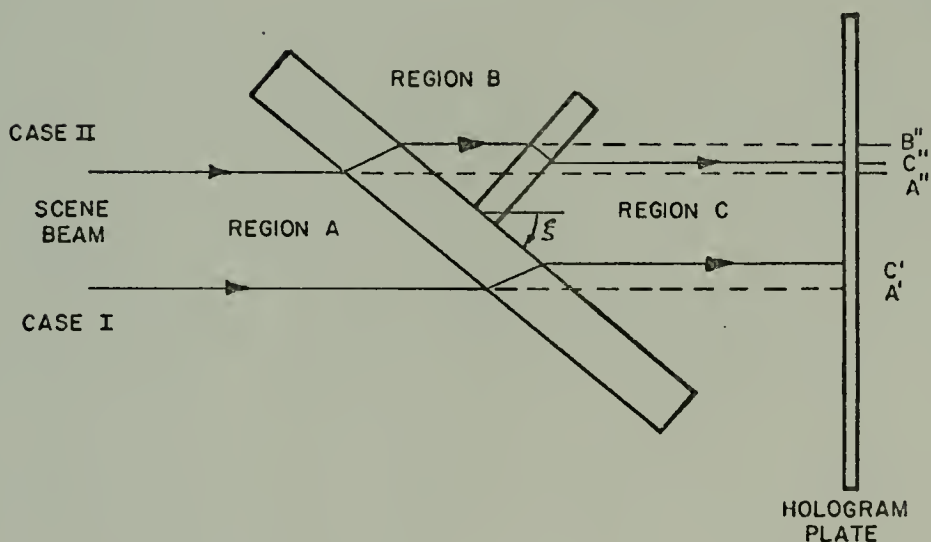
Figure 56. Schematic Illustrating the Problem of Different Fringe
Information Being Superimposed on One Beam Caused by the
Model Plastic
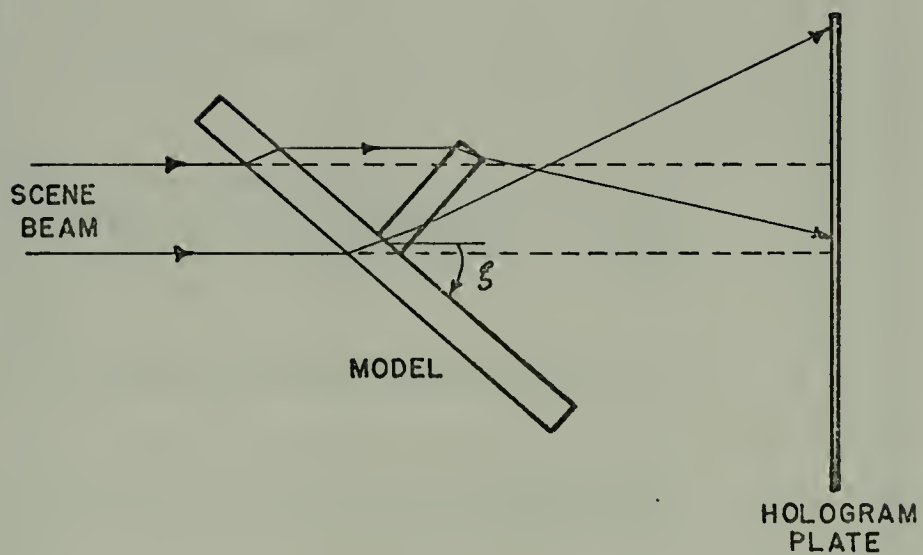
Figure 52.   Schematic Illustrating the Scene Beam Refraction in the
Fin Root and Tip Areas

Table I. Tabulation of Fringe Shift Data Taken From the Drawing of Photo 4

Line No.	Distance Above Aligned Plane			$\bigcirc' = \bigcirc + .055$	Fringe Location (inches) $\bigcirc$	Fringe Change $f = \bigcirc - \bigcirc$	Fringe Number $g = \frac{f}{h}$	Amount of 1.1 Fringe Correction Required	Corrected Values	
	Measured (inches)	Normalized $\bigcirc$ wing height	Corrected Distance from Tables						Y'	g
1	.190	.075	.071	.126	.360	.170	1.641	1.1	.081	2.74
2	.330	.131	.124	.179	.460	.130	1.255	1.1	.134	2.36
3	.465	.185	.176	.231	.590	.125	1.208	1.1	.186	2.31
4	.570	.226	.215	.270	.670	.100	.965	1.1	.225	2.07
5	.660	.262	.249	.304	.765	.105	1.013	1.1	.259	2.11
6	.745	.296	.281	.336	.860	.115	1.110	1.1	.291	2.21
7	.825	.327	.311	.366	.950	.125	1.208	1.1	.321	2.31
8	.950	.377	.358	.413	1.090	.140	1.352	1.1	.368	2.45
9	1.060	.421	.400	.455	1.240	.180	1.737	1.1	.410	2.84
10	1.180	.468	.445	.500	1.350	.170	1.641	1.1	.455	2.74
11	1.245	.494	.469	.524	1.500	.255	2.172	1.1	.479	3.27
12	1.350	.536	.509	.564	1.620	.270	2.607	.5	.543	3.11
13	1.430	.567	.539	.594	1.750	.320	3.090	.1	.590	3.19
14	1.533	.609	.579	.634	1.850	.315	3.041	0.	.634	3.04
15	1.625	.649	.617	.672	1.940	.315	3.041	0.	.672	3.04
16	1.720	.683	.649	.704	2.030	.310	2.994	0.	.704	2.99
17	1.830	.726	.690	.745	2.120	.290	2.800	0.	.745	2.80
18	1.955	.776	.737	.792	2.220	.265	2.560	0.	.792	2.56
19	2.080	.825	.783	.838	2.290	.210	2.028	0.	.838	2.03
20	2.180	.865	.821	.876	2.340	.160	1.545	0.	.876	1.55
21	2.315	.919	.872	.927	2.400	.085	.820	0.	.927	.82
22	2.400	.952	.904	.959	2.500	.100	.965	0.	.959	.97
23	2.500	.992	.942	.997	2.580	.080	.772	0.	.997	.77
24	2.570	1.020	.969	1.024	2.670	.100	.965	0.	1.024	.97
25	2.680	1.063	1.009	1.064	2.790	.110	1.062	0.	1.064	1.06
26	2.780	1.103	1.048	1.103	2.885	.115	1.110	0.	1.103	1.11

Wing height = 2.52 inches

Wing length = 2.92 inches

Average fringe interval = .1036 inches

96

Line No.	Distance Above Aligned Plane			Corrected Distance from Tables ③	Y' ④ = ③ + .055	Fringe Location (inches) ⑤	Fringe Change f = ⑤ − ④	Fringe Number $g = \frac{f}{b}$
	Measured (inches) ①	Corrected to Free Stream (inches) ②	Normalized $\frac{②}{\text{(wing height)}}$					
1	.190*	.076	.032	.030	.085	.270	.194	1.867
2	.290*	.176	.073	.069	.124	.390	.214	2.050
3	.410*	.296	.123	.117	.172	.450	.154	1.482
4	.525*	.411	.171	.162	.217	.560	.149	1.434
5	.615*	.501	.208	.198	.253	.650	.149	1.434
6	.710*	.596	.247	.235	.290	.725	.129	1.242
7	.800*	.686	.285	.271	.326	.830	.144	1.386
8	.910*	.796	.330	.314	.369	.980	.184	1.771
9	1.020*	.906	.376	.357	.412	1.140	.234	2.252
10	1.120*	1.006	.417	.396	.451	1.290	.284	2.738
11	1.230*	1.116	.463	.440	.495	1.420	.304	2.926
12	1.330*	1.216	.505	.480	.535	1.580	.364	3.503
13	1.370	1.370	.568	.540	.595	1.670	.300	2.887
14	1.460	1.460	.606	.576	.631	1.770	.310	2.984
15	1.560	1.560	.647	.615	.670	1.860	.300	2.887
16	1.660	1.660	.689	.655	.710	1.960	.300	2.887
17	1.760	1.760	.730	.694	.749	2.020	.260	2.502
18	1.880	1.880	.780	.741	.796	2.100	.220	2.117
19	2.000	2.000	.830	.788	.843	2.190	.190	1.829
20	2.110	2.110	.876	.832	.887	2.305	.195	1.877
21	2.220	2.220	.921	.875	.930	2.390	.170	1.704
22	2.330	2.330	.967	.919	.974	2.480	.150	1.444
23	2.445	2.445	1.015	.964	1.019	2.590	.145	1.396
24	2.570	2.570	1.066	1.013	1.068	2.680	.110	1.059
25	2.680	2.680	1.112	1.056	1.111	2.760	.080	.770
26	2.805	2.805	1.164	1.106	1.161	2.860	.055	.529

* Locations to be corrected to free stream conditions

Table II. Tabulation of Fringe Shift Data Taken From the Photographic Enlargement of Photo 4

REDUCTION OF AN INTERFEROGRAM TO OBTAIN FRINGE SHIFT DATA

The fringe shift reduction process was accomplished using two techniques. The first involved projecting the interferogram negative onto a sheet of white paper using a photo-enlarger. The light fringes offered the best contrast and were therefore traced out in Figures 30-34. In each drawing it was necessary to begin tracing the fringes above the fin and work towards the fin root since the transition across the fin tip determined the correct connection of the fringes across the fin leading edge shock. In order to determine the fringe change, one fringe line in the free stream region forward of the fin which appeared the straightest and paralleled the majority of other fringe lines was selected. A straight line, called the fringe reference line, was drawn over its centerline and extended to cross the y' axis. The remaining reference lines were then drawn parallel to the first and along the centerlines of the remaining free stream fringes. In reducing the drawings it was not realized until later that the free stream fringe patterns before and after the plate leading edge Prandtl-Meyer expansion differed considerably. This effect was taken into account later.

A ruler scaled to 0.01 inches was then placed along the y' axis and the distances of the fringes and reference lines above and below the aligned y' plane were then recorded in Table I for Photograph 4. The fin width and length were then measured and the average values were recorded. The average fringe interval was determined by measuring the distance between the first and last fringes used and dividing by the number of intervals. The fringe change was found by subtracting the fringe crossing

point. The fringe number was calculated by dividing the change by the average fringe interval. The reference line location was then normalized with respect to the measured fin height. Since the actual fin height was very close to one inch, the above number was considered to be the number of inches above or below the aligned plane. Thus the table computing the tunnel wall and grid refraction displacements in Appendix B could be entered to determine the actual reference line location with respect to the aligned plane of the drawing (see Figure 29). The locations were then converted to the y' axis system by adding the normalized location of the aligned plane. After realizing that not all the reference lines were referenced to the free stream density forward of the plate leading edge, the enlarged photographs (Figures 35-39) were checked against the drawings. It was found that the Prandtl-Meyer expansion caused a fringe number change of approximately 1.1. Consequently each reference line in the drawing was compared with the enlarged photograph and an appropriate percentage of the 1.1 fringe number was used as a correction (see Table I). The calculated fringe numbers had the correction fringe number added to them while the y' locations were corrected by

$$y'_{corr} = y'_{orig} - \frac{(1.1 \text{ Fringe no.}) \times (\text{Fringe Interval})}{(\text{Fin Height})} \qquad (A-1)$$

The second reduction technique was to use enlarged photographs made from the interferogram negatives to obtain the fringe change. The fringe lines were first traced over lightly with a pencil and then verified against the other photographs to ensure correct tracing. A datum fringe reference line was chosen as before and drawn. The remaining reference lines for the upper free stream fringe lines forward of the Prandtl-Meyer expansion were then drawn parallel to the datum. When it became impossible

99

to use fringe lines forward of the expansion, the reference lines were

then drawn along the centerline of the fringes between the expansion

and the fin. The same ruler was used to obtain the fringe crossing

points, the reference crossing points, fin measurements, and the average

fringe interval and they were recorded in Table 2. The reference line

crossing points were then corrected to free stream conditions, using a 1.1

Fringe number correction for those referenced to the pattern between the

expansion and fin leading edge. The fringe number and reference fin

locations were calculated as before. This method was considered more

accurate because the reference lines and fringe lines could easily be

rechecked for accuracy and corrected in the event that a fringe line

was traced incorrectly or a reference line was misaligned. The accuracy

was directly proportional to the hologram resolution which was not true

for the drawings since the reference lines are drawn parallel to hand-

drawn fringe lines.

APPENDIX B

CALCULATION OF TUNNEL WALL AND GRID PLASTIC REFRACTION CORRECTION

In the interferogram photographs used to obtain the fringe change, every point off the alignment axis will be slightly distorted due to the plastic tunnel wall and grid. This effect is illustrated in Figure 19. From Snells Law of Refraction, the angles of incidence and refraction are related by

$$\sin \alpha = n \sin \beta \qquad (B-1)$$

where n is the index of refraction between plastic and air. Then can be written

$$\beta = \sin^{-1} \left(\frac{\sin \alpha}{n} \right) \qquad (B-2)$$

Since the tunnel wall and grid have the same index of refraction, they can be considered on material with thickness t = ab in Figure 19. Then consider the height bd which can be written

$$bd = t \tan \alpha \qquad (B-3)$$

The beam displacement, Δy, is then

$$\Delta Y = bd - bc = t \tan \alpha - t \tan \beta \qquad (B-4)$$

but $\tan \alpha$ is

$$\tan \alpha = \frac{Y_{observed}}{L} \qquad (B-5)$$

Combining Equation (B-2), (B-4), and (B-5) the beam displacement becomes

$$\Delta Y = t \left[\frac{Y_{observed}}{L} - \tan \left[\sin^{-1} \left(\frac{\sin \alpha}{n} \right) \right] \right] \qquad (B-6)$$

The true location of the observed point is then

$$Y_{true} = Y_{observed} - \Delta Y \qquad (B-7)$$

101

A FORTRAN computer program was written to generate a table giving the true locations versus the observed locations. In the program the constants and variables from the above equations were defined as

$$Y_{observed} = Y$$

$$Y_{true} = YTRUE$$

$$\Delta Y = DY$$

$$\alpha = ALFA$$

$$L = L$$

$$n = N$$

Since the computer cannot calculate Equations (B-2) and (B-6) as written, they were constructed by parts using such letters as AA, AB, etc. The program and tables are included in the next few pages.

```
C      ***********************************************************
C      **                                                       **
C      **    THIS PROGRAM COMPUTES THE CORRECTION FOR THE       **
C      **    OFF AXIS TUNNEL WALL PARALLAX. THE FOLLOWING       **
C      **    INPUT PARAMETERS ARE REQUIRED:                     **
C      **    L = DISTANCE FROM HOLOGRAM PLANE TO THE MODEL      **
C      **        CENTER LINE                                    **
C      **    N = INDEX OF REFRACTION FOR TUNNEL WALL            **
C      **    T = THICKNESS OF TUNNEL AND GRID PLEXIGLAS         **
C      **    Y = OBSERVED DISTANCE OF THE POINT IN THE          **
C      **        PHOTOGRAPH FROM THE ALIGNED POINT              **
C      **    YTRUE = TRUE DISTANCE FROM ALIGNED POINT TO        **
C      **            THE POINT ON THE MODEL PLANE               **
C      **    YMAX = MAXIMUM DISTANCE OF INTEREST FROM THE       **
C      **           ALIGNED POINT                               **
C      **                                                       **
C      ***********************************************************
C
       REAL*4 L,N
C
C          INPUT PARAMETERS
C
       L=15.0
       N=1.5
       T=2.25
       YMAX=2.5
       PI=3.141593
C
C          OUTPUT FORMAT
C
       WRITE(6,100)L,N,T
  100  FORMAT('1',T25,'THE FOLLOWING TABLE IS TO ACCOUNT FOR'
      1' THE PARALLAX'/T25,'ERROR IN VIEWING THE MODEL '
      2'THROUGH GLASS WALLS AT'/T25,'ANY OTHER POINT THAN '
      3'AT THE ALIGNMENT POINT. INPUT'/T25,'PARAMETERS ARE:'
      4/T35,'(1) L = ',F6.3,' INCHES'/T35,'(2) N = ',F6.3,
      5' INCHES'/T35,'(3) T = ',F6.3,' INCHES')
       WRITE(6,110)
  110  FORMAT(' ',T24,'OBSERVED',T40,'TRUE',T54,'ERROR',T70,
      1'RAY'/T24,'DISTANCE',T38,'DISTANCE',T69,'ANGLE'/T24,
      2'(INCHES)',T38,'(INCHES)',T53,'(INCHES)',T67,
      3'(DEGREES)'/)
C
C          CALCULATIONS
C
       Y=0.0
   10  DO 15 I=1,2000
       AA=Y/L
       AB=ATAN(AA)
       ALFA=AB*180.0/PI
       AC=SIN(AB)/N
       BETA=ARSIN(AC)
       AD=TAN(BETA)
       DY=T*(AA-AD)
       YTRUE=Y-DY
C
       WRITE(6,200)Y,YTRUE,DY,ALFA
  200  FORMAT(' ',T24,F7.4,T38,F7.4,T53,F8.6,T67,F8.4)
       IF(MOD(I,10).EQ.0)WRITE(6,201)
  201  FORMAT(' ')
       IF(MOD(I,60).EQ.0)GO TO 11
       GO TO 12
   11  WRITE(6,202)
  202  FORMAT('1')
       WRITE(6,110)
   12  Y=.002*FLOAT(I)
       IF(Y.GE.YMAX)GO TO 20
   15  CONTINUE
   20  STOP
       END
```

THE FOLLOWING TABLE IS TO ACCOUNT FOR THE PARALLAX
ERROR IN VIEWING THE MODEL THROUGH GLASS WALLS AT
ANY OTHER POINT THAN AT THE ALIGNMENT POINT. INPUT
PARAMETERS ARE:
(1) L = 15.000 INCHES
(2) N =   1.500 INCHES
(3) T =   2.250 INCHES

OBSERVED DISTANCE (INCHES)	TRUE DISTANCE (INCHES)	ERROR (INCHES)	RAY ANGLE (DEGREES)
0.0	0.0	0.0	0.0
0.0020	0.0019	0.000100	0.0076
0.0040	0.0038	0.000200	0.0153
0.0060	0.0057	0.000300	0.0229
0.0080	0.0076	0.000400	0.0306
0.0100	0.0095	0.000500	0.0382
0.0120	0.0114	0.000600	0.0458
0.0140	0.0133	0.000700	0.0535
0.0160	0.0152	0.000800	0.0611
0.0180	0.0171	0.000900	0.0688
0.0200	0.0190	0.001000	0.0764
0.0220	0.0209	0.001100	0.0840
0.0240	0.0228	0.001200	0.0917
0.0260	0.0247	0.001300	0.0993
0.0280	0.0266	0.001400	0.1070
0.0300	0.0285	0.001500	0.1146
0.0320	0.0304	0.001600	0.1222
0.0340	0.0323	0.001700	0.1299
0.0360	0.0342	0.001800	0.1375
0.0380	0.0361	0.001900	0.1451
0.0400	0.0380	0.002000	0.1528
0.0420	0.0399	0.002100	0.1604
0.0440	0.0418	0.002200	0.1681
0.0460	0.0437	0.002300	0.1757
0.0480	0.0456	0.002400	0.1833
0.0500	0.0475	0.002500	0.1910
0.0520	0.0494	0.002600	0.1986
0.0540	0.0513	0.002700	0.2063
0.0560	0.0532	0.002800	0.2139
0.0580	0.0551	0.002900	0.2215
0.0600	0.0570	0.003000	0.2292
0.0620	0.0589	0.003100	0.2368
0.0640	0.0608	0.003200	0.2445
0.0660	0.0627	0.003300	0.2521
0.0680	0.0646	0.003400	0.2597
0.0700	0.0665	0.003500	0.2674
0.0720	0.0684	0.003600	0.2750
0.0740	0.0703	0.003700	0.2827
0.0760	0.0722	0.003800	0.2903
0.0780	0.0741	0.003900	0.2979
0.0800	0.0760	0.004000	0.3056
0.0820	0.0779	0.004100	0.3132
0.0840	0.0798	0.004200	0.3209
0.0860	0.0817	0.004300	0.3285
0.0880	0.0836	0.004400	0.3361
0.0900	0.0855	0.004500	0.3438
0.0920	0.0874	0.004600	0.3514
0.0940	0.0893	0.004700	0.3590
0.0960	0.0912	0.004800	0.3667
0.0980	0.0931	0.004900	0.3743
0.1000	0.0950	0.005000	0.3820
0.1020	0.0969	0.005100	0.3896
0.1040	0.0988	0.005200	0.3972
0.1060	0.1007	0.005300	0.4049
0.1080	0.1026	0.005400	0.4125
0.1100	0.1045	0.005500	0.4202
0.1120	0.1064	0.005600	0.4278
0.1140	0.1083	0.005700	0.4354
0.1160	0.1102	0.005800	0.4431
0.1180	0.1121	0.005900	0.4507

OBSERVED DISTANCE (INCHES)	TRUE DISTANCE (INCHES)	ERROR (INCHES)	RAY ANGLE (DEGREES)
0.1200	0.1140	0.006000	0.4584
0.1220	0.1159	0.006100	0.4660
0.1240	0.1178	0.006200	0.4736
0.1260	0.1197	0.006300	0.4813
0.1280	0.1216	0.006400	0.4889
0.1300	0.1235	0.006500	0.4966
0.1320	0.1254	0.006600	0.5042
0.1340	0.1273	0.006700	0.5118
0.1360	0.1292	0.006800	0.5195
0.1380	0.1311	0.006900	0.5271
0.1400	0.1330	0.007000	0.5347
0.1420	0.1349	0.007100	0.5424
0.1440	0.1368	0.007200	0.5500
0.1460	0.1387	0.007300	0.5577
0.1480	0.1406	0.007400	0.5653
0.1500	0.1425	0.007500	0.5729
0.1520	0.1444	0.007600	0.5806
0.1540	0.1463	0.007700	0.5882
0.1560	0.1482	0.007800	0.5959
0.1580	0.1501	0.007901	0.6035
0.1600	0.1520	0.008001	0.6111
0.1620	0.1539	0.008101	0.6188
0.1640	0.1558	0.008201	0.6264
0.1660	0.1577	0.008301	0.6340
0.1680	0.1596	0.008401	0.6417
0.1700	0.1615	0.008501	0.6493
0.1720	0.1634	0.008601	0.6570
0.1740	0.1653	0.008701	0.6646
0.1760	0.1672	0.008801	0.6722
0.1780	0.1691	0.008901	0.6799
0.1800	0.1710	0.009001	0.6875
0.1820	0.1729	0.009101	0.6952
0.1840	0.1748	0.009201	0.7028
0.1860	0.1767	0.009301	0.7104
0.1880	0.1786	0.009401	0.7181
0.1900	0.1805	0.009501	0.7257
0.1920	0.1824	0.009601	0.7333
0.1940	0.1843	0.009701	0.7410
0.1960	0.1862	0.009801	0.7486
0.1980	0.1881	0.009901	0.7563
0.2000	0.1900	0.010001	0.7639
0.2020	0.1919	0.010101	0.7715
0.2040	0.1938	0.010201	0.7792
0.2060	0.1957	0.010301	0.7868
0.2080	0.1976	0.010401	0.7944
0.2100	0.1995	0.010501	0.8021
0.2120	0.2014	0.010601	0.8097
0.2140	0.2033	0.010701	0.8174
0.2160	0.2052	0.010801	0.8250
0.2180	0.2071	0.010901	0.8326
0.2200	0.2090	0.011001	0.8403
0.2220	0.2109	0.011101	0.8479
0.2240	0.2128	0.011201	0.8556
0.2260	0.2147	0.011301	0.8632
0.2280	0.2166	0.011401	0.8708
0.2300	0.2185	0.011502	0.8785
0.2320	0.2204	0.011602	0.8861
0.2340	0.2223	0.011702	0.8937
0.2360	0.2242	0.011802	0.9014
0.2380	0.2261	0.011902	0.9090

OBSERVED DISTANCE (INCHES)	TRUE DISTANCE (INCHES)	ERROR (INCHES)	RAY ANGLE (DEGREES)
0.2400	0.2280	0.012002	0.9167
0.2420	0.2299	0.012102	0.9243
0.2440	0.2318	0.012202	0.9319
0.2460	0.2337	0.012302	0.9396
0.2480	0.2356	0.012402	0.9472
0.2500	0.2375	0.012502	0.9548
0.2520	0.2394	0.012602	0.9625
0.2540	0.2413	0.012702	0.9701
0.2560	0.2432	0.012802	0.9778
0.2580	0.2451	0.012902	0.9854
0.2600	0.2470	0.013002	0.9930
0.2620	0.2489	0.013102	1.0007
0.2640	0.2508	0.013202	1.0083
0.2660	0.2527	0.013302	1.0159
0.2680	0.2546	0.013402	1.0236
0.2700	0.2565	0.013502	1.0312
0.2720	0.2584	0.013602	1.0388
0.2740	0.2603	0.013703	1.0465
0.2760	0.2622	0.013803	1.0541
0.2780	0.2641	0.013903	1.0618
0.2800	0.2660	0.014003	1.0694
0.2820	0.2679	0.014103	1.0770
0.2840	0.2698	0.014203	1.0847
0.2860	0.2717	0.014303	1.0923
0.2880	0.2736	0.014403	1.0999
0.2900	0.2755	0.014503	1.1076
0.2920	0.2774	0.014603	1.1152
0.2940	0.2793	0.014703	1.1229
0.2960	0.2812	0.014803	1.1305
0.2980	0.2831	0.014903	1.1381
0.3000	0.2850	0.015003	1.1458
0.3020	0.2869	0.015103	1.1534
0.3040	0.2888	0.015203	1.1610
0.3060	0.2907	0.015304	1.1687
0.3080	0.2926	0.015404	1.1763
0.3100	0.2945	0.015504	1.1839
0.3120	0.2964	0.015604	1.1916
0.3140	0.2983	0.015704	1.1992
0.3160	0.3002	0.015804	1.2069
0.3180	0.3021	0.015904	1.2145
0.3200	0.3040	0.016004	1.2221
0.3220	0.3059	0.016104	1.2298
0.3240	0.3078	0.016204	1.2374
0.3260	0.3097	0.016304	1.2450
0.3280	0.3116	0.016404	1.2527
0.3300	0.3135	0.016504	1.2603
0.3320	0.3154	0.016605	1.2679
0.3340	0.3173	0.016705	1.2756
0.3360	0.3192	0.016805	1.2832
0.3380	0.3211	0.016905	1.2908
0.3400	0.3230	0.017005	1.2985
0.3420	0.3249	0.017105	1.3061
0.3440	0.3268	0.017205	1.3138
0.3460	0.3287	0.017305	1.3214
0.3480	0.3306	0.017405	1.3290
0.3500	0.3325	0.017505	1.3367
0.3520	0.3344	0.017605	1.3443
0.3540	0.3363	0.017705	1.3519
0.3560	0.3382	0.017806	1.3596
0.3580	0.3401	0.017906	1.3672

OBSERVED DISTANCE (INCHES)	TRUE DISTANCE (INCHES)	ERROR (INCHES)	RAY ANGLE (DEGREES)
0.3600	0.3420	0.018006	1.3748
0.3620	0.3439	0.018106	1.3825
0.3640	0.3458	0.018206	1.3901
0.3660	0.3477	0.018306	1.3977
0.3680	0.3496	0.018406	1.4054
0.3700	0.3515	0.018506	1.4130
0.3720	0.3534	0.018606	1.4206
0.3740	0.3553	0.018706	1.4283
0.3760	0.3572	0.018807	1.4359
0.3780	0.3591	0.018907	1.4435
0.3800	0.3610	0.019007	1.4512
0.3820	0.3629	0.019107	1.4588
0.3840	0.3648	0.019207	1.4665
0.3860	0.3667	0.019307	1.4741
0.3880	0.3686	0.019407	1.4817
0.3900	0.3705	0.019507	1.4894
0.3920	0.3724	0.019607	1.4970
0.3940	0.3743	0.019708	1.5046
0.3960	0.3762	0.019808	1.5123
0.3980	0.3781	0.019908	1.5199
0.4000	0.3800	0.020008	1.5275
0.4020	0.3819	0.020108	1.5352
0.4040	0.3838	0.020208	1.5428
0.4060	0.3857	0.020308	1.5504
0.4080	0.3876	0.020408	1.5581
0.4100	0.3895	0.020509	1.5657
0.4120	0.3914	0.020609	1.5733
0.4140	0.3933	0.020709	1.5810
0.4160	0.3952	0.020809	1.5886
0.4180	0.3971	0.020909	1.5962
0.4200	0.3990	0.021009	1.6039
0.4220	0.4009	0.021109	1.6115
0.4240	0.4028	0.021209	1.6191
0.4260	0.4047	0.021310	1.6268
0.4280	0.4066	0.021410	1.6344
0.4300	0.4085	0.021510	1.6420
0.4320	0.4104	0.021610	1.6497
0.4340	0.4123	0.021710	1.6573
0.4360	0.4142	0.021810	1.6649
0.4380	0.4161	0.021910	1.6726
0.4400	0.4180	0.022011	1.6802
0.4420	0.4199	0.022111	1.6878
0.4440	0.4218	0.022211	1.6955
0.4460	0.4237	0.022311	1.7031
0.4480	0.4256	0.022411	1.7107
0.4500	0.4275	0.022511	1.7184
0.4520	0.4294	0.022611	1.7260
0.4540	0.4313	0.022712	1.7336
0.4560	0.4332	0.022812	1.7413
0.4580	0.4351	0.022912	1.7489
0.4600	0.4370	0.023012	1.7565
0.4620	0.4389	0.023112	1.7642
0.4640	0.4408	0.023212	1.7718
0.4660	0.4427	0.023312	1.7794
0.4680	0.4446	0.023413	1.7870
0.4700	0.4465	0.023513	1.7947
0.4720	0.4484	0.023613	1.8023
0.4740	0.4503	0.023713	1.8099
0.4760	0.4522	0.023813	1.8176
0.4780	0.4541	0.023913	1.8252

OBSERVED DISTANCE (INCHES)	TRUE DISTANCE (INCHES)	ERROR (INCHES)	RAY ANGLE (DEGREES)
0.4800	0.4560	0.024014	1.8328
0.4820	0.4579	0.024114	1.8405
0.4840	0.4598	0.024214	1.8481
0.4860	0.4617	0.024314	1.8557
0.4880	0.4636	0.024414	1.8634
0.4900	0.4655	0.024515	1.8710
0.4920	0.4674	0.024615	1.8786
0.4940	0.4693	0.024715	1.8863
0.4960	0.4712	0.024815	1.8939
0.4980	0.4731	0.024915	1.9015
0.5000	0.4750	0.025015	1.9092
0.5020	0.4769	0.025116	1.9168
0.5040	0.4788	0.025216	1.9244
0.5060	0.4807	0.025316	1.9320
0.5080	0.4826	0.025416	1.9397
0.5100	0.4845	0.025516	1.9473
0.5120	0.4864	0.025617	1.9549
0.5140	0.4883	0.025717	1.9626
0.5160	0.4902	0.025817	1.9702
0.5180	0.4921	0.025917	1.9778
0.5200	0.4940	0.026017	1.9855
0.5220	0.4959	0.026118	1.9931
0.5240	0.4978	0.026218	2.0007
0.5260	0.4997	0.026318	2.0083
0.5280	0.5016	0.026418	2.0160
0.5300	0.5035	0.026518	2.0236
0.5320	0.5054	0.026619	2.0312
0.5340	0.5073	0.026719	2.0389
0.5360	0.5092	0.026819	2.0465
0.5380	0.5111	0.026919	2.0541
0.5400	0.5130	0.027019	2.0618
0.5420	0.5149	0.027120	2.0694
0.5440	0.5168	0.027220	2.0770
0.5460	0.5187	0.027320	2.0846
0.5480	0.5206	0.027420	2.0923
0.5500	0.5225	0.027521	2.0999
0.5520	0.5244	0.027621	2.1075
0.5540	0.5263	0.027721	2.1152
0.5560	0.5282	0.027821	2.1228
0.5580	0.5301	0.027921	2.1304
0.5600	0.5320	0.028022	2.1380
0.5620	0.5339	0.028122	2.1457
0.5640	0.5358	0.028222	2.1533
0.5660	0.5377	0.028322	2.1609
0.5680	0.5396	0.028423	2.1686
0.5700	0.5415	0.028523	2.1762
0.5720	0.5434	0.028623	2.1838
0.5740	0.5453	0.028723	2.1914
0.5760	0.5472	0.028824	2.1991
0.5780	0.5491	0.028924	2.2067
0.5800	0.5510	0.029024	2.2143
0.5820	0.5529	0.029124	2.2220
0.5840	0.5548	0.029225	2.2296
0.5860	0.5567	0.029325	2.2372
0.5880	0.5586	0.029425	2.2448
0.5900	0.5605	0.029525	2.2525
0.5920	0.5624	0.029626	2.2601
0.5940	0.5643	0.029726	2.2677
0.5960	0.5662	0.029826	2.2754
0.5980	0.5681	0.029926	2.2830

OBSERVED DISTANCE (INCHES)	TRUE DISTANCE (INCHES)	ERROR (INCHES)	RAY ANGLE (DEGREES)
0.6000	0.5700	0.030027	2.2906
0.6020	0.5719	0.030127	2.2982
0.6040	0.5738	0.030227	2.3059
0.6060	0.5757	0.030327	2.3135
0.6080	0.5776	0.030428	2.3211
0.6100	0.5795	0.030528	2.3287
0.6120	0.5814	0.030628	2.3364
0.6140	0.5833	0.030729	2.3440
0.6160	0.5852	0.030829	2.3516
0.6180	0.5871	0.030929	2.3593
0.6200	0.5890	0.031029	2.3669
0.6220	0.5909	0.031130	2.3745
0.6240	0.5928	0.031230	2.3821
0.6260	0.5947	0.031330	2.3898
0.6280	0.5966	0.031431	2.3974
0.6300	0.5985	0.031531	2.4050
0.6320	0.6004	0.031631	2.4126
0.6340	0.6023	0.031731	2.4203
0.6360	0.6042	0.031832	2.4279
0.6380	0.6061	0.031932	2.4355
0.6400	0.6080	0.032032	2.4431
0.6420	0.6099	0.032133	2.4508
0.6440	0.6118	0.032233	2.4584
0.6460	0.6137	0.032333	2.4660
0.6480	0.6156	0.032434	2.4736
0.6500	0.6175	0.032534	2.4813
0.6520	0.6194	0.032634	2.4889
0.6540	0.6213	0.032735	2.4965
0.6560	0.6232	0.032835	2.5041
0.6580	0.6251	0.032935	2.5118
0.6600	0.6270	0.033035	2.5194
0.6620	0.6289	0.033136	2.5270
0.6640	0.6308	0.033236	2.5346
0.6660	0.6327	0.033336	2.5423
0.6680	0.6346	0.033437	2.5499
0.6700	0.6365	0.033537	2.5575
0.6720	0.6384	0.033637	2.5651
0.6740	0.6403	0.033738	2.5728
0.6760	0.6422	0.033838	2.5804
0.6780	0.6441	0.033938	2.5880
0.6800	0.6460	0.034039	2.5956
0.6820	0.6479	0.034139	2.6033
0.6840	0.6498	0.034239	2.6109
0.6860	0.6517	0.034340	2.6185
0.6880	0.6536	0.034440	2.6261
0.6900	0.6555	0.034541	2.6337
0.6920	0.6574	0.034641	2.6414
0.6940	0.6593	0.034741	2.6490
0.6960	0.6612	0.034842	2.6566
0.6980	0.6631	0.034942	2.6642
0.7000	0.6650	0.035042	2.6719
0.7020	0.6669	0.035143	2.6795
0.7040	0.6688	0.035243	2.6871
0.7060	0.6707	0.035343	2.6947
0.7080	0.6726	0.035444	2.7024
0.7100	0.6745	0.035544	2.7100
0.7120	0.6764	0.035645	2.7176
0.7140	0.6783	0.035745	2.7252
0.7160	0.6802	0.035845	2.7328
0.7180	0.6821	0.035946	2.7405

OBSERVED DISTANCE (INCHES)	TRUE DISTANCE (INCHES)	ERROR (INCHES)	RAY ANGLE (DEGREES)
0.7200	0.6840	0.036046	2.7481
0.7220	0.6859	0.036146	2.7557
0.7240	0.6878	0.036247	2.7633
0.7260	0.6897	0.036347	2.7710
0.7280	0.6916	0.036448	2.7786
0.7300	0.6935	0.036548	2.7862
0.7320	0.6954	0.036648	2.7938
0.7340	0.6973	0.036749	2.8014
0.7360	0.6992	0.036849	2.8091
0.7380	0.7011	0.036950	2.8167
0.7400	0.7029	0.037050	2.8243
0.7420	0.7048	0.037150	2.8319
0.7440	0.7067	0.037251	2.8395
0.7460	0.7086	0.037351	2.8472
0.7480	0.7105	0.037452	2.8548
0.7500	0.7124	0.037552	2.8624
0.7520	0.7143	0.037652	2.8700
0.7540	0.7162	0.037753	2.8776
0.7560	0.7181	0.037853	2.8853
0.7580	0.7200	0.037954	2.8929
0.7600	0.7219	0.038054	2.9005
0.7620	0.7238	0.038155	2.9081
0.7640	0.7257	0.038255	2.9157
0.7660	0.7276	0.038355	2.9234
0.7680	0.7295	0.038456	2.9310
0.7700	0.7314	0.038556	2.9386
0.7720	0.7333	0.038657	2.9462
0.7740	0.7352	0.038757	2.9538
0.7760	0.7371	0.038858	2.9615
0.7780	0.7390	0.038958	2.9691
0.7800	0.7409	0.039059	2.9767
0.7820	0.7428	0.039159	2.9843
0.7840	0.7447	0.039259	2.9919
0.7860	0.7466	0.039360	2.9996
0.7880	0.7485	0.039460	3.0072
0.7900	0.7504	0.039561	3.0148
0.7920	0.7523	0.039661	3.0224
0.7940	0.7542	0.039762	3.0300
0.7960	0.7561	0.039862	3.0376
0.7980	0.7580	0.039963	3.0453
0.8000	0.7599	0.040063	3.0529
0.8020	0.7618	0.040164	3.0605
0.8040	0.7637	0.040264	3.0681
0.8060	0.7656	0.040365	3.0757
0.8080	0.7675	0.040465	3.0834
0.8100	0.7694	0.040566	3.0910
0.8120	0.7713	0.040666	3.0986
0.8140	0.7732	0.040767	3.1062
0.8160	0.7751	0.040867	3.1138
0.8180	0.7770	0.040968	3.1214
0.8200	0.7789	0.041068	3.1291
0.8220	0.7808	0.041169	3.1367
0.8240	0.7827	0.041269	3.1443
0.8260	0.7846	0.041369	3.1519
0.8280	0.7865	0.041470	3.1595
0.8300	0.7884	0.041570	3.1671
0.8320	0.7903	0.041671	3.1748
0.8340	0.7922	0.041772	3.1824
0.8360	0.7941	0.041872	3.1900
0.8380	0.7960	0.041973	3.1976

OBSERVED DISTANCE (INCHES)	TRUE DISTANCE (INCHES)	ERROR (INCHES)	RAY ANGLE (DEGREES)
0.8400	0.7979	0.042073	3.2052
0.8420	0.7998	0.042174	3.2128
0.8440	0.8017	0.042274	3.2204
0.8460	0.8036	0.042375	3.2281
0.8480	0.8055	0.042475	3.2357
0.8500	0.8074	0.042576	3.2433
0.8520	0.8093	0.042676	3.2509
0.8540	0.8112	0.042777	3.2585
0.8560	0.8131	0.042877	3.2661
0.8580	0.8150	0.042978	3.2738
0.8600	0.8169	0.043078	3.2814
0.8620	0.8188	0.043179	3.2890
0.8640	0.8207	0.043280	3.2966
0.8660	0.8226	0.043380	3.3042
0.8680	0.8245	0.043481	3.3118
0.8700	0.8264	0.043581	3.3194
0.8720	0.8283	0.043682	3.3270
0.8740	0.8302	0.043782	3.3347
0.8760	0.8321	0.043883	3.3423
0.8780	0.8340	0.043983	3.3499
0.8800	0.8359	0.044084	3.3575
0.8820	0.8378	0.044185	3.3651
0.8840	0.8397	0.044285	3.3727
0.8860	0.8416	0.044386	3.3803
0.8880	0.8435	0.044486	3.3880
0.8900	0.8454	0.044587	3.3956
0.8920	0.8473	0.044688	3.4032
0.8940	0.8492	0.044788	3.4108
0.8960	0.8511	0.044889	3.4184
0.8980	0.8530	0.044989	3.4260
0.9000	0.8549	0.045090	3.4336
0.9020	0.8568	0.045190	3.4412
0.9040	0.8587	0.045291	3.4489
0.9060	0.8606	0.045392	3.4565
0.9080	0.8625	0.045492	3.4641
0.9100	0.8644	0.045593	3.4717
0.9120	0.8663	0.045693	3.4793
0.9140	0.8682	0.045794	3.4869
0.9160	0.8701	0.045895	3.4945
0.9180	0.8720	0.045995	3.5021
0.9200	0.8739	0.046096	3.5097
0.9220	0.8758	0.046197	3.5174
0.9240	0.8777	0.046297	3.5250
0.9260	0.8796	0.046398	3.5326
0.9280	0.8815	0.046499	3.5402
0.9300	0.8834	0.046599	3.5478
0.9320	0.8853	0.046700	3.5554
0.9340	0.8872	0.046800	3.5630
0.9360	0.8891	0.046901	3.5706
0.9380	0.8910	0.047002	3.5782
0.9400	0.8929	0.047102	3.5858
0.9420	0.8948	0.047203	3.5935
0.9440	0.8967	0.047304	3.6011
0.9460	0.8986	0.047404	3.6087
0.9480	0.9005	0.047505	3.6163
0.9500	0.9024	0.047606	3.6239
0.9520	0.9043	0.047706	3.6315
0.9540	0.9062	0.047807	3.6391
0.9560	0.9081	0.047908	3.6467
0.9580	0.9100	0.048009	3.6543

OBSERVED DISTANCE (INCHES)	TRUE DISTANCE (INCHES)	ERROR (INCHES)	RAY ANGLE (DEGREES)
0.9600	0.9119	0.048109	3.6619
0.9620	0.9138	0.048210	3.6695
0.9640	0.9157	0.048310	3.6771
0.9660	0.9176	0.048411	3.6848
0.9680	0.9195	0.048512	3.6924
0.9700	0.9214	0.048613	3.7000
0.9720	0.9233	0.048713	3.7076
0.9740	0.9252	0.048814	3.7152
0.9760	0.9271	0.048915	3.7228
0.9780	0.9290	0.049015	3.7304
0.9800	0.9309	0.049116	3.7380
0.9820	0.9328	0.049217	3.7456
0.9840	0.9347	0.049318	3.7532
0.9860	0.9366	0.049418	3.7608
0.9880	0.9385	0.049519	3.7684
0.9900	0.9404	0.049620	3.7760
0.9920	0.9423	0.049720	3.7836
0.9940	0.9442	0.049821	3.7913
0.9960	0.9461	0.049922	3.7989
0.9980	0.9480	0.050023	3.8065
1.0000	0.9499	0.050123	3.8141
1.0020	0.9518	0.050224	3.8217
1.0040	0.9537	0.050325	3.8293
1.0060	0.9556	0.050426	3.8369
1.0080	0.9575	0.050526	3.8445
1.0100	0.9594	0.050627	3.8521
1.0120	0.9613	0.050728	3.8597
1.0140	0.9632	0.050829	3.8673
1.0160	0.9651	0.050929	3.8749
1.0180	0.9670	0.051030	3.8825
1.0200	0.9689	0.051131	3.8901
1.0220	0.9708	0.051232	3.8977
1.0240	0.9727	0.051332	3.9053
1.0260	0.9746	0.051433	3.9129
1.0280	0.9765	0.051534	3.9205
1.0300	0.9784	0.051635	3.9281
1.0320	0.9803	0.051735	3.9357
1.0340	0.9822	0.051836	3.9433
1.0360	0.9841	0.051937	3.9509
1.0380	0.9860	0.052038	3.9586
1.0400	0.9879	0.052139	3.9662
1.0420	0.9898	0.052240	3.9738
1.0440	0.9917	0.052340	3.9814
1.0460	0.9936	0.052441	3.9890
1.0480	0.9955	0.052542	3.9966
1.0500	0.9974	0.052643	4.0042
1.0520	0.9993	0.052743	4.0118
1.0540	1.0012	0.052844	4.0194
1.0560	1.0031	0.052945	4.0270
1.0580	1.0050	0.053046	4.0346
1.0600	1.0069	0.053147	4.0422
1.0620	1.0088	0.053248	4.0498
1.0640	1.0107	0.053348	4.0574
1.0660	1.0125	0.053449	4.0650
1.0680	1.0144	0.053550	4.0726
1.0700	1.0163	0.053651	4.0802
1.0720	1.0182	0.053752	4.0878
1.0740	1.0201	0.053853	4.0954
1.0760	1.0220	0.053953	4.1030
1.0780	1.0239	0.054054	4.1106

OBSERVED DISTANCE (INCHES)	TRUE DISTANCE (INCHES)	ERROR (INCHES)	RAY ANGLE (DEGREES)
1.0800	1.0258	0.054155	4.1182
1.0820	1.0277	0.054256	4.1258
1.0840	1.0296	0.054357	4.1334
1.0860	1.0315	0.054458	4.1410
1.0880	1.0334	0.054559	4.1486
1.0900	1.0353	0.054660	4.1562
1.0920	1.0372	0.054760	4.1638
1.0940	1.0391	0.054861	4.1714
1.0960	1.0410	0.054962	4.1790
1.0980	1.0429	0.055063	4.1866
1.1000	1.0448	0.055164	4.1942
1.1020	1.0467	0.055265	4.2018
1.1040	1.0486	0.055366	4.2094
1.1060	1.0505	0.055467	4.2170
1.1080	1.0524	0.055568	4.2246
1.1100	1.0543	0.055668	4.2322
1.1120	1.0562	0.055769	4.2398
1.1140	1.0581	0.055870	4.2474
1.1160	1.0600	0.055971	4.2550
1.1180	1.0619	0.056072	4.2626
1.1200	1.0638	0.056173	4.2702
1.1220	1.0657	0.056274	4.2778
1.1240	1.0676	0.056375	4.2854
1.1260	1.0695	0.056476	4.2929
1.1280	1.0714	0.056577	4.3005
1.1300	1.0733	0.056678	4.3081
1.1320	1.0752	0.056779	4.3157
1.1340	1.0771	0.056880	4.3233
1.1360	1.0790	0.056981	4.3309
1.1380	1.0809	0.057082	4.3385
1.1400	1.0828	0.057183	4.3461
1.1420	1.0847	0.057284	4.3537
1.1440	1.0866	0.057385	4.3613
1.1460	1.0885	0.057486	4.3689
1.1480	1.0904	0.057586	4.3765
1.1500	1.0923	0.057687	4.3841
1.1520	1.0942	0.057788	4.3917
1.1540	1.0961	0.057889	4.3993
1.1560	1.0980	0.057990	4.4069
1.1580	1.0999	0.058091	4.4145
1.1600	1.1018	0.058192	4.4221
1.1620	1.1037	0.058293	4.4297
1.1640	1.1056	0.058394	4.4373
1.1660	1.1075	0.058495	4.4448
1.1680	1.1094	0.058596	4.4524
1.1700	1.1113	0.058697	4.4600
1.1720	1.1132	0.058798	4.4676
1.1740	1.1151	0.058899	4.4752
1.1760	1.1170	0.059000	4.4828
1.1780	1.1189	0.059101	4.4904
1.1800	1.1208	0.059202	4.4980
1.1820	1.1227	0.059303	4.5056
1.1840	1.1246	0.059404	4.5132
1.1860	1.1265	0.059506	4.5208
1.1880	1.1284	0.059607	4.5284
1.1900	1.1303	0.059708	4.5360
1.1920	1.1322	0.059809	4.5436
1.1940	1.1341	0.059910	4.5511
1.1960	1.1360	0.060011	4.5587
1.1980	1.1379	0.060112	4.5663

OBSERVED DISTANCE (INCHES)	TRUE DISTANCE (INCHES)	ERROR (INCHES)	RAY ANGLE (DEGREES)
1.2000	1.1398	0.060213	4.5739
1.2020	1.1417	0.060314	4.5815
1.2040	1.1436	0.060415	4.5891
1.2060	1.1455	0.060516	4.5967
1.2080	1.1474	0.060617	4.6043
1.2100	1.1493	0.060718	4.6119
1.2120	1.1512	0.060819	4.6195
1.2140	1.1531	0.060920	4.6270
1.2160	1.1550	0.061021	4.6346
1.2180	1.1569	0.061123	4.6422
1.2200	1.1588	0.061224	4.6498
1.2220	1.1607	0.061325	4.6574
1.2240	1.1626	0.061426	4.6650
1.2260	1.1645	0.061527	4.6726
1.2280	1.1664	0.061628	4.6802
1.2300	1.1683	0.061729	4.6878
1.2320	1.1702	0.061830	4.6954
1.2340	1.1721	0.061931	4.7029
1.2360	1.1740	0.062032	4.7105
1.2380	1.1759	0.062134	4.7181
1.2400	1.1778	0.062235	4.7257
1.2420	1.1797	0.062336	4.7333
1.2440	1.1816	0.062437	4.7409
1.2460	1.1835	0.062538	4.7485
1.2480	1.1854	0.062639	4.7560
1.2500	1.1873	0.062740	4.7636
1.2520	1.1892	0.062842	4.7712
1.2540	1.1911	0.062943	4.7788
1.2560	1.1930	0.063044	4.7864
1.2580	1.1949	0.063145	4.7940
1.2600	1.1968	0.063246	4.8016
1.2620	1.1987	0.063348	4.8092
1.2640	1.2006	0.063448	4.8167
1.2660	1.2024	0.063550	4.8243
1.2680	1.2043	0.063651	4.8319
1.2700	1.2062	0.063752	4.8395
1.2720	1.2081	0.063854	4.8471
1.2740	1.2100	0.063955	4.8547
1.2760	1.2119	0.064056	4.8622
1.2780	1.2138	0.064157	4.8698
1.2800	1.2157	0.064258	4.8774
1.2820	1.2176	0.064360	4.8850
1.2840	1.2195	0.064461	4.8926
1.2860	1.2214	0.064562	4.9002
1.2880	1.2233	0.064663	4.9078
1.2900	1.2252	0.064764	4.9153
1.2920	1.2271	0.064865	4.9229
1.2940	1.2290	0.064967	4.9305
1.2960	1.2309	0.065068	4.9381
1.2980	1.2328	0.065169	4.9457
1.3000	1.2347	0.065270	4.9533
1.3020	1.2366	0.065372	4.9608
1.3040	1.2385	0.065473	4.9684
1.3060	1.2404	0.065574	4.9760
1.3080	1.2423	0.065675	4.9836
1.3100	1.2442	0.065777	4.9912
1.3120	1.2461	0.065878	4.9987
1.3140	1.2480	0.065979	5.0063
1.3160	1.2499	0.066081	5.0139
1.3180	1.2518	0.066182	5.0215

OBSERVED DISTANCE (INCHES)	TRUE DISTANCE (INCHES)	ERROR (INCHES)	RAY ANGLE (DEGREES)
1.3200	1.2537	0.066283	5.0291
1.3220	1.2556	0.066384	5.0366
1.3240	1.2575	0.066486	5.0442
1.3260	1.2594	0.066587	5.0518
1.3280	1.2613	0.066688	5.0594
1.3300	1.2632	0.066789	5.0670
1.3320	1.2651	0.066891	5.0745
1.3340	1.2670	0.066992	5.0821
1.3360	1.2689	0.067093	5.0897
1.3380	1.2708	0.067195	5.0973
1.3400	1.2727	0.067296	5.1049
1.3420	1.2746	0.067398	5.1124
1.3440	1.2765	0.067499	5.1200
1.3460	1.2784	0.067600	5.1276
1.3480	1.2803	0.067701	5.1352
1.3500	1.2822	0.067803	5.1428
1.3520	1.2841	0.067904	5.1503
1.3540	1.2860	0.068005	5.1579
1.3560	1.2879	0.068107	5.1655
1.3580	1.2898	0.068208	5.1731
1.3600	1.2917	0.068309	5.1806
1.3620	1.2936	0.068411	5.1882
1.3640	1.2955	0.068512	5.1958
1.3660	1.2974	0.068614	5.2034
1.3680	1.2993	0.068715	5.2110
1.3700	1.3012	0.068816	5.2185
1.3720	1.3031	0.068918	5.2261
1.3740	1.3050	0.069019	5.2337
1.3760	1.3069	0.069121	5.2413
1.3780	1.3088	0.069222	5.2488
1.3800	1.3107	0.069323	5.2564
1.3820	1.3126	0.069425	5.2640
1.3840	1.3145	0.069526	5.2716
1.3860	1.3164	0.069628	5.2791
1.3880	1.3183	0.069729	5.2867
1.3900	1.3202	0.069830	5.2943
1.3920	1.3221	0.069932	5.3019
1.3940	1.3240	0.070033	5.3094
1.3960	1.3259	0.070135	5.3170
1.3980	1.3278	0.070236	5.3246
1.4000	1.3297	0.070338	5.3322
1.4020	1.3316	0.070439	5.3397
1.4040	1.3335	0.070540	5.3473
1.4060	1.3354	0.070642	5.3549
1.4080	1.3373	0.070743	5.3624
1.4100	1.3392	0.070845	5.3700
1.4120	1.3411	0.070946	5.3776
1.4140	1.3430	0.071048	5.3852
1.4160	1.3448	0.071149	5.3927
1.4180	1.3467	0.071251	5.4003
1.4200	1.3486	0.071352	5.4079
1.4220	1.3505	0.071454	5.4154
1.4240	1.3524	0.071555	5.4230
1.4260	1.3543	0.071657	5.4306
1.4280	1.3562	0.071758	5.4382
1.4300	1.3581	0.071860	5.4457
1.4320	1.3600	0.071961	5.4533
1.4340	1.3619	0.072063	5.4609
1.4360	1.3638	0.072164	5.4684
1.4380	1.3657	0.072266	5.4760

OBSERVED DISTANCE (INCHES)	TRUE DISTANCE (INCHES)	ERROR (INCHES)	RAY ANGLE (DEGREES)
1.4400	1.3676	0.072367	5.4836
1.4420	1.3695	0.072469	5.4912
1.4440	1.3714	0.072571	5.4987
1.4460	1.3733	0.072672	5.5063
1.4480	1.3752	0.072774	5.5139
1.4500	1.3771	0.072875	5.5214
1.4520	1.3790	0.072977	5.5290
1.4540	1.3809	0.073078	5.5366
1.4560	1.3828	0.073180	5.5441
1.4580	1.3847	0.073281	5.5517
1.4600	1.3866	0.073383	5.5593
1.4620	1.3885	0.073484	5.5668
1.4640	1.3904	0.073586	5.5744
1.4660	1.3923	0.073687	5.5820
1.4680	1.3942	0.073789	5.5895
1.4700	1.3961	0.073891	5.5971
1.4720	1.3980	0.073992	5.6047
1.4740	1.3999	0.074094	5.6122
1.4760	1.4018	0.074196	5.6198
1.4780	1.4037	0.074297	5.6274
1.4800	1.4056	0.074399	5.6349
1.4820	1.4075	0.074500	5.6425
1.4840	1.4094	0.074602	5.6501
1.4860	1.4113	0.074704	5.6576
1.4880	1.4132	0.074805	5.6652
1.4900	1.4151	0.074907	5.6728
1.4920	1.4170	0.075009	5.6803
1.4940	1.4189	0.075110	5.6879
1.4960	1.4208	0.075212	5.6955
1.4980	1.4227	0.075314	5.7030
1.5000	1.4246	0.075415	5.7106
1.5020	1.4265	0.075517	5.7182
1.5040	1.4284	0.075618	5.7257
1.5060	1.4303	0.075720	5.7333
1.5080	1.4322	0.075822	5.7408
1.5100	1.4341	0.075923	5.7484
1.5120	1.4360	0.076025	5.7560
1.5140	1.4379	0.076127	5.7635
1.5160	1.4398	0.076229	5.7711
1.5180	1.4417	0.076330	5.7787
1.5200	1.4436	0.076432	5.7862
1.5220	1.4455	0.076534	5.7938
1.5240	1.4474	0.076635	5.8013
1.5260	1.4493	0.076737	5.8089
1.5280	1.4512	0.076839	5.8165
1.5300	1.4531	0.076940	5.8240
1.5320	1.4550	0.077042	5.8316
1.5340	1.4569	0.077144	5.8391
1.5360	1.4588	0.077246	5.8467
1.5380	1.4607	0.077347	5.8543
1.5400	1.4625	0.077449	5.8618
1.5420	1.4644	0.077551	5.8694
1.5440	1.4663	0.077653	5.8769
1.5460	1.4682	0.077754	5.8845
1.5480	1.4701	0.077856	5.8921
1.5500	1.4720	0.077958	5.8996
1.5520	1.4739	0.078060	5.9072
1.5540	1.4758	0.078161	5.9147
1.5560	1.4777	0.078263	5.9223
1.5580	1.4796	0.078365	5.9299

OBSERVED DISTANCE (INCHES)	TRUE DISTANCE (INCHES)	ERROR (INCHES)	RAY ANGLE (DEGREES)
1.5600	1.4815	0.078467	5.9374
1.5620	1.4834	0.078568	5.9450
1.5640	1.4853	0.078670	5.9525
1.5660	1.4872	0.078772	5.9601
1.5680	1.4891	0.078874	5.9676
1.5700	1.4910	0.078976	5.9752
1.5720	1.4929	0.079078	5.9827
1.5740	1.4948	0.079179	5.9903
1.5760	1.4967	0.079281	5.9979
1.5780	1.4986	0.079383	6.0054
1.5800	1.5005	0.079485	6.0130
1.5820	1.5024	0.079587	6.0205
1.5840	1.5043	0.079689	6.0281
1.5860	1.5062	0.079790	6.0356
1.5880	1.5081	0.079892	6.0432
1.5900	1.5100	0.079994	6.0508
1.5920	1.5119	0.080096	6.0583
1.5940	1.5138	0.080198	6.0659
1.5960	1.5157	0.080300	6.0734
1.5980	1.5176	0.080402	6.0810
1.6000	1.5195	0.080503	6.0885
1.6020	1.5214	0.080605	6.0961
1.6040	1.5233	0.080707	6.1036
1.6060	1.5252	0.080809	6.1112
1.6080	1.5271	0.080911	6.1187
1.6100	1.5290	0.081013	6.1263
1.6120	1.5309	0.081115	6.1338
1.6140	1.5328	0.081217	6.1414
1.6160	1.5347	0.081319	6.1489
1.6180	1.5366	0.081421	6.1565
1.6200	1.5385	0.081523	6.1640
1.6220	1.5404	0.081624	6.1716
1.6240	1.5423	0.081726	6.1791
1.6260	1.5442	0.081828	6.1867
1.6280	1.5461	0.081930	6.1942
1.6300	1.5480	0.082032	6.2018
1.6320	1.5499	0.082134	6.2093
1.6340	1.5518	0.082236	6.2169
1.6360	1.5537	0.082338	6.2244
1.6380	1.5556	0.082440	6.2320
1.6400	1.5575	0.082542	6.2395
1.6420	1.5594	0.082644	6.2471
1.6440	1.5613	0.082746	6.2546
1.6460	1.5632	0.082848	6.2622
1.6480	1.5650	0.082950	6.2697
1.6500	1.5669	0.083052	6.2773
1.6520	1.5688	0.083154	6.2848
1.6540	1.5707	0.083256	6.2924
1.6560	1.5726	0.083358	6.2999
1.6580	1.5745	0.083460	6.3075
1.6600	1.5764	0.083562	6.3150
1.6620	1.5783	0.083664	6.3226
1.6640	1.5802	0.083766	6.3301
1.6660	1.5821	0.083868	6.3377
1.6680	1.5840	0.083970	6.3452
1.6700	1.5859	0.084072	6.3528
1.6720	1.5878	0.084174	6.3603
1.6740	1.5897	0.084276	6.3679
1.6760	1.5916	0.084378	6.3754
1.6780	1.5935	0.084480	6.3829

OBSERVED DISTANCE (INCHES)	TRUE DISTANCE (INCHES)	ERROR (INCHES)	RAY ANGLE (DEGREES)
1.6800	1.5954	0.084583	6.3905
1.6820	1.5973	0.084685	6.3980
1.6840	1.5992	0.084787	6.4056
1.6860	1.6011	0.084889	6.4131
1.6880	1.6030	0.084991	6.4207
1.6900	1.6049	0.085093	6.4282
1.6920	1.6068	0.085195	6.4358
1.6940	1.6087	0.085297	6.4433
1.6960	1.6106	0.085399	6.4508
1.6980	1.6125	0.085501	6.4584
1.7000	1.6144	0.085603	6.4659
1.7020	1.6163	0.085706	6.4735
1.7040	1.6182	0.085808	6.4810
1.7060	1.6201	0.085910	6.4886
1.7080	1.6220	0.086012	6.4961
1.7100	1.6239	0.086114	6.5036
1.7120	1.6258	0.086216	6.5112
1.7140	1.6277	0.086318	6.5187
1.7160	1.6296	0.086421	6.5263
1.7180	1.6315	0.086523	6.5338
1.7200	1.6334	0.086625	6.5413
1.7220	1.6353	0.086727	6.5489
1.7240	1.6372	0.086829	6.5564
1.7260	1.6391	0.086932	6.5640
1.7280	1.6410	0.087034	6.5715
1.7300	1.6429	0.087136	6.5790
1.7320	1.6448	0.087238	6.5866
1.7340	1.6467	0.087340	6.5941
1.7360	1.6486	0.087443	6.6017
1.7380	1.6505	0.087545	6.6092
1.7400	1.6524	0.087647	6.6167
1.7420	1.6543	0.087749	6.6243
1.7440	1.6561	0.087851	6.6318
1.7460	1.6580	0.087954	6.6393
1.7480	1.6599	0.088056	6.6469
1.7500	1.6618	0.088158	6.6544
1.7520	1.6637	0.088260	6.6620
1.7540	1.6656	0.088363	6.6695
1.7560	1.6675	0.088465	6.6770
1.7580	1.6694	0.088567	6.6846
1.7600	1.6713	0.088669	6.6921
1.7620	1.6732	0.088772	6.6996
1.7640	1.6751	0.088874	6.7072
1.7660	1.6770	0.088976	6.7147
1.7680	1.6789	0.089079	6.7222
1.7700	1.6808	0.089181	6.7298
1.7720	1.6827	0.089283	6.7373
1.7740	1.6846	0.089385	6.7448
1.7760	1.6865	0.089488	6.7524
1.7780	1.6884	0.089590	6.7599
1.7800	1.6903	0.089692	6.7674
1.7820	1.6922	0.089795	6.7750
1.7840	1.6941	0.089897	6.7825
1.7860	1.6960	0.089999	6.7900
1.7880	1.6979	0.090102	6.7976
1.7900	1.6998	0.090204	6.8051
1.7920	1.7017	0.090306	6.8126
1.7940	1.7036	0.090409	6.8202
1.7960	1.7055	0.090511	6.8277
1.7980	1.7074	0.090613	6.8352

OBSERVED DISTANCE (INCHES)	TRUE DISTANCE (INCHES)	ERROR (INCHES)	RAY ANGLE (DEGREES)
1.8000	1.7093	0.090716	6.8428
1.8020	1.7112	0.090818	6.8503
1.8040	1.7131	0.090921	6.8578
1.8060	1.7150	0.091023	6.8654
1.8080	1.7169	0.091125	6.8729
1.8100	1.7188	0.091228	6.8804
1.8120	1.7207	0.091330	6.8879
1.8140	1.7226	0.091433	6.8955
1.8160	1.7245	0.091535	6.9030
1.8180	1.7264	0.091637	6.9105
1.8200	1.7283	0.091740	6.9181
1.8220	1.7302	0.091842	6.9256
1.8240	1.7321	0.091945	6.9331
1.8260	1.7340	0.092047	6.9406
1.8280	1.7358	0.092150	6.9482
1.8300	1.7377	0.092252	6.9557
1.8320	1.7396	0.092355	6.9632
1.8340	1.7415	0.092457	6.9708
1.8360	1.7434	0.092559	6.9783
1.8380	1.7453	0.092662	6.9858
1.8400	1.7472	0.092764	6.9933
1.8420	1.7491	0.092867	7.0009
1.8440	1.7510	0.092969	7.0084
1.8460	1.7529	0.093072	7.0159
1.8480	1.7548	0.093174	7.0234
1.8500	1.7567	0.093277	7.0310
1.8520	1.7586	0.093379	7.0385
1.8540	1.7605	0.093482	7.0460
1.8560	1.7624	0.093584	7.0535
1.8580	1.7643	0.093687	7.0611
1.8600	1.7662	0.093790	7.0686
1.8620	1.7681	0.093892	7.0761
1.8640	1.7700	0.093995	7.0836
1.8660	1.7719	0.094097	7.0912
1.8680	1.7738	0.094200	7.0987
1.8700	1.7757	0.094302	7.1062
1.8720	1.7776	0.094405	7.1137
1.8740	1.7795	0.094507	7.1213
1.8760	1.7814	0.094610	7.1288
1.8780	1.7833	0.094713	7.1363
1.8800	1.7852	0.094815	7.1438
1.8820	1.7871	0.094918	7.1513
1.8840	1.7890	0.095020	7.1589
1.8860	1.7909	0.095123	7.1664
1.8880	1.7928	0.095226	7.1739
1.8900	1.7947	0.095328	7.1814
1.8920	1.7966	0.095431	7.1889
1.8940	1.7985	0.095533	7.1965
1.8960	1.8004	0.095636	7.2040
1.8980	1.8023	0.095739	7.2115
1.9000	1.8042	0.095841	7.2190
1.9020	1.8061	0.095944	7.2265
1.9040	1.8080	0.096047	7.2340
1.9060	1.8098	0.096149	7.2416
1.9080	1.8117	0.096252	7.2491
1.9100	1.8136	0.096355	7.2566
1.9120	1.8155	0.096457	7.2641
1.9140	1.8174	0.096560	7.2716
1.9160	1.8193	0.096663	7.2792
1.9180	1.8212	0.096765	7.2867

OBSERVED DISTANCE (INCHES)	TRUE DISTANCE (INCHES)	ERROR (INCHES)	RAY ANGLE (DEGREES)
1.9200	1.8231	0.096868	7.2942
1.9220	1.8250	0.096971	7.3017
1.9240	1.8269	0.097073	7.3092
1.9260	1.8288	0.097176	7.3167
1.9280	1.8307	0.097279	7.3242
1.9300	1.8326	0.097382	7.3318
1.9320	1.8345	0.097484	7.3393
1.9340	1.8364	0.097587	7.3468
1.9360	1.8383	0.097690	7.3543
1.9380	1.8402	0.097793	7.3618
1.9400	1.8421	0.097895	7.3693
1.9420	1.8440	0.097998	7.3769
1.9440	1.8459	0.098101	7.3844
1.9460	1.8478	0.098204	7.3919
1.9480	1.8497	0.098306	7.3994
1.9500	1.8516	0.098409	7.4069
1.9520	1.8535	0.098512	7.4144
1.9540	1.8554	0.098615	7.4219
1.9560	1.8573	0.098718	7.4294
1.9580	1.8592	0.098820	7.4370
1.9600	1.8611	0.098923	7.4445
1.9620	1.8630	0.099026	7.4520
1.9640	1.8649	0.099129	7.4595
1.9660	1.8668	0.099232	7.4670
1.9680	1.8687	0.099335	7.4745
1.9700	1.8706	0.099437	7.4820
1.9720	1.8725	0.099540	7.4895
1.9740	1.8744	0.099643	7.4970
1.9760	1.8763	0.099746	7.5045
1.9780	1.8782	0.099849	7.5121
1.9800	1.8800	0.099952	7.5196
1.9820	1.8819	0.100054	7.5271
1.9840	1.8838	0.100157	7.5346
1.9860	1.8857	0.100260	7.5421
1.9880	1.8876	0.100363	7.5496
1.9900	1.8895	0.100466	7.5571
1.9920	1.8914	0.100569	7.5646
1.9940	1.8933	0.100672	7.5721
1.9960	1.8952	0.100775	7.5796
1.9980	1.8971	0.100878	7.5871
2.0000	1.8990	0.100981	7.5946
2.0020	1.9009	0.101084	7.6021
2.0040	1.9028	0.101186	7.6096
2.0060	1.9047	0.101289	7.6172
2.0080	1.9066	0.101392	7.6247
2.0100	1.9085	0.101495	7.6322
2.0120	1.9104	0.101598	7.6397
2.0140	1.9123	0.101701	7.6472
2.0160	1.9142	0.101804	7.6547
2.0180	1.9161	0.101907	7.6622
2.0200	1.9180	0.102010	7.6697
2.0220	1.9199	0.102113	7.6772
2.0240	1.9218	0.102216	7.6847
2.0260	1.9237	0.102319	7.6922
2.0280	1.9256	0.102422	7.6997
2.0300	1.9275	0.102525	7.7072
2.0320	1.9294	0.102628	7.7147
2.0340	1.9313	0.102731	7.7222
2.0360	1.9332	0.102834	7.7297
2.0380	1.9351	0.102937	7.7372

OBSERVED DISTANCE (INCHES)	TRUE DISTANCE (INCHES)	ERROR (INCHES)	RAY ANGLE (DEGREES)
2.0400	1.9370	0.103040	7.7447
2.0420	1.9389	0.103143	7.7522
2.0440	1.9408	0.103246	7.7597
2.0460	1.9426	0.103349	7.7672
2.0480	1.9445	0.103453	7.7747
2.0500	1.9464	0.103556	7.7822
2.0520	1.9483	0.103659	7.7897
2.0540	1.9502	0.103762	7.7972
2.0560	1.9521	0.103865	7.8047
2.0580	1.9540	0.103968	7.8122
2.0600	1.9559	0.104071	7.8197
2.0620	1.9578	0.104174	7.8272
2.0640	1.9597	0.104277	7.8347
2.0660	1.9616	0.104380	7.8422
2.0680	1.9635	0.104483	7.8497
2.0700	1.9654	0.104587	7.8572
2.0720	1.9673	0.104690	7.8647
2.0740	1.9692	0.104793	7.8722
2.0760	1.9711	0.104896	7.8797
2.0780	1.9730	0.104999	7.8872
2.0800	1.9749	0.105102	7.8947
2.0820	1.9768	0.105205	7.9022
2.0840	1.9787	0.105309	7.9097
2.0860	1.9806	0.105412	7.9172
2.0880	1.9825	0.105515	7.9246
2.0900	1.9844	0.105618	7.9321
2.0920	1.9863	0.105721	7.9396
2.0940	1.9882	0.105825	7.9471
2.0960	1.9901	0.105928	7.9546
2.0980	1.9920	0.106031	7.9621
2.1000	1.9939	0.106134	7.9696
2.1020	1.9958	0.106238	7.9771
2.1040	1.9977	0.106341	7.9846
2.1060	1.9996	0.106444	7.9921
2.1080	2.0015	0.106547	7.9996
2.1100	2.0033	0.106650	8.0071
2.1120	2.0052	0.106754	8.0146
2.1140	2.0071	0.106857	8.0220
2.1160	2.0090	0.106960	8.0295
2.1180	2.0109	0.107064	8.0370
2.1200	2.0128	0.107167	8.0445
2.1220	2.0147	0.107270	8.0520
2.1240	2.0166	0.107374	8.0595
2.1260	2.0185	0.107477	8.0670
2.1280	2.0204	0.107580	8.0745
2.1300	2.0223	0.107683	8.0820
2.1320	2.0242	0.107787	8.0894
2.1340	2.0261	0.107890	8.0969
2.1360	2.0280	0.107993	8.1044
2.1380	2.0299	0.108097	8.1119
2.1400	2.0318	0.108200	8.1194
2.1420	2.0337	0.108303	8.1269
2.1440	2.0356	0.108407	8.1344
2.1460	2.0375	0.108510	8.1419
2.1480	2.0394	0.108613	8.1493
2.1500	2.0413	0.108717	8.1568
2.1520	2.0432	0.108820	8.1643
2.1540	2.0451	0.108924	8.1718
2.1560	2.0470	0.109027	8.1793
2.1580	2.0489	0.109131	8.1868

OBSERVED DISTANCE (INCHES)	TRUE DISTANCE (INCHES)	ERROR (INCHES)	RAY ANGLE (DEGREES)
2.1600	2.0508	0.109234	8.1943
2.1620	2.0527	0.109337	8.2017
2.1640	2.0546	0.109441	8.2092
2.1660	2.0565	0.109544	8.2167
2.1680	2.0584	0.109647	8.2242
2.1700	2.0602	0.109751	8.2317
2.1720	2.0621	0.109854	8.2392
2.1740	2.0640	0.109958	8.2466
2.1760	2.0659	0.110061	8.2541
2.1780	2.0678	0.110165	8.2616
2.1800	2.0697	0.110268	8.2691
2.1820	2.0716	0.110372	8.2766
2.1840	2.0735	0.110475	8.2840
2.1860	2.0754	0.110579	8.2915
2.1880	2.0773	0.110682	8.2990
2.1900	2.0792	0.110786	8.3065
2.1920	2.0811	0.110889	8.3140
2.1940	2.0830	0.110993	8.3214
2.1960	2.0849	0.111096	8.3289
2.1980	2.0868	0.111200	8.3364
2.2000	2.0887	0.111303	8.3439
2.2020	2.0906	0.111407	8.3514
2.2040	2.0925	0.111510	8.3588
2.2060	2.0944	0.111614	8.3663
2.2080	2.0963	0.111717	8.3738
2.2100	2.0982	0.111821	8.3813
2.2120	2.1001	0.111924	8.3887
2.2140	2.1020	0.112028	8.3962
2.2160	2.1039	0.112131	8.4037
2.2180	2.1058	0.112235	8.4112
2.2200	2.1077	0.112339	8.4187
2.2220	2.1096	0.112442	8.4261
2.2240	2.1115	0.112546	8.4336
2.2260	2.1133	0.112650	8.4411
2.2280	2.1152	0.112753	8.4486
2.2300	2.1171	0.112857	8.4560
2.2320	2.1190	0.112960	8.4635
2.2340	2.1209	0.113064	8.4710
2.2360	2.1228	0.113168	8.4784
2.2380	2.1247	0.113271	8.4859
2.2400	2.1266	0.113375	8.4934
2.2420	2.1285	0.113479	8.5009
2.2440	2.1304	0.113582	8.5083
2.2460	2.1323	0.113686	8.5158
2.2480	2.1342	0.113790	8.5233
2.2500	2.1361	0.113893	8.5308
2.2520	2.1380	0.113997	8.5382
2.2540	2.1399	0.114101	8.5457
2.2560	2.1418	0.114205	8.5532
2.2580	2.1437	0.114308	8.5606
2.2600	2.1456	0.114412	8.5681
2.2620	2.1475	0.114516	8.5756
2.2640	2.1494	0.114620	8.5830
2.2660	2.1513	0.114723	8.5905
2.2680	2.1532	0.114827	8.5980
2.2700	2.1551	0.114931	8.6055
2.2720	2.1570	0.115034	8.6129
2.2740	2.1589	0.115138	8.6204
2.2760	2.1608	0.115242	8.6279
2.2780	2.1627	0.115346	8.6353

OBSERVED DISTANCE (INCHES)	TRUE DISTANCE (INCHES)	ERROR (INCHES)	RAY ANGLE (DEGREES)
2.2800	2.1645	0.115450	8.6428
2.2820	2.1664	0.115553	8.6503
2.2840	2.1683	0.115657	8.6577
2.2860	2.1702	0.115761	8.6652
2.2880	2.1721	0.115865	8.6727
2.2900	2.1740	0.115969	8.6801
2.2920	2.1759	0.116072	8.6876
2.2940	2.1778	0.116176	8.6951
2.2960	2.1797	0.116280	8.7025
2.2980	2.1816	0.116384	8.7100
2.3000	2.1835	0.116488	8.7174
2.3020	2.1854	0.116592	8.7249
2.3040	2.1873	0.116695	8.7324
2.3060	2.1892	0.116799	8.7398
2.3080	2.1911	0.116903	8.7473
2.3100	2.1930	0.117007	8.7548
2.3120	2.1949	0.117111	8.7622
2.3140	2.1968	0.117215	8.7697
2.3160	2.1987	0.117319	8.7772
2.3180	2.2006	0.117423	8.7846
2.3200	2.2025	0.117527	8.7921
2.3220	2.2044	0.117631	8.7995
2.3240	2.2063	0.117735	8.8070
2.3260	2.2082	0.117839	8.8145
2.3280	2.2101	0.117942	8.8219
2.3300	2.2120	0.118046	8.8294
2.3320	2.2138	0.118150	8.8368
2.3340	2.2157	0.118254	8.8443
2.3360	2.2176	0.118358	8.8518
2.3380	2.2195	0.118462	8.8592
2.3400	2.2214	0.118566	8.8667
2.3420	2.2233	0.118670	8.8741
2.3440	2.2252	0.118774	8.8816
2.3460	2.2271	0.118878	8.8890
2.3480	2.2290	0.118982	8.8965
2.3500	2.2309	0.119086	8.9040
2.3520	2.2328	0.119190	8.9114
2.3540	2.2347	0.119294	8.9189
2.3560	2.2366	0.119398	8.9263
2.3580	2.2385	0.119502	8.9338
2.3600	2.2404	0.119606	8.9412
2.3620	2.2423	0.119711	8.9487
2.3640	2.2442	0.119815	8.9561
2.3660	2.2461	0.119919	8.9636
2.3680	2.2480	0.120023	8.9711
2.3700	2.2499	0.120127	8.9785
2.3720	2.2518	0.120231	8.9860
2.3740	2.2537	0.120335	8.9934
2.3760	2.2556	0.120439	9.0009
2.3780	2.2575	0.120543	9.0083
2.3800	2.2594	0.120647	9.0158
2.3820	2.2612	0.120751	9.0232
2.3840	2.2631	0.120856	9.0307
2.3860	2.2650	0.120960	9.0381
2.3880	2.2669	0.121064	9.0456
2.3900	2.2688	0.121168	9.0530
2.3920	2.2707	0.121272	9.0605
2.3940	2.2726	0.121376	9.0679
2.3960	2.2745	0.121480	9.0754
2.3980	2.2764	0.121585	9.0828

OBSERVED DISTANCE (INCHES)	TRUE DISTANCE (INCHES)	ERROR (INCHES)	RAY ANGLE (DEGREES)
2.4000	2.2783	0.121689	9.0903
2.4020	2.2802	0.121793	9.0977
2.4040	2.2821	0.121897	9.1052
2.4060	2.2840	0.122001	9.1126
2.4080	2.2859	0.122106	9.1201
2.4100	2.2878	0.122210	9.1275
2.4120	2.2897	0.122314	9.1350
2.4140	2.2916	0.122418	9.1424
2.4160	2.2935	0.122523	9.1498
2.4180	2.2954	0.122627	9.1573
2.4200	2.2973	0.122731	9.1647
2.4220	2.2992	0.122835	9.1722
2.4240	2.3011	0.122940	9.1796
2.4260	2.3030	0.123044	9.1871
2.4280	2.3049	0.123148	9.1945
2.4300	2.3067	0.123253	9.2020
2.4320	2.3086	0.123357	9.2094
2.4340	2.3105	0.123461	9.2168
2.4360	2.3124	0.123565	9.2243
2.4380	2.3143	0.123670	9.2317
2.4400	2.3162	0.123774	9.2392
2.4420	2.3181	0.123879	9.2466
2.4440	2.3200	0.123983	9.2541
2.4460	2.3219	0.124087	9.2615
2.4480	2.3238	0.124191	9.2689
2.4500	2.3257	0.124296	9.2764
2.4520	2.3276	0.124400	9.2838
2.4540	2.3295	0.124505	9.2913
2.4560	2.3314	0.124609	9.2987
2.4580	2.3333	0.124713	9.3061
2.4600	2.3352	0.124818	9.3136
2.4620	2.3371	0.124922	9.3210
2.4640	2.3390	0.125027	9.3285
2.4660	2.3409	0.125131	9.3359
2.4680	2.3428	0.125235	9.3433
2.4700	2.3447	0.125340	9.3508
2.4720	2.3466	0.125444	9.3582
2.4740	2.3484	0.125549	9.3657
2.4760	2.3503	0.125653	9.3731
2.4780	2.3522	0.125758	9.3805
2.4800	2.3541	0.125862	9.3880
2.4820	2.3560	0.125967	9.3954
2.4840	2.3579	0.126071	9.4028
2.4860	2.3598	0.126176	9.4103
2.4880	2.3617	0.126280	9.4177
2.4900	2.3636	0.126385	9.4251
2.4920	2.3655	0.126489	9.4326
2.4940	2.3674	0.126594	9.4400
2.4960	2.3693	0.126698	9.4474
2.4980	2.3712	0.126803	9.4549
2.5000	2.3731	0.126907	9.4623

APPENDIX C

APPLICATION OF COMPUTER PROGRAM "HOLOFER"

The computer program is an adptation of the inversion first proposed
by C. D. Maldonado [9, 10, 11] and is designed to invert fringe numbers
across a field to the density field. It can be operated in three dif-
ferent modes as described below:

   (a) Mode 1

      Mode 1 is utilized as a self-test of the computer program. It
can either generate its own input density field using Subroutine FUNCT
or read in a density field through Subroutine FREAD. The program then
generates the fringe array and inverts the array back to the original
density field. This mode was utilized in the present investigation to
determine the value of the scale factor, α , required to obtain the
correct density across the fin.   .

   (b) Mode 2

      This mode reads in irregularly spaced fringe data and generates
the fringe array at regular intervals across the field using Subroutine
SHEET. By specifying NCODE = 1, the fringe array can be generated by one
of the functions in Subroutine FUNCT. Mode 2 was not utilized .

   (c) Mode 3

      Mode 3 reads in the fringe data at regularly spaced intervals and
inverts the array to density data across the field. The Subroutine GARRAY
calls Subroutine READ to read in the fringe data. The first two cards
preceeding the fringe data provide the program with the fringe field size,
location, and symmetry.

The following parameters were used in considering the symmetric field
case:

PARAMETER	INPUT
NOF	Run Number
IMAX	201
JMAX	1
ISYM	101
JSYM	1
IMS	2
JMS	100
Z	0.387
XO	0.0
YO	0.0
PHISYM	0.0

References [3] and [12] contain further details and applications
of the computer program. A print-out of the program is included in the
next few pages of this appendix.

```
C     **********************HOLOVERT*******************************             CAL00001C
C                                                                              CAL00020
C     HOLOVERT INVERTS THE FIELD AT AN ARRAY OF POINTS IN A VARIABLE           CAL00030
C     COORDINATE SYSTEM. IT SURVEYS NPTS POINTS EACH FOR A SET OF NLINS        CAL00040
C     LINES ACROSS THE FIELD.                                                  CAL00050
C                                                                              CAL00060
      COMMON IMAX,JMAX,IIMX,JJMX,ALPHA,SIZE,EPS,MODE,BOX,SD,IX,Z               CAL00070
      COMMON /TAB/ INDEX,KEXTRA,MEXTRA,KLIMIT,MLIMIT,KOUT,MOUT                  CAL00080
      COMMON /TAB2/ IPT,KPT,BND,NPTS,NLINS,RHOINF,RLAMDA,BETA                   CAL00090
      COMMON /OUT/ XP,THEO,CALC,ERR,RHO,CA,FA                                   CAL00100
      COMMON /EQPARA/ A,B,C,D,E,P,Q,S,T,U,V,W,RO,RA,NO,NA,NOF,NAF               CAL00110
      COMMON /SYM/ ISYM,JSYM,MSYM,FCU,IMS,JMS,QSYM                             CAL00120
      COMMON /IO/ CMS,IN1,IN2,IN4                                              CAL00130
      DATA BL,PL,ST,EX,OH,SC,DH,BR/1H ,1H+,1H*,1HX,1HO,1H:,1H-,1H|/            CAL00140
      DIMENSION RB(7),TL(62),RO(101),RA(101)                                   CAL00150
C                                                                              CAL00160
      DIMENSION G(5151),GA(5151),H(202,5),SCF(73,6),BDA(4000)                  CAL00170
      DIMENSION THEO(51,11),CALC(51,11),ERR(51),RHO(51)                        CAL00180
      DIMENSION CA(51),FA(51,11),AR(42),XP(51),YP(51)                          CAL00190
      CMS=0.                                                                   CAL00200
C                                                                              CAL00220
      REWIND 3                                                                 CAL00230
      IN1=5                                                                    CAL00240
      IN2=5                                                                    CAL00250
      IN4=5                                                                    CAL00260
      IF(CMS.NE.1.) GO TO 20                                                   CAL00270
      IN1=1                                                                    CAL00280
      IN2=2                                                                    CAL00290
      IN4=4                                                                    CAL00300
      IF(CMS.EQ.1.) REWIND 4                                                   CAL00310
   20 READ(IN4,89) (AR(I),I=1,42)                                              CAL00320
      IMAX=AR(1)                                                               CAL00330
      JMAX=AR(2)*2.                                                            CAL00340
      IF(JMAX.LE.0) JMAX=1                                                     CAL00350
      KLIMIT=AR(3)                                                             CAL00360
      MLIMIT=AR(4)                                                             CAL00370
      KEXTRA=AR(5)                                                             CAL00380
      MEXTRA=AR(6)                                                             CAL00390
      JSYM=AR(14)                                                              CAL00400
      ALPHA=AR(7)                                                              CAL00410
      SIZE=AR(8)                                                               CAL00420
      EPS=AR(9)                                                                CAL00430
      MODE=AR(13)                                                              CAL00440
      DGN=AR(17)                                                               CAL00450
      RHOINF=AR(10)                                                            CAL00460
      RLAMDA=AR(11)*1.E-8                                                       CAL00470
      BETA=AR(12)
```

127

```
      NPTS=AR(15)                                                       CAL00480
      NLINS=AR(16)                                                      CAL00490
      SD=AR(18)                                                         CAL00500
      PHIZ=AR(19)                                                       CAL00510
      DELPHI=AR(20)                                                     CAL00520
      YPZERO=AR(21)                                                     CAL00530
      YPRNG=AR(22)                                                      CAL00540
      XPZERO=AR(23)                                                     CAL00550
      XPRNG=AR(24)                                                      CAL00560
      NOF=AR(25)                                                        CAL00570
      NAF=AR(26)                                                        CAL00580
      IPT=AR(27)                                                        CAL00590
      KPT=AR(28)                                                        CAL00600
      LPT=AR(29)                                                        CAL00610
      BND=AR(30)                                                        CAL00620
      A=AR(31)                                                          CAL00630
      B=AR(32)                                                          CAL00640
      C=AR(33)                                                          CAL00650
      D=AR(34)                                                          CAL00660
      E=AR(35)                                                          CAL00670
      P=AR(36)                                                          CAL00680
      S=AR(37)                                                          CAL00690
      T=AR(38)                                                          CAL00700
      U=AR(39)                                                          CAL00710
      V=AR(40)                                                          CAL00720
      W=AR(41)                                                          CAL00730
      Q=AR(42)                                                          CAL00740
      WRITE(6,90)
      WRITE(6,98)
      WRITE(6,91)(AR(I),I=7,12)
      WRITE(6,92)(AR(I),I=13,18)
      WRITE(6,93)(AR(I),I=19,24)
      WRITE(6,94)(AR(I),I=25,30)
      WRITE(6,95)(AR(I),I=31,36)
      WRITE(6,96)(AR(I),I=37,42)
      WRITE(6,97)(AR(I),I=1,75)
      WRITE(6,98)(ST,I=1,75)
   90 FORMAT(//,' THE INPUT PARAMETERS FOR THIS RUN ARE :',///)
   91 FORMAT(/5X,'* IMAX * JMAX/2 * KLIMIT * MLIMIT * KEXTRA *',SET00310
     1  MEXTRA  /3X,?/3X,?/3X,?
   92 FORMAT(/5X,'* SIZE * ALPHA * EPS. * RHO-INF * LAMBDA *',SET00340
     1  BETA  *F10.6,2X,F8.7,F9.1,F11.6)
   93 FORMAT(/5X,'* MODE * SYM. * POINTS * LINES * DIAGNOS *',SET00360
     1  STD.DEV /2F10.3,2X,F11.6,2X,F10.3)
   94 FORMAT(/5X,'* DELPHI * PHIZERO * YPZERO * XPZERO *',
     1  XPRANGE /2X,5F10.0,F10.3)
   95 FORMAT(/5X,'* ADD FUN * TST FUN * GARRAY * GRAPH * LIN PRT *',SET00400
     1  MAP BND /2X,6F10.0)
```

```
96  FORMAT (/5X,'**      A      *      B      *      C      *      D      *      E      *',   SET00420
   1P        '(/4X,6F10.3)
97  FORMAT (/5X,'**      S      *      T      *      U      *      V      *      M      *',   SET00440
   1Q        '(/4X,6F10.3)
98  FORMAT (/3X,75A1)                                              CAL00750
    IF(DGN.GE.4) WRITE (6,89) (AR(I),I=1,42)                       CAL00760
    NNN=2                                                          CAL00770
    IF(MODE.LT.0) NNN=1                                            CAL00780
    IF(MODE.GT.5) NNN=3                                            CAL00790
    IF(MODE.GT.5) MODE=MODE-10                                     CAL00800
    NGP=0                                                          CAL00810
    IF(KLIMIT.LT.KEXTRA) KEXTRA=KLIMIT                             CAL00820
    IF(MLIMIT.LT.MEXTRA) MEXTRA=MLIMIT                             CAL00830
    IF(IPT.LT.0) NGP=IPT                                           CAL00840
    IF(IPT.LT.0) IPT=-IPT                                          CAL00850
    ISYM=2.-(FLOAT(JSYM)/2.-FLOAT(JSYM/2))*2                       CAL00860
    IF(JSYM.EQ.0) ISYM=1                                           CAL00870
    IF(JSYM.GT.JMAX) ISYM=2                                        CAL00880
    IF(ISYM.EQ.1) JMAX=((JMAX+1)/2)*2.                             CAL00890
    RJMX=JMAX                                                      CAL00900
    MSYM=JSYM                                                      CAL00910
    IF((MSYM.EQ.0).OR.(MSYM.GT.JMAX)) MSYM=1                       CAL00920
    FCU=ISYM*JSYM*JMAX                                             CAL00930
    IF((JSYM.GT.JMAX).OR.(JSYM.EQ.0)) FCU=JMAX                     CAL00940
    QSYM=FCU/RJMX                                                  CAL00950
    IMS=(IMAX+ISYM-1)/ISYM                                         CAL00960
    JMS=JMAX                                                       CAL00970
    IF(ISYM.EQ.1) JMS=(JMAX/2+1)/2                                 CAL00980
    IF(JSYM.EQ.0) JMS=JMAX/2                                       CAL00990
    MODE=ABS(AR(13))                                               CAL01000
    XO=0.                                                          CAL01010
    YO=0.                                                          CAL01020
    ZD=0.                                                          CAL01030
    PHISYM=0.                                                      CAL01040
    HS=SIZE/2.                                                     CAL01050
    RHOS=1.286                                                     CAL01060
    BOX=RHOINF*BETA/RHOS/RLAMDA                                    CAL01070
    RPTS=NPTS                                                      CAL01080
    XPR=0.                                                         CAL01090
    IF(NPTS.GT.1) XPR=XPRNG/(RPTS-1.)/2.                           CAL01100
    XPM=-XPR                                                       CAL01110
    PIE=3.141592653589793                                         CAL01120
    MONE=1                                                         CAL01130
    WRITE (6,58) IMAX,JMAX,IMS,JMS,ISYM,JSYM,MSYM,QSYM,FCU         CAL01140
58  FORMAT(3X,'IMAX,JMAX,IMS,JMS,ISYM,JSYM,MSYM,QSYM,FCU',/        CAL01150
   1 7I5,2F7.3/)                                                   CAL01160
    NTWO=2                                                         CAL01170
    IX=IMAX+JMAX
```

```
        NF=IN1
        IF((MODE.EQ.1.).AND.(NOF.EQ.8).AND.(DGN.GE.1.)) WRITE (6,69)
        IF((MODE.EQ.1).AND.(NOF.EQ.8)) CALL FREAD (NO,RO,NF,ZD)
        Z=ZD
        IF(DGN.GE.1.) WRITE (6,68)
        CALL GARRAY (G,GA,NOF,DGN,MONE,XO,YO,PHISYM)
        LM=1
        IF((LPT.EQ.0).AND.(BND.EQ.0)) LM=0
        IIMX=IMAX+1
        JJMX=JMAX+1
        IJMX=IMAX*JMAX
        NBD=1
        IF(JSYM.EQ.0) NBD=2
        KBD=KLIMIT*NBD
        DO 15 IJ=1,IJMX
   15   GA(IJ)=0.
        NF=IN2
        IF((NAF.EQ.8).AND.(DGN.GE.1.) WRITE (6,69)
        IF((NAF.EQ.8) CALL FREAD (NA,RA,NF,ZD)
        MST=MODE
        MODE=1
        IF(DGN.GE.1.) WRITE (6,68)
        IF((NAF.NE.0) CALL GARRAY (GA,G,NAF,DGN,NTWO,XO,YO,PHISYM)
        MODE=MST
        DO 6 IJ=1,IJMX
    6   G(IJ)=G(IJ)+GA(IJ)
   16   RLINS=NLINS
        IF((NAF.EQ.8) WRITE (6,88) NA,(RA(L),L=1,NA)
        IF((NOF.EQ.8) WRITE (6,87) NO,(RO(I),I=1,NO)
        IF(LM.EQ.0) GO TO 14
        RB(1)=-1.+.7
        DO 1 I=2,7
    1   RB(I)=RB(I-1)+.5
        TPIE=2.*PIE
        MPIE=-PIE
        DYP=0..
        DXP=0..
        IF((NLINS.GT.1) DYP=YPRNG/(RLINS-1.)
        IF((NPTS.GT.1) DXP=XPRNG/(RPTS-1.)
        IF((NNN.EQ.2) .AND.(DGN.GE.2)) WRITE (6,64)
        IF(NNN.EQ.2) CALL BDGEN (G,H,SCF,DGN,NBD,BDA,KBD)
        DO 5 J=1,NLINS
        IF(DGN.GE.1.) WRITE (6,67) J
        RJM=J-1
        PHI=PHIZ+DELPHI*RJM
        YP(J)=YPZERO+DYP*RJM
        PSI=(PHI+90.)*PIE/180.
```

```
      TAU=PSI-PHISYM
      IF(LPT.EQ.1) GO TO 9
      IF(LPT.LE.1) WRITE(6,78) (ST,I=1,124)
      IF(LPT.GT.1) WRITE(6,74) (ST,I=1,95)
      IF((CMS.EQ.1.).AND.(LPT.GT.1)) READ(5,79) ZZ
      WRITE(6,86) Z,PHI,YP(J)
      WRITE(6,85) Z,PHI,YP(J)
      WRITE(6,76)
      IF(MODE.EQ.1) WRITE(6,83) (RB(I),I=1,7)
      IF(MODE.GT.1) WRITE(6,80) (RB(I),I=1,7)
      WRITE(6,81) (DH,I=1,54),(PL,II=1,13)
      IC=0
      DO 3 I=1,NPTS
      RIM=I-1
      THEO(I,J)=0.
      CA(I,J)=0.
      ERR(I,J)=0.
      RHO(I)=XPZERO+DXP*RIM
      XP(I)=ABS(XP(I))
      XPII=SQRT(XP(I)**2+YP(J)**2)/HS
      RS=SQRT(XP(I)**2+YP(J)**2)
      IF(RS.GT.1.E-10) GO TO 13
      THT=ATANM(YP(J),XP(I))
      IF(RS.EQ.0.) THT=0.
      SIG=TAU-PIE/2.+THT
      IF(SIG.GT.PIE) SIG=SIG-TPIE
      IF(SIG.LT.MPIE) SIG=SIG+TPIE
      XS=RS*COS(SIG)
      YS=RS*SIN(SIG)
      IF(DGN.GE.5) WRITE(6,44) SIG
   44 FORMAT(' ',E10.3)
      WRITE(6,57) PHI,DELPHI,PSI,TAU,THT,SIG,SIGI,XS,YS
   57 FORMAT(' ANGLES=',10E10.3)
      RI=I
      F=0.
      IF(DGN.GE.2.) WRITE(6,66) I
      IF(FUNCT.EQ.1) CALL FUNCT(XS,YS,F,NAF,DGN,NTWO)
      IF(MODE.EQ.1) CALL FUNCT(XS,YS,F,NOF,DGN,MONE)
      THEO(I,J)=F
      IF(NNN.GE.2) REWIND 3
      IF(NNN.GE.2) CALL FIELD (RS,SIGI,SOLN,NBD,BDA,DGN,KBD)
      IF(NNN.GE.1) CALL FIELD2 (RS,SIGI,SOLN,G,H,SCF,DGN)
      CA(I)=SOLN/BOX/HS
      CALC(I,J)=CA(I)-FA(I,J)
```

```
CAL01660
CAL01670
CAL01680
CAL01690
CAL01700
CAL01710
CAL01720
CAL01730
CAL01740
CAL01750
CAL01760
CAL01770
CAL01780
CAL01790
CAL01800
CAL01810
CAL01820
CAL01830
CAL01840
CAL01850
CAL01860
CAL01870
CAL01880
CAL01890
CAL01900
CAL01910
CAL01920
CAL01930
CAL01940
CAL01950
CAL01960
CAL01970
CAL01980
CAL01990
CAL02000
CAL02010
CAL02020
CAL02030
CAL02040
CAL02050
CAL02060
CAL02070
CAL02080
CAL02090
CAL02100
CAL02110
CAL02120
CAL02130
```

```
      RHO(I)=RHOINF*(CALC(I,J)+1.)                                      CALO2140
      ERR(I)=CA(I)                                                      CALO2150
      IF(MODE.EQ.1) ERR(I)=(CALC(I,J)-THEO(I,J))                        CALO2160
      IF(MODE.GT.1) THEO(I,J)=FA(I,J)                                   CALO2170
      IF(LPT.EQ.0) GO TO 3                                             CALO2180
      LC=0                                                             CALO2190
      TTL=0                                                            CALO2200
 13   TTL(1)=BL                                                        CALO2210
      IF((XP(I).GT.XPM).AND.(XP(I).LT.XPR)) TTL=1.                      CALO2260
      IF(IC.EQ.5) IC=0                                                 CALO2270
      IF(IC.EQ.0) TL(1)=PL                                             CALO2280
      DO 2 L=2,62                                                      CALO2290
      IF((I.EQ.1).OR.(TTL.EQ.1.).OR.(I.EQ.NPTS)) TL(L)=PL              CALO2300
      IF(LC.EQ.10) LC=0                                                CALO2310
      IF((IC.EQ.0).AND.(LC.EQ.0)) TL(L)=PL                             CALO2320
      LC=LC+1                                                          CALO2330
 2    TL(2)=PL                                                         CALO2340
      TL(22)=PL                                                        CALO2350
      TL(62)=PL                                                        CALO2360
      IC=IC+1                                                          CALO2370
      RLW=(CA(I)+1.)*20.+2.5                                           CALO2380
      LW=RLW                                                           CALO2390
      IF(LW.GT.62) LW=62                                               CALO2400
      IF(LW.LT.2) LW=2                                                 CALO2410
      TL(LW)=SC                                                        CALO2420
      RLY=(FA(I,J)+1.)*20.+2.5                                         CALO2430
      LY=RLY                                                           CALO2440
      IF(LY.GT.62) LY=62                                               CALO2450
      IF(LY.LT.2) LY=2                                                 CALO2460
      IF(NAF.NE.0) TL(LY)=ST                                           CALO2470
      RLX=(THEO(I,J)+1.)*20.+2.5                                       CALO2480
      LX=RLX                                                           CALO2490
      IF(LX.GT.62) LX=62                                               CALO2500
      IF(LX.LT.2) LX=2                                                 CALO2510
      IF(MODE.EQ.1) TL(LX)=OH                                          CALO2520
      RLZ=(CALC(I,J)+1.)*20.+2.5                                       CALO2530
      LZ=RLZ                                                           CALO2540
      IF(LZ.GT.62) LZ=62                                               CALO2550
      IF(LZ.LT.2) LZ=2                                                 CALO2560
      TL(LZ)=EX                                                        CALO2570
      WRITE(6,82)MOUT,KOUT,INDEX,THEO(I,J),ERR(I),CALC(I,J),RHO(I),    CALO2580
     1XP(I),(TL(L),L=1,62)
      IF((NPTS.LE.20).AND.(I.NE.NPTS)) WRITE (6,79)                    CALO2590
 3    CONTINUE                                                         CALO2600
      IF(LPT.NE.0) WRITE (6,81) (DH,I=1,54),(PL,I=1,13)                CALO2610
      TMAX=0.
      TMIN=0.
```

132

```
      IE=0
      BE=0.
      EB=0.
      DO 4 I=1,NPTS
      TH=THEO(I,J)
      IF(TH.GT.TMAX) TMAX=TH
      IF(TH.LT.TMIN) TMIN=TH
      ER=ABS(CALC(I,J)-TH)
      IF(ER.LE.BE) GO TO 4
      BE=ER
      IE=I
    4 CONTINUE
      TMM=TMAX-TMIN
      EB=RHOINF*(CALC(IE,J)-THEO(IE,J))
      IF(TMM.NE.0.) BE=(CALC(IE,J)-THEO(IE,J))*100./TMM
      IF((MODE.EQ.1).AND.(LPT.NE.0)) WRITE(6,75) EB,XP(IE),BE
      IF(DELPHI.NE.0.) YP(J)=PHI
    5 CONTINUE
      IF(BND) GO TO 14
      IF((LPT.EQ.0).OR.(LPT.GT.1)) WRITE(6,78) (ST,I=1,124)
      IF((LPT.GT.1).AND.(LPT.GT.1)) WRITE(6,74) (ST,I=1,95)
      IF((DGN.GE.1).AND.(NPTS.NE.0)) WRITE(6,63) READ(5,79) ZZ
      CALL MAP,NLINS,CALC,NOF,Z,BND)
   14 IF(NAF.EQ.0+NAF) GO TO 10
      NAO=10*NOF+NAF
      IF((DGN.GE.1).AND.(NGP.EQ.-3)) WRITE(6,62)
      IF((NGP.EQ.-3) CALL GPUNCH (Z,XO,YO,PHISYM,NAO,IMAX,JMAX,G)
    7 G(IJ)=G(IJ)-GA(IJ)
   10 DO 7 IJ=1,IJMX
      IF((IPT.EQ.3).OR.(IPT.GE.4)) WRITE (6,78) (ST,I=1,124)
      IF((IPT.EQ.1).OR.(IPT.GE.4)) WRITE (6,74) (ST,I=1,95)
      IF((IPT.EQ.2).OR.(IPT.GE.4)) READ (5,79) ZZ
      IF((CMS.EQ.1).AND.(IPT.EQ.2)) READ (5,79) ZZ
      CALL GPRINT (G,MONE)
      IF((NGP.EQ.-1) CALL GPUNCH (Z,XO,YO,PHISYM,NOF,IMAX,JMAX,G)
      IF((IPT.EQ.3) WRITE (6,78) (ST,I=1,124)
      IF((IPT.GE.4) WRITE (6,74) (ST,I=1,95)
      IF((CMS.EQ.1).AND.(IPT.GE.4)) READ (5,79) ZZ
      CALL GPRINT (GA,NTWO)
   11 IF((KPT.EQ.3) GO TO 12
      IF((KPT.EQ.1).OR.(KPT.EQ.3)) WRITE (6,78) (ST,I=1,124)
      IF((KPT.EQ.2).OR.(KPT.GE.4)) WRITE (6,74) (ST,I=1,95)
      IF((CMS.EQ.1).AND.(KPT.EQ.2)) READ (5,79) ZZ
      IF((DGN.GE.1).AND.(KPT.EQ.2).OR.(KPT.EQ.2)) WRITE (6,61)
      CALL GPLOT(G,GA,JMS)
   12 WRITE (6,78) (EX,I=1,124)
      AGAIN=ST
```

133

```
      IF (CMS.NE.1.) READ(5,60) AGAIN
      IF (AGAIN.EQ.BL) GO TO 20
      WRITE (6,77)
   89 FORMAT (6F12.7)
   88
   87 1 POINTS) WAS:'/' THE INPUT DATA FOR ADD-ON FUNCTION NO.8 (',I3,
   87 FORMAT (/)
   86 1 POINTS) WAS:'/' THE INPUT DATA FOR THE TEST FUNCTION NO.8, (',I3,
   86 FORMAT (/)
   85 1H1/)' THE INVERTED CROSS SECTION FOR:')
   85 FORMAT (1H1/)
   84 ='.F8.3.' CM.'/10X,'PHI='.F8.3,' DEGREES'/10X,
   84 14HY= ,F8.3,' CM. = ORIGINAL FUNCTION'/
   83 270X,' ADD-ON FUNCTION AND RETURN.')
   83 FORMAT (' ADJUST PAGE, HIT SPACE AND RETURN.')
   82 1 ORIGINAL ABS. COMPUTED (MG/CC)'/'
   82 K TERM MAX LIMIT ORIGINAL FUNCTION DENSITY ',6H X' ,F4.1,
   82 FORMAT (2X,I2,1X,I3,1X,I4,1X,F9.4,1X,F9.4,F7.3,1X,F9.4,1X,F7.3,
   81 1F7.3,1X,(4X,A1))
   81 FORMAT (3X,A1,I2(4X,A1))
   80 26F10.1)
   80 K TERM:'2X,'FUNCTION',5X,'SUM',3X,'FUNCTION DENSITY ',
   80 1 MAX:'3X,'ADD-ON',6X,'THE',4X,'DENSITY (MG/CC)',
   80 FORMAT (F4.1,6F10.3)
   79 26H INVERTED FUNCTION = (RHO/RHO-INFINITY)-1.0',33X,': = THE'
   78 2FORMAT (1X,6F10.3)
   77 FORMAT (1X,124A1)
   76 4X,'INVERTED SUM'/70X,': = COMPUTED FUNCTION')
   75 1,'' ,4X,F10.2,' LARGEST ERROR:',F8.6,' GMS/CC: AT ',3HX'='.F6.3
   75 1 47A1,PERCENT.'/)
   74 FORMAT (1X,47A1,' SETUP PAGE, HIT SPACE, RETURN ',48A1)
   69 FORMAT (' LINE I3,')    CALL FREAD
   68 FORMAT (' POINT I3,')   CALL GARRAY
   67 FORMAT (' ')            DO LOOP')
   66 FORMAT (' ')            CALL FIELD
   65 FORMAT (' ')            CALL BDGEN
   64 FORMAT (' ')            CALL MAP
   63 FORMAT (' ')            CALL GPUNCH
   62 FORMAT (' ')            CALL GPLOT
   61 FORMAT (80A1)           CALL FUNCT')
   60 STOP
      END
C 0C0001
C
```

```fortran
      SUBROUTINE BDGEN (G,H,SCF,DGN,NBD,BDA,KBD)
C
C     BDGEN EVALUATES THE B AND D COEFFICIENTS FOR ALL M AND K, AND WRITES
C     THE ARRAY LINEARLY ON DISK.
C
      COMMON      IMAX,JMAX,IIMX,JJMX,IJMX,ALPHA,SIZE,EPS,MODE,BOX,SD,IX,Z
      COMMON /TAB/ INDEX,KEXTRA,MEXTRA,KLIMIT,MLIMIT,KOUT,MOUT
      COMMON /SYM/ ISYM,JSYM,MSYM,FCU,IMS,JMS,QSYM
      DIMENSION G(IJMX),H(IIMX,5),SCF(JJMX,6),BDA(KBD)
C     INITIALIZE THE VALUES:
      INDEX=0
      KL2=NBD*KLIMIT
      REWIND 3
      JJMX6=JJMX*6
      IIMX2=(IIMX+1)/2
      PIE=3.141592653589793
      RIMAX=IMAX
      KLMP=KLIMIT+1
      DX=2./RIMAX
      RJMAX=JMAX
      DXI=2.*PIE/FCU
C     INITIALIZE THE MODIFIED HERMITE POLYNOMIAL ARRAY;  VECTORS:
C     (1)=H1,(2)=H2,(3)=ALPHA*X(I),(4)=HM+2 STORED,(5)=HM+1 STORED
      DO 1 II=1,IIMX2
      RII=II
      IIM=IIMX-II+1
      H(II,3)=ALPHA*(RII*DX-DX-1.)
      H(IIM,3)=-H(II,3)
      H(II,1)=2.*H(II,3)
      H(IIM,1)=-H(II,1)
      H(II,2)=(2.*H(II,3)*H(II,1)-1.)/3.
      H(IIM,2)=H(II,2)
      H(II,5)=H(II,2)
      H(IIM,5)=H(II,5)
      H(II,4)=H(II,1)
    1 H(IIM,4)=H(IIM,1)
C     INITIATE THE SIN/COS ARRAY:
      SIGN=1.
      DO 2 J=1,JJMX
      RJM=J-1
      SCF(J,1)=0.
      SCF(J,2)=1.
      SCF(J,3)=SIN(RJM*DXI-PIE/2.)
      SCF(J,4)=COS(RJM*DXI-PIE/2.)
      SCF(J,5)=0.
    2 SCF(J,6)=0.
      MS=0
C     COMMENCE THE M LOOP:
```

```fortran
      DO 7 MP=1,MLIMIT
      M=MP-1
      RM=M
      SIGN=-SIGN
C     IF(DGN.LE.-4) WRITE (6,88) SCF(1,1),SCF(2,1),SCF(1,2),SCF(2,2)      SUB00510
C     TEST FOR SYMMETRY SKIPS:                                           SUB00520
      IF(MS.EQ.MSYM) MS=0                                                SUB00530
      TOTAL=0.                                                           SUB00540
      MS=MS+1                                                            SUB00550
      IF(MS.NE.1) GO TO 6                                                SUB00560
C     COMMENCE THE K LOOP:                                               SUB00570
      DO 5 KP=1,KLIMIT                                                   SUB00580
      K=KP-1                                                             SUB00590
      PK=K                                                               SUB00600
      RK=K                                                               SUB00610
C     CALL THE B & D COEFFICIENTS AND WRITE THEM ON DISK:                SUB00620
      INDEX=INDEX+1                                                      SUB00630
      CALL BD (M,K,G,H,SCF,B,D,JJMX6)                                    SUB00640
      IF(DGN.EQ.3.) WRITE(6,89) M,K,B,D                                  SUB00650
      IF(DGN.LE.-2) WRITE (6,89) M,K,B,D                                 SUB00660
      IF(DGN.LE.-4) WRITE (6,88) H(1,1),H(1,2),H(1,4),H(1,5)             SUB00670
      KK=K*NBD+1                                                         SUB00680
      K2=K*NBD                                                           SUB00690
      BDA(KK)=B                                                          SUB00700
      BDA(K2)=D                                                          SUB00710
C     GENERATE THE NEXT ORDER OF THE SET OF HERMITE POLYNOMIALS FOR NEW K:  SUB00720
      ORDER=M+2*KP+1                                                     SUB00730
      HA=SQRT((PK+RM))/ORDER                                             SUB00740
      HB=2.*SQRT((PK+1.)*(RM+PK+1.))/(ORDER+1.)/(ORDER+2.)              SUB00750
      DO 5 IIMX2                                                         SUB00760
      IIMX-I,II+1                                                        SUB00770
      H(II,1)=2.*(H(II,3)*H(II,1))                                       SUB00780
      H(II,1)=SIGN*H(II,1)                                               SUB00790
    5 H(II,2)=HB*(H(II,3)*H(II,1)-ORDER*H(II,2))                         SUB00800
C     ADVANCE THE SIN/COS ARRAY FOR THE NEXT M:                         SUB00810
      DO 3 J=1,JMX                                                       SUB00820
      IF(DGN.LE.-5) WRITE (6,87) (SCF(J,NT),NT=1,6)                      SUB00830
   87 FORMAT(' SIN/COS MXI:',8E10.3)                                     SUB00840
      STEMP=SCF(J,1)                                                     SUB00850
      SCF(J,1)=SCF(J,1)*SCF(J,4)+SCF(J,2)*SCF(J,3)                       SUB00860
      SCF(J,2)=SCF(J,2)*SCF(J,4)-STEMP*SCF(J,3)                          SUB00870
    3 DO 4 J=1,JMAX                                                      SUB00880
      SCF(J,5)=SCF(J+1,1)-SCF(J,1)                                       SUB00890
      SCF(J,6)=SCF(J+1,2)-SCF(J,2)                                       SUB00900
    4 WRITE(6,88) (BDA(I),I=1,KBD)                                       SUB00910
      IF(DGN.LE.-3) WRITE(6,88) (BDA(I),I=1,10)                          SUB00920
    6 IF(JSYM.GT.JMAX) RETURN                                            SUB00930
      RM=RM+1                                                            SUB00940
```

```
C     REGENERATE THE HERMITE ARRAY FOR NEW M, K=0:
      DO 7 II=1,IIMX2
      IIM=II+1
      IIMX-II=II+1
      H(II,2)=H(II,4)*SQRT(RM)/(RM+1.)
      H(IIM,1)=-SIGN*H(II,5)
      H(II,2)=2.*SQRT(RM+1.)*(H(II,3)*H(II,1)-(RM+1.)*H(II,2))
      H(II,2)=H(II,1)
      H(II,4)=H(II,2)/(RM+2.)/(RM+3.)
      H(II,5)=H(II,2)
7     FORMAT( ,I4,' ',      K=',I4,',       B=',E10.4,',       D=',E10.4)
89    FORMAT(1H ,'M=',I4,' ',
88    FORMAT(2X,10E10.3)
      RETURN
      END
C000002
C
      SUBROUTINE FIELD (RS,SIG,SOLN,NBD,BDA,DGN,KBD)
C
C     FIELD EVALUATES THE VALUE OF THE FIELD FUNCTION AT A PARTICULAR
C     POINT DESIGNATED IN CYLINDRICAL COORDINATES, BY USING THE INVERSION
C     EQUATION OF MALDONADO, ET-AL. FIELD USES THE ARRAY OF B & D
C     COEFFICIENTS GENERATED IN SUBROUTINE BDGEN.
C
      COMMON IMAX,JMAX,IIMX,JJMX,KEXTRA,IJMX,ALPHA,SIZE,EPS,MODE,BOX,SD,IX,Z
      COMMON /TAB/ INDEX,KEXTRA,MEXTRA,KLIMIT,MLIMIT,KOUT,MOUT
      COMMON /SYM/ JSYM,MSYM,FCU,IMS,JMS,QSYM
      DIMENSION BDA(KBD), STK(52), STM(52)
C     INITIALIZE THE VALUES:
      INDEX=0
      MTIMER=0
      KOUT=0
      MMAX=0
      KMAX=0
      TOTAL=0.
      JJMX6=JJMX*6
      REWIND 3
      AR=ALPHA*RS
      ARG=AR**2
      EXPON=EXP(-ARG)
      PIE=3.141592653589793
      APP=ALPHA/PIE/PIE
      M=0
      RM=M
      RIMAX=IMAX
      DX=2./RIMAX
```

```
      RJMAX=JMAX
      SIGN=1.
      STK(1)=0.
      STM(1)=0.
      SMS=0.
      CMS=1.
      SMI=SIN(SIG)
      CMI=COS(SIG)
      MEP=MEXTRA+1
      DO 16 MB=1,MEP
   16 STM(MB)=0.
      FM=1.
C
C     COMMENCE THE M LOOP:
    2 SIGN=-SIGN
      K=0
      RK=K
      RM=M
      ARM=1.
      IF(M.NE.0) ARM=AR**M
      KTIMER=KEXTRA+1
      KEP=KEXTRA+1
      DO 15 KB=1,KEP
   15 STK(KB)=0.
      SIGNK=-1.
C     COMPUTE THE K=0 & K=1 ORDERS OF LAGUERRE POLYNOMIAL FOR GIVEN M:
      PM=0.
      P=SQRT(1./FM)
      PP=(RM+1.-ARG)*SQRT(1./FM/(RM+1.))
C     TEST FOR SYMMETRY SKIPS:
      IF(MS+1.EQ.MSYM) MS=0
      MS=MS+1
C
      IF(MS.NE.1) GO TO 7
C     READ A LINE OF B & D COEFFICIENTS FOR GIVEN M:
      READ(3) (BDA(I),I=1,KBD)
      IF(DGN.LE.-6) WRITE(6,88) (BDA(I),I=1,10)
C     COMMENCE THE K LOOP:
      INDEX=INDEX+1
    3 SIGNK=-SIGNK
C     COMPUTE THE M,K SUMMATION TERM:
      KK=K*NBD+1
      B=BDA(KK)
      D=0.
      IF(NBD.EQ.2) D=BDA(KK+1)
      BRAKET=B
      IF(RM.EQ.0.) GO TO 4
      BRAKET=B*CMS+D*SMS
    4 ADD=SIGNK*BRAKET*P*ARM
```

```
      TOTAL=TOTAL+ADD
      IF (DGN.GT.-5) GO TO 5
      STOT=TOTAL*EXPON*APP/BOX/SIZE
      WRITE (6,89) M,K,STOT,ADD,BRAKET,P,ARM,B,CMS,D,SMS
C     ESTABLISH CHECK AS THE RELATIVE SIZE OF THE M,K TERM OF THE SERIES:
5     CHECK=ABS(ADD)
      IF (TOTAL.GT.EPS) CHECK=ABS(ADD/TOTAL)
C     ADVANCE THE K INDEX:
      K=K+1
      RK=K
      DO 10 KA=1,KEXTRA
      KB=KEXTRA-KA+1
      STK(KB+1)=STK(KB)
10    STK(2)=TOTAL
      ORDER=M+2*K+1
C     GENERATE THE NEXT ORDER OF LAGUERRE POLYNOMIAL FOR NEW K:
      PM=P
      P=PP
      PP=P*(ORDER-ARG)-PM*SQRT(RK*(RM+RK))
      PP=PP/SQRT((RK+1.)*(RM+RK+1.))
C     SET KTIMER TO PROVIDE EXTRA K TERMS AFTER CHECK < EPS:
      KTIMER=KTIMER+1
      IF (K.GE.KLIMIT) GO TO 6
      IF (CHECK.GE.EPS) KTIMER=0
      IF (KTIMER.LE.KEXTRA) GO TO 3
      GO TO 7
6     KOUT=KOUT+1
      IF (KEXTRA.EQ.0) GO TO 7
      TOTAL=0.
      DO 11 KA=1,KEXTRA
11    TOTAL=TOTAL+STK(KA+1)
      RKX=KEXTRA
      TOTAL=TOTAL/RKX
C     END OF K LOOP; ADVANCE M:
7     M=M+1
      RM=M
      STP=SMS
      SMS=SMS*CMI+CMS*SMI
      CMS=CMS*CMI-STP*SMI
      IF (K.GT.KMAX) KMAX=K
      FM=FM*RM
      DO 12 MA=1,MEXTRA
      MB=MEXTRA-MA+1
12    STM(MB+1)=STM(MB)
      STM(2)=TOTAL
C     SET MTIMER FOR EXTRA M TERMS:
      IF (MS.EQ.1) MTIMER=MTIMER+1
      IF (JSYM.GT.JMAX) GO TO 9
```
```
SUB01920
SUB01930
SUB01940
SUB01950
SUB01960
SUB01970
SUB01980
SUB01990
SUB02000
SUB02010
SUB02020
SUB02030
SUB02040
SUB02050
SUB02060
SUB02070
SUB02080
SUB02090
SUB02100
SUB02110
SUB02120
SUB02130
SUB02140
SUB02150
SUB02160
SUB02170
SUB02180
SUB02190
SUB02200
SUB02210
SUB02220
SUB02230
SUB02240
SUB02250
SUB02260
SUB02270
SUB02280
SUB02290
SUB02300
SUB02310
SUB02320
SUB02330
SUB02340
SUB02350
SUB02360
SUB02370
SUB02380
SUB02390
```

139

```
       IF (K.GT.KEXTRA) MTIMER=0
       IF (M.GE.MLIMIT) GO TO 13
  13   IF (MTIMER.LE.MEXTRA) GO TO 2
       IF (MEXTRA.EQ.0) GO TO 9
       DO 14 MA=1,MEXTRA
  14   TOTAL=TOTAL+STM(MA+1)
       RMX=MEXTRA
       TOTAL=TOTAL/RMX
C      END OF M LOOP;  COMPUTE OUTPUT SOLN.
  9    MOUT=M-1
       IF (KOUT.EQ.0) KOUT=KMAX-1
       SOLN=TOTAL*EXPON*APP/2.
  89   FORMAT (M=',I4,',', K=',I4,',',   SUBTOTAL=',9E10.3)
  88   FORMAT (2X,10E10.3)
       RETURN
       END
C000003
C

       SUBROUTINE BD (M,K,G,H,SCF,B,D,JJMX6)
C
C  BD EVALUATES THE FIRST (B) AND SECOND (D) COEFFICIENTS IN THE
C  INVERSION EQUATION, FOR A PARTICULAR SET OF INDEXES M & K.
C  BD MAKES USE OF THE HERMITE POLYNOMIAL ARRAY GENERATED BY
C  SUBROUTINE FIELD AS M & K ADVANCE.
C
       COMMON IMAX,JMAX,IIMX,JJMX,IJMX,ALPHA,SIZE,EPS,MODE,BOX,SD,IX,Z
       COMMON /SYM/ ISYM,JSYM,MSYM,FCU,IMS,JMS,QSYM
       DIMENSION G(IJMX),SCF(JJMX6),H(IIMX)
       PIE=3.14159265358979793
       B=0.
       D=0.
       RM=M
       RK=K
       RJMAX=JMAX
       JJMX4=4*JJMX
       DXI=2.*PIE/FCU
  200  FORMAT(IIX,I10,/)
       IF (M.NE.0) GO TO 2
       S=DXI
       DO 1 J=1,JMAX
       DO 1 I=1,IMAX
       II=I+1
       IJ=IMAX*(J-1)+I
```

```
      SUB02850
      SUB02860
      SUB02870
      SUB02880
      SUB02890
      SUB02900
      SUB02910
      SUB02920
      SUB02930
      SUB02940
      SUB02950
      SUB02960
      SUB02970
      SUB02980
      SUB02990
      SUB03000
      SUB03010
      SUB03020
      SUB03030
      SUB03040
      SUB03050
      SUB03060
      SUB03070
      SUB03080
      SUB03090
      SUB03100
      SUB03110
      SUB03120
      SUB03130
      SUB03140
      SUB03160
      SUB03170
      SUB03180
      SUB03190
      SUB03200
      SUB03210
      SUB03220
      SUB03230
      SUB03240
      SUB03250
      SUB03260
      SUB03270
      SUB03280
      SUB03290
      SUB03300

1     DH=H(II)-H(I)
      B=B+G(IJ)*S*DH
      B=B*QSYM/2.
      RETURN
2     DO 3 J=1,JMAX
      JS=J+JMX4
      S=SCF(JS)/RM
      DO 3 I=1,IMAX
      II=I+1
      IJ=IMAX*(J-1)+I
      DH=H(II)-H(I)
      B=B+G(IJ)*S*DH
3     B=B*QSYM
      RETURN
4     IF(M.NE.0) GO TO 6
      S=DXI
      DO 5 J=1,JMAX
      DO 5 I=1,IMAX
      II=I+1
      IJ=IMAX*(J-1)+I
      DH=H(II)-H(I)
5     B=B+G(IJ)*S*DH
      B=B/2.
      RETURN
6     DO 7 J=1,JMAX
      JS=J+JMX4
      J2=JS+JJMX
      S=SCF(JS)/RM
      CC=SCF(J2)/RM
      DO 7 I=1,IMAX
      II=I+1
      IJ=IMAX*(J-1)+I
      DH=H(II)-H(I)
      B=B+G(IJ)*S*DH
      D=D-G(IJ)*C*DH
      RETURN
66    FORMAT(' BD:',4I5,10F6.2)
7     RETURN
      END
C000004
C
      SUBROUTINE FIELD2 (RS,SIG,SOLN,G,H,SCF,DGN)
C
C  FIELD2 COMPUTES THE SAME INVERSION AS SUBROUTINE FIELD, EXCEPT THAT
C  THE COEFFICIENTS B AND D ARE COMPUTED INDIVIDUALLY AS USED BY
C  CALLING BD. DISK STORAGE IS NOT REQUIRED, BUT COMPUTING TIME IS
C  MUCH GREATER. FIELD2 IS UTILIZED BY SPECIFYING A NEGATIVE MODE ON
```

```
C     THE INPUT PARAMETER. VALUE OF THE FIELD FUNCTION AT A PARTICULAR        SUB03310
C     FIELD EVALUATES THE FIELD FUNCTION AT A PARTICULAR                      SUB03320
C     POINT DESIGNATED IN CYLINDRICAL COORDINATES, BY USING THE INVERSION     SUB03330
C     EQUATION OF MALDONADO, ET AL.  FIELD CALLS SUBROUTINES BD & GARRAY.     SUB03340
                                                                              SUB03350
      COMMON IMAX,JMAX,IIMX,JJMX,IJMX,ALPHA,SIZE,EPS,MODE,BOX,SD,IX,Z         SUB03360
      COMMON /TAB/ INDEX,KEXTRA,MEXTRA,KLIMIT,MLIMIT,KOUT,MOUT                SUB03370
      COMMON /SYM/ ISYM,JSYM,MSYM,FCU,IMS,JMS,QSYM                            SUB03380
      DIMENSION G(IJMX),H(IIMX,5),SCF(JJMX,6)                                 SUB03390
C     INITIALIZE THE VALUES:                                                  SUB03400
      INDEX=0                                                                 SUB03410
      MTIMER=0                                                                SUB03420
      KOUT=0                                                                  SUB03430
      MOUT=0                                                                  SUB03440
      MMAX=0                                                                  SUB03450
      KMAX=0                                                                  SUB03460
      TOTAL=0.                                                                SUB03470
      JJMX6=JJMX*6                                                            SUB03480
      IIMX2=(IIMX+1)/2                                                        SUB03490
      AR=ALPHA*RS                                                             SUB03500
      ARG=AR**2                                                               SUB03510
      EXPON=EXP(-ARG)                                                         SUB03520
      PIE=3.141592653589793                                                   SUB03530
      APP=ALPHA/PIE/PIE                                                       SUB03540
      M=0                                                                     SUB03550
      RM=M                                                                    SUB03560
      RIMAX=IMAX                                                              SUB03570
      DX=2./RIMAX                                                             SUB03580
      RJMAX=JMAX                                                              SUB03590
      DXI=2.*PIE/FCU                                                          SUB03600
C     INITIALIZE THE MODIFIED HERMITE POLYNOMIAL ARRAY:  VECTORS:            SUB03610
C     (1)=H1, (2)=H2, (3)=ALPHA*X(I), (4)=HM+2 STORED, (5)=HM+1 STORED       SUB03620
      DO 1, II=1,IIMX2                                                        SUB03630
      RII=IIMX-II+1                                                           SUB03640
      H(II,3)=ALPHA*(RII*DX-DX-1.)                                            SUB03650
      H(IIM,3)=-H(II,3)                                                       SUB03660
      H(II,1)=2.*H(II,3)                                                      SUB03670
      H(II,2)=(H(II,3)*H(II,1)-1.)/3.                                         SUB03680
      H(IIM,1)=-H(II,1)                                                       SUB03690
      H(IIM,2)=H(II,2)                                                        SUB03700
      H(IIM,5)=H(II,2)                                                        SUB03710
      H(II,5)=H(II,2)                                                         SUB03720
      H(IIM,4)=H(II,1)                                                        SUB03730
      H(II,4)=H(IIM,1)                                                        SUB03740
      SIGN=1.                                                                 SUB03750
    1 FM=1.                                                                   SUB03760
C     INITIATE THE SIN/COS ARRAY:                                            SUB03770
                                                                              SUB03780
```

142

```
      DO 11 J=1,JJMX
      RJM=J-1
      SCF(J,1) =0.
      SCF(J,2)=1.
      SCF(J,3)=SIN(RJM*DXI-PIE)
      SCF(J,4)=COS(RJM*DXI-PIE)
      SCF(J,5)=0.
   11 SCF(J,6)=0.
C     COMMENCE THE M LOOP:
    2 SMS=0
      SIGN=-SIGN
      K=0
      RK=K
      ARM=1.
      IF(M.NE.0) ARM=AR**M
      KTIMER=0
      SIGNK=-1.
C     COMPUTE THE K=1 ORDERS OF LAGUERRE POLYNOMIAL FOR GIVEN M:
      PM=0.
      P=SQRT(1./FM)
      PP=(RM+1.-ARG)*SQRT(1./FM/(RM+1.))
C     ADVANCE THE SIN/COS ARRAY FOR NEW M:
      DO 12 J=1,JJMX
      SCF(J,1)=SCF(J,1)*SCF(J,4)+SCF(J,2)*SCF(J,3)
   12 SCF(J,2)=SCF(J,2)*SCF(J,4)-SCF(J,1)*SCF(J,3)
      DO 13 J=1,JMAX
      SCF(J,5)=SCF(J+1,1)-SCF(J,1)
   13 SCF(J,6)=SCF(J+1,2)-SCF(J,2)
C     TEST FOR SYMMETRY SKIPS:
      IF(MS.EQ.MSYM) MS=0
      TOTAL=0.
      MS=MS+1
      IF(MS.NE.1) GO TO 7
      RMS=RM*SIG
      CMS=COS(RMS)
      SMS=SIN(RMS)
C     COMMENCE THE K LOOP:
    3 INDEX=INDEX+1
      SIGNK=-SIGNK
C     CALL THE B & D COEFFICIENTS AND COMPUTE THE M,K SUMMATION TERM:
      CALL BD (M,K,G,H,SCF,B,D,JJMX6)
      IF(DGN.LE.-2.) WRITE (6,89) M,K,B,D
      BRAKET=B
      IF(RM.EQ.0.) GO TO 4
      BRAKET=B*CMS+D*SMS
    4 ADD=SIGNK*BRAKET*P*ARM
      TOTAL=TOTAL+ADD
C     ESTABLISH CHECK AS THE RELATIVE SIZE OF THE M,K TERM OF THE SERIES:
```

```
      CHECK=ABS(ADD)                                                     SUB04270
      IF(TOTAL.GT.EPS) CHECK=ABS(ADD/TOTAL)                              SUB04280
C     ADVANCE THE K INDEX:                                              SUB04290
      K=K+1                                                             SUB04300
      RK=K                                                              SUB04310
      ORDER=M+2*K+1                                                     SUB04320
C     GENERATE THE NEXT ORDER OF LAGUERRE POLYNOMIAL FOR NEW K:         SUB04330
      PM=P                                                              SUB04340
      PP=PP                                                             SUB04350
      PP=P*(ORDER-ARG)-PM*SQRT(RK*(RM+RK))                              SUB04360
      PP=PP/SQRT((RK+1.)*(RM+RK+1.))                                    SUB04370
C     GENERATE THE NEXT ORDER OF THE SET OF HERMITE POLYNOMIALS FOR NEW K: SUB04380
      HA=SQRT((RK+RM))/ORDER                                            SUB04390
      HB=2.*SQRT((RK+1.)*(RM+RK+1.))*((RM+RK+1.)/(ORDER+2.)             SUB04400
      DO 5 II=1,IIMX2                                                   SUB04410
      IIM=IIMX-II+1                                                     SUB04420
      H(II,1)=2.*(H(II,3)*H(II,2)-HA*H(II,1))                           SUB04430
      H(II,2)=SIGN*(H(II,3)*H(II,1)-ORDER*H(II,2))                      SUB04440
C     PROVIDE EXTRA K TERMS AFTER CHECK < EPS:                          SUB04450
C     SET K TIMER:                                                      SUB04460
      KTIMER=KTIMER+1                                                   SUB04470
      IF(K.GE.KLIMIT) GO TO 6                                           SUB04480
      IF(MTIMER.LE.MEXTRA) GO TO 2                                      SUB04490
      IF(CHECK.GE.EPS) KTIMER=0                                         SUB04500
      IF(KTIMER.LE.KEXTRA) GO TO 3                                      SUB04510
      GO TO 7                                                           SUB04520
C     END OF K LOOP:  ADVANCE M AND COMPUTE NEW TOTAL:                  SUB04530
6     KOUT=KOUT+1                                                       SUB04540
7     M=M+1                                                             SUB04550
      IF(K.GT.KMAX) KMAX=K                                              SUB04560
      RM=M                                                              SUB04570
      FM=FM*RM                                                          SUB04580
C     REGENERATE THE HERMITE ARRAY FOR NEW M, K=0:                      SUB04590
      DO 8 II=1,IIMX2                                                   SUB04600
      IIM=IIMX-II+1                                                     SUB04610
      H(II,2)=H(II,4)*SQRT(RM)/(RM+1.)                                  SUB04620
      H(II,1)=-(H(IIM,5))*H(II,2)                                       SUB04630
      H(II,2)=2.*SQRT(RM+2.)*(H(IIM,1)*(H(II,3)*H(II,1)-(RM+1.)*H(II,2)) SUB04640
      H(II,3)=2.*SQRT(RM+1.)/(RM+2.)                                    SUB04650
      H(II,2)=H(II,1)                                                   SUB04660
      H(II,4)=H(II,2)                                                   SUB04670
C     SET M TIMER FOR EXTRA M TERMS:                                    SUB04680
8     IF(MS.EQ.1) MTIMER=MTIMER+1                                       SUB04690
      IF(JSYM.GT.JMAX) GO TO 9                                          SUB04700
      IF(K.GT.KEXTRA) MTIMER=0                                          SUB04710
      IF(M.GE.MLIMIT) GO TO 9                                           SUB04720
C     END OF M LOOP:  COMPUTE OUTPUT SOLN.                              SUB04740
```

```
      MOUT=M-1                                                         SUB04750
      IF(KOUT.EQ.0) KOUT=KMAX-1                                        SUB04760
9     SOLN=TOTAL*EXPON*APP/2.                                          SUB04770
89    FORMAT(' M=',I4,',',   K=',I4,',',   B=',E10.4,',',   D=',E10.4) SUB04780
      RETURN                                                           SUB04790
      END                                                              SUB04800
                                                                       SUB04810
                                                                       SUB04820
C000005                                                                SUB00010
C                                                                      SUB00020

      SUBROUTINE GARRAY (G,GA,NOF,DGN,NUMB,XO,YO,PHISYM)               SUB00030
C     GARRAY FILLS THE DATA ARRAY OVER AN ORTHOGONAL AREA WITH         SUB00040
C     THE REGULAR DATA OBTAINED BY THE METHOD CORRESPONDING TO THE     SUB00050
C     PARTICULAR MODE:                                                 SUB00060
C                                                                      SUB00070
C     MODE 1  -   DATA OBTAINED BY SAMPLING A KNOWN FUNCTION SUPPLIED  SUB00080
C                 IN SUBROUTINE FUNCT AND SAMPLED IN SUBROUTINE GOLF.  SUB00090
C                                                                      SUB00100
C     MODE 2  -   DATA OBTAINED BY GENERATING A REGULAR ARRAY FROM     SUB00110
C                 IRREGULAR EXPERIMENTAL INPUT DATA READ IN.  CALLS    SUB00120
C                 SUBROUTINE EXPERIMENTAL (EXPERIMENTAL DATA MAY       SUB00130
C                 BE SIMULATED, SEE SHEET.)                            SUB00140
C                                                                      SUB00150
C     MODE 3  -   UTILIZES RAW DATA TAKEN AT THE PROPER INTERVAL,      SUB00160
C                 OR PREVIOUSLY GENERATED, AND READ DIRECTLY INTO THE  SUB00170
C                 GARRAY.  CALLS SUBROUTINE READ.                      SUB00180
C                                                                      SUB00190
      COMMON IMAX,JMAX,IIMX,JJMX,IJMX,ALPHA,SIZE,EPS,MODE,BOX,SD,IX,Z  SUB00200
      COMMON /SYM/ IISYM,JISYM,MSYM,FCU,IMS,JMS,QSYM                   SUB00210
      COMMON /IO/ CMS,IN1,IN2,IN4                                      SUB00220
      DIMENSION G(IMAX,JMAX),GA(IMAX,JMAX)                             SUB00230
      PIE=3.141592653589793                                           SUB00240
      HS=SIZE/2.                                                       SUB00250
      IF(MODE.GT.3) MODE=1                                             SUB00260
      RIMX=IMAX                                                        SUB00270
      RJMX=JMAX                                                        SUB00280
      DELR=SIZE/RIMX                                                   SUB00290
      DELXI=2.*PIE/FCU                                                 SUB00300
      IF(MODE.GT.1) GO TO 2                                            SUB00310
      DO 1 J=1,JMS                                                     SUB00320
      RJ=J                                                             SUB00330
      XI=(RJ-.5)*DELXI-PIE                                             SUB00340
      J2=J+2*(JMS-J)                                                   SUB00350
      J3=J+JMAX/2                                                      SUB00360
      J4=J2+JMAX/2                                                     SUB00370
                                                                       SUB00380
```

145
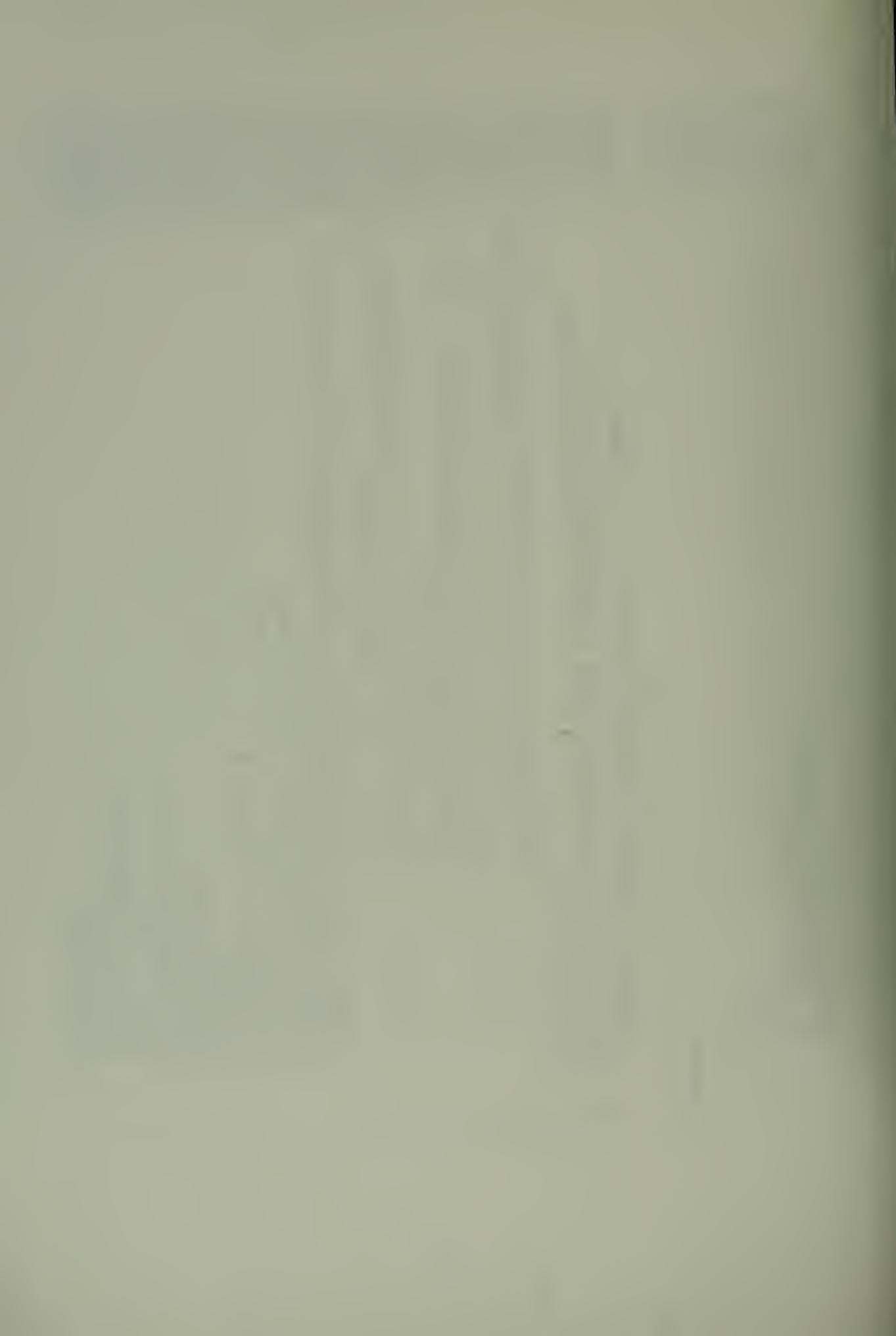
```
          DO 1  I=1,IMS
          RI=I
          II=IMAX+1-I
          R=(RI-.5)*DELR-HS
          CALL GOLF (R,XI,GIJ,NOF,DGN,NUMB)
          G(I,J)=GIJ
          IF(ISYM.EQ.2) G(II,J)=GIJ
          IF(ISYM.EQ.2) GO TO 1
          G(II,J3)=GIJ
          IF(JSYM.EQ.0) GO TO 1
          G(I,J2)=GIJ
          G(II,J4)=GIJ
   1      CONTINUE
          GO TO 4
   2      IF(MODE.GT.2) GO TO 3
          CALL SHEET (G,GA,XO,YO,PHISYM,NOF)
          GO TO 4
   3      CALL READ (Z,XO,YO,PHISYM,NOF,IMAX,JMAX,G)
   4      IF(DGN.GE.2) WRITE (6,39)
          RETURN
  39      FORMAT ('   GARRAY RETURNS')
          END
C000006
C

          SUBROUTINE GOLF (R,XI,GIJ,NOF,DGN,NUMB)
C
C     GOLF COMPUTES THE FUNCTION G(R,XI) FOR A PARTICULAR LINE OF SIGHT
C     FROM A KNOWN FUNCTION CONTAINED IN SUBROUTINE FUNCT.
C
          COMMON IMAX,JMAX,IIMX,JJMX,IIMX,JJMX,IJMX,ALPHA,SIZE,EPS,MODE,BOX,SD,IX,Z
          ZERO=0.
          LMAX=IMAX*3
          RLMAX=LMAX
          DELXP=SIZE/RLMAX
          SXI=SIN(XI)
          CXI=COS(XI)
          DELXS=DELXP*CXI
          DELYS=DELXP*SXI
          XP=DELXP*.5-SIZE/2.
          XS=XP*CXI-R*SXI
          YS=XP*SXI+R*CXI
          GIJ=0.
          DO 1  L=1,LMAX
          RL=L
          CALL FUNCT(XS,YS,F,NOF,DGN,NUMB)
          GIJ=GIJ+F
```
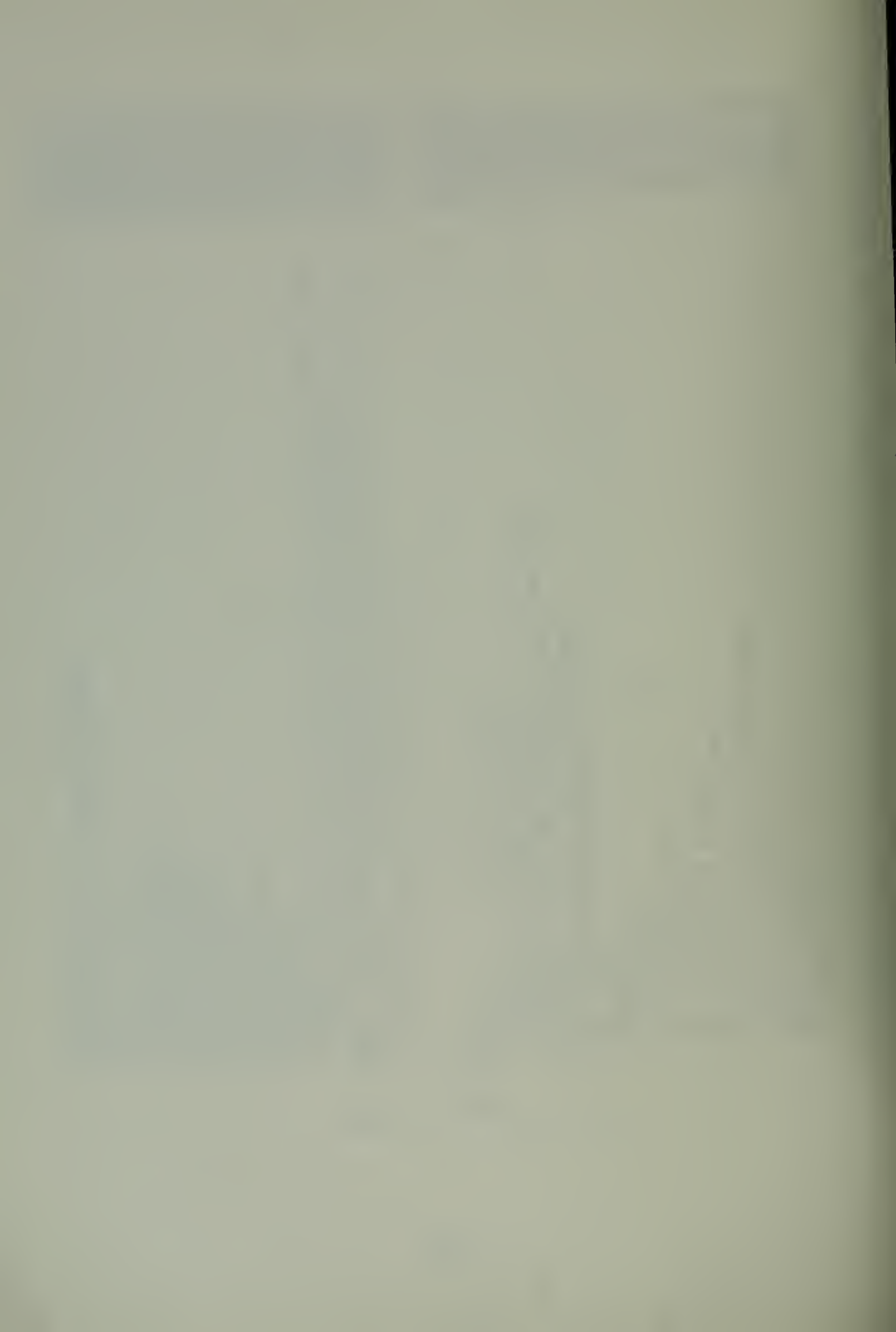
```
        XS=XS+DELXS                                                        SUB00850
        YS=YS+DELYS                                                        SUB00860
        IF (GIJ.NE.0.) GIJ=GIJ*DELXP*BOX                                   SUB00870
        IF ((SD.EQ.0.).OR.(NUMB.EQ.1)) GO TO 2                             SUB00880
        IF (DGN.GE.3) WRITE (6,28) IX                                      SUB00890
        CALL GAUSS (IX,SD,ZERO,RV)                                         SUB00900
        GIJ=GIJ+RV                                                         SUB00910
        IF (DGN.GE.3) WRITE (6,29) R,XI,GIJ                                SUB00920
        RETURN                                                             SUB00930
 29     FORMAT ('    R=',F8.3,'  XI=',F8.3,'  GIJ=',F8.3)                  SUB00940
 28     FORMAT (' GAUSS, IX=',I8)                                          SUB00950
        END                                                                SUB00960
C000007                                                                    SUB00970
C                                                                          SUB00980

        SUBROUTINE FUNCT (XS,YS,F,NOF,DGN,NUMB)                            SUB00990
C                                                                          SUB01000

CP67USERID  1095BOXJ                                                       SUB01020
C                                                                          SUB01030
C   FUNCT EVALUATES AS INPUT FUNCTION AT POSITION (X,Y) IN THE TEST        SUB01040
C   SECTION COORDINATE SYSTEM.  NOF IDENTIFIES THE EQUATION USED.          SUB01050
C                                                                          SUB01060
        COMMON IMAX,JMAX,IIMX,JJMX,IJMX,ALPHA,SIZE,EPS,MODE,BOX,SD,IX,Z    SUB01070
        COMMON /EQPARA/ A,B,C,D,E,P,Q,S,T,U,V,W,RO,RA,NO,NA,N1,N2          SUB01080
        DIMENSION RO(101),RA(101)                                          SUB01090
        AA=A                                                               SUB01100
        BB=B                                                               SUB01110
        CC=C                                                               SUB01120
        DD=D                                                               SUB01130
        EE=E                                                               SUB01140
        PP=P                                                               SUB01150
        IF (NUMB.LE.1) GO TO 50                                            SUB01160
        AA=S                                                               SUB01170
        BB=T                                                               SUB01180
        CC=U                                                               SUB01190
        DD=V                                                               SUB01200
        EE=W                                                               SUB01210
        PP=Q                                                               SUB01220
 50     PIE=3.14159265358979793                                           SUB01230
        HS=SIZE/2.                                                         SUB01240
        R=SQRT(XS**2+YS**2)/HS                                             SUB01250
        F=0.                                                               SUB01260
        IF (R.GT.1.) GO TO 11                                             SUB01270
        IF (NOF.LE.0) GO TO 11                                            SUB01280
C
C   1.  AXISYMMETRIC GAUSSIAN:
```

```
   1      IF (NOF.GT.1) GO TO 2
          F=AA*EXP(-1.*(R*HS/BB)**2)
          GO TO 11
C     ADJUSTABLE RECTANGULAR STEP FUNCTION:
   2    2 IF (NOF.GT.2) GO TO 3
          F=PP
          IF ((ABS(XS-DD).LE.BB).AND.(ABS(YS-EE).LE.CC))  F=AA
          GO TO 11
C     DISPLACABLE ELLIPTICAL GAUSSIAN:
   3    3 IF (NOF.GT.3) GO TO 4
          F=AA*EXP(-1.*(((XS-DD)/BB)**2+((YS-EE)/CC)**2))
          GO TO 11
C     CONSTANT:
   4    4 IF (NOF.GT.4) GO TO 5
          F=AA
          GO TO 11
C     ADJUSTABLE AND DISPLACABLE ELLIPTIC RAMP FUNCTION:
   5    5 IF (NOF.GT.5) GO TO 6
          RBC=SQRT(((XS-DD)/BB)**2+((YS-EE)/CC)**2)
          F=0.
          IF (RBC.LT.1.)  F=AA*((1.-RBC)**PP)
          GO TO 11
C     DISPLACABLE ELLIPTIC STEP FUNCTION:
   6    6 IF (NOF.GT.6) GO TO 7
          RBC=SQRT(((XS-DD)/BB)**2+((YS-EE)/CC)**2)
          F=0.
          IF (RBC.LT.1.)  F=AA
          GO TO 11
C     CIRCULAR COSINE-SQUARED FUNCTION OF BB MAXIMA:
   7    7 IF (NOF.GT.7) GO TO 8
          F=AA*COS((2.*BB-1.)*PIE*R/2.)**2
          GO TO 11
C     NUMERICAL FUNCTION:  REQUIRES AN INPUT ARRAY READ IN BY
C     SUBROUTINE FREAD: N POINT VALUES FOLLOWED BY N POINT VALUES. (101 MAX)
C     A CONSTANT VALUE AA IS ADDED TO THE FUNCTION.
   8    8 IF (NOF.GT.8) GO TO 9
          IF (NUMB.LE.1) N=NO
          IF (NUMB.GT.1) N=NA
          NM=N-1
          NMM=N-2
          RN=N
```

148

```
      RI=R*(RN-1.)+1.                                                   SUB01770
      IR=INT(RI)                                                        SUB01780
      RIR=FLOAT(IR)                                                     SUB01790
      DI=RI-RIR                                                         SUB01800
      IF(NUMB..LE.1)  F=RO(IR)                                          SUB01810
      IF(NUMB..GT.1)  F=RA(IR)                                          SUB01820
      IF((IR..NE.N)..AND.(NUMB..LE.1))   F=F+DI*(RO(IR+1)-RO(IR))       SUB01830
      IF((IR..NE.N)..AND.(NUMB..GT.1))   F=F+DI*(RA(IR+1)-RA(IR))       SUB01840
      F=F*AA+BB                                                         SUB01850
      GO TO 11                                                          SUB01860
C                                                                       SUB01870
C  9.  SPECIAL FUNCTION: MAY BE WRITTEN FOR THE OCCASION AND            SUB01880
C      INSERTED IN SUBROUTINE SPFUN                                     SUB01890
    9 IF(NOF.GT.9) GO TO 10                                             SUB01900
      CALL SPFUN (XS,YS,F)                                              SUB01910
      GO TO 11                                                          SUB01920
C                                                                       SUB01930
C 10.  EQUATIONS NO. 10 AND BEYOND ARE SET TO ZERO.                     SUB01940
   10 F=0.                                                              SUB01950
C                                                                       SUB01960
   11 IF (DGN..GE.4) WRITE (6,99) XS,YS,F                               SUB01970
   99 FORMAT(' XS=',F8.3,',',YS=',F8.3,',',     F=',F8.3)               SUB01980
      RETURN                                                            SUB01990
      END                                                               SUB02000
C00000C8                                                                SUB02010
C                                                                       SUB02020
                                                                        SUB02030

      SUBROUTINE SPFUN (XS,YS,F)                                        SUB02040
C                                                                       SUB02050
C  SPFUN IS A SPECIAL ROUTINE FOR EQ'N NO. 9.  ANY FUNCTION MAY BE      SUB02060
C  ENTERED.                                                             SUB02070
C                                                                       SUB02080
      COMMON /EQPARA/ A,B,C,D,E,P,Q,S,T,U,V,W,RO,RA,NO,NA,N1,N2         SUB02090
      DIMENSION RO(101),RA(101)                                         SUB02100
      F=0.                                                              SUB02110
      IF ((ABS(XS)..LE.B)..AND.(ABS(YS)..LE.C))   F=A                   SUB02120
      RETURN                                                            SUB02130
      END                                                               SUB02140
C00000C9                                                                SUB02150
C                                                                       SUB02160
```

149

```fortran
      SUBROUTINE SHEET (G,D,XO,YO,PHISYM,NOF)                        SUB02170
C                                                                    SUB02180
C SHEET READS IRREGULARLY SPACED VALUES OF THE LINE INTEGRAL, AS     SUB02190
C OBTAINED FROM HOLOGRAPHIC INTERFEROGRAMS. THE INTEGRAL LINES MAY BE SUB02200
C DEFINED EITHER BY GRID INTERCEPT POSITIONS, OR BY ANGLE AND RADIUS SUB02210
C ABOUT THE CENTER OF THE LABORATORY COORDINATE SYSTEM CENTER. HIGHEST SUB02220
C MUST BE ENTERED IN CONSECUTIVE ORDER FROM LOWEST (NEG.) TO HIGHEST SUB02230
C (POS.) RADIUS. DATA MAY BE SIMULATED BY SPECIFYING NCODE=1, SUBFUNCT. SUB02240
C FOLLOWED BY APERATURE POSITIONS FOR A FUNCTION NUMBER IN 'SUBFUNCT'. SUB02250
C                                                                    SUB02260
      COMMON IMAX,JMAX,IIMX,JJMX,IJMX,ALPHA,SIZE,EPS,MODE,BOX,SD,IX,Z SUB02270
      COMMON /SYM/ISYM,JSYM,MSYM,FCU,IMS,JMS,QSYM                     SUB02280
      COMMON /IO/CMS,IN1,IN2,IN4                                      SUB02290
      DIMENSION G(303),D(IMAX,JMAX),XI(303),RR(303)                  SUB02300
      DIMENSION XG(303),YG(303),XD(303),YD(303),XY(303)              SUB02310
      NAR=303                                                        SUB02320
      PIE=3.141592653589793                                          SUB02330
      MPIE=-1.*PIE                                                   SUB02340
      MPPIE=2.*PIE                                                   SUB02350
      MPPIT=PIE*PIE/2.                                               SUB02360
      PIET=PIE*PIE/2.                                                SUB02370
C                                                                    SUB02380
C ZERO THE ARRAYS:                                                   SUB02390
      DO 1 J=1,JMAX                                                  SUB02400
      DO 1 I=1,IMAX                                                  SUB02410
      G(I,J)=0.                                                      SUB02420
    1 D(I,J)=0.                                                      SUB02430
      DO 2 I=1,NAR                                                   SUB02440
      XG(I)=0.                                                       SUB02450
      YG(I)=0.                                                       SUB02460
      XD(I)=0.                                                       SUB02470
      YD(I)=0.                                                       SUB02480
      XY(I)=0.                                                       SUB02490
      XI(I)=0.                                                       SUB02500
    2 RR(I)=0.                                                       SUB02510
C                                                                    SUB02520
C READ THE BASIC DATA:                                               SUB02530
      IF(CMS.EQ.1.) REWIND 1                                         SUB02540
      READ(IN1,59) NOF,NCODE                                         SUB02550
      READ(IN1,58) Z,XO,YO,PHISYM,XMX,XMN,YMX,YMN                    SUB02560
      READ(IN1,59) JM                                                SUB02570
      RIMX=IMAX                                                      SUB02580
      DR=SIZE/RIMX                                                   SUB02590
      R=(-DR-SIZE)/2.                                                SUB02600
      RZO=SQRT(XO**2+YO**2)                                          SUB02610
      GAM=ATANM(YO,XO)                                               SUB02620
      TP=3-ISYM                                                      SUB02630
      BT=JSYM                                                        SUB02640
      DAN=PIE*TP/BT
      HS=SIZE/2.
```

```
      MXY=1
      IF((XMX.NE.0.).OR.(XMN.NE.0.).OR.(YMX.NE.0.).OR.(YMN.NE.0.))MXY=0
      IF((MXY.EQ.1) GO TO 3
      XMX=XO++HS
      YMX=YO+HS
      XMN=XO-HS
      YMN=YO-HS
C     COMMENCE THE READ AND FILL LOOP:
3     DO 12 J=1,JM
      READ (IN1,59)IM
      MN=0.
      XH=0.
C     READ THE LINES, DETERMINE CODE, CALCULATE RADIUS & ANGLE FOR CODE 1:
      DO 5 I=1,IM
      IF(NCODE.LE.0)READ(IN1,58) XD(I),YD(I),XG(I),YG(I),D(I,J),RR(I),
     1XI(I),XY(I)
      IF(NCODE.GE.1)CALL SIM(XD(I),YD(I),XG(I),YG(I),RR(I),XI(I),
     1XY(I),XO,YO,PHISYM,XMX,XMN,YMX,YMN,NOF,I,IM)
      IF(XY(I).EQ.3.) GO TO 5
      IF((YD(I).NE.0.).OR.(YG(I).NE.0.)) XY(I)=1.
      IF((XD(I).NE.0.).OR.(XG(I).NE.0.)) XY(I)=1.
      IF((RR(I).NE.0.).AND.(XI(I).NE.0.)) XY(I)=2.
      IF((XY(I).EQ.0.).AND.(XY(I).EQ.0.)) XY(I)=2.
      IF((XY(I).EQ.1.).AND.(D(I,J).NE.0.)) GO TO 4
      DEN=SQRT((XG(I)-XD(I))**2+(YG(I)-YD(I))**2)
      IF((DEN.EQ.0.).OR.(XY(I).EQ.4.) GO TO 4
      RR(I)=((XO-XD(I))*(YG(I)-YD(I))-(XG(I)-XD(I))*(YO-YD(I)))/DEN
      XIM=ATANM((YG(I)-YD(I)),(XG(I)-XD(I)))
      XIM=XI(I)
4     IF((XY(I).EQ.2.) XIM=XI(I)
      XIN=XIM
      IF((XY(I).EQ.2.) RR(I)=RR(I)+RZO*SIN(GAM-XI(I))
5     CONTINUE
C     COMPUTE MAX AND MIN ANGLE INDEXES FOR APERATURE POSITION LOCATION:
      DO 6 I=1,IM
      IF((XY(I).NE.1.).OR.(XY(I).NE.2.)) GO TO 6
      IF((XI(I).GT.XIM) IMT=XI(I)
      IF((XI(I).GT.XIM) IMT=I
      IF((XI(I).LT.XIN) XIN=XI(I)
      IF((XI(I).LE.XIN) INT=I
6     CONTINUE
C     DETERMINE APERATURE LOCATION:
      LPR=0
      XID=XI(IMT)-XI(INT)
      IF(ABS(XID).LT..00001) LPR=1
      XIH=(XI(IMT)+XI(INT))/2.
```

```
      RRH=100CO.*COS(XIH)                                              SUB03130
      XH=RRH*COS(XIH)                                                  SUB03140
      YH=RRH*SIN(XIH)                                                  SUB03150
      IF(LPR.EQ.1) GO TO 7                                             SUB03160
      YTX=-RR(IMT)*SIN(XI(IMT))-YO                                     SUB03170
      YTN=-RR(INT)*SIN(XI(INT))-YO                                     SUB03180
      XTX=RR(IMT)*COS(XI(IMT))-XO                                      SUB03190
      XTN=RR(INT)*COS(XI(INT))-XO                                      SUB03200
      UA=TAN(XI(IMT))                                                  SUB03210
      UC=TAN(XI(INT))                                                  SUB03220
      UB=YTX-UA*XTX                                                    SUB03230
      UD=YTN-UC*XTN                                                    SUB03240
      XH=(UD-UB)/(UA-UC)                                               SUB03250
      YH=XH*UA+UB                                                      SUB03260
      RRH=SQRT((XH-XO)**2+(YH-YO)**2)                                  SUB03270
      XIH=ATANM((YH-YO),(XH-XO))                                       SUB03280
7     CONTINUE                                                         SUB03290
C     FILL THE ANGLE AND RADIUS FOR ANY CODE 3 OR 4 LINES:            SUB03300
      DO 9 I=1,IM                                                      SUB03310
      IF(XY(I).NE.3.) GO TO 8                                          SUB03320
      BAS=SQRT(RRH**2-RR(I)**2)                                        SUB03330
      XI(I)=XIH-ATANM(RR(I),BAS)                                       SUB03340
      GO TO 9                                                          SUB03350
8     XI(I)=ATANM((YH-YD(I)),(XH-XD(I)))                              SUB03360
      RR(I)=RRH*SIN(XI(I)-XIH)                                         SUB03370
9     CONTINUE                                                         SUB03380
C     ANGLES AND RADII ARE NOW FILLED FOR ALL POINTS IN THIS LINE.    SUB03390
C     VACATE THE SET OF VECTORS TO BE USED AS TEMPORARY STORAGE:      SUB03400
      DO 10 I=1,IM                                                     SUB03410
      XD(I)=0.                                                         SUB03420
      YD(I)=0.                                                         SUB03430
      XG(I)=0.                                                         SUB03440
      XY(I)=0.                                                         SUB03450
      RR(I)=D(I,I)                                                     SUB03460
10    D(I,J)=0.                                                        SUB03470
C     CONVERT THE LINE TO REGULAR RADII USING INTERPOLATION:          SUB03480
      RR(1)=R+DR                                                       SUB03490
      CALL SPLINE(YG,XY,IM,RR(1),D(1,J))                              SUB03500
      DO 11 I=2,IMAX                                                   SUB03510
      RI=R+DR*RI                                                       SUB03520
11    RR(I)=R+DR*RI                                                    SUB03530
C     GENERATE THE VECTOR OF ANGLES FOR THIS COLUMN AND STORE IN G ARRAY: SUB03540
      CALL SPLINN(YG,XY,IM,RR(I),D(I,J))                              SUB03550
      DO 12 I=1,IMAX                                                   SUB03560
      BAS=SQRT(RRH**2-RR(I)**2)                                        SUB03570
      G(I,J)=XIH-ATANM(RR(I),BAS)                                      SUB03580
                                                                       SUB03590
                                                                       SUB03600
```

152

```
      YG(I)=0.
      D(I,J)=XY(I)
   12 XY(I)=0.
C     COLUMNS ARE NOW ALL REGULARLY FILLED.                             SUB03610
C     NEXT,INTERPOLATE EACH ROW REGULARLY OVER THE ANGLES.
      DO 23 I=1,IMAX
C     EXPAND THE DATA TO 2 SETS TO ESTABLISH SMOOTH INTERPOLATION.
      JM3=3*JM
      II=IMAX+1-I
      IF(JSYM.NE.0) GO TO 14
   13 DO 13 J=1,JMS
      J2=J+JMS
      J3=J2+JMS
      XD(J1)=D(II,J)
      XD(J2)=D(II,J)-TPIE-PHISYM
      XD(J3)=D(II,J)-PIE-PHISYM
      XG(J1)=G(II,J)-PIE-PHISYM
      XG(J2)=G(II,J)-PHISYM
      GO TO 16
   14 DO 15 J=1,JMS
      J1=JMS+J
      J2=JMS+1-J
      J3=JM3+1-J
      XD(J1)=D(II,J)
      XD(J2)=D(II,J)
      XD(J3)=D(II,J)
      XG(J1)=G(II,J)-2.*(G(I,J)-PHISYM)-PIE-PHISYM
      XG(J2)=PIE-PHISYM
      XG(J3)=J+2.*(DAN+PHISYM-G(II,J))-PIE-PHISYM
   15 CONTINUE
   16 JM2=2*JMS
      JP=JMS/2
   17 DO 17 J=1,JM2
      XD(J)=XD(J+JP)
      XG(J)=XG(J+JP)
      JJS=JM2+1
   18 DO 18 J=JJS,JM3
      XG(J)=0.
C     FIND THE SMALLEST ANGLE
      XY(1)=1.
      SA=XG(1)
   19 DO 19 J=1,JM2
      IF(XG(J).GE.SA) GO TO 19
      SA=XG(J)
      XY(1)=J
   19 CONTINUE
```

```
C     FIND THA MAX ANGLE IN THE ROW:
      XY(JM2)=JM2                                                        SUB04090
      SB=XG(JM2)                                                         SUB04100
      DO 20 J=1,JM2                                                      SUB04110
      IF (XG(J).LE.SB) GO TO 20                                          SUB04120
      SB=XG(J)                                                           SUB04130
      XY(JM2)=J                                                          SUB04140
   20 CONTINUE                                                           SUB04150
C     DETERMINE THE ORDER OF INCREASING ANGLE IN THE ROW                SUB04160
      JJ=2                                                               SUB04170
   21 JSA=XY(JJ-1)                                                       SUB04180
      SA=XG(JJ-1)                                                        SUB04190
      JTS=0                                                              SUB04200
      DO 22 J=1,JM2                                                      SUB04210
      IF (XG(J).LE.SA) GO TO 22                                          SUB04220
      IF (XG(J).GT.SB) GO TO 22                                          SUB04230
      SB=XG(J)                                                           SUB04240
      XY(JJ)=J                                                           SUB04250
      JTS=1                                                              SUB04260
   22 CONTINUE                                                           SUB04270
      IF (JTS.EQ.0) JM2=JJ                                               SUB04280
      JJ=JJ+1                                                            SUB04290
      IF (JJ.LE.JM2) GO TO 21                                            SUB04300
      DO 23 J=1,JM2                                                      SUB04310
      JX=XY(J)                                                           SUB04320
      YD(J)=XD(JX)                                                       SUB04330
C     INTERPOLATE:                                                       SUB04340
      DXI=2.*PIE/FCU                                                     SUB04350
      XI(J)=DXI/2.-PIE-PHISYM                                            SUB04360
      CALL SPLINE(XG,YD,JM2,XI(J),G(I,J))                               SUB04370
      DO 24 J=2,JMS                                                      SUB04380
      XI(J)=XI(J-1)+DXI                                                  SUB04390
      CALL SPLINN(XG,YD,JM2,XI(J),G(I,J))                               SUB04400
   24 DO 25 J=1,JMS                                                      SUB04410
      XIJ=XI(J)                                                          SUB04420
      XU=XMX                                                             SUB04430
      IF ((XIJ.GE.0.).AND.(XIJ.LT.PIE)) XU=XMN                          SUB04440
      YU=YMN                                                             SUB04450
      IF ((XIJ.GE.MPIT).AND.(XIJ.LT.PIT)) YU=YMX                        SUB04460
      XL=XMN                                                             SUB04470
      IF ((XIJ.GE.0.).AND.(XIJ.LT.PIE)) XL=XMX                          SUB04480
      YL=YMX                                                             SUB04490
      IF ((XIJ.GE.MPIT).AND.(XIJ.LT.PIT)) YL=YMN                        SUB04500
      SXIJ=SIN(XIJ)                                                      SUB04510
      CXIJ=COS(XIJ)                                                      SUB04520
      RMN=(XO-XL)*SXIJ-(YO-YL)*CXIJ                                      SUB04530
      RMX=(XO-XU)*SXIJ-(YO-YU)*CXIJ                                      SUB04540
```

```
      DO 25 I=1,IMAX                                              SUB04570
      IF(RR(I).LT.RMN) G(I,J)=0.                                  SUB04580
      IF(RR(I).GT.RMX) G(I,J)=0.                                  SUB04590
25    CONTINUE                                                    SUB04600
C     EXPAND SYMMETRY SECTOR INTO AN ORTHOGONAL INTERVAL.         SUB04610
      IF(ISYM.EQ.2) GO TO 27                                      SUB04620
      DO 26 J=1,JMS                                               SUB04630
      J2=JMAX/2+I-J                                               SUB04640
      J3=JMAX/2+J                                                 SUB04650
      J4=JMAX+1-J                                                 SUB04660
      DO 26 II=1,IMAX                                             SUB04670
      II=IMAX+1-I                                                 SUB04680
      G(II,J2)=G(I,J)                                             SUB04690
      G(II,J3)=G(I,J)                                             SUB04700
      G(II,J4)=G(I,J)                                             SUB04710
26    RETURN                                                      SUB04720
C     FOR EVEN SYMMETRY, AVERAGE THE GARRAY COLUMNS.             SUB04730
27    IMS=(2*IMAX+1)/2                                            SUB04740
      DO 28 J=1,JMAX                                              SUB04750
      DO 28 I=1,IMS                                               SUB04760
      II=IMAX+1-I                                                 SUB04780
      GST=(G(I,J)+G(II,J))/2.                                     SUB04790
      G(I,J)=GST                                                  SUB04800
28    G(II,J)=GST                                                 SUB04810
      RETURN                                                      SUB04820
59    FORMAT (5I5)                                                SUB04830
58    FORMAT (10F7.3)                                             SUB04840
      END                                                         SUB04850
C0000010                                                          SUB04860
C
      FUNCTION ATANM(Y,X)                                         SUB04870
C                                                                 SUB04880
C     COMPUTES THE ARCTAN OF Y/X BETWEEN -PI AND +PI.            SUB04890
C                                                                 SUB04900
      PIE=3.14159265358979                                        SUB04910
      PI2=PIE/2.                                                  SUB04920
      ATANM=SIGN(PI2,Y)                                           SUB04930
      IF(X.NE.0.) ATANM=ATAN(Y/X)                                 SUB04940
      IF(X.GE.0.) RETURN                                          SUB04950
      IF(Y.GE.0.) ATANM=PIE+ATANM                                 SUB04960
      IF(Y.LT.0.) ATANM=-PIE+ATANM                                SUB04970
      RETURN                                                      SUB04980
      END                                                         SUB04990
C0000011                                                          SUB05000
C                                                                 SUB05010
```

155

```
      SUBROUTINE SIM (XD,YD,XG,YG,D,R,XI,XY,XO,YO,PS,XM,XN,YM,YN,I,IM,     SUB05020
     1DG,NF)                                                               SUB05030
C     SIM SIMULATES THE FRINGE NUMBER DATA ONE WOULD OBTAIN FROM THE       SUB05040
C     HOLOGRAPHIC INTERFEROGRAM PROCESS FOR A KNOWN FUNCTION AS THE        SUB05050
C     CONTAINED IN SUBROUTINE FUNCT. THE GRID BOX DIMENSIONS MUST          SUB05060
C     EXCEED THE INVERSION CIRCLE SIZE, AND APERATURE POINTS SPECIFIED     SUB05070
C     MUST FALL BETWEEN XI=-40 DEGREES, AND XI=+130 DEGREES.               SUB05080
                                                                           SUB05090
      COMMON IMAX,JMAX,IIMX,JJMX,IJMX,ALF,SIZ,EPS,MOD,BOX,SD,IX,Z          SUB05100
      COMMON /IO/ CMS,INI,IN2,IN4                                          SUB05110
      READ (IN1,29) XH,YH                                                  SUB05120
      ZER=0.                                                               SUB05130
      RIM=IM                                                               SUB05140
      RI=I                                                                 SUB05150
      DX=(XM-XN)/(RIM-1.)                                                  SUB05160
      DY=(YM-YN)/(RIM-1.)                                                  SUB05170
      XI1=XM-(RIM-1.)*DX                                                   SUB05180
      YI1=YM-(RIM-1.)*DY                                                   SUB05190
      XI1=ATANM (YH-Y1,XH-X1)-PS                                           SUB05200
      RRH=SQRT((XH-XO)**2+(YH-YO)**2)                                      SUB05210
      XIO=ATANM(YH-YO,XH-XO)-PS                                            SUB05220
      RI1=RRH*SIN(XI1-XIO)                                                 SUB05230
      IF ((I.GT.1).AND.(I.LT.IM)) GO TO 1                                  SUB05240
      IF ((ABS(RI).LT.SIZ/2.) R1=SIGN(SIZ/2.,R1)                           SUB05250
      XY=3.                                                                SUB05260
      GO TO 2                                                              SUB05270
    1 CALL GOLF (R,XI,D,NR,ZER,ZER)                                        SUB05280
      XD=XN                                                                SUB05290
      YD=YN                                                                SUB05300
      IF (XH.NE.X1) YD=Y1-(X1-XN)*(YH-Y1)/(XH-X1)                          SUB05310
      IF (YS.GE.YN) GO TO 2                                                SUB05320
      YD=YN                                                                SUB05330
      IF (YH.NE.Y1) XD=X1-(Y1-YN)*(XH-X1)/(YH-Y1)                          SUB05340
      RETURN                                                               SUB05350
   29 FORMAT (10F7.3)                                                      SUB05360
      END                                                                  SUB05370
                                                                           SUB05380
C000012                                                                    SUB00010
                                                                           SUB00020

      SUBROUTINE FREAD (NO,RO,NF,ZZ)                                       SUB00030
C     FREAD READS THE NUMERIC ARRAY WHICH IS USED FOR EQUATION 8 OF        SUB00040
C     SUBROUTINE FUNCT. FIRST CARD IS NUMBER OF POINTS (N.GE.1),           SUB00050
C     FOLLOWED BY ONE POINT PER CARD.                                      SUB00060
                                                                           SUB00070
      DIMENSION RO(101)                                                    SUB00080
                                                                           SUB00090
```

156

```
      READ (NF,89) NO,ZZ                                               SUB00100
      WRITE(6,90) NO,ZZ
      DO 10 I=1,NO                                                     SUB00120
      READ(NF,88) RO(I)
      WRITE(6,88) RO(I)
   10 CONTINUE                                                         SUB00140
   89 FORMAT(I5,F9.3)                                                  SUB00150
   88 FORMAT(F8.5)                                                     SUB00160
   90 FORMAT(1X,I5,F9.3)                                               SUB00170
      RETURN
      END
C000013
C
      SUBROUTINE GPRINT (G,NUMB)
C
C     GPRINT PRINTS THE DATA ARRAY 'G'  WHICH WAS INPUT TO
C     THE PROGRAM IN SUBROUTINE GARRAY.
C
      COMMON IMAX,JMAX,IIMX,JJMX,IJMX,ALPHA,SIZE,EPS,MODE,BOX,SD,IX,Z   SUB00180
      DIMENSION G(IJMX)                                                SUB00190
      DIMENSION X(15)                                                  SUB00200
      DATA HYP,VERT/1H-,1HI/                                           SUB00210
      IF (NUMB.EQ.1) WRITE (6,99) MODE,Z                               SUB00220
      IF (NUMB.EQ.2) WRITE (6,92) Z                                    SUB00230
      JM2=JMAX/2                                                       SUB00240
      RIMAX=IMAX                                                       SUB00250
      RJMAX=JMAX                                                       SUB00260
      DX=SIZE/RIMAX                                                    SUB00270
      DXI=360./RJMAX                                                   SUB00280
C     INTRVL SETS THE NUMBER OF TERMS PRINTED PER LINE. IF IT IS ALTERED, SUB00290
C     ONE MUST ALSO REDIMENSION X AND ALTER FORMATS 98, 97, AND 95.    SUB00300
      INTRVL=15                                                        SUB00310
      IB=1                                                             SUB00320
    1 IT=IB+INTRVL-1                                                   SUB00330
      IF (IT.GT.IMAX) IT=IMAX                                          SUB00340
      IBT=IT-IB+1                                                      SUB00350
      WRITE (6,98) (II,II=IB,IT)                                       SUB00360
      DO 2 I=1,IBT                                                     SUB00370
      RI=IB-1+I                                                        SUB00380
      X(I)=-SIZE/2.+(RI-.5)*DX                                         SUB00390
    2 LM=7*IBT+1                                                       SUB00400
      WRITE (6,97) (X(I),I=1,IBT)                                      SUB00410
      WRITE (6,96) (HYP,L=1,LM),VERT                                   SUB00420
      JMH=JM2+1                                                        SUB00430
      DO 3 J=JMH,JMAX                                                  SUB00440
      RJ=J                                                             SUB00450
```

157

```
      XI=-180.+DXI*(RJ-.5)
      IGB=(J-1)*IMAX+IB                                              SUB00510
      IGT=IGB-IB+IT                                                  SUB00520
      WRITE (6,95) J,XI,(G(L),L=IGB,IGT)                            SUB00530
      WRITE (6,94) (HYP,L=1,LM),VERT                                SUB00550
      IB=IB+INTRVL                                                   SUB00560
      ITOLD=IT                                                       SUB00570
      IT=IT+INTRVL                                                   SUB00580
      IF (ITOLD.LT.IMAX) GO TO 1                                    SUB00590
      WRITE (6,93)                                                   SUB00600
   99 FORMAT(1H1//'       THE ARRAY OF INPUT DATA (G), OBTAINED BY GARRAY,SUB00610
     1MODE = ',I1,'   FOR Z= ',F7.3,'  CM:')                        SUB00620
   98 FORMAT(//I1,'  I= ',15I7)                                     SUB00630
   97 FORMAT(11X,'  X= ',15F7.3)                                    SUB00640
   96 FORMAT(11X,'  XI= ',15F7.3)                                   SUB00650
   95 FORMAT(2X,I3,F9.2,'',15F7.3)                                  SUB00660
   94 FORMAT(14X,3,'',115A1)                                        SUB00670
   93 FORMAT(//5X)                                                   SUB00680
   92 FORMAT(1H1//'    THE ADD-ON FUNCTION GARRAY FOR Z=',F7.3,' CM:')SUB00690
      RETURN                                                         SUB00700
      END                                                            SUB00710
C00014                                                               SUB00720
C                                                                    SUB00730

      SUBROUTINE GPUNCH (Z,XO,YO,PHS,NOF,IMX,JMX,G)                 SUB00740
C                                                                    SUB00750
C     GPUNCH PUNCHES OUT THE FIRST NON-SYMMETRIC PORTION OF GARRAY  SUB00760
C     (OR WRITES IT ON FILE 7 IN CMS VERSION)                       SUB00770
C                                                                    SUB00780
      COMMON /SYM/ ISM,JSM,MSM,FCU,IMS,JMS,QSM                      SUB00790
      DIMENSION G(IMX,JMX)                                           SUB00800
      WRITE(7,39) NOF,IMX,JMX,ISM,JSM,IMS,JMS                       SUB00810
      WRITE(7,38) ((G(I,J),I=1,IMS),J=1,JMS)                        SUB00820
   39 FORMAT(10I5)                                                   SUB00830
   38 FORMAT(10F7.3)                                                 SUB00840
      RETURN                                                         SUB00850
      END                                                            SUB00860
C00015                                                               SUB00870
C                                                                    SUB00880

      SUBROUTINE READ (Z,XO,YO,PHISYM,NOF,IMAX,JMAX,G)             SUB00890
C                                                                    SUB00900
C     READS THE NON-SYMMETRIC PORTION OF THE GARRAY AND EXPANDS IT TO ANSUB00910
C     ORTHOGONAL SET. NOTE, INSURE SUFFICIENT DIMENSIONS IN MAIN PROGRAM.SUB00920
C                                                                    SUB00930
      COMMON /SYM/ ISYM,JSYM,MSYM,FCU,IMS,JMS,QSYM                  SUB00940
```

```
      COMMON /IO/ CMS,IN1,IN2,IN4
      DIMENSION G(IMAX,JMAX)
      READ(IN1,39) Z,NOF,IMAX,JMAX,ISYM,JSYM,IMS,JMS
      READ(IN1,40) Z,XO,YO,PHISYM
   10 DO 10 J=1,JMS
      READ(IN1,38) (G(I,J),I=1,IMS)
      WRITE(6,37) NOF,Z,XO,YO,PHISYM,IMAX,JMAX,JSYM
      RJMX=JMAX
      MSYM=JSYM
      IF((ISYM.EQ.0).OR.(MSYM.GT.JMAX)) MSYM=1
      FCU=ISYM*JSYM*JMAX
      IF(JSYM.GT.JMAX) FCU=JMAX
      QSYM=FCU/RJMX
      DO 4 J=1,JMS
    1 IF(ISYM.EQ.1) GO TO 2
      II=1,IMS
      II=IMAX+I-I
    1 G(II,J)=G(I,J)
      GO TO 4
    2 J2=JMAX/2+1-J
      J3=JMAX/2+J
      J4=JMAX+1-J
      DO 3 I=1,IMAX
      II=IMAX+I-I
      G(II,J2)=G(I,J)
      G(II,J3)=G(I,J)
      G(II,J4)=G(I,J)
    3 CONTINUE
    4 CONTINUE
   39 FORMAT(10I5)
   40 FORMAT(4F7.3)
   38 FORMAT(10F7.3)
   37 FORMAT(///' MODE 3 READS GARRAY DIRECTLY:',NOF=',I4/'
     1' ',' XO=',F7.3,' YO=',F7.3,' IMAX=',I4,
     2' ',' JMAX=',I4,' PHISYM=',F7.3,' Z=',F7.3,
     ' JSYM=',I4//)
      RETURN
      END
C000016
C
      SUBROUTINE MAP (IM,JM,A,N,Z,BAND)
C
C     MAP CALLS SUBROUTINE MIMPII AND PLOTS A CONTOUR MAP OF THE ARRAY
C
      DIMENSION A(IM,JM),T(24)
      DATA BL/1H /
      DO 1 I=1,24
    1 T(I)=BL
```

159

```
      ICON=1
      IF(BAND.LT.0.) ICON=0                                             SUB01390
      IF(BAND.LT.0.) BAND=-BAND                                         SUB01400
      AMIN=0.                                                           SUB01410
      IJT=0                                                             SUB01420
      AZ=1.                                                             SUB01430
      BZ=0.•                                                            SUB01440
      WRITE(6,49) N,Z                                                   SUB01450
      CALL MTMPII (A,IM,JM,T,BAND,AZ,BZ,AMIN,IJT,ICON)                  SUB01460
   49 FORMAT (1H1//' THE FUNCTION SURFACE, TEST NO.'I3,'   Z='F5.3//)   SUB01470
      RETURN                                                            SUB01480
      END                                                               SUB01490
C000017                                                                 SUB01500
C                                                                       SUB01510
                                                                        SUB01520
      SUBROUTINE GPLOT (G,GA,JMS)                                       SUB01530
C                                                                       SUB01540
C GPLOT PRINTS A ROUGH PLOT OF THE LINE INTEGRAL FUNCTIONS IN GARRAY.   SUB01550
C                                                                       SUB01560
      COMMON IMAX,JMAX,IIMX,JJMX,IJMX,ALPHA,SIZE,EPS,MODE,BOX,SD,IX,Z   SUB01570
      COMMON /TAB/ INDEX(7),JSYM,ISYM                                   SUB01580
      COMMON /TAB2/ IPT,KPT,LPT,MPT,REST(5)                            SUB01590
      DIMENSION G(IMAX,JMAX),GA(IMAX,JMAX),ROW(101)                     SUB01600
      DIMENSION A(201),B(101),C(201),D(101)                            SUB01610
      JM=101                                                            SUB01620
      DATA BL,PL,ST,DH,EX/1H ,1H+,1H*,1H-,1HX/                          SUB01630
      JMS2=JMAX/2+1                                                     SUB01640
      IF(ISYM.EQ.2)JMS2=1                                               SUB01650
      JMS3=JMS2+JMS-1                                                   SUB01660
      DO 8 J=JMS2,JMS3                                                  SUB01670
      WRITE(6,67)(ST,I=1,120)                                           SUB01680
      DO 1 I=1,IMAX                                                     SUB01690
      A(I)=G(I,J)                                                       SUB01700
    1 C(I)=GA(I,J)                                                      SUB01710
      AS=.5                                                             SUB01720
      BS=•.0                                                            SUB01730
      CALL INTERP (A,IMAX,AS,B,JM,BS)                                   SUB01740
      CALL INTERP (C,IMAX,AS,D,JM,BS)                                   SUB01750
      WRITE(6,69) J                                                     SUB01760
      BIG=0.                                                            SUB01770
      SMALL=0.                                                          SUB01780
      DO 2 I=1,IMAX                                                     SUB01790
      IF(A(I).GT.BIG) BIG=A(I)                                          SUB01800
      IF(C(I).GT.BIG) BIG=C(I)                                          SUB01810
      IF(A(I).LT.SMALL) SMALL=A(I)                                      SUB01820
    2 IF(C(I).LT.SMALL) SMALL=C(I)                                      SUB01830
      RANGE=BIG-SMALL                                                   SUB01840
```

160

```
      RINK=RANGE/80.                                                SUB01850
      TOP=BIG+RINK                                                  SUB01860
      CEN=BIG                                                       SUB01870
      BOT=BIG-RINK                                                  SUB01880
      KC=0                                                          SUB01890
      DO 7 K=1,41                                                   SUB01900
      IC=0                                                          SUB01910
      DO 6 I=1,101                                                  SUB01920
      ROW(I)=BL                                                     SUB01930
      IF((I.EQ.1).OR.(I.EQ.51).OR.(I.EQ.101))ROW(I)=PL             SUB01940
      IF((K.EQ.1).OR.(K.EQ.41))ROW(I)=PL                            SUB01950
      IF((TOP.GE.0.).AND.(BOT.LE.0.)) ROW(I)=DH                     SUB01960
      IF(IC.EQ.5) GO TO 3                                           SUB01970
      GO TO 4                                                       SUB01980
    3 ROW(I)=PL                                                     SUB01990
      IF(KC.EQ.10) ROW(I)=PL                                        SUB02000
    4 IF(KPT.LE.2) GO TO 5                                          SUB02010
      IF((D(I).LE.TOP).AND.(D(I).GE.BOT))  ROW(I)=ST               SUB02020
      IF((B(I).LE.TOP).AND.(B(I).GE.BOT))  ROW(I)=EX               SUB02030
    5 IC=IC+1                                                       SUB02040
      IF(KC.EQ.5) KC=0                                              SUB02050
      IF(KC.NE.0) WRITE (6,65) (ROW(I),I=1,101)                    SUB02060
    6 IF(KC.EQ.0) WRITE (6,68) CEN,(ROW(I),I=1,101)                SUB02070
      TOP=TOP-2.*RINK                                               SUB02080
      CEN=CEN-2.*RINK                                               SUB02090
      BOT=BOT-2.*RINK                                               SUB02100
    7 KC=KC+1                                                       SUB02110
      WRITE (6,66)  (ST,I=1,120)                                    SUB02120
   66 FORMAT (//,J=-.,I3//)                                         SUB02130
   69 FORMAT (1X,F8.3,/,121A1//)                                    SUB02140
   68 FORMAT (1H1,/,121A1//)                                        SUB02150
   67 FORMAT (//,121A1//)                                           SUB02160
   65 FORMAT (10X,101A1)                                            SUB02170
      RETURN                                                        SUB02180
      END                                                           SUB02190
C0C0018                                                             SUB02200
C                                                                   SUB02210

      SUBROUTINE INTERP (A,IM,AS,B,JM,BS)                           SUB02220
C                                                                   SUB02230
C     INTERP CONVERTS A REGULAR VECTOR A OF IM POINTS TO A REGULAR VECTOR SUB02240
C     B OF JM POINTS. QS=.5 FOR A VECTOR WITH POINTS DEFINED IN THE SUB02250
C     CENTER OF THE INTERVAL, AS AND BS ARE THE % OF AN INTERVAL FROM THE SUB02260
C     EDGE OF THE FIELD TO THE FIRST POINT (.0 OR .5 FOR EDGE OR CENTER  SUB02270
C     DEFINED POINTS)                                               SUB02280
C                                                                   SUB02290
      DIMENSION A(IM),B(JM)                                         SUB02300
```

```
      RIM=IM
      RJM=JM
      RAT=(RIM-1.+2.*AS)/(RJM-1.+2.*BS)                         SUBO02310
      DO 2 I=1,JM                                               SUBO02320
      BI=I                                                      SUBO02330
      AI=RAT*(BI+BS)-AS                                         SUBO02340
      IA=AI                                                     SUBO02350
      F=AI-FLOAT(IA)                                            SUBO02360
      IF((IA.EQ.0).OR.(IA.EQ.JM)) GO TO 1                       SUBO02370
      B(I)=A(IA)+F*(A(IA+1)-A(IA))                              SUBO02380
      GO TO 2                                                   SUBO02390
    1 IF(IA.EQ.0) B(I)=A(1)*(F-AS)/(1.-AS)                      SUBO02400
      IF(IA.EQ.JM) B(I)=A(JM)*F/(1.-AS)                         SUBO02410
    2 CONTINUE                                                  SUBO02420
      RETURN                                                    SUBO02430
      END                                                       SUBO02440
C000019                                                         SUBO02450
C-------------------------------------------------------------- SUBO02460
C                                                               SUBO02470
C     SUBROUTINE SPLINE                                         SPL00010
C                                                               SPL00020
C     PURPOSE                                                   SPL00030
C        PROVIDES INTERPOLATED VALUE USING "CUBIC SPLINE FITTING" SPL00040
C                                                               SPL00050
C     USAGE                                                     SPL00060
C        FIRST CALL TO SUBROUTINE:                              SPL00070
C        CALL SPLINE(X,Y,M,XINT,YINT)                           SPL00080
C                                                               SPL00090
C        SUBSEQUENT CALLS:                                      SPL00100
C        CALL SPLINN(X,Y,M,XINT,YINT)                           SPL00110
C                                                               SPL00120
C                                                               SPL00130
C     DESCRIPTION OF PARAMETERS                                 SPL00140
C        X:    MONOTONICALLY INCREASING ABSCISSA ARRAY          SPL00150
C        Y:    ONE-FOR-ONE CORRESPONDING ORDINATE ARRAY         SPL00160
C        M:    NUMBER OF X AND Y VALUES SUPPLIED (<OR=300       SPL00170
C        XINT: VALUE OF ABSCISSA FOR WHICH CORRESPONDING ORDINATE SPL00180
C              IS TO BE INTERPOLATED (OR EXTRAPOLATED)          SPL00190
C        YINT: INTERPOLATED (OR EXTRAPOLATED) ORDINATE VALUE    SPL00200
C                                                               SPL00210
C                                                               SPL00220
C     REMARKS                                                   SPL00240
C        IF SPECIFIED X FALLS OUTSIDE OF RANGE, AN EXTRAPOLATED SPL00250
C        VALUE WILL BE SUPPLIED                                 SPL00260
C                                                               SPL00270
C                                                               SPL00280
C     SUBROUTINES AND FUNCTION SUBPROGRAMS REQUIRED             SPL00290
C        SUBROUTINE SPLICO IS INCLUDED IN SUBROUTINE SPLIN PACKAGE SPL00300
C                                                               SPL00310
```

162

```
C     MATHEMATICAL METHOD
C        UPON FIRST ENTRY TO SPLIN, A CALL TO SPLICO IS MADE TO
C        DETERMINE THE COEFFICIENTS. TO BE USED IN PERFORMING THE
C        INTERPOLATIONS. SEARCH FOR BRACKETING ABSCISSA VALUES IS
C        ALWAYS MADE FROM THE REFERENCE LAST USED IN INTERPOLATING.
C
C     REFERENCE
C        PENNINGTON, RALPH H., "INTRODUCTORY COMPUTER METHODS AND
C        NUMERICAL ANALYSIS", THE MACMILLAN COMPANY, NEW YORK, 1965
C
      SUBROUTINE SPLINE(X,Y,M,XINT,YINT)                                 SPL00440
      DIMENSION X(M),Y(M),C(4,300)                                       SPL00460
      CALL SPLICO(X,Y,M,C)                                              SPL00470
      K=1                                                               SPL00480
      ENTRY SPLIN(X,Y,M,XINT,YINT)                                      SPL00490
      IF(XINT-X(1)) 70,1,2                                              SPL00500
70    K=1                                                              SPL00510
 3    GO TO 7                                                          SPL00520
 1    YINT=Y(1)                                                        SPL00530
      RETURN                                                           SPL00540
 2    IF(XINT-X(K+1)) 6,4,5                                            SPL00550
 4    YINT=Y(K+1)                                                      SPL00560
      RETURN                                                           SPL00570
 5    K=K+1                                                            SPL00580
      IF(M-K) 71,71,3                                                  SPL00590
71    K=M-1                                                            SPL00600
 6    IF(XINT-X(K)) 13,12,11                                           SPL00610
12    YINT=Y(K)                                                        SPL00620
      RETURN                                                           SPL00640
13    K=K-1                                                            SPL00650
      GO TO 6                                                          SPL00660
 7    PRINT 101,XINT                                                   SPL00670
101   FORMAT(8H0XINT = E18.9,32H, OUT OF RANGE FOR INTERPOLATION)      SPL00680
11    YINT=(X(K+1)-XINT)*(C(1,K)*(X(K+1)-XINT)**2+C(3,K))              SPL00690
      YINT=YINT+(XINT-X(K))*(C(2,K)*(XINT-X(K))**2+C(4,K))             SPL00700
      RETURN                                                           SPL00710
      END                                                              SPL00720
```

```
      SUBROUTINE SPLICO(X,Y,M,C)                                        SPL00730
      DIMENSION X(M),Y(M),C(4,300),D(300),P(300),E(300),A(300,3),B(300),SPL00740
     1Z(300)                                                            SPL00750
      MM=M-1                                                            SPL00760
      DO 2 K=1,MM                                                       SPL00770
      D(K)=X(K+1)-X(K)                                                  SPL00780
      P(K)=D(K)/6.                                                      SPL00790
    2 E(K)=(Y(K+1)-Y(K))/D(K)                                          SPL00800
      DO 3 K=2,MM                                                       SPL00810
    3 B(K)=E(K)-E(K-1)                                                  SPL00820
      A(1,2)=-1.-D(1)/D(2)                                              SPL00830
      A(1,3)=D(1)/D(2)                                                  SPL00840
      A(2,3)=P(2)-P(1)*A(1,3)                                           SPL00850
      A(2,2)=2.*(P(1)+P(2))-P(1)*A(1,2)                                 SPL00860
      A(2,3)=A(2,3)/A(2,2)                                              SPL00870
      B(2)=B(2)/A(2,2)                                                  SPL00880
      DO 4 K=3,MM                                                       SPL00890
      A(K,2)=2.*(P(K-1)+P(K))-P(K-1)*A(K-1,3)                           SPL00900
      B(K)=B(K)-P(K-1)*B(K-1)                                           SPL00910
      A(K,3)=P(K)/A(K,2)                                                SPL00920
    4 B(K)=B(K)/A(K,2)                                                  SPL00930
      Q=D(M-2)/D(M-1)                                                   SPL00940
      A(M,1)=1.+Q+A(M-2,3)                                              SPL00950
      A(M,2)=-Q-A(M,1)*A(M-1,3)                                         SPL00960
      B(M-1)=B(M-2)-A(M,1)*B(M-1)                                       SPL00970
      Z(M)=B(M)/A(M,2)                                                  SPL00980
      MN=M-2                                                            SPL00990
      DO 6 I=1,MN                                                       SPL01000
      K=M-I                                                             SPL01010
    6 Z(K)=B(K)-A(K,3)*Z(K+1)                                           SPL01020
      Z(1)=-A(1,2)*Z(2)-A(1,3)*Z(3)                                     SPL01030
      DO 7 K=1,MM                                                       SPL01040
      Q=1./(6.*D(K))                                                    SPL01050
      C(1,K)=Z(K)*Q                                                     SPL01060
      C(2,K)=Z(K+1)*Q                                                   SPL01070
      C(3,K)=Y(K)/D(K)-Z(K)*P(K)                                        SPL01080
    7 C(4,K)=Y(K+1)/D(K)-Z(K+1)*P(K)                                    SPL01090
      RETURN                                                            SPL01100
      END                                                              SPL01110
                                                                        SPL01120
C000020                                                                 MET000010
C*******************************************************************    MET000020
C                                                                       MET000030
C      SUBROUTINE MTMPII                                                MET000040
C                                                                       MET000050
C      PURPOSE                                                          MET000060
```

164

```
C     MTMPII WILL PRODUCE,ON THE PRINTER, A CONTOUR MAP             METO0070
C     OF ANY SINGLE PRECISION TWO DIMENSIONAL ARRAY.                METO0080
C                                                                   METO0090
C     USAGE                                                         METO0100
C                                                                   METO0110
C          CALL MTMPII(Y,N,M,T,BND,AZ,BZ,AMIN,IJT,ICON)            METO0120
C                                                                   METO0130
C     DESCRIPTION OF PARAMETERS                                     METO0140
C                                                                   METO0150
C          Y   - THE ARRAY TO BE CONTOURED. DIMENSIONED Y(N,M)      METO0160
C          N   - NUMBER OF ROWS IN Y.                               METO0170
C          M   - NUMBER OF COLUMNS IN Y.                            METO0180
C          T   - ARRAY FOR PLOT TITLE. REAL*4. T(24).               METO0190
C          BND - A BANDWIDTH FOR THE CONTOURING. IF BND IS ZERO     METO0200
C                BND=(MAX(Y)-MIN(Y))/15. WILL BE CALCULATED AS FOLLOWS METO0210
C                                                                   METO0220
C          AZ  - A LINEAR TRANSFORMATION MAYBE PERFORMED ON         METO0230
C                THE ARRAY Y OF THE FOLLOWING FORM AZ*Y+BZ.         METO0240
C                IF AZ=0 THEN AZ=1.,MIM(Y)-1 WILL BE COMPUTED SUCH THAT, METO0250
C                MAX(IMAX(Y),IMIM(Y)-) WILL BE LESS THAN 1,         METO0260
C                AND BZ WILL BE LEFT AS INPUT.                      METO0270
C          BZ  - SEE UNDER AZ                                       METO0280
C          AMIN- THE LEVEL AT WHICH COUTOURING WILL BEGIN. IF       METO0290
C                AMIN=0. THEN AMIN WILL BE CALCULATED               METO0300
C                TO BE ,WITH REFERENCE AT ZERO,THE NEXT LOWER       METO0310
C                CONTOUR LEVEL FROM MIN(Y) AS DETERMINED BY         METO0320
C                BND.                                               METO0330
C          IJT - IF IJT=0 AMIN WILL BE CALCULATED AS DESCRIBED      METO0340
C                ABOVE.                                             METO0350
C          ICON- IF ICON=0 NO CONTOURING WILL BE DONE BUT THE       METO0360
C                ARRAY Y WILL BE PRINTED IN THE PLOT FORMAT.        METO0370
C                                                                   METO0380
C     REMARKS                                                       METO0390
C          MTMPII REQUIRES A PRINTER WITH 132 PRINT POSITIONS.      METO0400
C          IF NECESSARY THE MAP WILL BE SEGMENTED COLUMNWISE.       METO0410
C          THE ROWS AND COLUMNS ARE NUMBERED ALONG THE EDGES.       METO0420
C          THAT A SEGMENT MAYBE EASILY JOINED TOGETHER. SOME        METO0430
C          ONLY THREE SIGNIFICANT FIGURES WILL BE PRINTED AT.       METO0440
C          EACH POINT. THE POSITION OF THE FIRST SIGNIFICANT        METO0450
C          DIGIT WILL BE DETERMINED BY MAX(IMAX(Y),-IMIN(Y)).       METO0460
C          THE PLOT WILL BE PRODUCED CN A INCH GRID. IT IN          METO0470
C          WILL BE ASSUMED THAT THE SPACING BETWEEN POINTS IN       METO0480
C          BOTH DIRECTIONS IS THE SAME AND EQUAL FOR ALL POINTS     METO0490
C                                                                   METO0500
C     SUBROUTINES REQUIRED                                          METO0510
C          NONE                                                     METO0520
C                                                                   METO0530
C     METHOD                                                        METO0540
C          THE CONTOUR LEVELS ARE DETERMINED BY SIMPLE LINEAR
```

```
C      INTERPOLATION FROM THE FOUR SURROUNDING PIONTS.          MET00550
C***************************************************************MET00560
C***************************************************************MET00570
C                                                               MET00580
C      MTMPII SUBROUTINE FOR ONE-INCH GRID SPACING              MET00590
C      OAKES CODE 5105   15 JAN 69                              MET00600
C                                                               MET00610
                                                                MET00620

       SUBROUTINE MTMPII(Y,N,M,T,BND,AZ,BZ,AMIN,IJT,ICON)       MET00630
       REAL*4 IH,KG,ITJZ                                        MET00640
       DIMENSION A(140),B(140),C(140),D(140),IH(20),Y(N,M),TP(10),TPX(10) MET00650
      Z,TPM(10),XMT(10),BTM(10),BTX(10),BT(10),KG(10),T(24)     MET00660
       DIMENSION E(140),F(140),G(140),H(140)                    MET00670
C                                                               MET00680
C                                                               MET00690
       DATA DUE /4H    /,EPL/4H+   /,EMI/4H-   /,IH/1H0,1H ,1H1,1H2, MET00700
      1 1H0,1H3,1H ,1H4 ,1H5,1H ,1H6,1H ,1H7,1H ,1H8,1H ,1H9,1H ,KG/ MET00710
      2 1H0,1H1,1H2,1H3,1H4,1H5,1H6,1H7,1H8,1H9/,BLK/4H    /     MET00720
C                                                               MET00730
       YMIN=Y(1,1)                                              MET00740
       YMAX=Y(1,1)                                              MET00750
       DO 20 I=1,M                                              MET00760
       DO 10 J=1,N                                              MET00770
       YMIN=AMIN1(YMIN,Y(J,I))                                  MET00780
       YMAX=AMAX1(YMAX,Y(J,I))                                  MET00790
 10    CONTINUE                                                 MET00800
 20    CONTINUE                                                 MET00810
       DELY=YMAX-YMIN                                           MET00820
       IF(BND) 25,25,30                                         MET00830
 25    BND=DELY/15.0                                            MET00840
 30    IF (AMIN-YMIN) 31,31,32                                  MET00850
 31    IF (IJT) 33,32,33                                        MET00860
 32    PD=YMIN/BND                                              MET00870
       PF=ABS(PD-INT(PD))                                       MET00880
       IF (YMIN) 2,1,1                                          MET00890
 1     AMIN=YMIN-PF*BND                                         MET00900
       GO TO 33                                                 MET00910
 2     AMIN=YMIN-(1.0-PF)*BND                                   MET00920
 33    AHLD=AZ                                                  MET00930
       IF (AZ) 55,35,55                                         MET00940
 35    SM=AMAX1(ABS(YMIN),ABS(YMAX))                            MET00950
       NS=0                                                     MET00960
 40    NS=NS+1                                                  MET00970
       SM=10.0*SM                                               MET00980
       IF(SM-1.0)40,50,45                                       MET00990
 45    NS=NS-1                                                  MET01000
```

```fortran
      SM=SM/10.0
50    IF(SM-1.0)50,50,45
55    AHLD=10.0**NS
      HBND=BND/2.0
      PRINT 70,T
6     FORMAT(5X,24A4,//)
      PRINT 57,AHLD,BZ
57    FORMAT(1H0,65HTHE FOLLOWING TRANSFORMATION WAS PERFORMED ON THE IN
     1PUT MATRIX /5X,1H(,E12.5,8H*Y(I,J)+,E12.5,5,1H)//2X,73HAND THREE
     2 DIGITS TO THE RIGHT OF THE DECIMAL POINT ARE PRINTED IN THE MAP )
C
      PRINT 54,YMAX,YMIN
54    FORMAT(/4X,5HYMAX=,E15.7,5X,5HYMIN=,E15.7)
      IF(ICON)5,58,5
5     PRINT 11,BND
11    FORMAT(2X,17HTHE BAND WIDTH IS,E12.5,6H UNITS //4X,14HCONTOUR LEVE
     1LS
      I=0
      YTOP=AMIN
      IF(ABS(YMIN-YMAX)-100.0*BND)53,53,58
53    YB=YTOP
      YTOP=YTOP+BND
      I=I+1
      J=MOD(I,20)
      ITJZ=IH(J)
      IF(YB-YMAX)59,58,58
59    PRINT 61,YB,YTOP,ITJZ
61    FORMAT(/4X,E10.3,4H TO ,E10.3,2H =,1X,A1)
      GO TO 53
58    NCCP=0
      NCP=0
60    PRINT 70,T
70    FORMAT(1H1)
      PRINT 6,T
      NLINE=0
      NCCP=NCP+1
      NCP=NCP + 13
73    IF(NCP-M)80,80,75
75    NCP=M
80    CONTINUE
      J=-2
      NLINE=NLINE+1
      LLINE=N-NLINE+1
C  SET UP HEADING
85    IF(NCCP-1) 85,85,90
      J=1
90    DO 100 I = 1,135
```

METO01010
METO01020
METO01030
METO01040
METO01050
METO01060
METO01070
METO01080
METO01090
INMETO01100
THREEMETO01110
METO01120
METO01130
METO01140
METO01150
METO01160
LEVEMETO01170
METO01180
METO01190
METO01200
METO01210
METO01220
METO01230
METO01240
METO01250
METO01260
METO01270
METO01280
METO01290
METO01300
METO01310
METO01320
METO01330
METO01340
METO01350
METO01360
METO01370
METO01380
METO01390
METO01400
METO01410
METO01420
METO01430
METO01440
METO01450
METO01460
METO01470
METO01480

```
      A(I)=BLK
      B(I)=BLK
      H(I) = BLK
100   CONTINUE
110   DO 160 L=NCCP,NCP
      J = J+8
      KI=L
120   IF(KI-100) 130,120,120
      LL=KI/100
      A(J)=KG(LL+1)
      KI=KI-100*LL
      GO TO 135
130   A(J)=KG(1)
135   J=J+1
140   IF(KI-10) 150,140,140
      LL=KI/10
      A(J)=KG(LL+1)
      KI=KI-10*LL
      GO TO 155
150   A(J)=KG(1)
155   J=J+1
      A(J)=KG(KI+1)
160   CONTINUE
C SETUP FIRST ROW OF ARRAY
      GO TO 260
170   NLINE=NLINE+1
      LLINE=N-NLINE+1
      IF(NLINE-N) 180,180,380
180   DO 190 I=1,135
      A(I) = BLK
      B(I) = BLK
      C(I) = BLK
      D(I) = BLK
      E(I) = BLK
      F(I) = BLK
      G(I) = BLK
      H(I) = BLK
190   CONTINUE
      IF(ICON)195,260,195
195   NCY=NCCP-1
      J=4
      IF(NCY)200,200,210
200   J=5
210   NCY=NCY+1
      IF(NCY-NCP) 220,220,260
220   IF(NCY-M)230,260,260
230   NLINE = NLINE-1
      YD1 = Y(NLINE,NCY) - Y(NLINE+1,NCY)
```

```
      YD2=Y(NLINE,NCY+1)-Y(NLINE+1,NCY+1)                               METO1970
      TP(1)=Y(NLINE,NCY+1)-0.125*YD1                                    METO1980
      TPX(1)=Y(NLINE,NCY+1)-0.250*YD1                                   METO1990
      TPM(1)=Y(NLINE,NCY+1)-0.375*YD1                                   METO2000
      XMT(1)=Y(NLINE,NCY+1)-0.500*YD1                                   METO2010
      BTM(1)=Y(NLINE,NCY+1)-0.625*YD1                                   METO2020
      BTX(1)=Y(NLINE,NCY+1)-0.750*YD1                                   METO2030
      BT=Y(NLINE,NCY+1)-0.875*YD1                                       METO2040
      TP=Y(NLINE,NCY+1)-0.1250*YD2                                      METO2050
      TPM(1)=Y(NLINE,NCY+1)-0.2500*YD2                                  METO2060
      XMT(1)=Y(NLINE,NCY+1)-0.3750*YD2                                  METO2070
      BTM(1)=Y(NLINE,NCY+1)-0.5000*YD2                                  METO2080
      BTX(1)=Y(NLINE,NCY+1)-0.6250*YD2                                  METO2090
      BT=Y(NLINE,NCY+1)-0.7500*YD2                                      METO2100
      BT=Y(NLINE,NCY+1)-0.8750*YD2                                      METO2110
      NLINE=NLINE+1                                                     METO2120
      D1=X(TP(10))                                                      METO2130
      D2=X(TPX(10))                                                     METO2140
      D3=X(TPM(10))                                                     METO2150
      D4=X(XMT(10))                                                     METO2160
      D5=X(BTM(10))                                                     METO2170
      D6=X(BTX(10))                                                     METO2180
      D7=X(BT(10))                                                      METO2190
      DO 240 I=2,9                                                      METO2200
      TP=TP(I-1)+D1                                                     METO2210
      TPX(I-1)=TPX(I-1)+D2                                              METO2220
      TPM(I-1)=TPM(I-1)+D3                                              METO2230
      XMT(I-1)=XMT(I-1)+D4                                              METO2240
      BTM(I-1)=BTM(I-1)+D5                                              METO2250
      BTX(I-1)=BTX(I-1)+D6                                              METO2260
      BT(I-1)=BT(I-1)+D7                                                METO2270
  240 CONTINUE                                                         METO2280
      J=J+1                                                             METO2290
      I1=MOD(IFIX(TP(I)-AMIN)/BND),20)+1                                METO2300
      I2=MOD(IFIX(TPX(I)-AMIN)/BND),200),20)+1                          METO2310
      I3=MOD(IFIX(TPM(I)-AMIN)/BND),200),20)+1                          METO2320
      I4=MOD(IFIX(XMT(I)-AMIN)/BND),200),20)+1                          METO2330
      I5=MOD(IFIX(BTM(I)-AMIN)/BND),200),20)+1                          METO2340
      I6=MOD(IFIX(BTX(I)-AMIN)/BND),200),20)+1                          METO2350
      I7=MOD(IFIX(BT(I)-AMIN)/BND),20)+1                                METO2360
      A(J)=IH(I1)                                                       METO2370
      B(J)=IH(I2)                                                       METO2380
      C(J)=IH(I3)                                                       METO2390
      D(J)=IH(I4)                                                       METO2400
      E(J)=IH(I5)                                                       METO2410
      F(J)=IH(I6)                                                       METO2420
      G(J)=IH(I7)                                                       METO2430
  250 CONTINUE                                                         METO2440
```

240

250

169

```
250   CONTINUE
260   GO TO 210
      NCY=NCCP-1
      J=-2
265   IF(NCY)  265,265,270
      J=-1
270   GO TO 330
      NCY=NCY+1
280   IF(NCY-NCP)  280,280,310
      J=J+7
      THLD=AHLD*Y(NLINE,NCY)+BZ
285   IF(THLD)  285,290,290
      H(J)=EMI
290   GO TO 295
      H(J)=EPL
295   NUM=INT(ABS(THLD-INT(THLD))*1000.0+0.5)
      NDS=100
      DO 300 KK=1,3
      J=J+1
      KI=NUM/NDS
      H(J)=KG(KI+1)
      NUM=NUM-KI*NDS
      NDS=NDS/10
300   CONTINUE
310   GO TO 270
320   IF(NCP-M)  360,320,320
330   IF(J-127)  330,330,360
      J=J+3
      KI=NLINE
335   IF(KI-100)  340,335,335
      LL=KI/100
      H(J)=KG(LL+1)
      KI=KI-100*LL
      GO TO 343
343   H(J)=KG(1)
      J=J+1
345   IF(KI-10)  350,345,345
      LL=KI/10
      H(J)=KG(LL+1)
      KI=KI-10*LL
      GO TO 355
355   H(J)=KG(1)
      J=J+1
350   H(J)=KG(KI+1)
      J=J+5
      IF(NCY-1)  270,270,360
360   IF(NLINE-1)362,362,368
362   PRINT 370,(A(I),I=1,132),(B(IP1),IP1=1,132),(H(IP2),IP2=1,132)
```

```
      GO TO 170                                                         METO2930
368   PRINT 370,(A(I),I=1,132),(B(IP1),IP1=1,132),(C(IP2),IP2=1,132),  METO2940
     1(D(IP3),IP3=1,132),(E(IP4),IP4=1,132),(F(IP5),IP5=1,132),         METO2950
     2(G(IP6),IP6=1,132),(H(IP7),IP7=1,132)                             METO2960
370   FORMAT(132A1)                                                     METO2970
      GO TO 170                                                         METO2980
380   DO 390 I=1,135                                                    METO2990
      A(I)=BLK                                                          METO3000
      B(I)=BLK                                                          METO3010
      C(I)=BLK                                                          METO3020
      D(I)=BLK                                                          METO3030
390   CONTINUE                                                          METO3040
      J=-2                                                              METO3050
      IF(NCCP-1) 395,395,400                                           METO3060
395   J=-1                                                              METO3070
400   DO 430 L=NCCP,NCP                                                METO3080
      J=J+8                                                             METO3090
      KI=L                                                              METO3100
      IF(KI-100) 410,405,405                                           METO3110
405   LL=KI/100                                                         METO3120
      C(J)=KG(LL+1)                                                     METO3130
      KI=KI-100*LL                                                      METO3140
      GO TO 412                                                         METO3150
410   C(J)=KG(1)                                                        METO3160
412   J=J+1                                                             METO3170
      IF(KI-10) 420,415,415                                            METO3180
415   LL=KI/10                                                          METO3200
      C(J)=KG(LL+1)                                                     METO3210
      KI=KI-10*LL                                                       METO3220
      GO TO 422                                                         METO3230
420   C(J)=KG(1)                                                        METO3240
422   J=J+1                                                             METO3250
      C(J)=KG(KI+1)                                                     METO3260
430   CONTINUE                                                          METO3270
      PRINT 370,(B(IP1),IP1=1,132),(C(IP2),IP2=1,132)                  METO3280
      IF(NCP-M)60,500,500                                              METO3290
500   RETURN                                                            METO3300
      END

C000021
C     .....................................................
C     .                                                   .
C     .                                                   .
C     SUBROUTINE GAUSS                                      GAUS   10
C     .                                                   . GAUS   20
C     .                                                   . GAUS   30
C     PURPOSE                                               GAUS   40
C       COMPUTES A NORMALLY DISTRIBUTED RANDOM NUMBER WITH A GIVEN GAUS 50
C                                                            GAUS   60
C                                                            GAUS   70
```

171

```
C
C          MEAN AND STANDARD DEVIATION                                   GAUS  80
C                                                                        GAUS  90
C     USAGE                                                              GAUS 100
C        CALL GAUSS(IX,S,AM,V)                                           GAUS 110
C                                                                        GAUS 120
C     DESCRIPTION OF PARAMETERS                                          GAUS 130
C        IX - IX MUST CONTAIN AN ODD INTEGER NUMBER WITH NINE OR         GAUS 140
C             LESS DIGITS ON THE FIRST ENTRY TO GAUSS. THEREAFTER        GAUS 150
C             IT WILL CONTAIN A UNIFORMLY DISTRIBUTED INTEGER RANDOM     GAUS 160
C             NUMBER GENERATED BY THE SUBROUTINE FOR USE ON THE NEXT     GAUS 170
C             ENTRY TO THE SUBROUTINE.                                   GAUS 180
C        S  - THE DESIRED STANDARD DEVIATION OF THE NORMAL               GAUS 190
C             DISTRIBUTION.                                              GAUS 200
C        AM - THE DESIRED MEAN OF THE NORMAL DISTRIBUTION                GAUS 210
C        V  - THE VALUE OF THE COMPUTED NORMAL RANDOM VARIABLE           GAUS 220
C                                                                        GAUS 230
C     REMARKS                                                            GAUS 240
C        THIS SUBROUTINE USES RANDU WHICH IS MACHINE SPECIFIC            GAUS 250
C                                                                        GAUS 260
C     SUBROUTINES AND FUNCTION SUBPROGRAMS REQUIRED                      GAUS 270
C        RANDU                                                           GAUS 280
C                                                                        GAUS 290
C     METHOD                                                             GAUS 300
C        USES 12 UNIFORM RANDOM NUMBERS TO COMPUTE NORMAL RANDOM         GAUS 310
C        NUMBERS BY CENTRAL LIMIT THEOREM. THE RESULT IS THEN            GAUS 320
C        ADJUSTED TO MATCH THE GIVEN MEAN AND STANDARD DEVIATION.        GAUS 330
C        THE UNIFORM RANDOM NUMBERS COMPUTED WITHIN THE SUBROUTINE       GAUS 340
C        ARE FOUND BY THE POWER RESIDUE METHOD.                          GAUS 350
C                                                                        GAUS 360
C                                                                        GAUS 370
C                                                                        GAUS 380
      SUBROUTINE GAUSS(IX,S,AM,V)                                        GAUS 390
      A=0.0                                                              GAUS 400
      DO 50 I=1,12                                                       GAUS 410
      CALL RANDU(IX,IY,Y)                                                GAUS 420
      IX=IY                                                              GAUS 430
   50 A=A+Y                                                              GAUS 440
      V=(A-6.0)*S+AM                                                     GAUS 450
      RETURN                                                             GAUS 460
      END                                                                GAUS 470

C0000022
C                                                                        RAND  10
C                                                                        RAND  20
C                                                                        RAND  30
```

172

```
C                                                                       RAND  40
C     SUBROUTINE RANDU                                                  RAND  50
C                                                                       RAND  60
C     PURPOSE                                                           RAND  70
C        COMPUTES UNIFORMLY DISTRIBUTED RANDOM REAL NUMBERS BETWEEN     RAND  80
C        0 AND 1.0 AND RANDOM INTEGERS BETWEEN ZERO AND                 RAND  90
C        2**31.  EACH ENTRY USES AS INPUT AN INTEGER RANDOM NUMBER      RAND 100
C        AND PRODUCES A NEW INTEGER AND REAL RANDOM NUMBER.             RAND 110
C                                                                       RAND 120
C     USAGE                                                             RAND 130
C        CALL RANDU(IX,IY,YFL)                                          RAND 140
C                                                                       RAND 150
C     DESCRIPTION OF PARAMETERS                                         RAND 160
C        IX - FOR THE FIRST ENTRY THIS MUST CONTAIN ANY ODD INTEGER     RAND 170
C             NUMBER WITH NINE OR LESS DIGITS.  AFTER THE FIRST ENTRY,  RAND 180
C             IX SHOULD BE THE PREVIOUS VALUE OF IY COMPUTED BY THIS    RAND 190
C             SUBROUTINE.                                               RAND 200
C        IY - A RESULTANT INTEGER RANDOM NUMBER REQUIRED FOR THE NEXT   RAND 210
C             ENTRY TO THIS SUBROUTINE.  THE RANGE OF THIS NUMBER IS    RAND 220
C             BETWEEN ZERO AND 2**31                                    RAND 230
C        YFL- THE RESULTANT UNIFORMLY DISTRIBUTED, FLOATING POINT,      RAND 240
C             RANDOM NUMBER IN THE RANGE 0 TO 1.0                       RAND 250
C                                                                       RAND 260
C     REMARKS                                                           RAND 270
C        THIS SUBROUTINE IS SPECIFIC TO SYSTEM/360 AND WILL PRODUCE     RAND 280
C        2**29 TERMS BEFORE REPEATING.  THE REFERENCE BELOW DISCUSSES   RAND 290
C        SEEDS (65539 HERE), RUN PROBLEMS CONCERNING MACLAREN AND       RAND 300
C        RANDOM DIGITS USING THIS GENERATION SCHEME.  DISCUSS THE USE OF RAND 310
C        MARSAGLIA, JACM 12, P. 83-89, AND TESTS.  A TABLE CONGRUENTIAL RAND 320
C        GENERATION METHODS.  ONE FILLING A TABLE AND ONE PICKING FROM THE RAND 330
C        THE RANDU TYPE.  BENEFIT WHICH HAS BEEN GENERATORS OF THE      RAND 340
C        TABLE.  IS OF BITS OF THE GENERATED DEVIATE.  STATISTICAL PROPERTIES RAND 350
C        SUGGESTED AS A CASE BETTER DEVIATE.  AS                        RAND 360
C        FOR HIGH ORDER BITS OF THE REFERENCE BELOW.  IT SHOULD BE NOTED THAT RAND 370
C        SEEDS SHOULD BE CHOSEN IN ACCORDANCE WITH THE DISCUSSION       RAND 380
C        GIVEN IN THE REFERENCE BELOW.  ALSO, IT SHOULD BE              RAND 390
C        IF FLOATING POINT RANDOM NUMBERS ARE DESIRED, AS ARE          RAND 400
C        AVAILABLE FROM RANDU, THE RANDOM CHARACTERISTICS OF THESE      RAND 410
C        FLOATING POINT DEVIATES ARE MODIFIED AND IN FACT THESE        RAND 420
C        DEVIATES HAVE HIGH PROBABILITY OF HAVING A TRAILING LOW        RAND 430
C        ORDER ZERO BIT IN THEIR FRACTIONAL PART.                       RAND 440
C                                                                       RAND 450
C     SUBROUTINES AND FUNCTION SUBPROGRAMS REQUIRED                     RAND 460
C        NONE                                                           RAND 470
C                                                                       RAND 480
C     METHOD                                                            RAND 490
C        POWER RESIDUE METHOD DISCUSSED IN IBM MANUAL C20-8011,         RAND 500
C        RANDOM NUMBER GENERATION AND TESTING                          RAND 510
```

173

```
C ...........................................................  RAND 520
C ...........................................................  RAND 530

      SUBROUTINE RANDU(IX,IY,YFL)                              RAND 540
      IY=IX*65539                                              RAND 550
      IF(IY)5,6,6                                              RAND 560
    5 IY=IY+2147483647+1                                       RAND 570
    6 YFL=IY                                                   RAND 580
      YFL=YFL*.4656613E-9                                      RAND 590
      RETURN                                                   RAND 600
      END
```

BIBLIOGRAPHY

1. Caulfield, H. J. and Lee, Sun, <u>The Applications of Holography</u>, John Wiley and Sons, 1970.

2. Ellis, B. K. and Furey, R. J., <u>Wing-Body Interactions at a Mach Number of 9.5.</u>, Naval Ship Research and Development Center Report 2564, Aerodynamics Laboratory Research and Development Report 1133, September 1967.

3. Jagota, R. C., <u>The Application of Holographic Interferometry to the Determination of the Flow Field Around a Right Circular Cone at Angle of Attack</u>, Aeronautical Engineer Thesis, Naval Postgraduate School, December 1970.

4. Jagota, R. C. and Collins, D. J., "Finite Fringe Holographic Interferometry Applied to a Right Circular Cone at Angle of Attack", to be published in <u>Journal of Applied Mechanics</u>.

5. Kaufman, L. G. II and Meckler, L., <u>Pressure and Heat Transfer Measurements at Mach 5 and 8 for a Fin-Flat Plate Model</u>, Technical Documentary Report No. ASD-TDR 63-235, April 1963.

6. Kaufman, L. G. II, <u>Pressure Distributions and Oil Film Photographs for Mach 5 Flows Past Fins Mounted on a Flat Plate</u>, Technical Documentary Report No. ASD-TDR-63-755, September 1963.

7. Landenberg, R. W., et. al., ed., <u>Physical Measurements in Gas Dynamics and Combustion</u>, Princeton University Press, 1954.

8. Liepmann, H. W., and Roshko, A., <u>Elements of Gas Dynamics</u>, p. 165, John Wiley and Sons, Inc., 1957.

9. Maldonado, C. D., Caran, A. P., and Olsen, H. N., "New Method for Obtaining Emission Coefficients from Emitted Spectral Intensities. Part I--Circularly Symmetric Light Sources.", <u>Journal of the Optical Society of America</u>, Vol. 55, No. 10, pp. 1247-1254, October 1965.

10. Maldonado, C. D., "Note on Orthogonal Polynomials Which Are 'Invariant in Form' to Rotations of Axis", <u>Journal of Mathematical Physics</u> Vol. 6, No. 12, pp. 1935-1938, December 1965.

11. Maldonado, C. D. and Olsen, H. N., "New Method for Obtaining Emission Coefficients from Emitted Spectral Intensities. Part II--Asymmetrical Sources", <u>Journal of the Optical Society of America</u>, Vol 56, No. 10, pp. 1305-1313, October 1966.

12. Matulka, R. D., <u>The Application of Holographic Interferometry to the Determination of Asymmetric Three-Dimensional Density Fields in Free Jet Flow</u>, Ph. D. Thesis, Naval Postgraduate School, June, 1970.

13. Matulka, R. D. and Collins D. J., "Determination of Three-Dimensional Density Fields from Holographic Interferograms", <u>Journal of Applied Physics</u>, Vol. 42, No. 3, March 1971.

14. Okayama, H. and Emori, Y., "Polarization Effects in Holography",
    Applied Physics Letters, Vol. 19, No. 9, pp. 359-360, 1 November 1971

15. Olsen, H. N., Maldonado, C. D., Duckworth, G. D., and Caron, A. P.,
    Investigation of the Interaction of an External Magnetic Field with
    an Electric Arc, Aerospace Research Laboratories Report ARL 66-0016,
    January 1966.

16. Olsen, H. N., Maldonado, C. D., and Duckworth, G. D., "A Numerical
    Method for Obtaining Internal Emission Coefficients from Externally
    Measured Spectral Intensities of Asymmetrical Plasmas", _J. Quant._
    Spectrosc. Radiat. Transfer, Vol. 8, pp. 1419-1430, 1968.

17. Ragent, B. and Brown, R. M., editors, Holographic Instrumentation
    Applications, Conference held at Ames Research Center, Moffett Field,
    California, NASA Sp-248, January 13-14, 1970.

18. Roe, P. L., _Exploratory Flow Measurements in the Wing-Body Junction_
    of a Possible Mach Four Vehicle, Royal Aircraft Establishment Tech-
    nical Report No. 65257, November 1965.

19. Polutchko, R. J., _Hypersonic Flow Field About a Blunt Slab Wing at_
    Angle of Attack: Phase I, Aerospace Research Laboratories 64-213,
    December 1964.

20. Stewartson, K. and Treadgold, D. A., "Wing-Body Interference at
    Supersonic Speeds", Transonic Aerodynamics, AGARD Conference Pro-
    ceedings No. 35, pp. 19-1--19-9, September 1968.

21. Stewartson, K., _On Wing-Body Interference in Supersonic Flow_, Aero-
    nautical Research Council 27-715, 9 February 1966.

22. Stollery, J. K., _Hypersonic Viscous Interaction--An Experimental_
    Investigation of Flow over Flat Plates at Incidence and Around an
    Expansion Corner, Aerospace Research Laboratories 70-0125, July 1970.

23. Thomas, J. P., _Investigation of the Pressure Distribution on a Blunt-F_
    Blunt-Plate Combination at a Mach Number of 11.26, Aerospace Research
    Laboratories 66-0142, July 1966.

24. Thomas, J. P., _Flow Investigation About a Fin-Plate Model at a Mach_
    Number of 11.26, Aerospace Research Laboratories 67-0188, September 19

25. Weirich, R. L. and Vahl, W. A., _Flow-Field Properties Near an Arrow-_
    Wing-Body Model at Mach Numbers of 1.60, 2.36, and 2.96, NASA Tech-
    nical Note D-4809, October 1968.

26. Winkelmann, A. E., 'Flow Visualization Studies of a Fin Protuberance
    Partially Immersed in a Turbulent Boundary Layer at Mach 5", United Sta
    Naval Ordinance Laboratory NOLTR-70-93, 20 May 1970.

27. Winkelmann, A. E., "Aerodynamic Interaction Phenomena Produced by a Fin
    Protuberance Partially Immersed in a Turbulent Boundary Layer at Mach
    AGARD Conference Proceedings No. 71, September 1970.

INITIAL DISTRIBUTION LIST

		No. Copies
1.	Defense Documentation Center Cameron Station Alexandria, Virginia 22314	2
2.	Library, Code 0212 Naval Postgraduate School Monterey, California 93940	2
3.	Chairman, Department of Aeronautics Naval Postgraduate School Monterey, California 93940	1
4.	Professor D. J. Collins, Code 57Co Department of Aeronautics Naval Postgraduate School Monterey, California 93940	1
5.	LT Robert W. Heyer, USN 10811 Spring Lane Lemoore, California 93245	1

DOCUMENT CONTROL DATA · R & D

(Security classification of title, body of abstract and indexing annotation must be entered when the overall report is classified)

1 ORIGINATING ACTIVITY *(Corporate author)*	2a. REPORT SECURITY CLASSIFICATION
Naval Postgraduate School Monterey, California 93940	Unclassified
	2b. GROUP

3 REPORT TITLE

Holographic Interferometry of The Flow Field Between a Fin And Flat Plate

4. DESCRIPTIVE NOTES *(Type of report and inclusive dates)*

Master's Thesis; (March 1972)

5. AUTHOR(S) *(First name, middle initial, last name)*

Robert Ward Heyer

6 REPORT DATE	7a. TOTAL NO. OF PAGES	7b. NO. OF REFS
March 1972	178	27

8a. CONTRACT OR GRANT NO.	9a. ORIGINATOR'S REPORT NUMBER(S)
b. PROJECT NO.	
c.	9b. OTHER REPORT NO(S) *(Any other numbers that may be assigned this report)*
d.	

10. DISTRIBUTION STATEMENT

Approved for public release; distribution unlimited.

11. SUPPLEMENTARY NOTES	12. SPONSORING MILITARY ACTIVITY
	Naval Postgraduate School Monterey, California 93940

13. ABSTRACT

   This study was an attempt to map the density field in a fin-flat plate junction three-dimensionally using holographic interferometry. This investigation has extended the density studies by Matulka [12, 13] and Jagota [3, 4] to include, for the first time, interferometric fringe information obtained through a transparent model in supersonic flow. The fringe information was then inverted by a FORTRAN computer program to produce a plot of the density field around the model. The feasibility of the method was demonstrated.

   The factors which are thought to have limited the success of the experiment include vibration of the model, fluctuations of the tunnel flow and the fact that the model was somewhat too large in relation to the size of the wind tunnel test section. Schlieren photography was used to look through and around the model and to verify that the same flow was established as was reported by Thomas [23, 24] and Winkelmann [26, 27].

   The data reduction of holographic interferograms was, for the first time, accomplished using photographic enlargements. This technique is considered to be much easier and more accurate than the one used in the previous investigations. However, the data reduction step, because of the time and labor involved, is considered to be the rate controlling process of the whole analysis.

DD FORM 1473 (PAGE 1)
1 NOV 65

S/N 0101-807-6811

A-31408

KEY WORDS	LINK A		LINK B		LINK C	
	ROLE	WT	ROLE	WT	ROLE	WT
fin-flat plate flow field						
wing-root flow field						
holography						
three-dimensional density field						
three-dimensional flow field						
fin						
flat plate						
interferogram						
flow field						
fin flat plate junction						
wing root junction						
holographic interferometry						
supersonic flow						

DD FORM 1473 (BACK)
1 NOV 65
S/N 0101-807-6921

179

UNCLASSIFIED
Security Classification

A-31409